TECHNO-ECONOMIC ANALYSIS OF CONCENTRATED SOLAR POWER PROJECTS IN NORTHERN NIGERIA

By

OLUTOSIN ADEBAYO,OGUNLEYE
Matric No: 202187

B.Eng Electrical/Electronic Engineering (NDA), M.Eng Electronic/Communication Engineering (NDA)

A Thesis in the Department of Mineral, Petroleum, Energy Economics and Law,
Submitted to the Faculty of Multidisciplinary Studies
in partial fulfilment of the requirements for the Degree of

DOCTOR OF PHILOSOPHY

of the

UNIVERSITY OF IBADAN

AUGUST 2021

CERTIFICATION

We certify that this work was carried out by Mr O.A. Ogunleye in the Department of Mineral, Petroleum, Energy Economics and Law, University of Ibadan

……

Supervisor
A. Adenikinju,
Ph.D. (Ibadan)

……..……..

Supervisor
O.S Ohunakin,
Ph.D. (Covenant University)

DEDICATION

This thesis is dedicated to God, the Almighty for the gift of life, other blessings and grace to complete this work successfully.

ACKNOWLEDGEMENTS

I thank the Almighty God for the inspiration and grace to complete this work. It would have been impossible without Him. I also appreciate my supervisors, Prof A. Adenikinju and Prof O.S. Ohunakin, for their guidance and commitment to the success of the work.

I also thank Mr. Olalekan Akintade for his immense contribution to this work and Mr Emmanuel Onyeuche for assisting with the administrative aspect of this work. I also appreciate all staff of the Department of Mineral, Petroleum, Energy Economics and Law, University of Ibadan, University of Ibadan, particularly Mr. Abayomi Daramola, Ms. BimpeAiyegboyin and MrsEhiedu Blessing, for their commitment and support that contributed immensely to the successful completion of this work.

To my wife, Aderonke, and my sons, Daniel and David, thank you for your love, encouragement and support, and to my mum, Esther Ogunleye, I sincerely appreciate your love and prayers.

Finally, I want to thank my father, Late Venerable Joshua Ogunleye, for his encouragement and support. I wished he was here to see me obtain this doctoral degree, but God be praised for the immense impact he made in my life.

To every other person who has contributed to the success of this work, I say a big thank you. Thank you all and may God in His infinite mercies continue to bless you.

ABSTRACT

Electricity supply in Nigeria is far below its demand with an all-time peak power generation of 5,420.30 MW as against estimated demand of over 30,000 MW. Bridging the electricity Demand-Supply gap in a sustainable manner requires the utilisation of renewable energy that supports both grid-tied and distributed technology. Concentrated Solar Power (CSP) technologies offer such solution. Literature is however limited on the feasibility and economic viability of CSP technologies in Northern Nigeria. More so, despite the vast direct normal irradiance endowment in Northern Nigeria and the high efficiencies of thermal energy storage associated with CSP, the technology is yet to be incorporated into the electricity generation mix in Nigeria. This study was therefore designed to conduct a techno-economic mapping of CSP technologies across widely selected locations in Northern Nigeria.

The Theory on Solar Radiation formed the framework. Data comprised an 18-year (2001-2018) meteorological records from the Nigerian Meteorological Agency and the European Union Photovoltaic Geographic Information System. A comparative analysis of ten locations in Northern Nigeria was conducted using the Angstrom-Page and Hargreaves-Samani equations in linear, quadratic, and cubic forms. The top five locations suitable for CSP deployment were identified through a weighted approach, and solar radiation models were developed for them. Typical Meteorological Year 3 (TMY3) data were subsequently developed from Finkelstein-Schafer statistics to simulate energy output and Levelised Cost of Electricity (LCOE) or break-even cost. This study also determined optimal concentrator, through comparative analysis of variants of Parabolic trough concentrator (PTC) model of CSP, and other system requirements using the System Advisor Model (SAM) Software.

Two locations (Maiadua 13°08'54"N, 8°13'41"E and Malam-Fatori13°40'59"N,13°19'59"E) were suitable for a 100 MW CSP plants, while the other three (Machina 13°08'11"N,10°02'57"E, Gada 13°46'32"N, 5°39'47"E and Zaria 11°11′N, 8°14'28"E) were found suitable for 50 MW CSP plants. The annual estimated energy outputs from the five locations were 341,702,879KWh, 323,484,204 kWh, 179,176,312 kWh, 170,673,093kWh and 155,710,024kWh, while the estimated LCOE of the proposed plants were US¢15.7/kWh, US¢15.8/kWh, US¢14.7/kWh, US¢15.4/kWh and US¢16.5/kWh for Maiadua, Malam-Fatori, Machina, Gada, and Zaria, respectively. Sites within latitudes 13°N and 14°N were suited for the deployment of CSP in the region. Furthermore, Sky Fuel Sky Trough 80-mm OD receiver was the preferred concentrator, Therminol VP-1 was the preferred heat transfer fluid, and HITEC Solar Salt the preferred thermal energy storage medium. The CSP plants could only be sited when and where the security situation permitted.

Five locations in Northern Nigeria can accommodate and efficiently deploy 50 MW to 100 MW CSP plants. Thus, a sustainable model of electricity generation capable of supporting industrial applications in an environmentally friendly manner has been formulated. Government should support CSP investments in Northern Nigeria through favourable power purchase agreements and feed-in-tariffs.

Keywords: Power generation, Direct normal irradiance, Parabolic trough concentrator, Levelised cost of electricity, Typical meteorological year

Wordcount: 464

TABLE OF CONTENTS

LIST OF TABLES

LIST OF FIGURES

LIST OF PLATES

LIST OF ABBREVIATIONS

AEP	-	Annual Energy Production
CBN	-	Central Bank of Nigeria
CRS	-	Central Receiver System
CSP	-	Concentrated Solar Power
DCF	-	Discounted Cash Flow
DE	-	Dish Engine
DHI	-	Diffused Horizontal Irradiance
DNI	-	Direct Normal Irradiance
DSG	-	Direct Steam Generation
ESMAP	-	Energy Sector Management Assistance Program
EU-PVGIS	-	European Union Photovoltaic Geographic Information System
FIT	-	Feed-in-Tariff
FMP	-	Federal Ministry of Power
FMWR	-	Federal Ministry of Water Resources
GHI	-	Global Horizontal Irradiance
HTF	-	Heat Transfer Fluid
IEA	-	International Energy Agency
IEC	-	InternationalElectrotechnicalCommission
IIED	-	International Institute for Environment and Development
IPCC	-	Intergovernmental Panel on Climate Change
IRENA	-	International Renewable Energy Agency
JICA	-	Japan International Cooperation Agency
LCOE	-	Levelised Cost of Electricity
LFR	-	Linear Fresnel Reflector
MCM	-	Mean Monthly Discharge
MYTO	-	Multi-Year Tariff Order

NBS	-	National Bureau of Statistics
NERC	-	Nigerian Electricity Regulatory Commission
NIMET	-	Nigerian Meteorological Agency
NREL	-	National Renewable Energy Laboratory
NSRDB	-	National Solar Radiation Data Base
ORC	-	Organic Rankine Cycle
PEST	-	Political, Economic, Social and Technological
PESTEL	-	Political, Economic, Social, Technological, Environmental and Legal
PPA	-	Power Purchase Agreement
PT	-	Power Tower
PTC	-	Parabolic Trough Concentrator
PV	-	Photovoltaic
RC	-	Rankine Cycle
SAM	-	System Advisor Model
SAWS	-	South African Weather Services
SCA	-	Solar Collector Assembly
SDG	-	Sustainable Development Goal
SWOT	-	Strengths, Weaknesses, Opportunities and Threats
TCN	-	Transmission Company of Nigeria
TES	-	Thermal Energy Storage
TMY	-	Typical Meteorological Year
UNDP	-	United Nations Development Programme

CHAPTER ONE
INTRODUCTION

1.1 Background to the Study

Energy is very crucial to the socio-economic development and prosperity of nations (Lloyd, 2017). It is basically used for transport, cooking, heating and electricity generation. According to Oyedepo (2013), energy use has a direct relationship with industrial productivity, and by implication socio-economic development. The author also stated that electricity is the preferred means of energy supply for industrial production processes. The place of electricity as a prime form of energy was further highlighted by IEC (2020) who adjudged it as the most versatile and most efficient means of consuming energy. The IEC also described electricity asloss-free energy associated withefficient energy conversion without losses or pollution. Electricity has also been acclaimed as the purest form of energy, with about 30 % of global energy production being utilised for electricity generation (IEA, 2010). The prime position occupied by electricity amongst other forms of energy is attributed to its greater flexibility, cleanliness and high transmission efficiency amongst other qualities (Mehta and Mehta, 2008).

Despite the importance of energy to human well-being, a significant percentage of the world population have little or no access to it. Amongst other energy demands, about 1.2 billion people globally do not have access to electricity (UNDP, 2016). In Nigeria, about 60% of the population are not connected to electricity through the national grid, while the 40% that is connected to the grid experience power outages about 60% of the time (Aliyu *et al.*, 2015).In a bid to address the shortfall in global demand for electricity, several sources of energy are being harnessed. Some of these sources of energy could be conventional while others are non-conventional or renewable. Although energy is a major facilitator of socio-economic development globally, the way through which it is sourced, produced and used could lead to environmental and social problems as evident in the use of conventional energy sources.

Conventional sources of energy are exhaustible and environmentally unfriendly due to emissions of greenhouse gases (GHGs), especially carbon-dioxide (CO_2) with its attendant harmful effect on the environment leading to global warming (Oyedepo, 2013). Thus, depletion in available reserve of conventional energy sources and the adverse effects of its utilisation on the environment makes development from conventional energy sources unsustainable. The environmental degradation occasioned by emissionsfrom conventional sources of energy led to a clamour for energy transition from conventional to renewable sources of energy. Unlike the conventional energy sources, renewable sources of energy or renewable energy (RE) including wind, hydro and solar energies amongst others are replenished naturally and hardly emit any GHG.

RE is highly beneficial to the socio-economic development of nations as posited by Schwerhoff and Mouhamadou (2017), who highlighted the large potential of RE in contributing to the attainment of the Sustainable Development Goals (SDGs) of the United Nations (UN). Particularly, RE was highlighted as crucial to the attainment of 10 out of the 17 SDGs of the UN, prominent among which are SDGs 7 and 13 on ensuring access to affordable, reliable, sustainable and modern energy for all, and taking urgent action to combat climate change and its impacts respectively. They further highlighted that the natural conditions in Africa are well suited for the deployment of RE.Amongst these renewable energy sources, the Sun is the predominant because other sources depend on it (Chu, 2011). Furthermore, Solar energy is one of the cleanest sources of energy and its application promotes economic growth and environmental integrity, especially in developing nations (Mohammed *et al*., 2017). Therefore, harnessing energy from the Sun for electricity generation has great potential for solving the energy deficiency in Nigeria. Furthermore, concentrated solar power (CSP) offers great potentialfor large scale power generation as well as ensuring grid stability. Although Nigeria generally has high level of solar radiation, northern Nigeria is more endowed in terms of direct solar radiation which is the major requirement for CSP applications.

1.2 Statement of the Problem

Nigeria's all-time peak power generation stands at about 5,420.30MW of electricity, which is far less than its over 30,000 MW estimated demand as projected by the

Presidential Task Force on Power by 2020 as highlighted in Figure 1.1 (TCN, 2020; GIZ, 2015).The difference between the projections and available power indicates that there is a huge electricity supply gap in Nigeria. It is worth noting that the available power in the country, were produced from massive use of fossil energy sources with the attendant pollution of the environment.

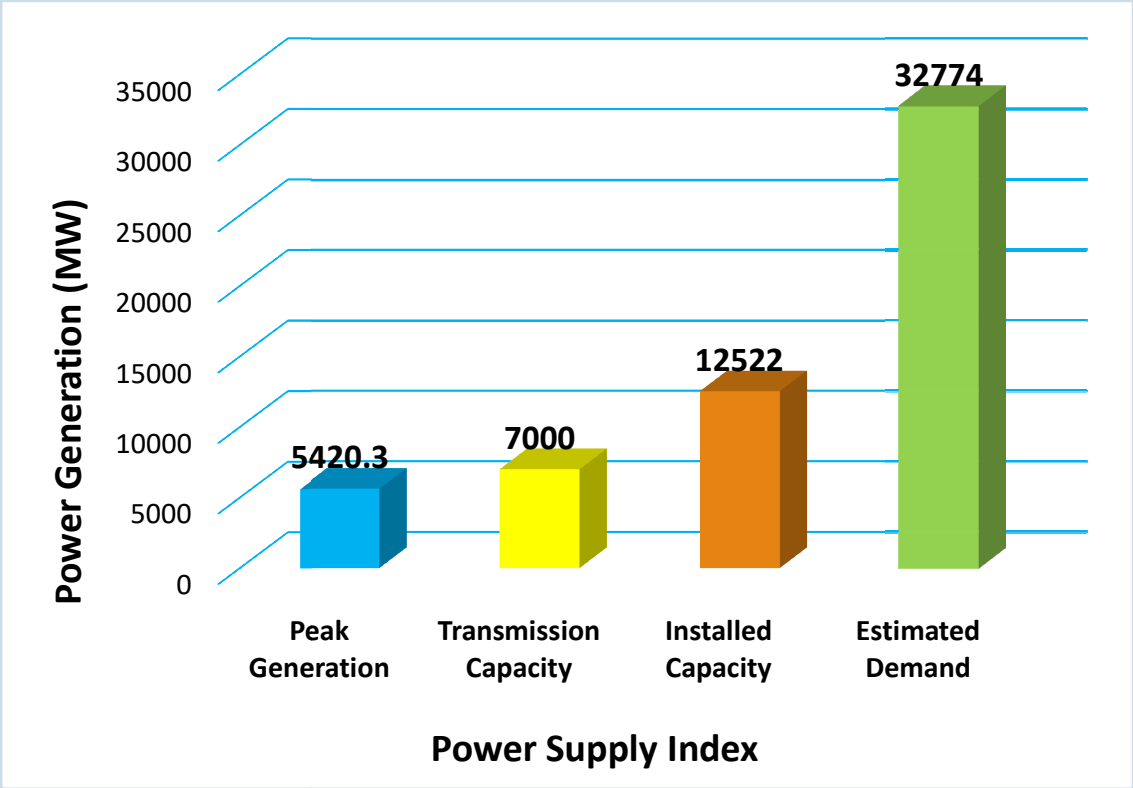

Figure 1.1: Estimated Power Demand versus Supply in Nigeria (Source: GIZ, 2015; TCN,2020)

Additionally, the electricity consumption per capita in Nigeria, which was 177.5 kWh/capita as of 2019, is very low relative to those of some thriving economies in Africa as indicated in Figure 1.2.

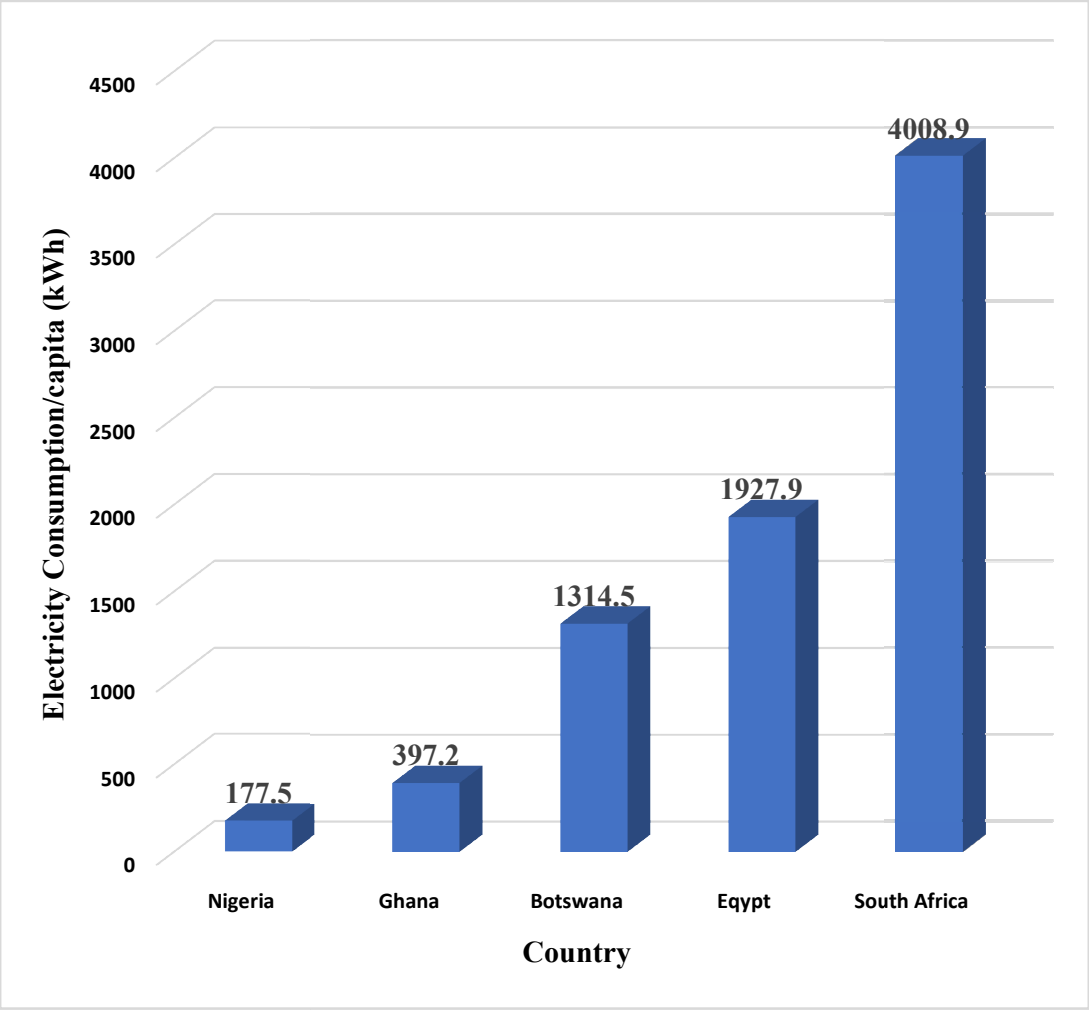

Figure 1.2: Electricity Consumption Per Capita of Nigeria and Some Thriving Economies in Africa (Source: BP, 2020)

Furthermore, power generation in Nigeria is majorly from hydropower plants and gas-fired thermal stations, constituting 15 % and 84 % of total installed power generation capacity respectively (Falobi, 2019). Apart from hydropower, power generation from other renewable sources that are found to be in vast deposit in the country, is still at an abysmal level, resulting into lean power generation mixin Nigeria due to inadequate exploitation of renewable energy sources, particularly solar thermal power such as concentrated solar power (CSP). For instance, in 2019, Nigeria generated about 2152 MW from renewable sources, out of which 2111 MW came from large hydropower, with only 28 MW coming from solar photovoltaics and 13 MW from other renewable sources as highlighted in Figure 1.3 (IRENA Renewable Energy Statistics, 2020). This study thus focussed on the utilisation of CSP to diversify Nigeria's electricity generation mix towards improved power supply in the country.

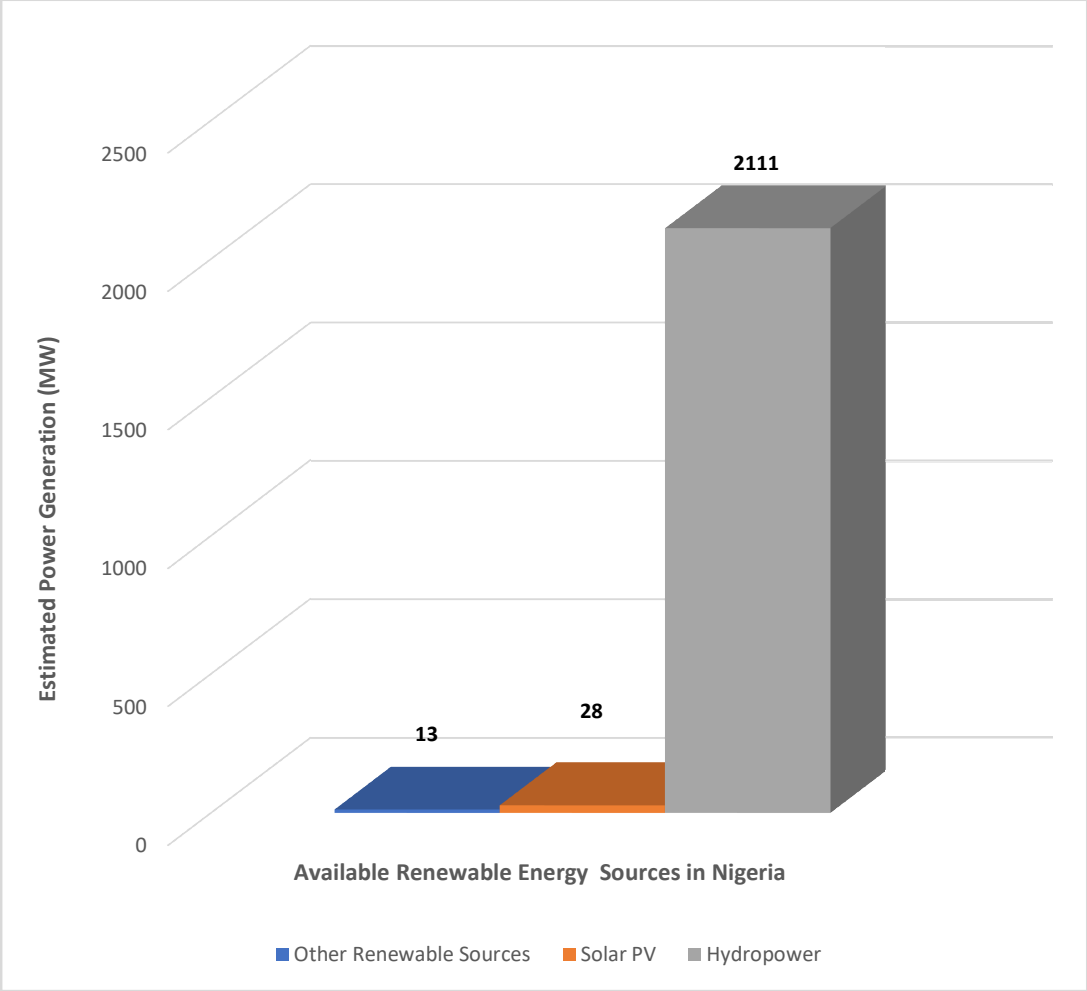

Figure 1.3: Estimated Power Generation from Renewable Sources in Nigeria as at 2019(Source: IRENA Renewable Energy Statistics, 2020)

Most of the power generated in Nigeria, from the largely untapped renewable sources like solar energy is at a small scale, and usually off grid. For instance, the solar energy in Nigeria is largely utilised for small-scale electricity generation such as solar home systems and street lighting using Solar Photovoltaic (PV) technology. If the country is to maximise its renewable resources potential, particularly solar energy, to generate power, efforts must be focussed on developing capacity for bothdistributed and grid-tied power generationthrough solar thermal electricity. The preference for solar thermal systems in this study is borne out of the need for higher grid stability relative to Solar PV. It has been projected that if only 5 % of suitable land in northern and central Nigeria is employed for solar thermal power generation, the country could generate about 427,000 MW of electricity through solar thermal systems (International Institute for Environment and Development, 2012). Solar thermal systems basically involve indirect conversion of solar energy into electricity or heat required for industrial purposes. CSP could thus be examined in this regard, owing to its potential for large-scale power generation and capability to support both grid-tied and distributed generation power supply. This is particularly essential for the northern parts of Nigeria where the rate of poverty is adjudged to be over 76 % (Ngbea and Achunike, 2014). This is premised on the fact that CSP could provide robust power supply for both small and medium enterprises as well as industrial processes. However, if CSP is to be utilised, a means of obtaining validatedDirect Normal Irradiance (DNI) data in the absence of pyrheliometers must be evolved to boost the confidence of potential investors in CSP projects.

1.3 Aim and Objectives of the Study

The aim of this work is to determine the techno-economic suitability of potential locations in northern Nigeria for the deployment of CSP plants. The specific objectives are to:

i. Conduct a general assessment of potential locations in northern Nigeria to determine suitability for power generation through CSP.
ii. Establish solar radiation models for the utilisation of CSP systems in suitable locations in northern Nigeria.
iii. Determine the annual electricity output from CSP plants in suitable locations in northern Nigeria.

iv. Determine the Levelised Cost of Electricity (LCOE) from CSP plants in suitable locations in northern Nigeria.

1.4 Justification for the Study

Satellite data ranging from 1994 to 2015 obtained from the World Bank Energy Sector Management Assistance Program (ESMAP), indicated that some locations in northern Nigeria possess adequateDirect Normal Irradiation (DNI)for CSP plants applications. Some of these locations possessannual DNI above 2000 kWh/m^2, exceeding the threshold design DNI value of 1800 kWh/m^2 for CSP plants (Sharma *et al*., 2015; Mashena and Alkishriwi, 2016).Furthermore, according to K¨oppen-GeigerClimate Classification, some locations in the northern part of Nigeria have arid and desert climatic conditions, similar to what is obtainable at the fringes of North Africa that are adjudged as one of the most fertile locations for CSP utilisation (World Bank ESMAP, 2011).

Ohunakin*et al.* (2013) indicated that similarity in latitude and topography of different locations is apossible means of predictingsimilarity in solar radiation.Thetopography and climate in some parts of northern Nigeriabears similarity with that oflocations in Northern Cape Province of South Africa where CSP is currently deployed. Although there is no latitudinal relationship between Nigeria and South Africa, the two countries being in different hemispheres, the climatic and topographic similarities of northern Cape Province in South Africa and northern Nigeria arousedthe author's interest to investigate possible similarities in solar radiation. This investigation could further elucidate the potential or otherwise of deploying CSP for power generation in northern Nigeria. The study is further compelled by the need to address the huge electricity supply gap in Nigeria while adhering to the nation's commitments to sustainable development.

The northern parts of Nigeria have been identified as areas of high solar resource. Since CSP offers capacity for large scale/grid-connected power generation, it would be expedient to investigate potential locations in northern Nigeria to determine their viability for deploying CSP plants in the region.The study assumes that insecurity issues in North East Nigeria would have been completely resolved by 2025.

1.5 Scope of the Study

The study focuses on one location in each of 10 selected states in northern Nigeria. These locations are Gada, Sokoto State (Latitude 13°46'32" N, Longitude 5°39'47"E), Yelwa, Kebbi State (Latitude 10°50'13"N, Longitude 4°44'35"E), Gamawa, Bauchi State (Latitude 12° 08′ N Longitude 10° 31'58"E), Maiadua, Katsina State (Latitude 13°08'54" N, Longitude8°13'41" E), Danbatta, Kano State (Latitude 12° 25′ 59″ N, Longitude 8° 30′ 55″ E),Gusau, Zamfara State (Latitude 12°9'46"N, Longitude 6°40'28" E), Mubi, Adamawa State (Latitude 10° 16′ N, Longitude 13° 16′ E), Zaria, Kaduna State (Latitude 11° 11′ N,Longitude 8° 14'28" E), Machina, Yobe State (Latitude 13°08'11" N, Longitude 10°02'57" E)and Malam-Fatori, Borno State (Latitude 13°40'59" N, Longitude 13°19'59" E).

The study utilised a general survey of locations in Nigeria through the European Union Photovoltaic Geographic Information System (EU-PVGIS) to determine potential locations based on value of DNI. Although Nigeria is generally endowed with high level of solar radiation, only some parts of northern Nigeria were observed as possible sites for CSP application based on the value of DNI obtainable from EU-PVGIS. The States where the locations of potential sites for CSP application are situated cover a total land space of about 433,987 km^2, which is about 47 % of the entire land area of Nigeria. Figure 1.4 shows the States of the locations under consideration. The area is also known to have peak temperatures of about 40ºC, which connotes a possible fertile area for solar resource, and lying within the high solar radiation zone in Nigeria (Abdulsalam *et al*, 2012).

Figure 1.4: Map of Nigeria showing the States where locations under Consideration are Situated.

CHAPTER TWO
LITERATURE REVIEW

2.1 Preamble

This chapter shall give a background to the study. It will also examine some literature relevant to CSP application to provide a conceptual basis for the study. The review shall be in fourparts: theoretical, economic and strategic, methodological and empirical reviews.

2.2 Solar Electricity Generation

Solar energy could be utilised for electricity generation either directly or indirectly.The direct conversion of solar energy to electricity occurs through photovoltaic (PV) effect. In the indirect approach, energy from the Sun is first converted to heat energy, which is then used to drive steam turbines to generate electricity as applicable in Concentrated Solar Plant (CSP) (Hayat *et al*., 2018).

Examples of Solar CSP applications include the Ivanpah Solar Electric Generating System in California, comprising 173,500 heliostats with an installed capacity of 392 MW, and was the largest CSP plant in the world until 2016 (NREL, 2018). In February 4, 2016, Morocco commissioned the 500 MW Noor-Ouarzazate CSP Complex which is currently the largest CSP plant in the world (World Bank, 2016).

Globally, the installed capacity of CSP for electricity as at 2017 was estimated at about 5.13 GW (SolarPACES, 2018). It is anticipated that global CSP capacity would rise to about 337 GW in 2030 and about 1089 GW by 2050. Furthermore, it was projected that CSP would provide about 11 % of global electricity and 15 % of the electricity in Africa by 2050. It is expected that North Africa and the Middle East would generate a majorproportion of the power to be realised from CSP (IEA CSP Technology Roadmap, 2010).

2.3 Climatic Considerations for Solar Power Plants

The K¨oppen-GeigerClimate Classification is a model that utilises widespread and long-term meteorologicalglobal dataset to classify geographical spaces. Itwas first developed by

Wladimir K¨oppen in 1900 and updated by Rudolf Geiger in 1954 and 1961. K¨oppen'sclassification was based on five vegetation groups comprisingthe equatorial zone, the arid zone, thewarm temperate zone, the snow zone and the polar zone, represented by the alphabets A- E respectively. In highlighting a zone in K¨oppen's climate classification, the first letter indicates the zone, the second letter indicates precipitation while the third letter indicates air temperature. For instance, Dfc indicates Snow, fully humid with cool summer (Peel *et al*., 2007; Kotte*et al*., 2006).

The initial work of K¨oppenthat led to the development of World Climate Map in 1923 was based on his discovery that plants are reliable indicators for many climatic elements. Studies over a century later such as Kalvova*et al*. (2003), Stern *et al*. (2000), Lohmann *et al*. (1993), Wang and Overland (2004), Gnanadesikan and Stouffer (2006) and Kleidon*et al*. (2000) all alluded to the veracity of K¨oppen's work. For instance, Kalvova*et al*. (2003) comparedglobal climate model outputs to the classification on K¨oppen'sWorld Climate map and observed just a minor difference of about 0.5%. Furthermore, Stern *et al*. (2000), had to rely on a modification of the Ko¨ppen climate classification to draw a new climatic map of Australia despite having access to all the climate data repository of the Australian Bureau of Meteorology. Despite all the works carried out to evolve climate classification, the original Ko¨ppen climate classification, which has been converted to digital map, is considered the most reliable and widely used climate classification for both teaching and research (Peel *et al*., 2007; Kotte*et al*., 2006).

The K¨oppen-Geiger climate classificationcategorised Nigeria into 4 climatic regions.These regions are the Warm Desert Climate (BWh), Warm Semi-Arid Climate (BSh), Monsoon Climate (Am) and the Tropical Savanna Climate (Aw) as illustrated in Figure 2.1.

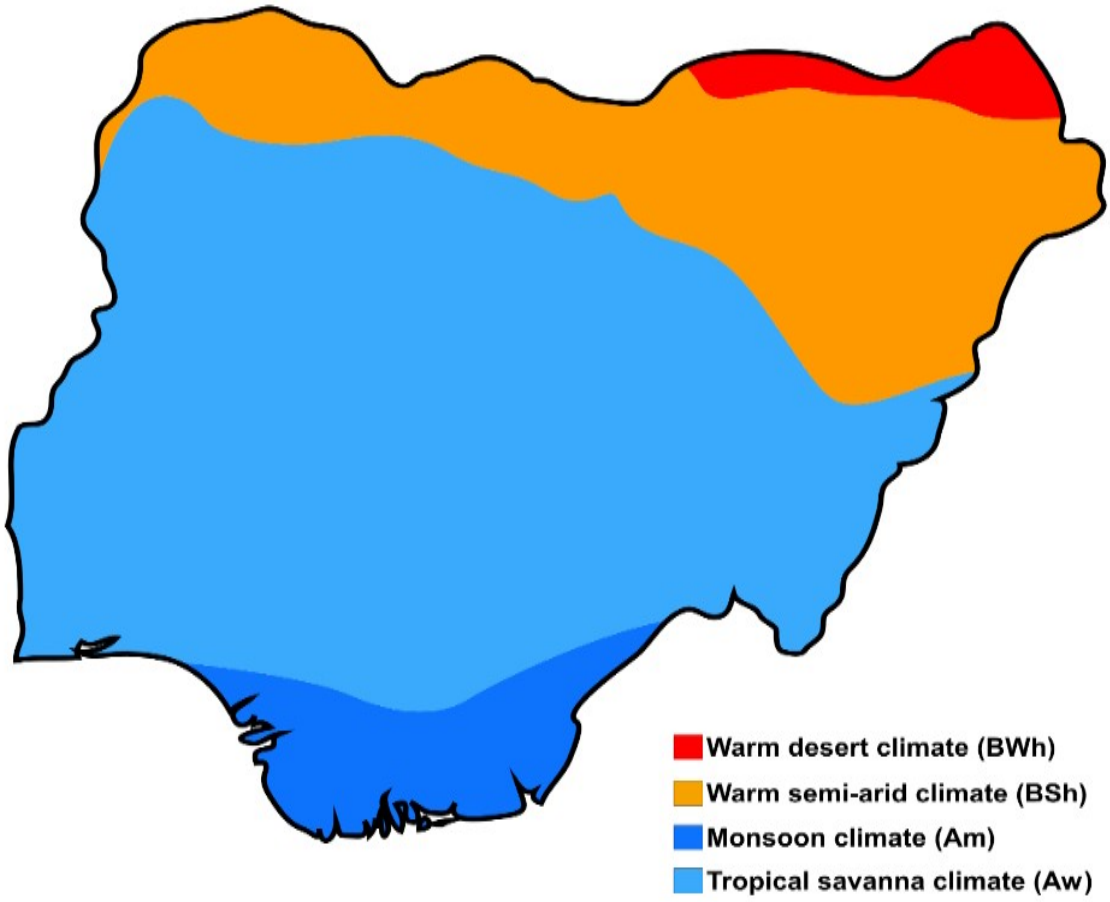

Figure 2.1: TheK¨oppen-Geiger Climate Classificationof Nigeria

Some of the northern states of Nigeria that lie within Latitudes 9^{o} to 14^{o}N and Longitudes 2^{o} to 15^{o}E fall within the BWh and BSh of the K¨oppen-Geiger climate classification.

The solar radiation potential of a site is paramount in determining its suitability for solar applications. A reliable online tool that provides an overview of solar radiation potential of sites and regions globally is the Global Solar Atlas, funded by the Energy Sector Management Assistance Program (ESMAP), a multi-donor trust fund administered by the World Bank. The Global Solar Atlas has 4 key features: interactive maps that affords visualisation of solar resource potential of sites and regions by indicating annual average values, PV energy yield calculator that enables calculation of long-term energy yield for PV systems, downloadable maps and Geographic Information System (GIS) data, and solar energy potential statistics for countries and regions that could provide insight to policymakers and researchers on the theoretical and practical potential of solar energy available at locations of interest (World Bank ESMAP, 2018).

The solar radiation at sites and locations are usually the Global Horizontal Irradiance (GHI) or the DNI. The GHI comprises the direct and diffused components of solar radiation (Hejase and Assi, 2014). The direct component of the GHI normal to the incident plane is the DNI and it is applicable in direct utilisation of solar radiation as in solar heating and CSP technology (Blanc *et al*., 2014). Solar PV technology however utilises GHI. Thus, DNI constitutes the major meteorological parameter that determines the energy output of a CSP plant. Hence, the DNI of locations in northern Nigeria was investigated using the online ESMAP Global Solar Atlas and the observations suggests that some locations in the northernmost part of Nigeria have high DNI values which may be suitable for CSP applications, as illustrated in the ESMAP DNI Solar Resource Map of Nigeria in Figure 2.2.

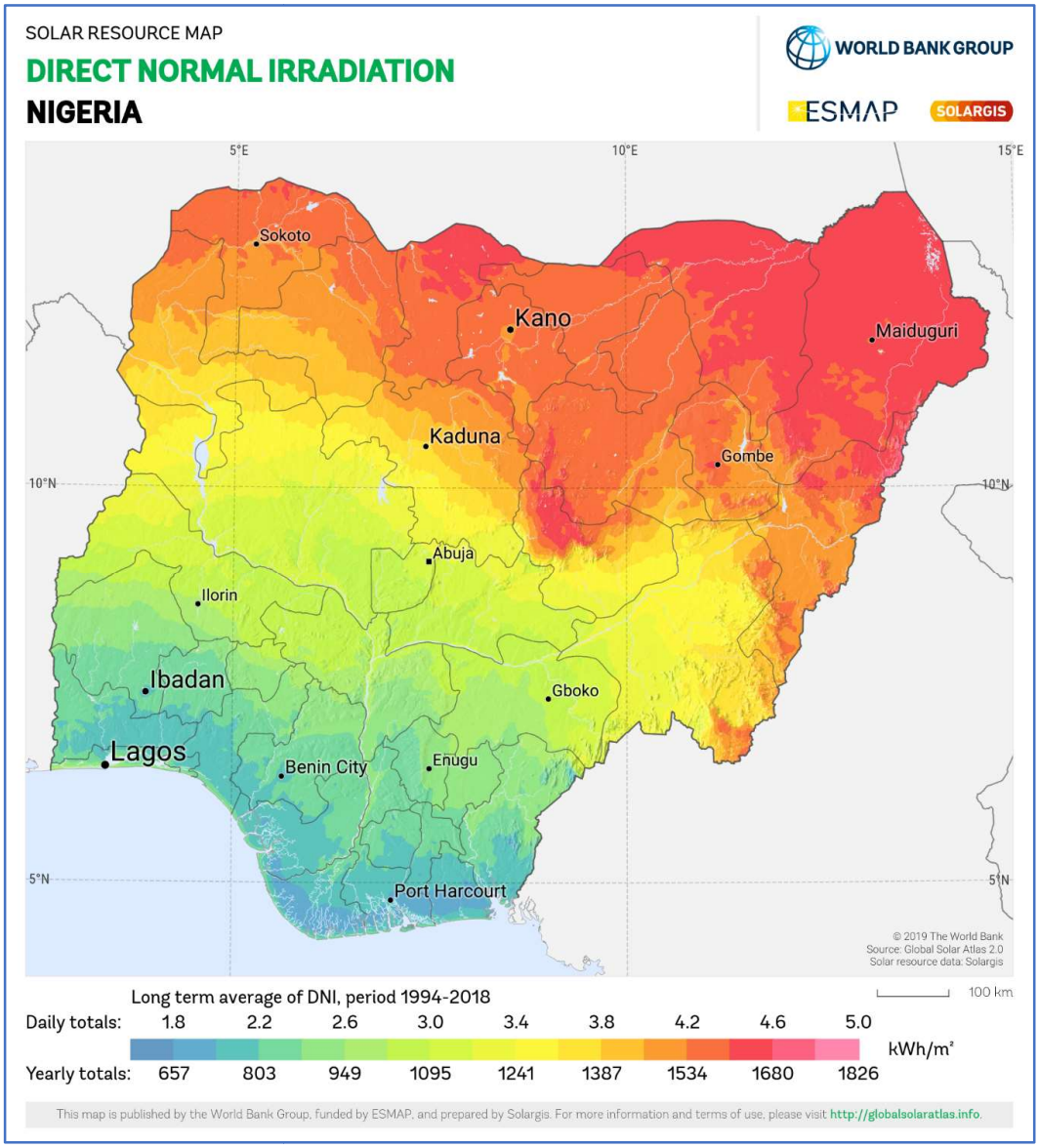

Figure 2.2: ESMAP DNI Solar Resource Map of Nigeria(Solargis, 2018).

The impact of other meteorological parameters like ambient temperature, wind speed, relative humidity, etc., is not quite significant except in extreme weather conditions like hurricane. Hence, such parameters are considered as auxiliary. DNI is not uniformly distributed across the globe like the Global Horizontal Irradiance (GHI). Locations in the subtropics around Latitudes 23°N or 23°S, with a spread of about ±10° or around 1000 km from the equator, have been identified as the most fertile for DNI harvesting. These bands on both sides of the equator are thus referred to as the 'sunbelts' (Meyer *et al*., 2012). The northernmost parts of Nigeria lie within Latitudes 13°N and 14°N, thereby falling within the global sunbelt.

2.4 Concentrated Solar Power System

CSP system refers to the combination of mirrors or lenses that harness direct solar radiation from the atmosphere to produce heat energy for electricity generation through a heat turbine (Lovegrove and Pye, 2012). A typical CSP system comprises a concentrator, receiver unit, heat transfer fluid (HTF) with its piping accessories, thermal energy storage (TES) and the power block. Mirrors or lenses are used as concentrators; the major types are trough, linear Fresnel, dish and tower. These concentrators could utilise either line-focussing or point-focussing principle. The trough and linear Fresnel concentrators utilise line-focussing principle, while the tower and dish concentrators utilise point-focussing principle. The line-focussing systems have a concentration factor of about 50-100 while the point-focussing systems have concentration factor of 500 and above. However, the line-focussing system are more commercially viable for large-scale on-grid electricity generation through CSP relative to the point-focussing system (IRENA, 2012).

Direct utilisation of solar energy is more pronounced than the indirect utilisation (IPCC, 2011). However, studies and recent developments revealthe huge potential that lies in the indirect utilisation of solar energy for electricity, especially CSP. CSP plants are more suitable for on-grid power generation in relation to Solar PV while it is also capable of providing large-scale heat for industries as well as water desalination systems. They are also easily adaptable for co-generation whereby energy sources such as gas or coal could be used to generate heat at periods of low solar resource to keep the plant running on a continuous basis. CSP also holds potential for providing energy for small and medium scale enterprises (SMEs) for the socio-economic development of developing nations like Nigeria (IEA Technology Roadmap CSP, 2010).

Receiver units intercepts the solar radiation from the concentrator and converts it to thermal energy. The dominant type of receiver is the single steel tube with a glass covering; the glass covering is meant to minimise convection heat losses. Other receiver units include those that employ several tubes to form hollow shapes and those directly submerged in the working fluid through volumetric absorption. Oil or molten salt are the preferred choice for HTF because of the transport properties and thermal stability. Heat could also be transferred from the receiver to the power block through Direct Steam Generation (DSG) whereby only one fluid serves as both the HTF and power-cycle working fluid,thereby eliminating the requirement for heat exchanger. Molten salt provides an efficient storage medium in TES systems amongst other storage media.The power block converts the thermal energy from solar radiation into electricity using turbines, particularly steam turbines (Lovegrove and Pye, 2012).The schematic diagram of a CSP system is shown in Figure 2.3.

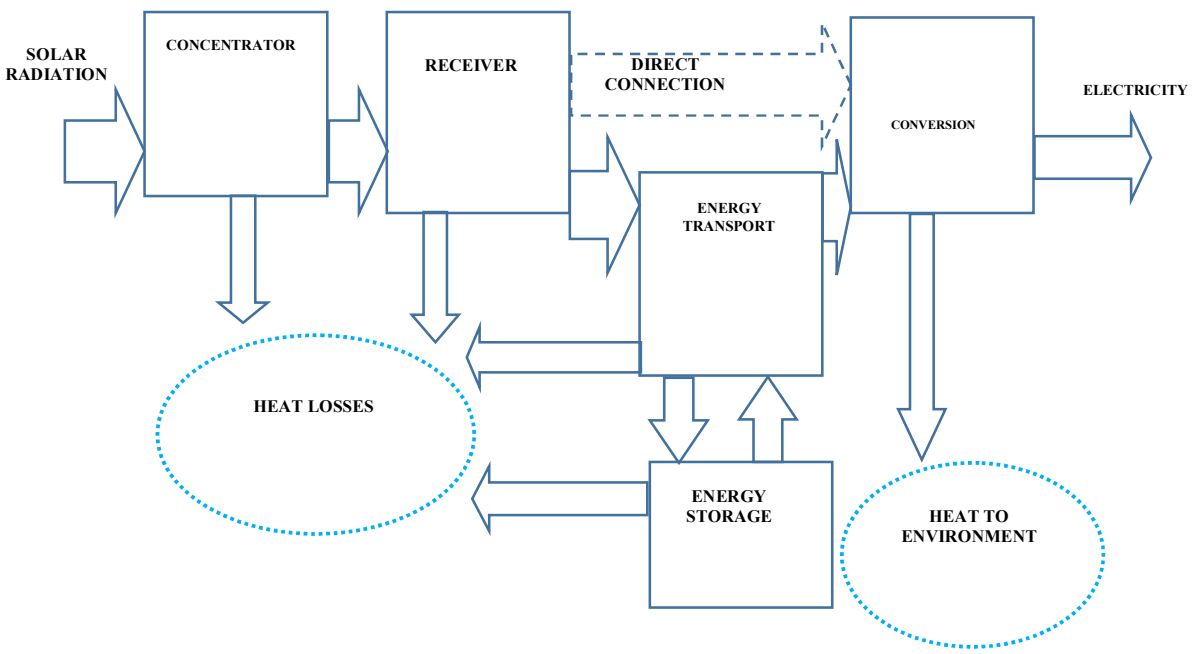

Figure 2.3: BlockDiagram of a CSP System (Source:Lovegrove and Pye, 2012).

CSP systems are largely based on four technologies.These are:(i) Central Receiver System (CRS)or Power Tower (ii) Dish Engine (DE)(iii) Linear Fresnel Reflector (LFR) and (iv) Parabolic Trough Concentrator (PTC) (World Bank ESMAP, 2011). The CRS and Dish Engine systems fall under the general category of point concentrating system, while the LFR and PTCare categorised under the line concentrating system(Moser *et al*. 2013).

2.4.1. Central Receiver System

A CRS also known as power tower (PT) CSP system, employs two-axis tracking heliostats bearing slightly concave mirrors to reflect direct solar radiation unto a central receiver on a tower. The receiver incorporates a steam generator with a circulating working fluid which then passes the generated steam in form of thermal energy unto a steam turbine to generate electricity (Storm, 2019).Typical CRS operates at temperatures up to 1200^{o}C due to high concentration factors of between 200-1000 (Alexopoulos and Hoffschmidt, 2017; Trieb*et al*., 2009). CRS is suitable for combined cycle application or co-generation of electricity through the utilisation of steam and gas in the same plant (Kearney*et al*., 2003; Palenzuela, 2015). The earliest CRS such as the Ivanpah in California and Khi Solar One in South Africa utilise steam as the HTF, but newer plants including the Gemasolarcommissioned in 2011, Crescent Dunes commissioned in 2013, and Noor III commissioned in 2018, utilise molten salts which has efficient heat transfer and energy storage capabilities (Kraemer, 2018). Furthermore, the high working temperatures used in CRS enables a lesser drop in power cycle performance relative to other solar thermal technologies (Palenzuela*et al*., 2015). However, CRS is not as matured as PTC technology, though it is gradually becoming common for large-scale generation or co-generation, as in the Ivanpah Plant in California, USA. A schematic model of a CRS system is shown in Figure 2.4.

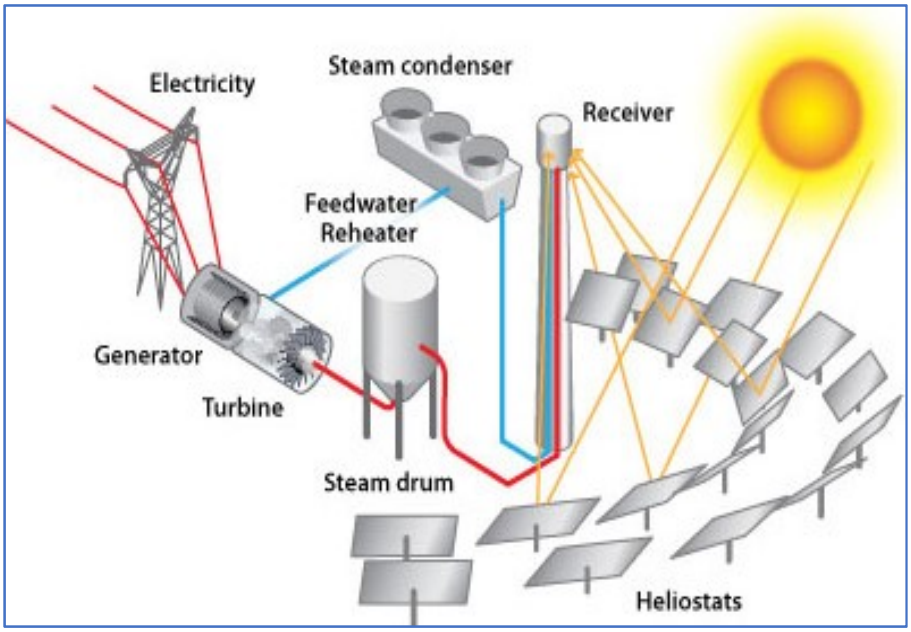

Figure 2.4: Schematic Model of CSP Central Receiver System (Source: PennState, 2018).

A pictorial model of a CRS system is also shown in Plate 2.1.

Plate 2.1: Pictorial Model of a CSP Central Receiver System (Source: U.S. Dept of Energy, 2013).

2.4.2 Dish Engine Technology

The Dish Engine Technology comprises a dish concentrator made of mirror that focuses heat energy onto a receiver fitted at a point equal to the focal length of the dish. A unique feature of the DE systems is its utilisation of mechanical energy instead of heat transfer fluid to produce electricity (World Bank ESMAP, 2011). A Stirling motor, which generates electricity directly from the focussed solar radiation, is also mounted close to the focus of the dish. The Stirling motor utilises helium or hydrogen obtained from solar radiation as its fuel for generating electricity. This offer advantages such as no requirement for water except for washing the mirrors and suitability for distributed generation (Palenzuela*et al*, 2015). Solar DEs have high concentration factors which enables high temperature generation of between 1500^{o}C – 4000^{o}C(Weinrebe and Ortmanns, 2007).They also have high solar energy toelectricity conversion efficiency of approximately 31.25 %. However, it is not suitable for large-scale electricity generation with estimated capacity of less than 25 kWe and future projections of not more than 1 MWe (Moser *et al*. 2013). A schematicmodelof a dish engine CSP system is shown in Figure 2.5.

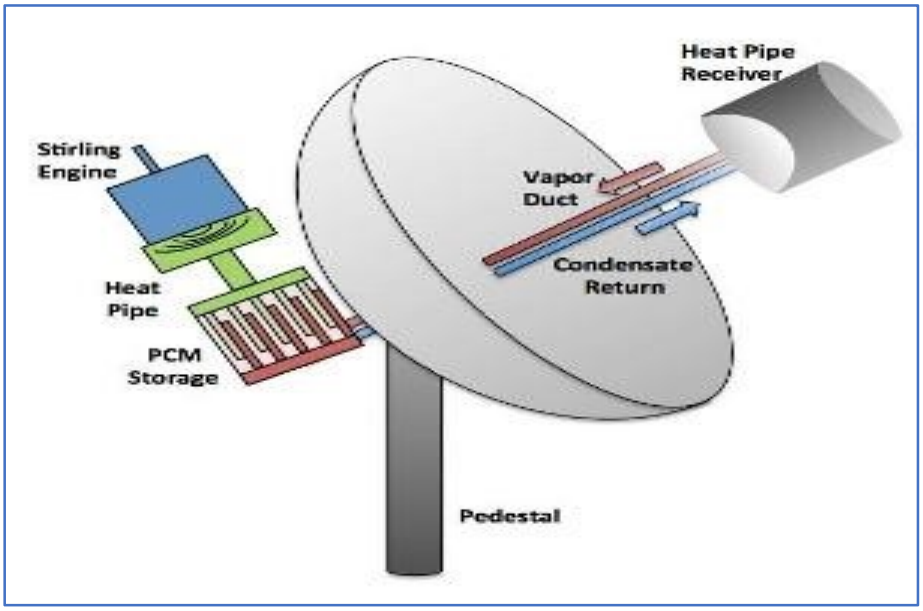

Figure 2.5: Schematic Model of Dish Engine CSP System (Source: Coventry and Andraka, 2017).

A pictorialmodel of a dish engine CSP system is also shown in Plate 2.2.

Plate 2.2: Pictorial Model of Dish Engine CSP System (Source: Greenoptimistic, 2012).

2.4.3 Linear Fresnel Reflector Technology

The Linear Fresnel Reflector (LFR) is a matured CSP technology comprising many mirror segments capable of tracking the sun individually. The absorber tubes of LFR system remain in a fixed position above the mirrors in the centre of the solar field, while the mirrors track the Sun. Some LFR designs utilise water directly in the receiver tubes at pressure of about 50 bar and temperature of about 280^{o}C, while some others use molten salts (USDoE, 2017). Direct Steam Generation (DSG) is the most common configuration of LFR plants. A distinct feature of the DSG concept is the utilisation of water or steam as the working fluid in the power block as well as the heat transfer fluid in the solar field (World Bank ESMAP, 2011). LFR systems have a relatively much lighter structure, which is about 80 % lighter per square meter in comparison to PTC systems. It also affords a more efficient use of land area andoffering about three times greater efficiency in land use than PTC; the reflectors can be positioned relatively closer to each other (Palenzuela*et al*., 2015) and elevated to enable farming underneath (Lubkoll*et al*., 2011). However, it has a relatively lesser optical efficiency, and requires about 33-38%additional aperture area for the same thermal energy output in comparison to PTC (Trieb*et al*., 2009). Furthermore, LFR operates at a relatively lower temperature of about 270^{o}C in comparison to that of PTC,which is about 350^{o}C, thereby resulting in a relatively lower steam cycle efficiency (Palenzuela*et al*., 2015). A major disadvantage of LFR systems is its technical inability to effectively incorporate a TES (World Bank ESMAP, 2011). A schematic model of LFR CSP system is illustrated in Figure 2.6.

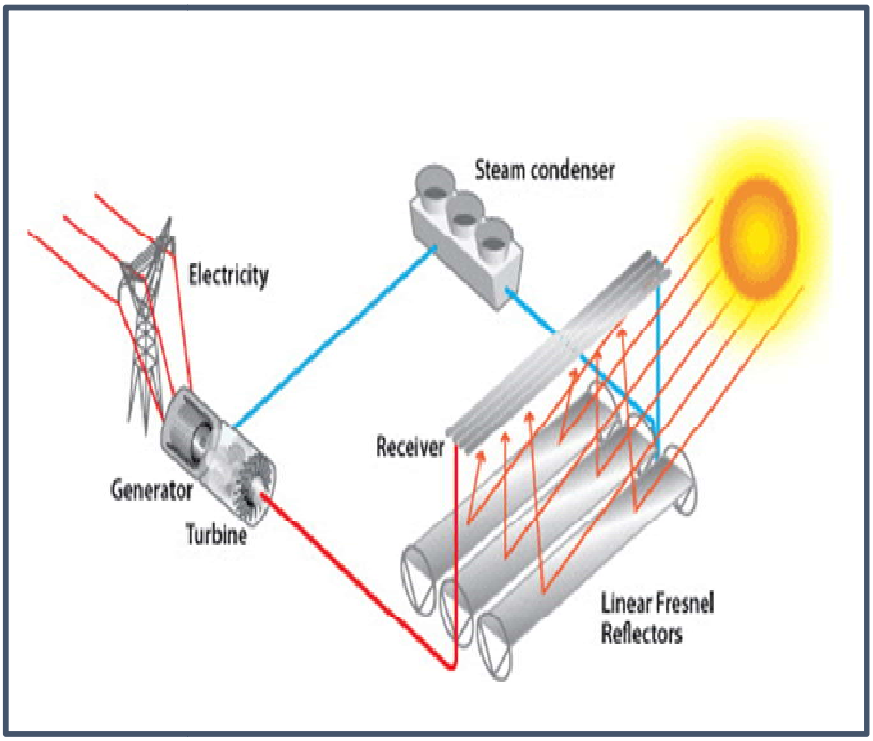

Figure 2.6: Schematic Model of LFR CSP System (Source: U.S. Dept of Energy, 2013).

A pictorialmodel of a LFR CSP system is also shown in Plate 2.3.

Plate 2.3: Pictorial Model of LFR CSP System (Source: The Solar Eclipse, 2016).

2.4.4 Parabolic Trough Concentrator Technology

The most matured CSP technology is the Parabolic Trough Concentrator**(**PTC), and accounting for approximately 88% of existing CSP plants (Moser *et al*., 2013).The PTC is made of long U-shaped mirrors with a linear axis tracking system, which reflects direct solar radiation unto an absorber tube along its focal line. The absorber tube is made of steel with selective coating, or aluminium in more recent designs, with the entire tube enveloped in an evacuated glass tube. A schematic model of PTC CSP system is shown in Figure 2.7.

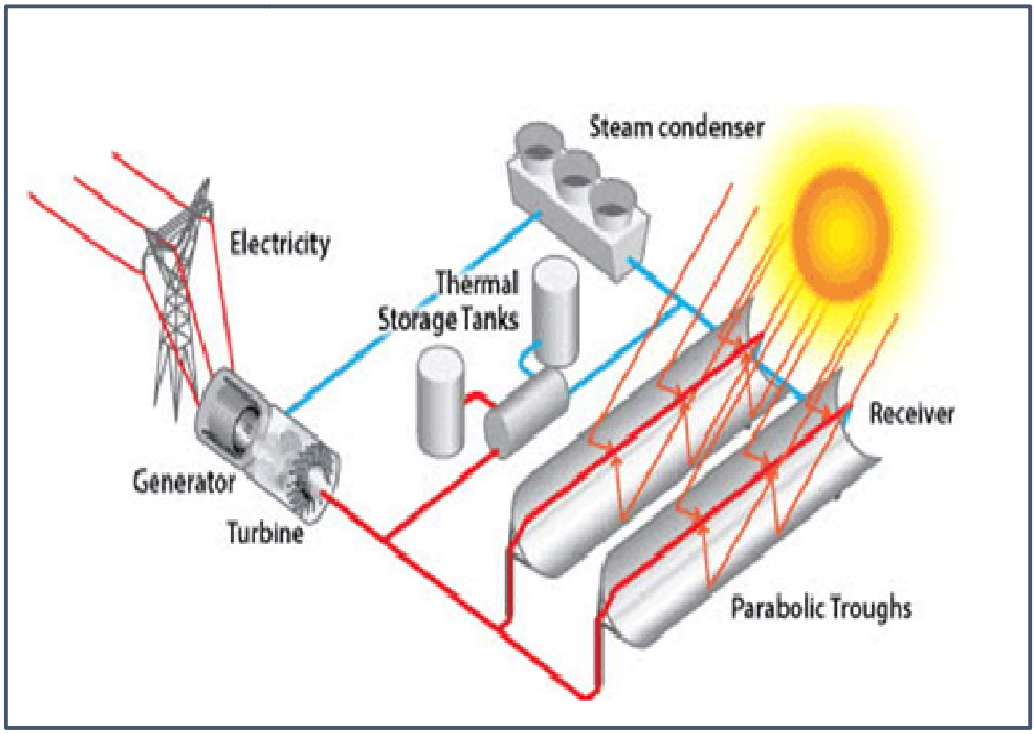

Figure 2.7: Schematic Model of PTC CSP System (Source: U.S. Dept of Energy, 2013).

A pictorialmodel of PTC CSP system is also shown in Plate 2.4.

Plate 2.4: Pictorial Model of PTC CSP System (Source: DLR, 2015).

The coating and enveloping of the steel absorber facilitate high absorbance of solar radiation and high emittance of heat to effectively raise the temperature of the HTF that flows through the tube. The heated HTF generates steam at a temperature of about 350 to 550^{o}C in a heat exchanger, and the steam discharged to a conventional Rankine cycle turbine to generate electricity (Trieb*et al*. 2009). A PTC CSP plant is usually designed to collect more radiation than the turbine can accept so that the excess could be channelled towards heating up the TES system. This is to ensure that the TES system provides the required thermal energy for the turbine when solar radiation is either low or unavailable. The operation of commercial PTC CSP plants spans over 20 years; the technology has largely matured over time, making it the most common CSP technology globally. As at 2019, PTC CSP plants accounted for 4952.05 MW of the 6442.45 MW, representing 76.87%of total operational CSP plants, which indicates its acceptance as the dominant CSP technology. It also accounts for1083 MW of the 1559 MW CSP plants projects and 214 MW of the 1816 MW of CSP plants under development (pre-construction stage with signed agreement).PTC thus constitute 69.5% and 12% of CSP plants under construction and those under development respectively. Moreover, the failure rate of PTC CSP plants is relatively low as it accounts for only 51.96 MW of the 403.96 MW (12.7%) CSP plants that are non-operational globallyas highlighted in Table 2.1 (NREL, 2020). The PTC technology is gradually becoming competitive with conventional thermal power plants (World Bank ESMAP, 2011).It could thus be considered as the preferable CSP option for large-scale/on-grid electricity generation in Nigeria.

Table 2.1: Global CSP Projects

Technology	Operational (MW)	Under Construction (MW)	Under development (MW)	Non-Operational (MW)
PTC	4952.05	1083	214	51.96
LFR	217.4	16	50	106
CRS/PT	1253	460	1552	243
DE	-	-	-	3
Total	**6442.45**	**1559**	**1816**	**403.96**

Source: NREL, 2020.

2.4.5 CSP Thermal Energy Storage

The Thermal Energy Storage (TES) could be grouped into three broad categories, which are:(i) sensible, (ii) latent heat, and (iii) thermo-chemical storages (Lovegrove and Pye, 2012). Sensible storage involves the heating and cooling of a material that does not result into phase change, latent heat storage is the melting and freezing of high-temperature phase-change materials, while thermo-chemical storage involves reversible chemical reactions used to store and discharge energy. The leading method of TES is the utilisation of molten-salt in a two-tank (hot and cold molten $NaNO_3$-KNO_3)based on the principle of heat transfer. A schematic diagram of a typical CSP TES is shown in Figure 2.8.

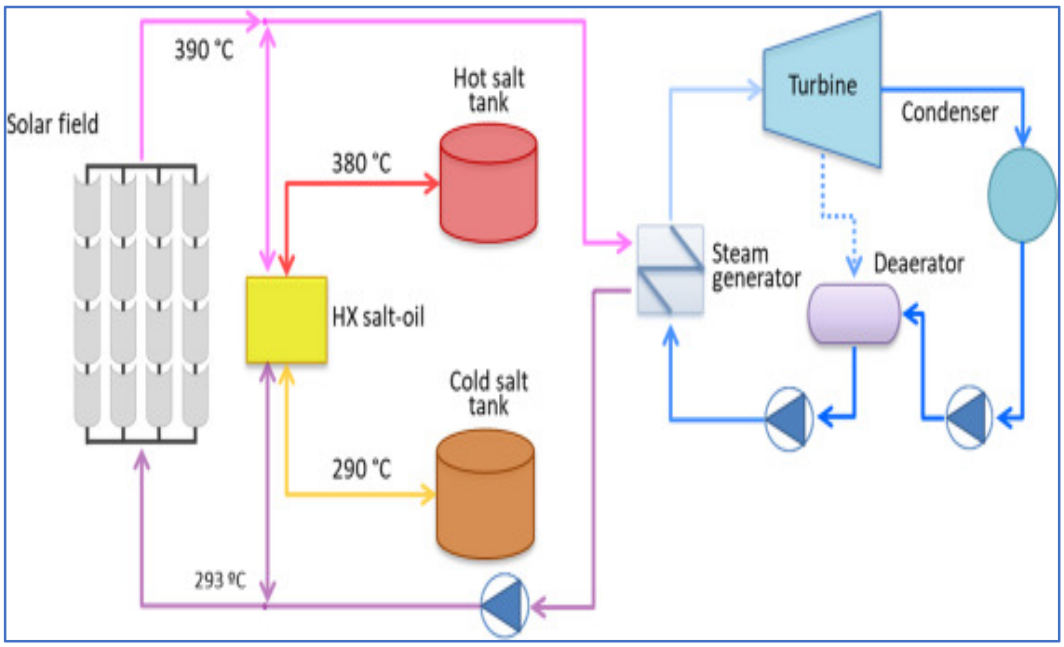

Figure 2.8: Schematic Diagram of TES System (Source: Walczak et al., 2018).

A pictorialmodel of a TES system is also shown in Plate 2.5.

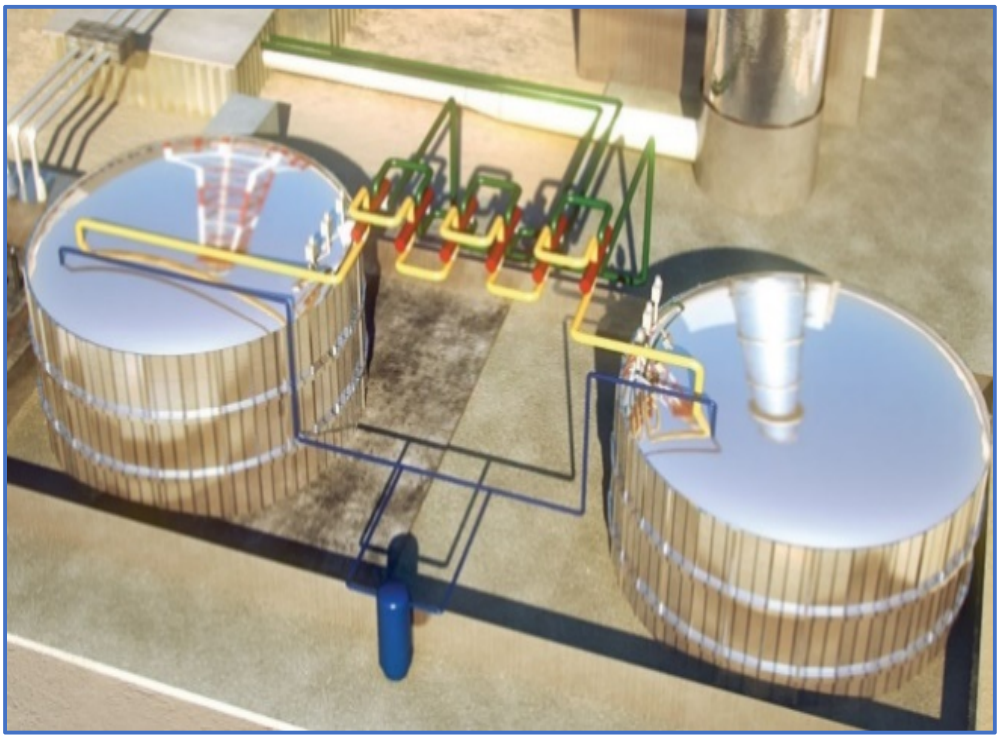

Plate 2.5: Pictorial Model of TES System (Source: Freund et al., 2021).

2.4.6 CSP Power Block

The final phase of a CSP plant is the power block where heat energy is converted into electricity by a turbine. Three major types of turbines are applicable in a CSP system. These are:(i) gas turbines, (ii) Stirling engines, and (iii) steam turbines (Lovegrove and Pye, 2012). Gas turbines operate based on the Brayton cycle, as employed in jet engines and turbogenerators of gas turbine power stations.In the Brayton cycle, solar heat is used to raise the temperature of compressed air to about 1,000°C for the turbine to operate efficiently. Such a temperature is only feasible in Central Receiver System (CRS) and Dish Engine CSP system, which are yet to attain large-scale deployment for electricity generation.The Brayton Cycle is depicted in Figure 2.9.

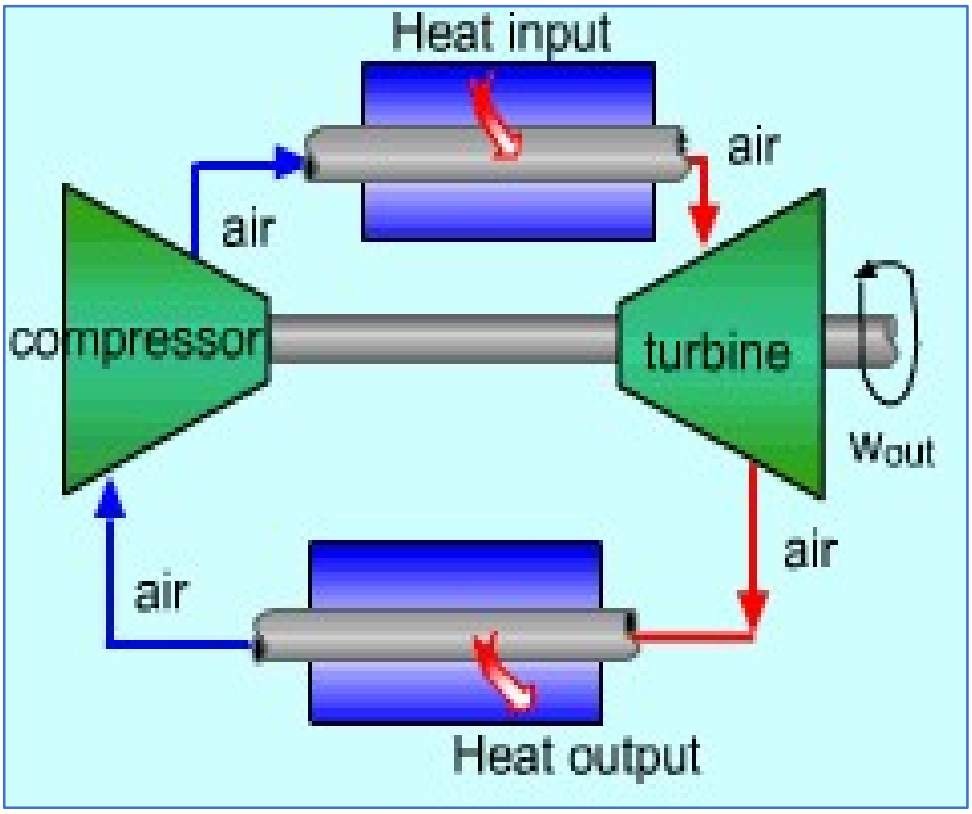

Figure 2.9: Schematic Diagram of Brayton Cycle (Source: Kaushik et.al, 2017).

Stirling engines are externally heated engines with reciprocating pistons operating on a fixed, enclosed amount of gas such as hydrogen, helium or air as its working fluid. The mounted Stirling engines comprise a receiver, engine and generator, positioned at the focus of the Dish Engine. The power generated by Stirling engines is usually in the kWerange;hence, they are only suitable for small-scale CSP applications. A typical example of Stirling engines in CSP are those mounted on Dish Engine. A typical Stirling engine mounted on a Dish Engine is shown in Figure 2.10.

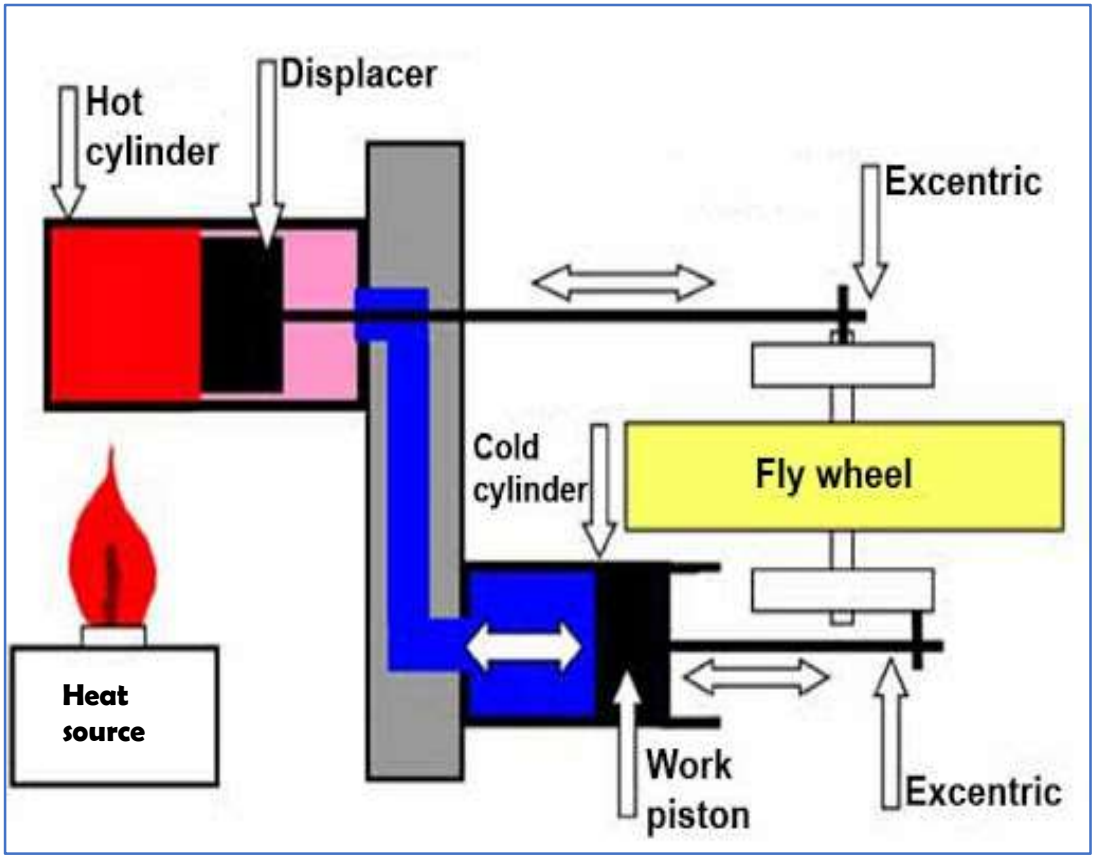

Figure 2.10: Schematic Diagram of Stirling Engine (Source:http://ridders.nu/Webpaginas/pagina_ervaringen_tips_stirlings/ervaringenstirlings_frametekst_engels.htm, 2021)

Steam turbines generate electricity by converting thermal energy of steam generated in a boilerinto mechanical energy using heat energy from an external source.There are two categories of steam turbines:(i) Rankine cycle (RC) and (ii) Organic Rankine cycle (ORC) turbines. The RC turbine expands the steam generated through an external heat source, in a boiler, to produce useful work while the excess steam is condensed for re-use in the cycle. The schematic diagram of a RC is shown in Figure 2.11.

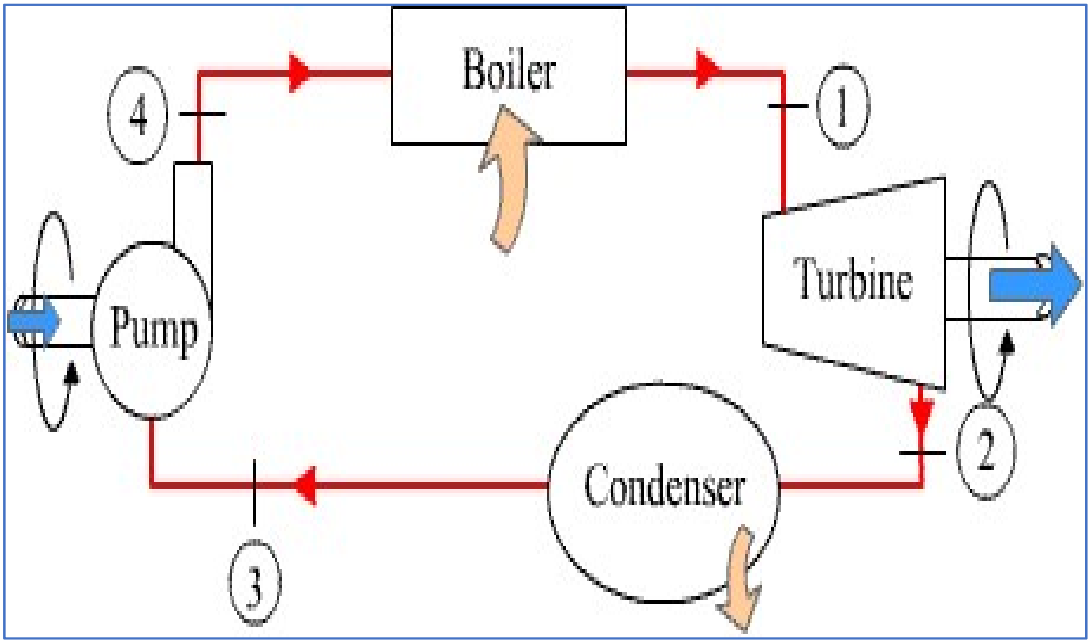

Figure 2.11: Schematic Diagram of Rankine Cycle (Source: Hussain and Maathe, 2014).

The ORC is very similar to the RC turbine, but less complex in configuration; it has a lower operating temperature and uses high complexity fluids such as refrigerants that allows for relatively lower temperature drops during the expansion process. They are rarely powered by fossil fuels and are only applicable in systems utilising low heat sources such as geothermal plants, biomass plants, waste heat recovery systems and small-scale solar thermal plants. Although, the efficiency of the ORC is lower than that of the conventional RC, it is considered a superior technology for low and medium heat sources or applications, due to the thermodynamic property of the working fluid that has higher heat retention capacity in comparison to steam (Astolfi, 2018). The schematic diagram of a typical ORC is shown in Figure 2.12.

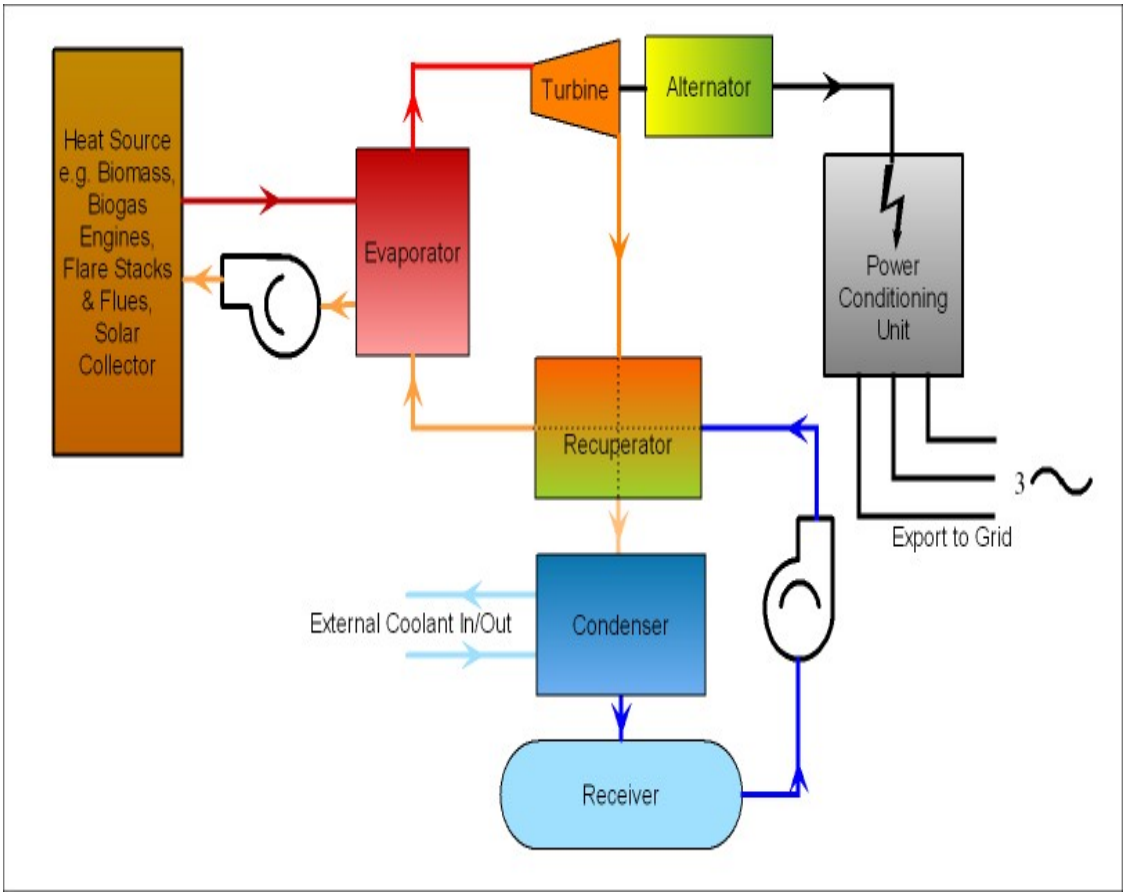

Figure 2.12: Schematic Diagram of Organic Rankine Cycle

(Source: https://www.zeintlplc.com/?page_id=46#, 2021).

Generally, steam turbines have the widest application amongst the various turbines employed for electricity generation, including CSP electricity generation.It is adaptable for all the concentrators employed for electricity generation through CSP. Steam engines could thus be a preferable option for CSP plants in Nigeria due to its versatility.

2.5 Theoretical Review on Thermal Performance of Concentrated Solar Power

CSP basically works on the principles of solar radiation, optics and heat transfer. These principles shall subsequently be examined.

2.5.1 Solar Radiation

Solar radiation incident on the earth contains energy. The total energy contained in the solar spectrum is referred to as the solar constant (G_{sc}). The "solar constant is the solar energy per unit time received on a unit surface area perpendicular to solar radiation's direction of propagation at mean earth-sun distance outsidethe atmosphere" (Duffie and Beckman, 2013). The accepted value of Gsc as given by the World Radiation Centre is 1367 W/m^2 or 4.921 MJ/m^2 (Duffie and Beckman, 2013). Total solar radiation, often called Global Horizontal Irradiance (GHI), have both the direct and diffuse components. The cosine of the solar zenith angle (θ_z) establishes a relationship between direct horizontal irradiance andDirect Normal Irradiance (DNI), which is the component required for CSP application. The diffused component is called Diffuse Horizontal Irradiance (DHI), which is the component of GHI affected by atmospheric attenuation, including scattering and absorption (Lovegrove and Stein, 2012). The effect of scattering and atmospheric absorption on direct irradiance is shown in Figure 2.13.

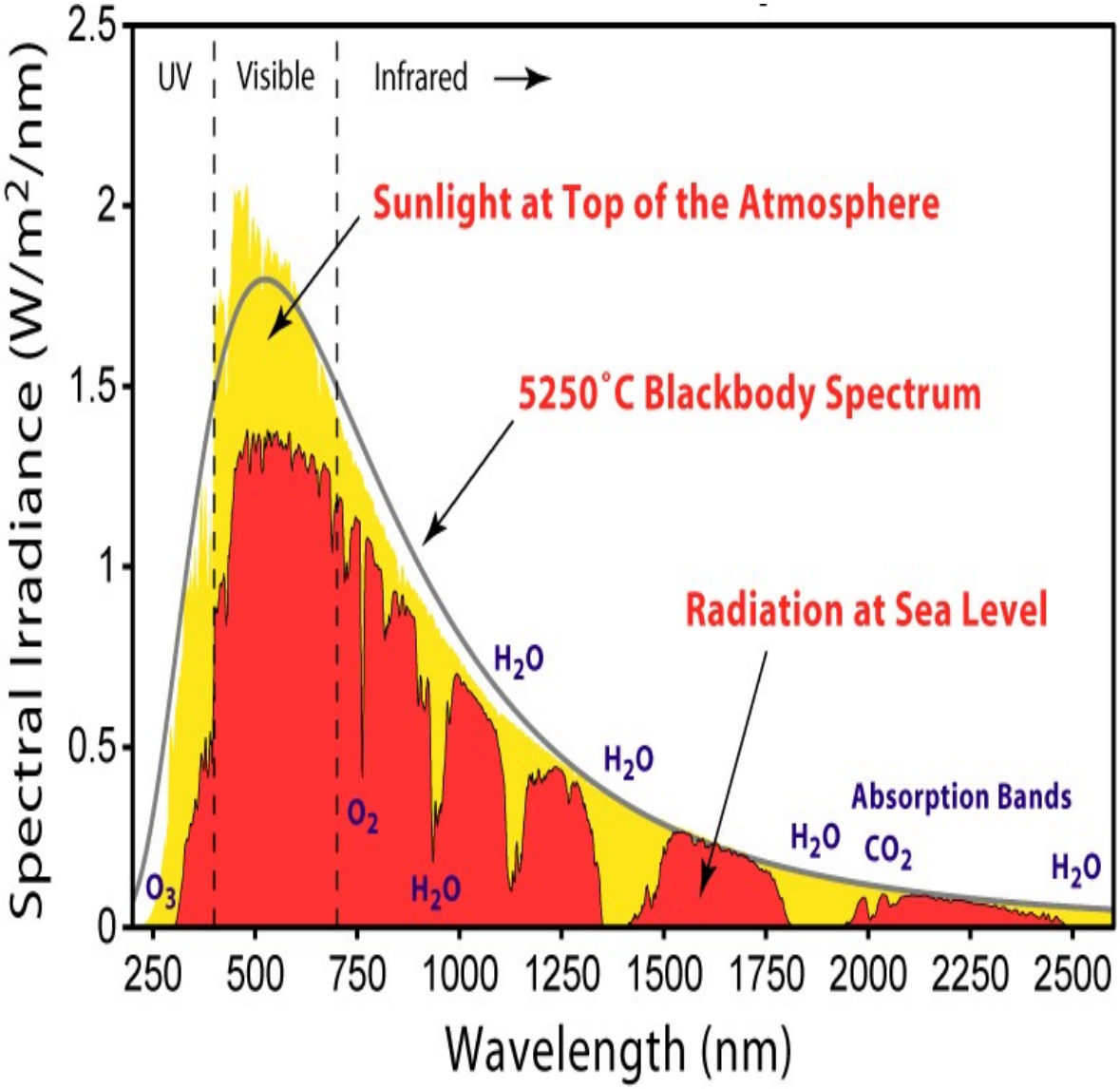

Figure 2.13: Effect of Scattering and Absorption on Direct Irradiance (Source: Mazzi, 2017).

In determining solar energy at specific locations on the earth, it is necessary to describe the position of the Sun relative to a fixed or moving plane by means of various angles including latitude (Ø), declination (δ), slope (β), surface azimuth angle (γ), hour angle, incident angle (θ), zenith angle (θ_z), solar altitude angle (α_s) and solar azimuth angle (γ_s) as indicated in Figure 2.14. These angles are necessary in determining the geometric factor (R_b) which is the ratio of direct radiation on a tilted plane to that on a horizontal plane. The geometric factor (R_b) is given as:

$$R_b = \frac{G_{bT}}{G_b} = \frac{G_{bn}\cos}{G_{bn}\cos\ _z} = \frac{\cos\theta}{\cos\theta_z} \quad (2.1)$$

where G_{bT} is the direct radiation on an inclined plane, G_b is direct radiation on a horizontal plane, and G_{bn} is direct radiation on a normal plane (Duffie and Beckman, 2013). For a flat plate collector on a horizontal plane,

$$\cos\ \theta = \sin\ \delta \sin\ \emptyset \cos\ \beta - \sin\ \delta \cos\ \emptyset \sin\ \beta \cos\ \gamma + \cos\ \delta \cos\ \emptyset \cos\ \beta \cos\ \omega + \cos\ \delta \sin\ \emptyset \sin\ \beta \cos\ \gamma \cos\ \omega + \cos\ \delta \sin\ \beta \sin\ \gamma \sin\ \omega \quad (2.2)$$

$$\cos\theta_z = \cos\emptyset \cos\delta \cos\omega + \sin\emptyset \sin\delta \quad (2.3)$$

For a concentrator that rotates on a horizontal East-West axis with continuous tracking,

$$\cos\theta = (1 - \cos^2\delta \sin^2\omega)^{0.5} \quad (2.4)$$

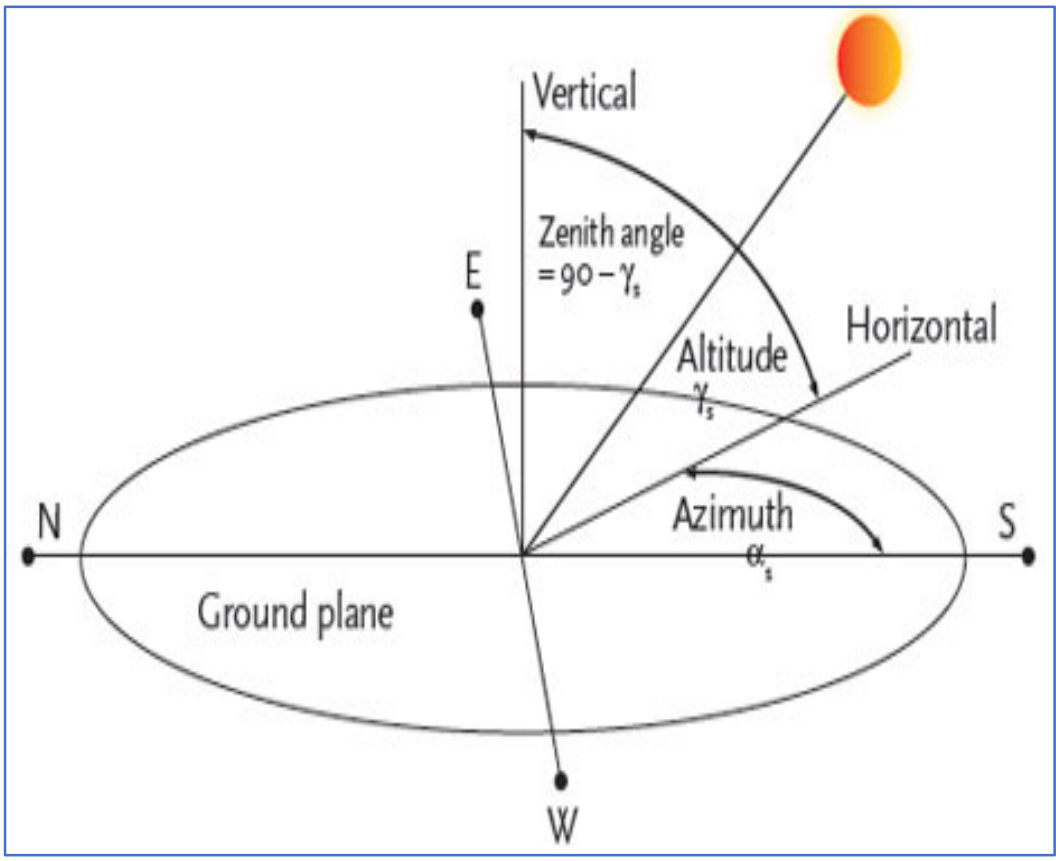

Figure 2.14: Representative Solar angles(Source: Duffie and Beckman, 2013)

The general relationship between GHI, DNI and DHI is given as:

$$GHI = G_b + G_d = \frac{DNI}{\cos_{\ z}} + DHI \quad (2.5)$$

where G_b is the direct horizontal irradiance, G_d is the diffused horizontal irradiance and θ_z is the solar zenith angle (Lovegrove and Stein, 2012). The uncertainty level of the calculated GHI is estimated at ±2 %and ±1 % when the atmosphere is cloudy and clear respectively (Vignola, 2012). The cloudiness or otherwise of an area largely determines the interplay between the variables in Equation (2.5). When it is completely cloudy, the value of G_b is approximately zero while the values of DHI and GHI are nearly equal, indicating a diffuse fraction of approximately one. However, when it is very sunny,the value of DHI is usually between 10 % and 20% of the value ofGHI, indicating a potential high value of G_b and DNI. Locations with a high level of clearness index of the sky would thus have a relatively high level of DNI (Vignola, 2012).

The daily average diffuse radiation H_d (Sawaqed*et al*. 2005), is given as:

$$\mathrm{H_d} = \mathrm{H}\{0.775 + 0.00653(\omega_s - 90) - [0.505 + 0.00455(\omega_s - 90)]$$
$$\cos(115\mathrm{K_T} - 103)\} \quad (2.6)$$

Where

$$\mathrm{K_T} = \frac{\mathrm{H}}{\mathrm{H_0}} \quad (2.7)$$

and$\mathrm{K_T} = \text{Clearness Index}$

$\mathrm{H} = \text{Daily radiation on a horizontal surface } (\mathrm{KJm^{-2}day^{-1}})$

$\mathrm{H_0} = \text{Daily extraterrestrial radiation } (\mathrm{KJm^{-2}day^{-1}})$

$\omega_s = \text{Sun hour angle (in degrees)} = \text{acos } (-\tan(\emptyset)\tan(\delta))$

$\emptyset = \text{Latitude of location (in degrees)}$

$\delta = \text{Solar declination angle (in degrees)} = 23.45 \sin [360\ \frac{284+\text{day}}{365}]$

Furthermore, the total hourly solar radiation incident on a horizontal plane, $\mathrm{I_{th}}$ in $\mathrm{Wm^{-2}}$as highlighted in Sawaqed*et al*. (2005) is given as:

$$\mathrm{I_{th}} = \frac{\mathrm{rH}}{3.6} \quad (2.8)$$

where r = ratio total hourly radiation to the total daily radiation, which is expressed as:

$$r = \frac{\pi}{24}(a + b\cos\omega)\left[\frac{\cos\omega - \cos\omega_s}{\sin\omega_s - \frac{\pi\omega_s}{180}\cos\omega_s}\right] \quad (2.9)$$

Where a = 0.4090 + 0.5016 $(\sin\omega_s - 60)$

b = 0.6609 - 0.4767 $(\sin\omega_s - 60)$

$\omega = Hour\ angle\ of\ the\ sun = \frac{360}{24}(h - 120)$

h = Time of the day

The hourly diffuse solar radiation I_d wasobtained fromSawaqed*et al.*(2005) as:

$$I_d = H_d \frac{24}{\pi}\left[\frac{\cos\omega - \cos\omega_s}{\sin\omega_s - \frac{\pi\omega_s}{180}\cos\omega_s}\right] \quad (2.10)$$

From Equation (2.5), total hourly solar radiation was inferred as follows (Sawaqed*et al.*, 2005):

$$I_{th} = I_{bh} + I_d \quad (2.11)$$

where $I_{bh} =$ Beam horizontal irradiance.

In designing solar systems with Sun tracking capability, it is essential to determine the hourly value of the direct solar radiation normal to a surface relative to the direction of the beam (I_{bn}) as:

$$I_{bn} = \frac{I_{bh}}{\cos\theta_z} \quad (2.12)$$

$$\theta_z = \cos\emptyset\cos\delta\cos\omega + \sin\emptyset\sin\delta \quad (2.13)$$

2.5.2 OpticalTheory

The principle of optics highlights three models of light including: wave, particle and ray models. The wave model describes the colour of light in terms of wavelength and the interaction of light with objects of sizes less than or approximately the wavelength of light (Crowell, 2006). The particle model describes the interaction of light with atoms while the

ray model traces the path of light.Light comprises both electric and magnetic fields, which accelerates the electrons emitted by the source of light. The emitted electrons move together to produce a beam of light whose behaviour is governed by two major rules when incident upon a surface. The first rule states that the angle of the reflected ray equals that of the incident ray while the second rule posits that the reflected ray lies in the plane of incidence with the incident ray and the normal or perpendicular line (Crowell, 2006).The interplay of these models could be observed from the propagation of light rays from the sun to its interactions in the atmosphere and behaviour when incident upon thermal concentrators.The reflection of light ray incident on parabolic mirrors to concentrate heat energy or photons at the focal point of the reflective surface for absorption by a receiver is fundamental to this research.

Consider an unpolarised radiation passing from one medium to another with each medium having different refractive indices n_1 and n_2.According to Fresnel's equation (Duffie and Beckman, 2013), reflection of rays perpendicular and parallel to the normal are given by Equations (2.14) and (2.15), respectively:

$$r_p = \frac{\mathrm{Sin}^2(\theta_2 - \theta_1)}{\mathrm{Sin}^2(\theta_2 + \theta_1)} \quad (2.14)$$

$$r_g = \frac{\tan^2(\theta_2 - \theta_1)}{\tan^2(\theta_2 + \theta_1)} \quad (2.15)$$

Reflection of unpolarised radiation as the average of the two components is given as:

$$r = \frac{r_p + r_g}{2} \quad (2.16)$$

Snell's law establishes the relationship between θ_1 and θ_2 as:

$$n_1 \sin\theta_1 = n_2 \sin\theta_2 \quad (2.17)$$

whereθ_1 and θ_2 are the angles of incidence and reflection/refraction respectively. When radiation occurs at normal incidence, θ_1 and θ_2 equals zero and Equations (2.16) and (2.17) together becomes(Duffie and Beckman, 2013):

$$r(0) = \frac{(n_1 - n_2)^2}{n_{1+}n_2} \quad (2.18)$$

When one of the media is air, the refractive index ≈1, and Equation (2.18) translates to:

$$r\,(0) = \frac{(n_1 - 1)^2}{n_{1+}n_2} \tag{2.19}$$

In line with the principle of energy conservation, Equation (2.20) highlights the relationship between incident power and the duo of reflected and transmitted powers:

$$P_i = P_r + P_t \tag{2.20}$$

where$\mathrm{P_i} = \text{Incident power}$, $\mathrm{P_r} = \text{Reflected power}$, and $\mathrm{P_t} = \text{Transmitted power}$

According to Peatross & Ware (2015), the fraction of reflected power, and reflectance in terms of Fresnel coefficients for s- and p- polarised fields are highlighted in Eqns (2.21) and (2.22) respectively:

$$\mathrm{R_s} \equiv \frac{\mathrm{P_r}^{(s)}}{\mathrm{P_i}^{(s)}} = \frac{\mathrm{I_r}^{(s)}}{\mathrm{I_i}^{(s)}} = \frac{\left|\mathrm{E_r}^{(s)}\right|^2}{\left|\mathrm{E_i}^{(s)}\right|^2} = |\mathrm{r_s}|^2 \tag{2.21}$$

$$\mathrm{R_p} \equiv \frac{\mathrm{P_r}^{(p)}}{\mathrm{P_i}^{(p)}} = \frac{\mathrm{I_r}^{(p)}}{\mathrm{I_i}^{(p)}} = \frac{\left|\mathrm{E_r}^{(p)}\right|^2}{\left|\mathrm{E_i}^{(p)}\right|^2} = \left|\mathrm{r_p}\right|^2 \tag{2.22}$$

where $\mathrm{R} = |\mathrm{r}|^2 = reflectance$, $I_r = \text{total reflected intensity}$, and $I_i = t\text{otal incident intensity}$.

$$I_r = I_r{}^{(s)} + I_r{}^{(p)} = R_s I_i{}^{(s)} + R_p I_i{}^{(p)} \tag{2.23}$$

Intensity of a field, I, could be defined as (Peatross & Ware, 2015):

$$I = \frac{1}{2} n \varepsilon_0 c \mathbf{E}_0 . \mathbf{E}_0{}^* = \left[|E_{0x}|^2 + \left|E_{0y}\right|^2 + |E_{0z}|^2\right] \tag{2.24}$$

Thus, the total incident intensity is given as (Peatross & Ware, 2015):

$$I_i = I_i{}^{(s)} + I_i{}^{(p)} = \frac{1}{2} n_i \varepsilon_0 c \left[\left|E_i{}^{(s)}\right|^2 + \left|E_i{}^{(p)}\right|^2\right] \tag{2.25}$$

From Equation (2.20), transmitted power in thes- and p- polarised fields are given in Equations (2.26) and (2.27) as:

$$P_t^{(s)} = P_i^{(s)} - P_r^{(s)} = (1 - R_s) P_i^{(s)} \quad (2.26)$$

$$P_t^{(p)} = P_i^{(p)} - P_r^{(p)} = (1 - R_p) P_i^{(p)} \quad (2.27)$$

Thus, the relationship between transmittance and reflectance, in the s- and p- polarised fields, could also be expressed as:

$$T_s \equiv \frac{P_t^{(s)}}{P_i^{(s)}} = 1 - R_s \text{ and } T_p \equiv \frac{P_t^{(p)}}{P_i^{(p)}} = 1 - R_p \quad (2.28)$$

The transmitted intensity, in terms of the Fresnel coefficients t_s and t_p, is given as:

$$I_t = I_t^{(s)} + I_t^{(p)} = \frac{1}{2} n_t \varepsilon_0 c \left[\left| E_t^{(s)} \right|^2 + \left| E_t^{(p)} \right|^2 \right] \quad (2.29)$$

n_t and n_i are the refractive indices of the propagation media. Since power is a product of intensity and area, transmittance could also be expressed as (Peatross and Ware, 2015):

$$T_s \equiv \frac{P_t^{(s)}}{P_i^{(s)}} = \frac{I_t^{(s)} A_t}{I_i^{(s)} A_i} = \frac{n_t \cos\theta_t}{n_i \cos\theta_i} |t_s|^2 \quad (2.30)$$

$$T_p \equiv \frac{P_t^{(p)}}{P_i^{(p)}} = \frac{I_t^{(p)} A_t}{I_i^{(p)} A_i} = \frac{n_t \cos\theta_t}{n_i \cos\theta_i} \left| t_p \right|^2 \quad (2.31)$$

If θ_t exceeds the critical angle, total internal reflection occurs hence Equations (2.30) and (2.31) would be invalid in such an instance.

Electromagnetic theory aptly explains the travel of light from one point to another. However, this study focusses on the energy content of light as it travels through a medium/media to its destination.Thus, it is essential to discuss the relationship between propagating electromagnetic fields and the energy conveyed through the propagating fields.According to Peatross and Ware (2015), this relationship, describing the connection between electromagnetic field and the energy content of light, was highlighted by Poynting's Theorem, which has its origin from two of Maxwell's equations as highlighted in Equations (2.32) and (2.33):

$$\nabla x E = - \frac{\partial B}{\partial t} \quad (2.32)$$

$$\nabla x \frac{\beta}{\mu_0} = \varepsilon_0 \frac{\partial E}{\partial t} + J \quad (2.33)$$

where E = Electric Field, B = Magnetic Field, J = Current Density, ε_0=Permittivity, and μ_0= Permeability.

Taking the dot product of $\frac{\beta}{\mu_0}$with Equation (2.32) and the dot product of E with Equation (2.33), we obtain:

$$\frac{\beta}{\mu_0} . (\nabla x \mathbf{E}) - \mathbf{E} . (\nabla x \frac{\beta}{\mu_0}) + \varepsilon_0 \mathbf{E} . \frac{\partial \mathbf{E}}{\partial t} + \frac{\beta}{\mu_0} . \frac{\partial \mathbf{B}}{\partial t} = -\mathbf{E}. \mathbf{J} \quad (2.34)$$

By employing the Vector Identity $\nabla . (f \times g) = g . (\nabla \times f) - f . (\nabla \times g)$to simplify thefirst two terms and identifying that the other two terms remaining are the time derivatives of $\varepsilon_0 E^2/2$ and $B^2/2\mu_0$respectively, Poynting's Theorem is obtained as highlighted in Equation (2.35) as:

$$\nabla . (\mathbf{E} x \frac{\mathbf{B}}{\mu_0}) + \frac{\partial}{\partial t} (\frac{\varepsilon_0 E^2}{2} + \frac{B^2}{2\mu_0}) = -\mathbf{E}. \mathbf{J} \quad (2.35)$$

Conventionally, Poynting's theorem is expressed as:

$$\nabla . \mathbf{S} + \frac{\partial}{\partial t} (u_{field} + u_{medium}) = 0 \quad (2.36)$$

where $\mathbf{S} \equiv \mathbf{E} x \frac{\mathbf{B}}{\mu_0}$ = Poynting vector (Irradiance).

$u_{field} = \frac{\varepsilon_0 E^2}{2} + \frac{B^2}{2\mu_0}$ = Energy per volume stored in the electric and magnetic fields.

$\frac{\partial u_{medium}}{\partial t} \equiv \mathbf{E}. \mathbf{J}$ = Power per volume delivered to the medium from the field.

2.5.3 Concept of Heat Transfer in Concentrated Solar Power Systems

In Concentrated Solar Power (CSP) systems, heat is transferred from the sun to a solar concentrator through the process of radiation whereby the sun emits energy as photons or electromagnetic waves (Ganjiet al., 2018). The energy contained in a photon is given as:

$$E = hv \quad (2.37)$$

where h = Planck's constant (6.6256 x 10^{-34}Js) and v = speed of light (Duffie and Beckman, 2013).The wavelength distribution of radiation emitted by a blackbody is given by Planck's law as:

$$E_{\lambda b} = \frac{2\pi h C_0^2}{\lambda^4 \left[\exp\left(\frac{hC_0}{\lambda KT}\right) - 1\right]} \quad (2.38)$$

where $2\pi hC_0 = C_1 = 3.7405 \times 10^8 \mu m4/m^2$ (Planck's first radiation constant) and C_2 =14,387.8 μm K (Planck's second radiation constant).

Stefan-Boltzmann's equation, highlighted as Equation (2.39) below, gives the total energy emitted per unit area by a blackbody (that is a perfect emitter), by integrating Planck's law over the entire wavelength.

$$E_b = \int_0^\infty E_{\lambda b} d\lambda = \sigma T^4 \quad (2.39)$$

where σ = Stefan-Boltzmann constant (5.6697 x 10^{-8} W/m^2 K^4 = 1.381 x 10^{-23} J/K) and T = source temperature in degrees Kelvin. Duffie and Beckman (2013) provided a simplified method of calculating blackbody radiation through Planck's law and Stefan-Boltzmann equation by integrating Equation (2.39) from zero to λ as highlighted in Equation (2.40) below, to obtain the value of energy from the blackbody radiation between the ranges of zero to λT as:

$$F_{0-\lambda T} = \frac{E_{0-\lambda T}}{\sigma T^4} = \int_0^{\lambda T} \frac{C_1 d(\lambda T)}{\sigma(\lambda T)^5 \left[\exp\left(\frac{C_2}{\lambda T}\right) - 1\right]} \quad (2.40)$$

Since the Sun is not a blackbody and losses occur during the radiation and collection of solar energy, it is expedient to determine the collector efficiency factor (F'), loss coefficient (U_L) and the collector heat removal factor (F_g) to determine the approximate usable energy(Duffie and Beckman, 2013). Considering a linear concentrator fitted with cylindrical absorbing tube surrounded by transparent covers,

$$Q_{loss1} = \frac{2\Pi k_{eff} L}{\left(\frac{D_r}{D_{ci}}\right)}(T_r - T_{ci}) + \frac{\Pi D_r L\sigma(T_r^4 - T_{ci}^4)}{\frac{1}{\varepsilon_r} + \frac{1-\varepsilon_c}{\varepsilon_c}\left(\frac{D_r}{D_{ci}}\right)}} \quad (2.41)$$

$$Q_{loss2} = \frac{2\Pi k_c L}{\ln\left(\frac{D_{co}}{D_{ci}}\right)}(T_{ci} - T_{co}) \quad (2.42)$$

$$Q_{loss3} = \Pi D_{co} L h_{sr}(T_{co} - T_o) + \varepsilon_c \Pi D_{co} L\sigma({T_{co}}^4 - {T_{sky}}^4) \quad (2.43)$$

where L = collector length, T_r = heat transfer from receiver, T_{ci} = heat transfer to the inside of the cover, T_{co} = heat transfer through the cover, T_{cr}, T_{sky} = heat transfer to the surrounding. Note that the subscript r represents the receiver, while ci and co represent the inner and outer cover of the receiver.K_c is the cover thermal conductivity, K_{eff} = effective conductivity for convection between receiver and the cover, h_{sr} = heat transfer coefficient:

$$h_{sr} = \frac{8.6v^{0.6}}{L^{0.4}} \quad (2.44)$$

At average wind speed (5m/s), and characteristic length of 8m, $h_{sr} \approx 10$ W/m^2 K.

$$\frac{k_{eff}}{k} = \max\left[1, 0.386\left(\frac{(P_r X R_{a*})}{0.861 + P_r}\right)^{1/4}\right] \quad (2.45)$$

$$R_{a*} = \frac{\left[\ln\left(\frac{D_o}{D_i}\right)^4\right]}{L^3({D_i}^{-3/5} + {D_o}^{-3/5})^5}(R_a L) \quad (2.46)$$

where R_a and P_r are the Rayleigh number and Prandtl number respectively. R_a and P_r enables the correlation of free convection heat transfer data. Nusselt number (Nu) could also be used for this correlation and the three parameters are defined as:

$$R_a = \frac{g\,\beta\,\delta T\,L^3}{v\alpha} \quad (2.47)$$

$$P_r = \frac{v}{\alpha} \quad (2.48)$$

$$Nu = \frac{hL}{k} \quad (2.49)$$

where h = heat transfer coefficient, L = distance between inner and outer cylinders, k =

thermal conductivity, g = gravitational constant, β = volumetric coefficient of expansion (β =1/T for ideal gas), δT = temperature difference between inner and outer cylinders, v = volumetric viscosity, and α = thermal diffusivity. The range of correlation of R_{a*} is given as:

$$R_{a*} \leq 10^7 \quad (2.50)$$

$$\text{At } R_{a*} \leq 100,\ K_{eff} = k \quad (2.51)$$

This implies that heat transfer is by conduction only, with convection completely suppressed. Thermal loss(Q_{loss}) cou1d be determined by first estimating T_{co} to determine the value closer to T_{ci} than T_r. Then, Equation (2.43) is calculated and substituted in Equation (2.42) to obtain an estimate of T_{ci}.Equation (2.41) is then used to confirm the initial guess of T_{co} by comparing Q_{loss} in Equation(2.43) with that obtained in Equation (2.41) (Duffie and Beckman, 2013).

The heat capacity of a substance, either at constant volume or pressure, could be expressed as:

$$C_v \equiv \left(\frac{\partial U}{\partial T}\right)_v \quad (2.52)$$

$$C_p \equiv \left(\frac{\partial H}{\partial T}\right)_p \quad (2.53)$$

where C_v = Constant volume heat capacity, C_p = Constant pressure heat capacity, U = Molar or specific internal energy, and H = Molar or specific enthalpy.

It was earlier mentioned that the effects of heat transfer, could be highlighted in three categories: sensible heat effects, latent heat effects and thermochemical heat effects. Sensible heat effect connotes heat transfer to a system resulting in change of temperature of the system without any corresponding phase transition, chemical reaction and change in composition.For a homogenous system with its specific internal energy expressed as a function of temperature and specific volume$U = U(T, V)$ where:

$$dU = \left(\frac{\partial U}{\partial T}\right)_v dT + \left(\frac{\partial U}{\partial V}\right)_T dV \quad (2.54)$$

Relating Equation (2.52) and (2.54):

$$dU = C_v dT + \left(\frac{\partial U}{\partial V}\right)_T dV \quad (2.55)$$

For a process with constant volume or if the internal energy is independent of volume, $\left(\frac{\partial U}{\partial V}\right)_T dV = 0.$

$dU = C_v dT$

hence,

$$\Delta U = \int_{T1}^{T2} C_v dT \quad (2.56)$$

If the process is mechanically reversible, Heat Q is defined as $Q = \Delta U$.Hence, heat is given as:

$$Q = \Delta U = \int_{T1}^{T2} C_v dT \quad (2.57)$$

Furthermore, molar or specific enthalpy as a function of temperature and pressure i.e., $H = H(T, P)$, is defined as:

$$dH = \left(\frac{\partial H}{\partial T}\right)_p dT + \left(\frac{\partial H}{\partial P}\right)_T dP \quad (2.58)$$

Using Equation (2.53), we have

$$dH = C_p dT + \left(\frac{\partial H}{\partial P}\right)_T dP \quad (2.59)$$

For a process with constant pressure or if the enthalpy is independent of volume, as in ideal gases, then:

$$dH = C_p dT \quad (2.60)$$

$$\Delta H = \int_{T1}^{T2} C_p dT \quad (2.61)$$

In a closed system with a mechanically reversible constant-pressure process, where heat transfer is in a steady-flow exchanger, Heat (Q)will be defined as:

$$Q = \Delta H = \int_{T1}^{T2} C_p dT \qquad (2.62)$$

Latent heat is synonymous to heat transfer resulting in phase change without change in temperature. Its effect is observed either when a solid substance is liquified, or a liquid substance is vaporised at constant pressure, with heat transfer occurring without change in the temperature of the substance. These effects are referred to as the latent heat of fusion and latent heat of vaporisation, respectively. Additionally, if a substance changes from one solid state to another, there are accompanying heats of transition such as in the structural change of rhombic crystalline to monolithic sulphur at a temperature of 95^{o}C (Smith *et al*., 2005). The latent heat in a phase change is solely a function of temperature, given as:

$$\Delta H = T\,\Delta V \frac{dP^{sat}}{dT} \qquad (2.63)$$

where ΔH = Latent heat,
T=Temperature,
ΔV = Accompanying volume change of the phase change,
P^{sat} = Saturation pressure.

Thermochemical effect is the resultant effect of heat transfer on the molecular structure and energy of products and reactants in a chemical process. The chemical processis also accompanied by heat transfer, temperature change or both. Thermochemical effects could be grouped into three categories. These are the standard heat of reaction, standard heat of formation and standard heat of combustion.The standard heat of reaction is "the enthalpy change when (a) moles of A, and (b) moles of B in their standard states at temperature T, react to form l mole of L and m moles of M in their standard states at the same temperature T" (Mastronardo& Coronado, 2020). This is represented mathematically as:

$$aA + bB \rightarrow lL + mM \qquad (2.64)$$

A formation reaction involves the combination of different elements to form a single compound while a combustion reaction is the product of the combination of oxygen with another element or compound. The standard enthalpy change of formation, $\Delta H°_{reaction}$, is highlighted in Equation (2.65) while a sample combustion reaction involving a mol of carbon and oxygen is at Equation (2.66) (Libretexts, 2020; Cengel& Boles, 2005).

$$\Delta H°_{reaction} = \sum \Delta H°_{(f)}(products) - \sum \Delta H°_{(f)}(reactants) \quad (2.65)$$

Where

$\Delta H°_{(f)}$= Standard enthalpy of formation

^{o} = A degree signifies that it's a standard enthalpy change.

f = The f indicates that the substance is formed from its elements

$$C + O_2 \rightarrow CO_2 \quad (2.66)$$

It is pertinent to note that in all the various categories of heat transfer discussed, it is impracticable for all of the heat to be converted to work or energy with the most efficient available systems attaining a maximum of 40 % efficiency (Smith *et al*., 2005).

The discourse on heat transfer in this work thus aligns with the second law of thermodynamics which places constraints upon the direction of heat transfer and the attainable efficiencies of heat engines. It highlights the impracticability of a receiver to absorb all the heat energy from a source and the impossibility of extracting all the heat from a hot reservoir to do work in a heat engine. This implies that the solar receiver cannot attain a higher temperature than that of the Sun, and the thermal efficiency of a heat engine can never be equal to 100 %, in line with Kelvin-Planck's statement of the second law of thermodynamics (Al-Shemmeri, 2010; Lovegrove and Pye, 2012) (Figure 2.15).

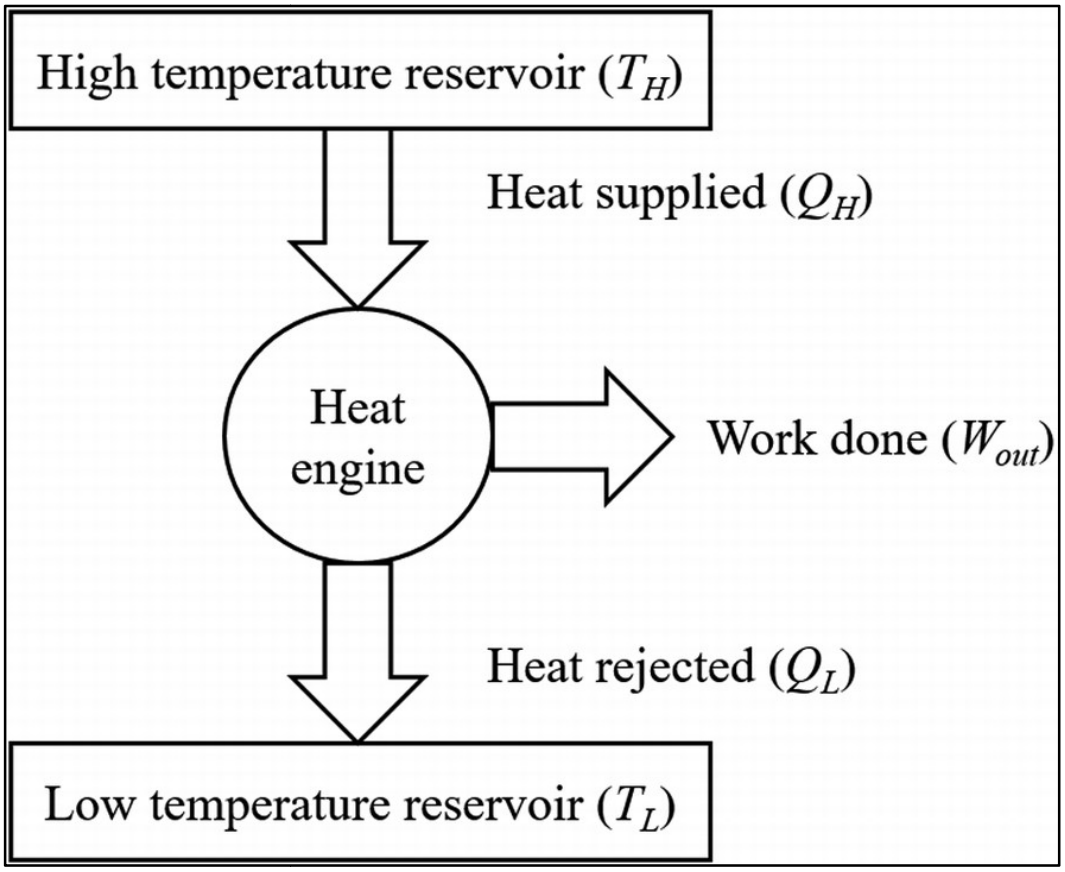

Figure 2.15: Illustration of the Second Law of Thermodynamics (Source: Patel et al., 2019).

The second law of thermodynamics is relevant to this research from the perspective of heat transfer from the Sun to the receiver unit of the CSP system as well as the conversion of thermal energy to electrical energy in the steam turbines of the system.

2.6 Economic and Strategic Review of Concentrated Solar Power System

The economics of energy is largely based on Levelised Cost of Electricity (LCOE), hence the concept of LCOE shall be examined based on some of its derivation methods. The study shall also examine some strategic tools for analysing a project or an organisation such as the political, economic, social and technological (PEST) analytical tool, the political, economic, social, technological, environmental and legal (PESTEL) analytical tool and the strengths, weaknesses, opportunities and threats (SWOT) analytical tool.

2.6.1 Levelised Cost of Electricity

It is very vital to determine the economic profitability of any power plant before embarking on the construction. A tested approach to determining the economic potential of a proposed power plant is the levelised cost of energy (LCOE). The LCOE is the constant per unit cost of energy, which over the system's lifetime will result in a total net present value (NPV) of zero. It is the break-even constant sale price of energy (Lovegrove and Pye, 2012).

$$\mathrm{NPV} = \sum_{i}^{N} \frac{C_i}{(1+DR)^i} \tag{2.67}$$

where, the cash flows C_i are those occurring in time interval *i* (year). DR is the discount rate and N is the total number of compounding periods. From the NPV, LCOE is calculated as:

$$\mathrm{LCOE} = \frac{NPV_{LCC}}{\sum_{i}^{N} \frac{\{E_{annual}\, x\, (1-T)\}}{(1+DR)^i}} \tag{2.68}$$

where, T = tax rate, NPV_{LCC}= net present value of all lifecycle costs, E_{annual} = annually generated electrical energy.

LCOE could also be viewed as an indicator of a balanced pricing of electricity, based on

equality of revenue and cost, including making a return on the capital invested equal to the discounted rate or weighted average cost of capital (WACC). An electricity price above the LCOE signifies a profitable venture while a price below it could indicate an unprofitable investment (IRENA, 2012). A viable approach to assessing the LCOE of a power plant is the discounted cash flow (DCF) analysis, which is based on discounting annual, quarterly or monthly financial flows to a common basis, while considering the time value of money. Based on DCF analysis, LCOE is calculated as:

$$LCOE = \frac{\Sigma^{(I_t+M_t+F_t)}/_{(1+r)^t}}{\Sigma^{N}/_{(1+r)^t}} \quad (2.69)$$

where, LCOE = average lifetime levelised cost of electricity generation, I_t = investment expenditure in the year (t), M_t = operations and maintenance expenditure in the year (t), F_t = fuel expenditure in the year (t), E_t= electricity generation in the year (t), r =discount rate, n = life of the system.

In considering the parameters for LCOE evaluation, the work of Parrado *et al*., (2016) employed the following parameters: total cost of the system in a reference year, land cost, discount rate, operations and maintenance cost, insurance cost, solar resource, tracking correction factor, performance factor, system lifespan and degradation factor. The LCOE was given as:

$$LCOE\ (t) = \frac{C(t)+L+\sum_{i=1}^{T}\left[\frac{C(t)(O\&M+I)}{(1+d)^i}\right]}{\sum_{i=1}^{T}\left[\frac{S.TF.\eta(1-DR)^i}{(1+d)^i}\right]} \quad (2.70)$$

where C (t) = total cost of the installed system in a certain year ($/W), L = land cost ($/W),T = estimated system lifespan (years), O&M = operations and maintenance Cost (%), d = discount rate (%), S = DNI (kWh/m^2/year), TF = tracking factor (%), η = performance factor (m^2/W), DR = degradation rate/factor (%), and I = insurance cost (%).

Equation (2.70) included some other location specific parameters such as DNI, performance factor, tracking correction factor and degradation factor, which are not included in Equation (2.68) for the calculation of LCOE. Zhuang *et al*., (2019) also

included learning rate/coefficient, which is an indication of past evolution of the system cost as a function of the global cumulative installed capacity, as a parameter in the calculation of the total cost of the system, given as:

$$C(t) = C(0)\left(\frac{Q_t}{Q_0}\right)^{\frac{log(1-LR)}{log2}} \quad (2.71)$$

where, $C(0)$ = total cost of the installed system in the reference year ($/W), Q_t = global cumulative installed capacity in a certain year (GW), Q_0 = cumulative installed capacity in the reference year (GW), LR =learning rate (%).

The degradation rate (DR) indicates the annual decrease in the energy output of the system. For a CSP system, DR is estimated as 0.2% (Parrado *et al*., 2016; Zhuang *et al*., 2019). Therefore, the electricity produced in subsequent years is given as:

$$E_i = E_0(1 - \left(\frac{DR}{100}\right)^i \quad (2.72)$$

where, E_0 = electricity produced at the inception of the system, i = respective years.

Furthermore, discount rate which indicates the time value of money and the risk associated with the investment is usually between 10% and 15% for CSP systems but a conservative 10% value is appropriate due to increased maturity of the technology (IEA, 2010, Parrado *et al*., 2016; Zhuang *et al*., 2019). The tracking factor of a 2-axis tracking system such as CRS CSP system is 100% while that of a single-axis tracking system like the PTC CSP is 97.11% (Hernandez-Moro and Martínez-Duart, 2012). Insurance cost was also determined to lie within 0.5-1% but a conservative 0.5% value is appropriate due to increased maturity of the technology. System lifespan is estimated to lie between 25 to 40 years, O&M cost estimated as 2%, while performance factor is given as (Parrado *et al*., 2016; Zhuang *et al*., 2019):

$$\eta = \frac{\text{Electricity produced per installed watt } \frac{kW}{W}}{\text{Utilized solar resource } \frac{kW}{m^2}} \quad (2.73)$$

A major concern about investing in large-scale renewable energy project such as CSP is its capital-intensive nature. However, studies revealed that the cost of CSP projects is

gradually becoming competitive. For instance, Mason and Raitze (2013) highlighted that a monolithic mirror CSP reflector significantly reduces the cost of CSP projects relative to the traditional glass mirrors. Apart from the monolithic coating of the mirror, which has a warranty of 20 years, the SkyTrough reflector uses aluminium space frames in place of the steel used in traditional mirrors. Using the monolithic SkyTrough and Euro Trough 150 CSP reflectors in a comparative study, it was observed that the cost of the SkyTrough was about 36 % lower than that of the Euro Trough. Furthermore, installation costs and LCOE of the Sky Trough were about 34 % and 17 % lower than that of the Euro Trough (IRENA, 2012). Although, the cost of solar thermal plants is still relatively high as shown in Table 2.2 (US DOE, 2017), the need to further diversify the energy mix of the nation's power supply system is essential as a means of enhancing the security of electricity supply. Furthermore, power purchase agreements (PPA) reduced the tariff of the SkyTrough CSP plant at the SEGS II in Dagett California to 6 cents/kWh, hence government support in terms of PPA with an economically suitable Feed-in-Tariff (FIT) for the investors are essential for the deployment of CSP technology in Nigeria.

Table 2.2: Relative LCOE of various Power Plants

Power Plant Type	Cost ($/kWh)
Coal	$0.11-0.12
Natural Gas	$0.053-0.11
Nuclear	$0.096
Wind	$0.044-0.20
Solar PV	$0.058
Solar Thermal	$0.184
Geothermal	$0.05
Biomass	$0.098
Hydro	$0.064

Source: US DoE Annual Energy Outlook, 2017

Projected evolution of LCOE indicates that for DNI levels of 2000 kWh/m^2/year and 2600 kWh/m^2/year, LCOE for CSP projects would decrease from about $300/MWh to $140/MWh and $200/MWh to $100/MWh respectively between 2010 and 2020 (IEA, 2010). Linear relationships could also be observed from 2020-2030 and 2030-2050 as highlighted in Figure 2.16. An observation in Figure 2.16 is an almost linear relationship between 2010 and 2020. Despite decreasing LCOE, CSP projects would require government support in the short term through initiatives such as favourable PPA or feed-in-tariff (FIT) to encourage prospective investors. Such an initiative would also demonstrate Government's commitment to sustainable development in addition to bridging the electricity supply gap in the country.

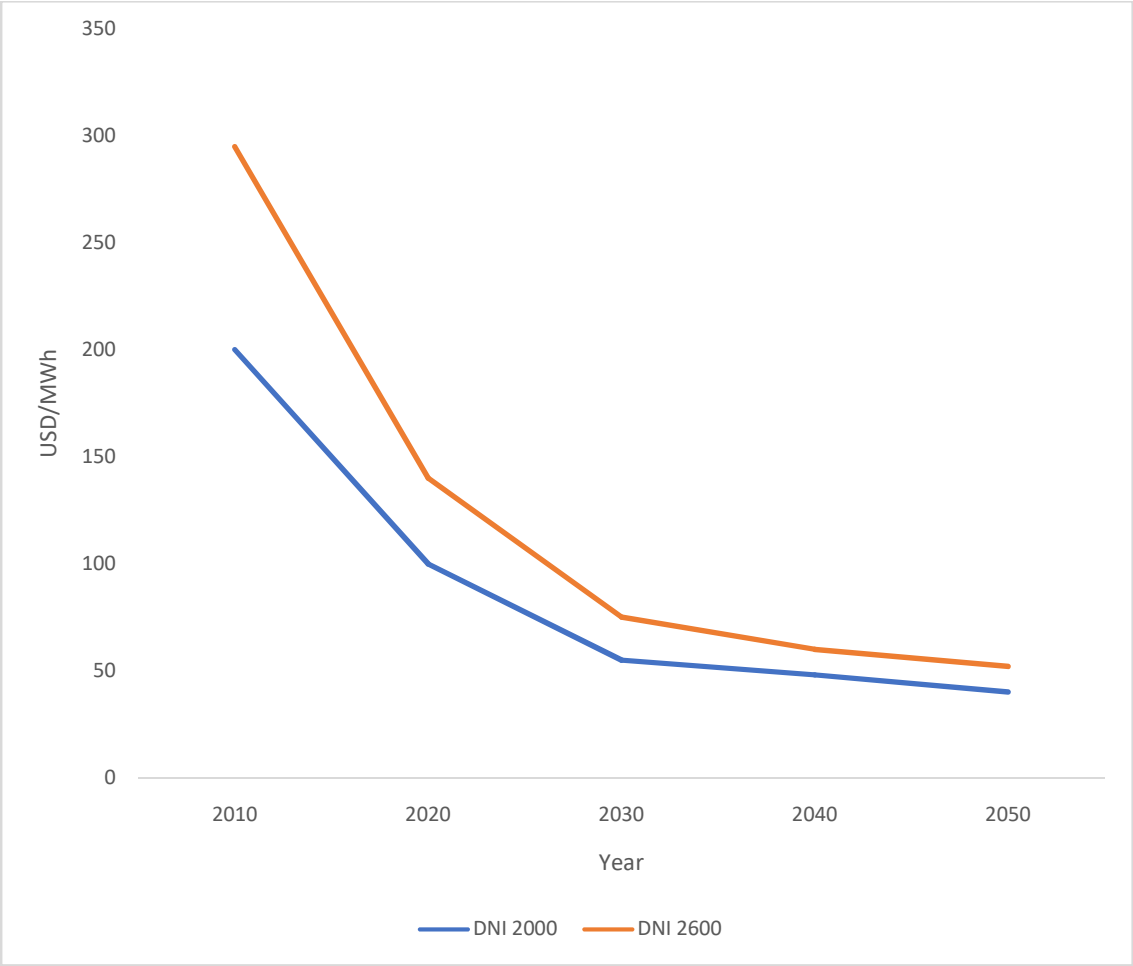

Figure 2.16: Projected Evolution of LCOE (Source: IEA Technology Roadmap CSP, 2010).

2.6.2 PEST/PESTEL Analytical Tool

PEST analytical tool is a framework comprising political, economic, social and technological forces utilised for the analysis of environmental factors (Thompson and Martin, 2006). The political factor covers government interventions and political lobbying activities in socio-economic issues such as tax policy, environmental regulations and merger restrictions. The economic factors cover the macro-economic conditions of the external environment and could involve seasonal or weather factors. Aspects considered under economic factors include GDP, exchange rate, interest rate and inflation rate. The social factors address social, cultural and demographic factors of the external environment and comprises living standards,language, demographics, consumer tastes, standard of education and gender roles. The technological factors comprisetechnological infrastructures,technological changes, technology incentives, and technology-related activities that affect the external environment. Aspects considered under technological factors include technological trends, technology legislation, innovations and breakthroughs, and infrastructure (Ho, 2014).

A similar tool, PESTEL, adds the environmental and legal factors to the PEST tool. Issues to be considered under the environmental factors include climate, recycling procedures, emissions, waste disposal and sustainability while the legal factors would address consumer law, health and safety, employment legislation, international as well as trade regulation and restrictions. A drawback of the PEST/PESTEL analytical tools is the focus mainly on the external environment.However, the outputs of PESTEL analysis could be used as inputs in the opportunities and threats columns in SWOT Analysis (Christodoulou and Cullinane, 2019). The investigation of the factors comprising the PEST/PESTEL analytical tools provides a broader scope of visualising the features that could impact on potential CSP plants in a location or environment.

2.6.3 SWOT Analytical Tool

Gurel and Tat (2017) described SWOT Analysis as a strategic planning framework used in

the evaluation of organisations, plans, businesses or projects.Thompson *et al*., (2006) also viewed it as a "simple but powerful tool for sizing up an organisation's resource capabilities and deficiencies, its market opportunities, and the external threats to its future".Ifediora*et al*., (2014) further posited that it is the most renowned tool for assessing and analysing the overall strategic position of a business or project relative to the operational environment.

SWOT analysis involves the identification of the strengths, weaknesses, opportunities and threats regarding the focus of the analysis. The strengths are the inherent traits that gives advantage over others while the weaknesses are the features that places an entity at a relative disadvantage. Furthermore, opportunities are the external elements that provides an advantage, while threats are the external elements that could jeopardise the functioning of a firm, project or business (Gurel and Tat, 2017). The positions as mentioned above suggests that SWOT analysis would be an effective tool for determining the viability of a project.

SWOT analysis basically helps in identifying the organisational and environmental factors impacting an organisation, business, plan or project. Essentially, it assists in identifying the strategies that will enable the creation of an efficient business model in line with an organisation or project’s resources and capabilities, while also considering the environment in which the organisation or project functions (Ifediora*et al*., 2014). There are two dimensions to SWOT analysis: (i) internal, and (ii) external dimensions. The internal dimension deals with organisational factors, which includes strengths and weaknesses, while the external dimension covers environmental factors comprising opportunities and threats as illustrated in Figure 2.17. The SWOT analysis would thus complement the empirical results obtained for a potential CSP plant thereby facilitating a more comprehensive approach to investment decisions.

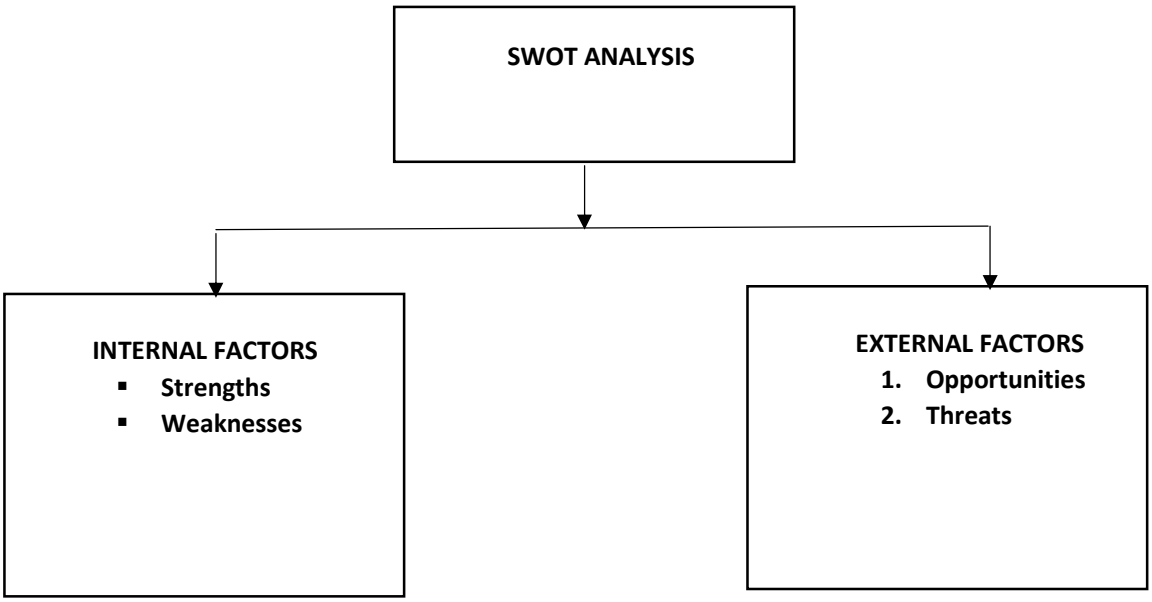

Figure 2.17: SWOT Analysis Framework (Source: Ifediora*et al*., 2014).

SWOT analyses is usually organised into four quadrants or a 2 by 2 matrix.The internal dimensions (strengths and weaknesses) are in the upper quadrants, while the external dimensions (opportunities and threats), and are in the lower quadrants. Additionally, the positive factors (strengths and opportunities) are in the first column while the negative factors (weaknesses and threat) are found in the second column as illustrated in Figure 2.18.

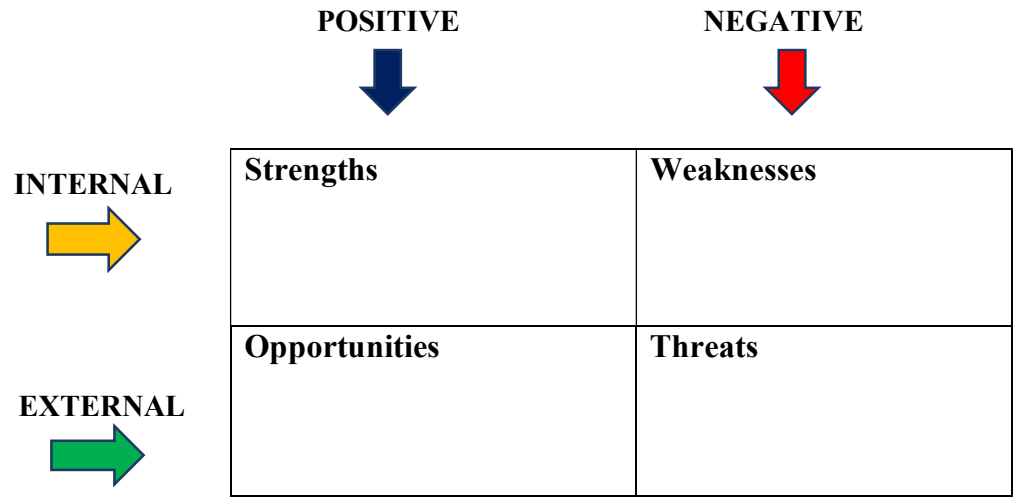

Figure 2.18: Illustration of SWOT Analysis Quadrant (Source: Ifediora*et al*., 2014).

SWOT analysis could be done either by matching strengths against weaknesses and opportunities against threats, or by matching all elements using the 2 x 2 matrix as illustrated in Table 2.3.

Table 2.3: Two-by-Two Matrix SWOT Analysis

	Strengths	**Weaknesses**
Opportunities	Achieve opportunities that greatly match the organisation's or project's strength	Overcome weaknesses to attain opportunities
Threats	Use strength to reduce the organisation's or project's vulnerability to threats	Prevent weaknesses to avoid making the organisation or project more prone to threats

(Source: Chermack and Kasshanna, 2007; Gurel and Tat, 2017).

In the employment of SWOT analysis for this study, internal dimensions shall be viewed as factors within the geographical space of Nigeria, while external dimensions shall be seen as factors outside the confines of the country.

2.7 Methodological Review

Several methods have been employed in previous studies regarding CSP plants. Duffie and Beckman (2013), Ohunakin*et al*. (2013) as well asRaziei and Pereira (2013) employed the Angstrom-Page (AP) model and the Hargreaves-Samani (HS) model, amongst others, either solely or comparatively. The HS and AP models highlights a relationship between irradiation on a horizontal plane and ambient temperature or sunshine duration respectively. Raziei and Pereira (2013) also employed other models such as the Penman-Monteith (PM) model and FAO-PM temperature model, although the work was based on evapotranspiration rate in some locations in Iran. The study however indicated a close relationship between HS model and PM as well as FAO-PM models. Some of the works especially that of Ohunakin*et al*., (2013) indicated that the results obtained from their various studies favoured HS model above other models.

Approaches to the technical analysis of CSP plants could be viewed under two categories:(i) inductive and (ii) deductive analyses/approaches.According to Thomas (2006), inductive analysis entails the derivation of concepts, themes, or a model through the interpretations of raw data by an evaluator or researcher". Deductive analysis, on the other hand, refers to the testing of the consistency of prior assumptions, theories or hypotheses by data analysis. In this research, inductive approach to CSP plant design is viewed as the design of a CSP plant from first principles while deductive approach is the design of a CSP plant using a reference plant(s) or results of previous CSP designs as a guide. The conceptual design and cost assessment of both dry and wet-cooled PTC CSP plants by WorleyParsons Group Inc. based on nominal design specifications by the

National Renewable Energy Laboratory (NREL) USA (Turchi, 2010), could be classified as inductive approach to CSP design. However, most of the available analysis employed the deductive approach since simulations provide avenue for observing the results of different combination of parameters.

A typical example of a CSP plant design using the inductive approach is the component-based cost model PTC CSP hypothetical plant developed by the NREL USA, with assistance from WorleyParsons Group Inc. (an experienced CSP system design and engineering firm), which formed the basis of the NREL System Advisor Model (SAM). The model was developed from specified conditions for a representative plant leading to a conceptual design and budgetary cost estimate from WorleyParsons(Turchi, 2010). The firm developed hypothetical wet-cooled and dry-cooled PTC CSP plants by evolving a line-item cost model that could be manipulated by users of SAM model to cater for prevalent indices for other locations that would be considered. The design was based on an Engineering, Procurement and Construction Management (EPCM) project but some typical project costs, notably owner's costs such as land cost, cost of permit, legal fees, survey costs, taxes etc., were observed to have been omitted. However, the omissions were considered as indirect costs in the NREL SAM model due to their importance in determining the LCOE.

The deductive approach was employed by Sharma *et al*. (2015) in the design of a 50 MW CSP plant for each of eight different locations in India using the PTC and LFR systems. The work was based on determining the optimal mix of design DNI, solar multiple and TES that gave the highest capacity factor with the least LCOE based on simulations using the NREL SAM. The annual DNI values of the locations ranged between 2085 kWh/m^2 and 2248 kWh/m^2 (~5708 Wh/m^2/day to 6155 Wh/m^2/day), similar to values obtainable in northern Nigeria. The study revealed that the lowest LCOE was obtained at solar multiples between 1.4–1.6 for PTC-based systems. The study further revealed that minimum LCOE was obtained at design DNI values ranging from 550 - 700 W/m^2 for the same system.The concept of LCOE has been employed in several works (Parrado *et al*., 2016; Sharma *et al*., 2015; Ohunakin*et al*., 2013), although different authors were observed to have used different approaches to the concept. Parrado *et al*. (2016) were of the view that the most suitable approach to determining LCOE for CSP and PV plants is the lifecycle cost method. Sharma *et al.* (2015) however employed the annual cost and capital recovery

factor approach while the work of Lovegrove and Pye (2012), employed the net present value approach to determining LCOE.

Bishoyi and Sudhakar (2017) employed the deductive approach in the design of a 100 MW PTC CSP plant in Udaipur, India. The study used a typical meteorological year 2 (TMY2) dataset as the database of the SAM NREL model, to simulate the energy output, LCOE, system efficiency and capacity factor of the hypothetical plant.However, the study did not state whether the satellite-based data used for simulation were validated through any other means. Furthermore, the study divided its method of selecting potential sites into two phases, using the minimum DNI value of 1800kWh/m^2/year for CSP power generation as the sole criteria for the first phase while the second phase involved the consideration of other parameters including land, water, communication and grid connectivity amongst others.The second phase also involved the simulation of outputs from the locations investigated. Although, DNI is the most important criteria in CSP deployment, it wasconsidered more desirable to include other important parameters at the initial phase, perhaps using a weightedapproach, to give a more realistic potential of the site under consideration.

2.8 Review of Empirical Literature

A study on the utilisation of a 2 MW LFR CSP plant for electricity generation in Spier Estate, South Africa was conducted in 2011. Some of the criteria considered for the plant's deployment include capital cost, LCOE, operation, and maintenance (O&M) cost. Other factors are potential for development, maturity of technology, minimal risks to soil contamination and fire explosion, and low system complexity (Lubkoll, 2011).

While most of these criteria are considered universal for CSP application, LCOE offers a more holistic picture of the economic viability of power plants, including CSP. Furthermore, the decision to utilise LFR CSP plant could have been dictated by the relatively low capacity of the plant in addition to its lack of a storage system as LFR plants have relative technical simplicity which allows high local value gain (Breeze, 2016). Furthermore, it utilises DSG which utilises water thereby reducing environmental risks in the event of fluid leakage (NREL, 2010). LFR technology are not adaptable for large scale electricity generation.

PTC CSP is the dominant technology for large-scale generation of electricity.Some prominent PTC plants are the 354 MW Solar Energy Generating System (SEGS) plants in California (Nixon*et al*., 2010) and the 360 MWNoor I and II plants in Morocco.The Noor I and II PTC CSP plants, with an additional 150 MW PT Noor III CSP Plant, are collectively the largest CSP plant in the world (NREL, 2020). It is also worth noting, that PTC CSP plants can be employed for both small and large-scale electricity generation. Small-scale CSP applications may utilise an ORC-based turbine due to higher efficiencies at lower temperatures. However,large-scaleCSP systems usually utilise a RC steam turbine operating at temperatures above 400°C (Lubkoll, 2011).

Studies have revealed that there is usually a disparity in satellite – based measurements of solar radiation with that of ground-based measurements (Olomiyesan and Oyedum, 2016; Ernst *et al.*, 2016).These disparities are attributable to aerosols, clouds, water vapour and terrain, which may be examined individually or collectively under the term "clearness index" (Sengupta *et al.*, 2018). While satellite-based data may be acceptable for small and medium-sized solar projects, it is usual to validate satellite-based data with ground-measured data at the specific site of the project for large-scale CSP plants; a process referred to as site adaptation (Polo *et al.*, 2016).

Satellite-based solar data is an integral over an area while ground-based solar data gives pinpoint measurements (Cebecauer and Suri, 2016). This leads to a mismatch when comparing the values obtained from the two observation instruments. For CSP projects, the pyrheliometer or alternatively a Rotating Shadowband Radiometer (RSR) used for the measurement of DNI at specific locations is not available at the weather stations in or near the locations investigated.The ground-measured data obtainable from the Nigerian Meteorological Agency (NIMET) is the GHI, which is useful for the planning of solar photovoltaic projects. Since pyrheliometers and RSR are not yet available in Nigeria, it is essential to develop an alternative means of validating satellite based DNI data for large-scale CSP plants.

Telsnig*et al*., (2013) used hourly irradiance data to predict the yield of different PTC plant configurations at two locations, which are Upington and Pretoria in South Africa. The study revealed that technical configurations and LCOE depends largely on a plant's location and the desired employment of the electricity generated. The electricity generated

by a CSP plant is influenced by several factors, particularly the designated or envisaged load in the electricity supply system.This envisaged role could eitherbe the supply of peak demand during daytime, whereby a storage system is not required or the transfer of base-load power into the grid, which may require a storage system. The study also examined the system configurations under three major components: (i) solar field, (ii) storage system, and (iii) power block, as earlier employed by Trieb*et al*., (2009). The work then conducted a cost optimisation for different power plant configurations based on the costs of the highlighted power plant components. It was then revealed that an adequate storage system coupled with a sufficiently large aperture area would translate into high-capacity factor for a CSP plant, although this may also lead to relatively high LCOE.

Raziei and Pereira (2013) studied evapotranspiration rate in some locations in Iran using models such as the Penman-Monteith, Hargreaves-Samani (HS) and FAO-PM temperature models. Evapotranspiration, which is a phenomenon describing the relationship between water balance and energy balance in the atmosphere (Zhao *et al*., 2013), bears a direct relationship with clearness index. The study revealed a close relationship in the results obtained from HS model and FAO-PM temperature models. This relationship suggests that HS model could serve as an effective tool for determining the clearness index of a location and would be worth investigating concerning locations being considered for CSP application in this study.

The work of Ohunakin*et al*., (2012) further highlighted the categorisation of clearness index into three: $K_T < 0.4$ (heavily overcast weather), $K_T \leq 0.4 \leq \leq 0.6$ (partly overcast weather) and $K_T > 0.7$ (clear weather). The work employed sunshine period-based model (Angstrom-Page equation) and two temperature-based models to calculate clearness index of Oshogbo, Nigeria. The study established that the correlation coefficients of the quadratic models were better than those of the linear models. Furthermore, the temperature-based models, particularly the quadratic form of Hargreaves-Samani model, are better suited for predicting the global solar radiation in Osogbo and other similar locations within reasonable level of accuracy. The authors also posited that the results obtained for Oshogbo could be adapted for locations having same latitude and similar altitudes. Since the quadratic models gave better results relative to the linear models, it would be necessary to investigate results of cubic models relative to linear and quadratic models, to determine if accuracy of such models could be enhanced.

Habib *et al*. (2012) posited that some locations in northern Nigeria with DNI values of about 4.1 kWh/m^2/day - 5 kWh/m^2/day are suitable for power generation using CSP. The study indicated that CSP plants are best cited in locations with adequate DNI and with flat terrain, having slope of about 3% or less. It wasdeduced from the study that if only 5% of the land area meeting the 3% slope condition in the 10 states under review are to be used for CSP applications, a total of 10,890 km^2 would be available for CSP application in those ten states collectively, thereby suggesting sufficient and suitable landmass for CSP plants. Thomas (2009) in Black & Veatch (2007) however, gave the ground slope requirement for CSP application as less than 1% while Bravo *et al*., (2007) indicated less than 2% ground slope as suitable for CSP deployment, but further stated that less than 7% gradient could be acceptable for grounds facing South-East to South-West.Using 5% of eligible land in northern Nigeria for CSP plants with an estimated generation of 50MW/km^2, 14 states in northern Nigeria could generate about 427,000 MW (Habib *et al*., 2012).

Ogunmodimu and Okoroigwe (2018) highlighted that DNI values in northern Nigeria varies between 6 kWh/m^2/day – 7.5 kWh/m^2/day, suggesting that the area could be suitable for CSP deployment since it meets the minimum threshold of 1800 kWh/m^2/year (Bishoyi and Sudhakar, 2017) or 1900 kWh/m^2/year (Ogunmodimu, 2012) utilised for CSP deployment.Ogunmodimu and Okoroigwe (2018) also analysed the various CSP technologies by considering operational, environmental and social factors for deployment in Nigeria. The study highlighted that even though PTC is the most expensive technology and relatively requires the largest landmass for deployment, it is the most matured and risk-free technology for short- and medium-term deployment of CSP plants.On the economics of CSP plants, their study identified the relatively higher investment cost of CSP projects in terms of LCOE, compared to conventional plants, with the investment cost accounting for about 80% of the total cost. They also stated that CSP plants have higher return on investment and a shorter payback period. The study further identified the need for environmental impact assessment as well as technical and economic feasibility study before the deployment of a CSP plant in Nigeria, the latter being the focus of this research.

Chhatbar and Meyer (2011) observed that although DNI is the most important parameter for determining the viability of a CSP plant, meteorological parameters including wind, ambient temperature and humidity are also worthy of consideration. They also observed

that months with same average DNI values may not necessarily produce the same energy yield due to variations in DNI frequency distribution. Poor DNI frequency distribution could lead to variation in energy yields within the range of ± 9% for locations with the same annual average of DNI. The study further highlighted that the ratio of annual energy production (AEP) to DNI, for PTC CSP systems, in the northern hemisphere decreases by 10 % for every 10^{o} increase in latitude, while same condition in the southern hemisphere results in 14 % decrease in AEP largely because of winter. The higher level of DNI decrease ratio in the southern hemisphere is thusbeing compensated for, by its higher levels of DNI.

In highlighting the effect of ambient temperature and wind speed on the efficiency of PTC CSP plants, Sabri and Benzirar (2015) indicated that system efficiency could drop by approximately 8 % when ambient temperature rises from 22^{o}C to 28^{o}C, and wind speed increases from 2.7 m/s to6.2m/s.The decrease in system efficiency due to increase in ambient temperature corroborates the fact that DNI levels and not necessarily high ambient temperatures is the predominant factor in determining the viability of a CSP system. The study suggests that the ideal operating temperature for CSP systems is 22^{o}C, which is not significantly different from the 25^{o}C employed as the standard in NREL SAM for simulation purposes. Regarding the wind speed at a PTC CSP site, a 4m/s to 5 m/s daytime velocity at heights of 50m above ground level was observed as the average wind speed at CSP plant locations. Moderate wind velocities have little or no effect on heat loss in CSP systems and could be assumed as zero for simulation purposes(Mittelman and Epstein, 2010).In this study, all the locations have higher wind speeds than 5 m/s. Wind speeds up to 6 and 6.5 m/s that are non-regular will be acceptable since the effect on CSP plants will not be very significant.In view of this fact, all the locations are found suitable for CSP siting.High relative humidity (RH) is known to have corrosion effects on metallic structures used for frame and some other components of a CSP system. It was indicated that the corrosive effect on metals begin to occur at RH of about 80 % (Francis, 2002).It is worth noting that most locations under investigation in this study all have mean monthly RH of less than 80 % except Yelwa with mean RH of about 80% in 4 months and Danbatta also having RH of about 80% in only one month (World Weather and Climate Information, 2019).

Simulation of the solar and other meteorological parameters of a potential site is usually

done prior to the deployment of a CSP plant to determine the viability of such a plant in a proposed location. The NRELSAM is a widely used software for the simulation of renewable energy systems such as CSP. The data used for simulation on SAM for some locations are available in the National Solar Radiation Data Base (NSRDB) in TMY data format. It was however observed that the NSRDB does not contain the TMY data of any location in Nigeria, necessitating the development of TMY data for locations in Nigeria with potential for CSP deployment.

Lovegrove and Pye(2012) defined TMY data format as "an assemblage of hourly data from long-term monthly and/or yearly averages of DNI, ambient temperature, humidity and wind speed to form the data of an artificial year, which caters for unusual or extreme days". It uses the weighted approach to cater for the level of importance of each parameter employed. A typical month is selected by determining the month that has the closest relation to the long-term monthly characteristics of the entire period under consideration, and usually 15 to 30 years but not less than 10 years. The original TMY dataset was developed in 1978 by the Sandia National Laboratories, USA. It comprised data of 248 locations covering the period 1952 - 1975. The TMY then evolved through the TMY2 and the more recent TMY3 comprising data of more than 1400 locations due to continuous update. These locations are mostly in the USA and Europe with some few locations in other parts of the world. The TMY3 data format is unique because it is written in the Comma Separated Value (CSV) format making it readable by several existing applications or programs, unlike the other TMY and TMY2 formats written in unfamiliar algorithms (Wilcox and Marion, 2008). It was observed that no TMY data of any location in Nigeria is available in the NSRDB and this would pose a challenge in the deployment of CSP plants in Nigeria since simulation is essential in determining the viability of locations for CSP plants' siting.

2.9 Summary

The chapter focussed on background to the study as well as the theoretical, methodological and empirical reviews of literature relevant to the study.The CSP system comprises the concentrator, Heat Transfer Fluid (HTF) with its associated mechanism as well as a power block. They are majorly of four different types including (i) Power Tower or Central Receiver System (CRS), (ii) Dish Engine (DE), (iii) Linear Fresnel Reflector (LFR) and (iv) Parabolic Trough Concentrator (PTC); PTC technology being the most matured and

widely deployed technology. The heat obtained through the concentrators are channelled to a power block where the heat is converted to electrical energy.The theoretical aspect focussed on solar radiation, optics and heat transfer theories, while methods examined the inductive and deductive approaches amongst others. Furthermore, the empirical review focussed on studies earlier conducted on CSP, which indicated that CSP is a technology of the present and more importantly the future. This suggests that further studies are required to effectively harness the potential of CSP for power generation towards meeting the energy needs of the future.

CHAPTER THREE
METHODOLOGY

3.1 Preamble

This chapter provides the context within which the research was conducted and sets it in proper perspective for easy understanding. It covers the theoretical framework, research questions, research design, data sources and methods of data analysis.

3.2 Theoretical Framework

The study was based on the solar radiation theory and examined the results of the clearness index of selected locations in northern Nigeria based on two equations:(i) Angstrom-Page, and (ii) Hargreaves-Samaniequations.The more suitable of these equations shall subsequently be determined through regression analysis using the Ordinary Least Square (OLS) method. In this regard, the linear, quadratic and cubic equations of potential locations for CSP deployment in northern Nigeria based on the two mentioned equations shall be compared to determine the most suitable.

3.2.1 Angstrom-Page Equation

The Angstrom-Page equationprovides a relationship between clearness index and sunshine fraction of the atmosphere at specific locations as presented in Equation (3.1).

$$\frac{H_m}{H_0} = a + b\frac{n}{N} \quad (3.1)$$

wherea and b = regression constants, n = monthly mean of the daily calculated sunshine hour duration, N = monthly mean of the daily calculated maximum possible sunshine hour duration (MJ/(m^2.d), H_o= monthly mean extra-terrestrial solar radiation on horizontal surface (MJ/(m^2.d), H_m= measured monthly mean daily global solar radiation on a horizontal surface.

$\frac{H_m}{H_0}$ = $K_T$and referred to as 'clearness index'.It is the ratio of the monthly averaged daily global solar radiation to the monthly averaged daily extra-terrestrial solar radiation. $\frac{n}{N}$is the ratio of the monthly averaged daily sunshine to the monthly averaged daylight hour (sunshine fraction).

$$H_o = \frac{24}{\Pi} Isc\left(1 + 0.033Cos\frac{360D_n}{365}\right)\left(Cos\phi\ Cos\delta\ Sin\ \omega_s + \frac{\Pi}{180}\omega_s\ Sin\phi\ Sin\delta\right) \quad (3.2)$$

$$N = \frac{2}{15}\omega_s \quad (3.3)$$

The daily sunshine duration can be computed using Equation (3.4) as:

$$n_o = (h/360) * arc\cos(tan\phi tan23.5cos(360D_n)/365.25)) \quad (3.4)$$

From Equation (3.4), the monthly mean sunshine duration (n) could be calculated, where h = 24 hours

$$\delta = 23.45\ Sin\{\frac{360\ (284+D_n)}{365}\} \quad (3.5)$$

$$\omega_s = \arccos(-\tan\phi\ \tan\delta) \quad (3.6)$$

where,Isc= solar constant with a mean value of 4.9212 MJ/(m^2.d), δ = solar declination, ω_s = Sunset hour angle, D_n = day number ranging from 1 to 365, ϕ = Latitude of the location

Equation (4.1) is a linear equation in the form $y = a + bx$ (3.7)

where,$y = \frac{H_m}{H_0}$and $x = \frac{n}{N}$

Linear form of the Angstrom-Page equation may not give the best fit for a regression analysis. In this regard, other forms of the equation such as the quadratic, exponential, logarithmic and power, have been developed (Ohunakin et.al, 2013). Sundram and Babu (2014) highlighted the quadratic and cubic forms of the Angstrom-Page equation as respectively shown in Equations (3.8) and (3.9).

$$\frac{H_m}{H_0} = a + b\frac{n}{N} + c(\frac{n}{N})^2 \quad (3.8)$$

$$\frac{H_m}{H_0} = a + b\frac{n}{N} + c(\frac{n}{N})^2 + d(\frac{n}{N})^3 \quad (3.9)$$

Equations (3.10) and (3.11) are second and third order equations that could be represented as:

$$y = a + bx + cx^2 \quad (3.10)$$

$$y = a + bx + cx^2 + dx^3 \quad (3.11)$$

The direct irradiation, which is the requirement for CSP application could be obtained by removing the diffused component ($\frac{H_d}{H}$) of H_m by either using the original correlation by Liu and Jordan (1960) for calculating the daily radiation or the correlation by Erbs*et al*., (1982) for calculating monthly radiation, both highlighted in Duffie and Beckman (2013) as follows:

For $\omega_s \leq 81.4^o$ and $0.3 \leq K_T \leq 0.8$,

$$\frac{H_d}{H} = 1.391 - 3.560K_T + 4.189\,K_T{}^2 - 2.137\,K_T{}^3 \quad (3.12)$$

For $\omega_s > 81.4^o$ and $0.3 \leq K_T \leq 0.8$,

$$\frac{H_d}{H} = 1.311 - 3.022K_T + 3.427K_T{}^2 - 1.821\,K_T{}^3 \quad (3.13)$$

3.2.2. Hargreaves-SamaniEquation

Zhang et.al. (2013) employed the Hargreaves method to relate the extra-terrestrial solar irradiation (H_0) to the average daily solar irradiation (H_m) by means of ambient temperature. Hargreaves method predicts clearness index K_T as:

$$K_T = K_{RS}(T_{max} - T_{min})^{0.5} \quad (3.14)$$

where, T_{max} = maximum temperature, T_{min} = minimum temperature, K_{RS} = adjustment coefficient.

K_{RS} ~ 0.16 for interior locations, where air masses are not strongly influenced by a large water body.

K_{RS} ~ 0.19 for coastal locations, on or adjacent coast of a large land mass and where air masses are influenced by a nearby water body.

Daily clearness index could be obtained from monthly averages using exponential variables established by Knight *et al*. (1991) as follows:

$$K_T = (1/\gamma)[\ln\{1-\alpha)e^{\gamma k}T_{min} + \alpha e^{\gamma k}T_{max}\}] \quad (3.15)$$

where, $\gamma = -1.498 + [1.184\xi - 27.182\, e^{(-1.5\xi)}] / (K_{T,\,max} - K_{T,\,min})$

$\xi = (K_{T,\,max} - K_{T,\,min}) / (K_{T,\,max} - K_{T,\,av})$

$K_{T,\,min} = 0.05$

$K_{T,\,max} = 0.6313 + 0.267\, K_{T,\,av} - 11.9\, (K_{T,\,av} - 0.75)^8$

$\alpha = n_{dk} - 0.5 / n_{dm}$

Where

n_{dk} = Day of the month, n_{dm} = Number of days in the month

Daily irradiation on a horizontal plane (H_{md}), could then be obtained from equation (3.16) as:

$$H_{md} = K_T . H_0 \quad (3.16)$$

Similarly, Ohunakin*et al*., (2013) highlighted the original HS equation(Hargreaves and Samani, 1982) as shown in Equation (3.17) as:

$$\frac{Hm}{Ho} = a + b\Delta T^{0.5} \quad (3.17)$$

The quadratic and cubic forms of the equation are highlighted in Equations (3.18) and (3.19)as:

$$\frac{H_m}{H_0} = a + b\Delta T^{0.5} + c(\Delta T^{0.5})^2 \quad (3.18)$$

$$\frac{H_m}{H_0} = a + b\Delta T^{0.5} + c(\Delta T^{0.5})^2 + d(\Delta T^{0.5})^3 \quad (3.19)$$

where, ΔT is the difference between the mean maximum and minimum monthly temperatures. The direct irradiation could also be obtained from the work of Liu and Jordan (1960) or Erbs correlation as earlier highlighted.

3.3 Research Questions

The study provided answers to the following questions:

i. Which locations in northern Nigeria are suitable for power generation through CSP?
ii. Which solar radiation model(s) would be suitable for the utilisation of CSP in potential locations in northern Nigeria?
iii. What is the annual electricity output from CSP plants in potential locations in northern Nigeria?
iv. What is the LCOE from CSP plants in potential locations in northern Nigeria?

3.4 Research Design

The study employed 18-year (2001-2018) daily average of solar radiation data obtained from the Nigerian Meteorological Agency (NIMET). It also used 21-year (1997-2017) daily average of solar radiationdata obtained from the South African Weather Services (SAWS),and 18-year (2001-2018) hourly data of DNI, GHI, DHI, dry bulb temperature, wind speed, wind direction, relative humidity and air pressure from the European Union Photovoltaic Geographic Information System (EU – PVGIS) and the National Solar Radiation Database (NSRDB) of the National Renewable Energy Laboratory (NREL) California, USA.The data of the nearest major town with a weather station was employed where such data was unavailable for location under investigation.The research is divided into four parts and employed the quantitative research approach.

The first part of the study is the initial selection of potential sites. The criteria for initial site selection comprised DNI, sunshine duration, mean temperature, land availability and

suitability, relative humidity and water availability.However, all locations under review adequately met the criteria for relative humidity, hence the criterion was not rated. Weighted points were allocated to each of the other stated criteria, using the assigned weights employed for the development of TMY data in the NSRDB of the NREL as a guide, and the use of upper and lower limits or establishment of benchmarks for each parameter based on the literature, previous studiesand models.

The weighting method was adopted because assigned weights of the various parameters in the development of TMY data could be allotted intuitively based on knowledge of the influence of the various parameters on the intended application (Sawaqed*et al.*, 2005). Similar data of two locations in South Africa (Pofadder and Upington) where CSP is currently deployed were also obtained from the SAWS and the EU-PVGIS. The essence of obtaining data from locations in South Africa where CSP is deployed is for validation with data of potential locations for CSP application in Nigeria through correlation analysis of these data.

The GHI data for the locations in Nigeria obtained from NIMET, were captured using the Gunn-Bellani distillate (mm). The Gunn Bellanni readings (H_{GB}) were converted to MJ/(m^2.d) by a conversion factor of 1.1364 recommended by Sambo and adopted in Ohunakin*et al.*, (2013).The solar radiation integrator of Gunn-Bellani distillates, provides a time integrated assessment of radiation incident on a black body by measuring the volume of the liquid distilled in a receiving graduated tube.The accuracy of its actinometer is ensured by calibrating it against standard solar radiation recorders such as the pyranometer and pyrheliometer.It is cheap, easy to observe and lacks any replaceable mechanical or electronic component. It is thus suitable for the measurement of meteorological data in several locations especially in a developing nation like Nigeria (Ohunakin*et. al*, 2013).

The daily duration of sunshine was measured by NIMET using the Campbell Stokes sunshine recorder, which uses a glass sphere with diameter of about 10 cm as a lens to produce the Sun's image on the reverse surface of the sphere. The placement of a strip of card along the focus of the lens ensures the focussed rays result into burn traces on the paper, with the length of the burn trace providing an index of the period of bright sunshine. Issues regarding the use of the Campbell Stokes recorder for the measurement of sunshine hours include the uncertainty in what constitutes a burnt portion of the paper, non-response to low level of radiations and the tendency of the paper to be affected by humidity (Duffie

and Beckman, 2013). However, high precision in the production of its components could enhance the accuracy of the equipment.

The second part of the research focusses on the derivation of solar radiation models and theoretical determination of DNI for the locations selected for the deployment of CSP plants in northern Nigeria.The solar radiation model for each location was derived through comparison of the results obtained from regression analysis using Angstrom-Page (AP) and Hargreaves-Samani (HS) equations. The results of the regression analysis in linear, quadratic and cubic forms, based on the two equations, were compared to determine the most suitable model. The theoretical DNI was then determined by synthesizing the daily GHI on a horizontal plane (measured in Gunn-Bellani) obtained from NIMETinto hourly DNI on a normal plane. The synthesis was necessary as pyrheliometer, which is the equipment required for on-site measurement of DNI, was not available for the study. The study consequently computed empirical values of DNI for the respective locations from meteorological data obtained from NIMET. From the daily total solar radiation for each hour (I_{th}) obtained from NIMET, hourly diffuse radiations, beam horizontal radiations (I_{bh}) and hourly direct solar radiations on a normal surface (I_{bn}) were subsequently calculated as illustrated in Figure 3.1.

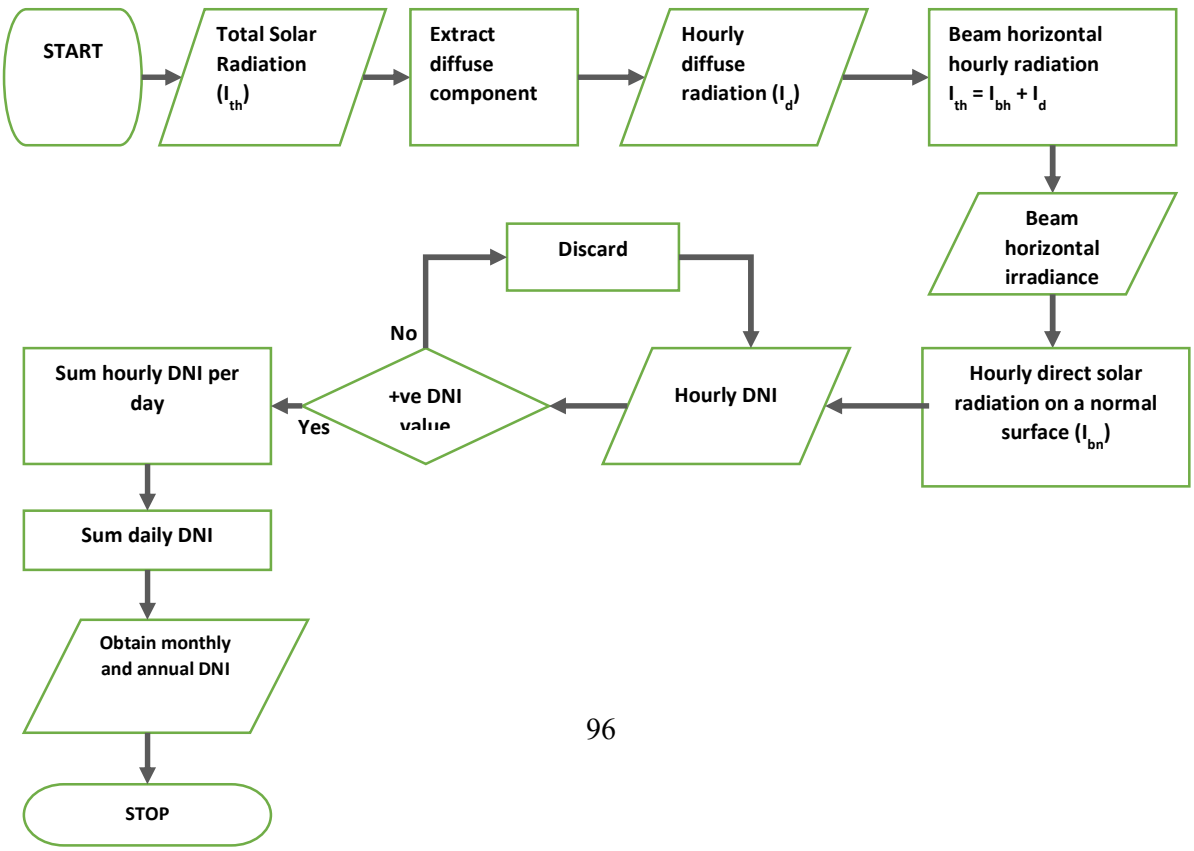

Figure 3.1: Flow Chart for the Theoretical Determination of Direct Normal Irradiance.

The theoretically determined DNI served as an alternative source of data comparison with the satellite based DNIwherepyrheliometers required for on-site measurement of DNI are not available.Locations having satellite based and theoretical DNI values above the minimum DNI value for CSP deployment (1800kWh/m^2/year) were considered suitable for siting CSP plants and subjected to further analysis. The locations further analysed were the top-5 ranked locations in the initial selection process.

The third part of the study was the investigation of the most suitable system component and requirements for the potential CSP plants. It also involved thesimulation of energy output as well as LCOE from potential CSP plants in the selected locations using NRELSAM. The technical configuration of the NREL Reference CSP Plant, that is the 100 MW dry-cooled PTC CSP Solar Energy Generating System (SEGS) VIII in California, was adopted where feasible while a scaled down 50 MW of the plant was adopted for the rest of the locations as applicable.

The simulation was based on the development of TMY data required to obtainenergy

output and LCOE from the proposed CSP plants using the NREL SAM.The TMY data was developed in the TMY3 format of the NSRDB (Wilcox and Marion, 2008),using the Finkelstein-Schafer (FS) statistics (Equation 3.20) employed in the original Sandia Method. However, direct component of solar radiation was incorporated in the TMY3 format since it is meant for a solar thermal system as indicatedin Table 3.1.The FS statistics employs weighted sum (WS) (Equation 3.21), based on relative importance of the parameters indicated in Table 3.1.

$$\mathrm{FS} = \frac{1}{\mathrm{n}}\sum_{\mathrm{i}=1}^{\mathrm{n}} \delta_{\mathrm{i}} \tag{3.20}$$

where,δ_i = absolute difference between the long-term CDF and the candidate month CDF at $x_{i.}$

n = the number of daily readings in a month.

$$\mathrm{WS} = \sum \mathrm{w_i}\,\mathrm{FS_i} \tag{3.21}$$

where,w_i = weighting for index, and FS_i = FS statistic for index.

The variations in the parameters for determining TMMs in the original Sandia Method and the TMY3 format include the addition of parameter ranges and relative humidity in Sawaqed*et al*., (2005) and the absence of dew point temperatures in both Sawaqed*et al*., (2005) and Ohunakin*et al*., (2018). Most importantly, the TMY3 data weighted direct radiation separately, unlike theSandia methods that provided weights for only global radiation. Since CSP works on DNI, the TMY3 format is considered most appropriate for the study.

Table 3.1: Comparison of Parameters and Weighted Sum for TMY Development

Parameter	**Sandia (Sawaqed*et al*., 2015)**	**Sandia (Ohunakin*et al*., 2018)**	**TMY3 (NSRDB)**
Max Dry Bulb Temp	1/24	1/12	1/20
Min Dry Bulb Temp	1/24	1/12	1/20
Mean Dry Bulb Temp	1/24	2/12	2/20
Dry Bulb Temp (range)	1/24	-	-
Max Dew Point Temp	-	-	1/20
Min Dew Point Temp	-	-	1/20
Mean Dew Point Temp	-	-	2/20
Max Wind Velocity	1/24	1/12	1/20
Mean Wind Velocity	1/24	1/12	1/20

Global Radiation	12/24	5/12	5/20
Direct Radiation	-	-	5/20
Relative Humidity (mean)	1/24	1/12	-
Relative Humidity (max)	1/24	-	-
Relative Humidity (min)	1/24	-	-
Relative Humidity (range)	1/24	-	-
Wind Velocity (min)	1/24	-	-
Wind Velocity (range)	1/24	-	-

Although Table 3.1 showed thatSawaqed*et al*., (2005) and Ohunakin*et al*., (2018) both used the Sandia Method, it can be observed that the researchers' knowledge and intuition led to slight changes in the allotment of weights to the parameters. However, for the simulation, the following parameters were used: GHI, DNI, DHI, dry point temperature, dew point temperature, relative humidity, air pressure, wind speed, wind direction and albedo.Two parameters required for the data simulation, which is dew point temperature and albedo, could not be obtained from both NIMET and EU-PVGIS.Hence, dew point temperature was calculated from an equation obtained from Lawrence (2005), as indicated in Equation (3.22).

$$T_d = T - \left(\frac{100-RH}{5}\right) \quad (3.22)$$

where, T_d = dew point temperature, T = dry bulb temperature, RH = relative humidity.

The Albedo (Alb) is the relationship between the reflected solar irradiance andthe global horizontal irradiance. In determining the adopted Alb for the locations investigated, the study adopted the Alb of Amapala (Honduras) as obtained from the NSRDB of the NREL. The decision to adopt the Alb of Amapala was based on the latitudinal relationship (13^{o}N) between Amapala and most of the locations investigated in northern Nigeria (Ohunakin*et. al*, 2013; NREL, 2017).

The simulation was based on the CSP Parabolic Trough (Physical) Performance Model and the LCOE Calculator (FCR method) financial model of the SAM 2017 version 9.5. The TMMs and the entire TMY3 dataset were developed using same method in Ohunakin*et al*., (2013). The technical configuration of the NREL Reference CSP Plant (i.e., the 100 MW Solar Energy Generating System (SEGS) VIII California, USA) using a solar multiple of two (2), was adopted for the simulation. However, the economic indices in the model were adjusted to suit Nigeria, so that the simulation can reflect prevailing economic realities in Nigeria (in place of default values representing USA). The adopted rates are shown in Table 3.2. Partial screenshots of the TMY3 data showing the parameters used for the simulation of relevant outputs of the locations investigated are shown in Appendix 1.

Table 3.2: Adopted Economic Indices for Nigeria

Parameter	**SAM Rate**	**Adopted Rate**
Analysis Period	20 years	25 years
Inflation Rate	2.5%/year	7.5%/year
Internal Rate of Return (Nominal)	13%/year	13%/year
Projected Term Debt	60% of Capital Cost	60% of Capital Cost
Nominal Debt Interest Rate	8%/year	12%/year
Effective Tax Rate	40%/year	30%/year
Nominal Construction Interest Rate	8%/year	12%/year
Capital Cost	$6,065/kW	$6,065/kW
Fixed Operating Cost (Annual)	$66/kW	$66/kW
Variable Operating Cost	0.004$/kWh	0.004$/kWh

The technical configuration of the proposed plants was based on deductive approach, in that the technical configuration of an existing plant was used to determine the potential outputs of hypothetical plants in other locations.The derived output comprises the estimated annual energy output, estimated monthly energy output, capacity factor, and LCOE amongst others.The economic model was based on derivation of LCOE for each of the respective proposed plants using three different methods including: (i) simulation of LCOE using the NREL SAM, (ii) theoretical calculation of LCOE,and (iii) derivation of current LCOE based on cost projections. The mean of the LCOE obtained from the three distinct methods was adopted as the derived LCOE. The calculated LCOE was determined using inputs from feasibility studies, prevailing economic indices, NREL SAM software and interpolation of values indicated in the Resettlement Action Plan (RAP) for the Ganjuwa 100 MW Solar Project in Bauchi Stateamongst others.The RAP was considered suitable because its total land requirement (2,240,000m^2) is approximately the same as that required for a 100 MW CSP Plant, although the former is for a Solar Photovoltaic system.

The RAP was also considered suitable as it was designed in accordance with Good International Industry Practice (GIIP) e.g., the African Development Bank (AfDB) Integrated Safeguard Systems (2013), AfDB Involuntary Resettlement Policy(2015) and the European Investment Bank's Environmental and Social Handbook (2013).

The LCOE based on cost projection wasobtained through linear interpolation,because a near linear relationship could be established in the LCOE from 2010-2020 (IEA,2010). Here, the linear interpolant was determined as the straight line, with coordinates (x, y), between two known points with coordinates (x_0,y_0) and (x_1,y_1) in Equation (3.23):

$$\frac{y-y_0}{x-x_0} = \frac{y_1-y_0}{x_1-x_0} \tag{3.23}$$

Once the value of x in Equation (3.23) is given, the value of y can be determined and vice versa. Furthermore, the use of the learning curve method in determining LCOE theoretically was considered generic since past evolution of the system cost as a function of the global cumulative installed capacity is considered in the determination of total cost. Hence, this study developed the total cost of the proposed system from first principles using prevailing economic indices in Nigeria.

The selection of concentrator, HTF, and TES medium was based on energy output, LCOE and the required solar aperture area within a range of solar multiples, using NREL SAM simulation.The fourth part of the study was the conduct of a strengths, weaknesses, opportunities and threats (SWOT) analysis of deploying CSP plants in northern Nigeria.The analysis elucidated the viability of employing CSP technology to boost power generation in Nigeria.

3.5 Data Sources

The research relied on secondary data sources including publications, books and journals. Other sources included data from NIMET, SAWS, World Bank, International Renewable Energy Agency (IRENA), International Energy Agency (IEA), Nigerian Electricity Regulatory Commission (NERC), Central Bank of Nigeria (CBN), National Bureau of Statistics (NBS), NSRDB of the NREL, European Commission Joint Research Centre,World BankESMAP and other relevant research institutions in Nigeria and across

the world.

3.6 Data Analysis

The research employed exploratory data analysis for parameters including DNI, sunshine duration, maximum temperature, minimum temperature, using correlation and linear regression analysis.Tools employed in the analyses are the NREL SAM, R software, EU Photovoltaic Geographic Information System (PVGIS) softwareand Excel spreadsheet.

3.7 Summary

The chapter focussed on the theoretical framework of the study, which involved a comparative analysis of the Angstrom-Page and HS models, while the research design involved four distinct parts including: (i) initial site selection, (ii) derivation of solar radiation models and theoretical determination of DNI, (iii) selection of system component and requirements, including simulation of energy output as well as LCOE(iv)SWOT analysis of deploying CSP plants in northern Nigeria. It also indicated the sources of data and methods of data analysis.

CHAPTER FOUR
RESULTS AND DISCUSSION

4.1 Preamble

This chapter presents the descriptive analysis of the various data employed for the study, and highlights the results obtained in line with the research design. The descriptive data analysis established the suitability of some locations in northern Nigeria for the deployment of CSP upon comparative study of three significant parameters: DNI, sunshine duration and temperature, with those of two locations where CSP is currently deployed in South Africa (Upington and Pofadder). The most suitable sites for CSP application in northern Nigeria was determined followed by derivation of solar radiation models for the most

suitable locations and the derivation of solar radiation models for each of the selected locations. The discussion of results obtained also forms part of this chapter.

4.2 Descriptive Data Analysis

The DNI values of all potential locations are presented in Table 4.1all meet the 1800 kWh/m^2/year (~5000Wh/m^2/day) design criteria specified for CSP applications (Bishoyi and Sudhakar, 2017), with Malam Fatori having the highest mean DNI of 5807Wh/m^2/day in Nigeria. The duration of sunshine in a location is also a major determinant for the suitability of a CSP project.

Table 4.1: Descriptive Statistics of Daily DNI Data for the Locations under Review

Location	Mean	Median	Range	Minimum	Maximum	Confidence Level (95.0%)
Pofadder	8057.69	8050.00	3770.00	6210.00	9980.00	759.58
Upington	7830.00	7830.00	3120.00	6350.00	9470.00	614.68
Gamawa	5447.69	5470.00	2390.00	3850.00	6240.00	429.84
Machina	5542.31	5790.00	2190.00	3990.00	6180.00	379.69
M/Fatori	5807.69	6160.00	2310.00	4030.00	6340.00	410.52
Gada	5480.00	5680.00	1930.00	4080.00	6010.00	333.81
Gasau	5268.46	5290.00	2670.00	3470.00	6140.00	488.14
Danbatta	5447.69	5470.00	2390.00	3850.00	6240.00	429.84
Maiadua	5509.23	5600.00	2340.00	3970.00	6310.00	395.84
Yelwa	5070.00	5090.00	2960.00	3110.00	6070.00	547.47
Mubi	5293.08	5290.00	3470.00	3150.00	6620.00	635.68

Zaria	5268.46	5290.00	2670.00	3470.00	6140.00	488.14

Sources: EU-PVGIS, 2019; South Africa Weather Services, 2018.

The DNI values of the potential locations arealso presented in Figure 4.1.

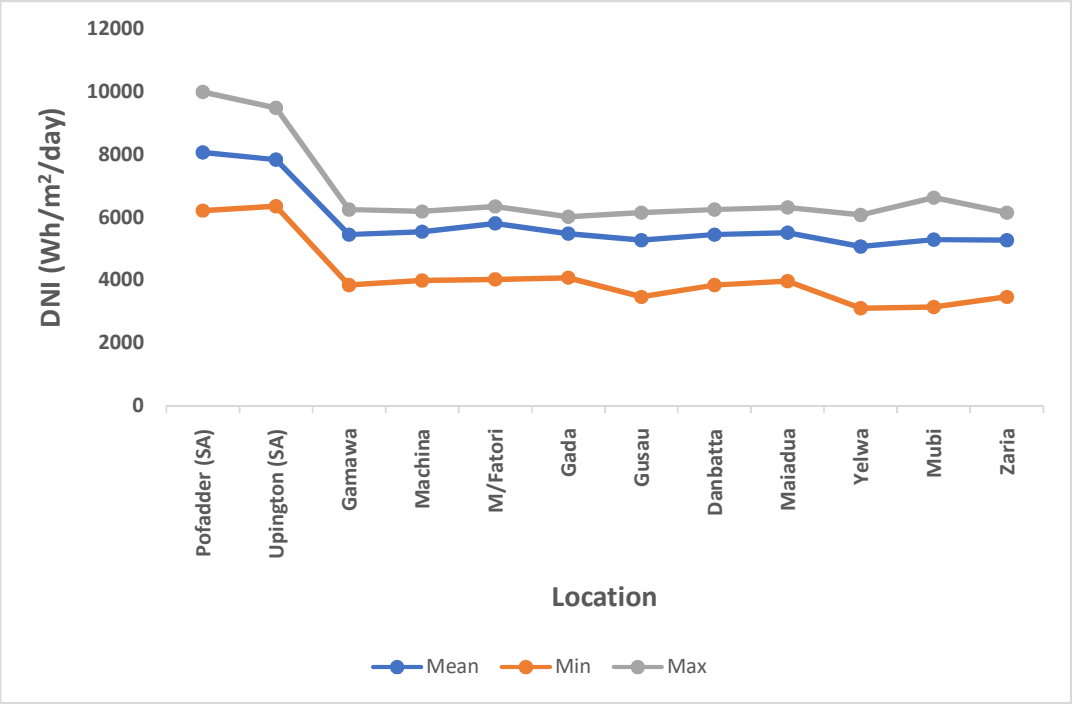

Figure 4.1: Plot of minimum, maximum and average DNI values for selected locations in Nigeria and South Africa

Figure 4.1 indicates that the two locations in South Africa, Pofadder and Upington, have higher mean, minimum and maximum DNI values compared to all the locations under consideration in Nigeria. Correlation analysis of the DNI values of all the locations (Table 4.2 and Figure 4.2), also reveal a positive relationship between the locations in South Africa and all the locations under consideration in Nigeria, suggesting that the data obtained for locations in Nigeria are suitable for modelling.

Table 4.2: Correlation Analysis of DNI Data

	Pofadder	Upington	Gamawa	Machina	M/Fatori	Gada	Gasau	Danbatta	Maiadua	Yelwa	Mubi	Zaria
Pofadder	1											
Upington	0.983279	1										
Gamawa	0.643461	0.522766	1									
Machina	0.513538	0.385792	0.979801	1								
M/Fatori	0.404437	0.281748	0.936078	0.981445	1							
Gada	0.567029	0.446194	0.985839	0.992239	0.972749	1						
Gasau	0.654552	0.534517	0.999072	0.977344	0.934118	0.984015	1					
Danbatta	0.643461	0.522766	0.953297	0.979801	0.936078	0.985839	0.999072	1				
Maiadua	0.583217	0.449963	0.984837	0.984094	0.940647	0.980464	0.983363	0.984837	1			
Yelwa	0.66957	0.548824	0.99563	0.968861	0.923056	0.976884	0.996987	0.99563	0.977228	1		
Mubi	0.733817	0.622117	0.979461	0.932581	0.884265	0.954203	0.981296	0.979461	0.946294	0.988739	1	
Zaria	0.654552	0.534517	0.999072	0.977344	0.934118	0.984015	0.985896	0.999072	0.983363	0.996987	0.981296	1

Correlation results indicate that Mubi has the highest degree of relationship with Pofadder

and Upington (0.734 and 0.622, respectively), followed by Yelwa (0.67 and 0.55, respectively), Zaria (0.654 and 0.534, respectively), Gasau (0.654 and 0.534 respectively), Danbatta (0.643 and 0.523, respectively) and Gamawa (0.643 and 0.523, respectively). These five locations in Nigeria have positive and relatively higher DNI relationships with Pofadder and Upington in South Africa relative to the other five locations.

Another observation is that all the selected locations in Nigeria have remarkably high correlation with one another. This could be attributed to the locations being under the same climatic region, and with same latitudes (Ohunakin*et. al*, 2013). However, correlation of DNI values for locations in different hemispheres may not be a reliable criterion for determining the viability of locations for CSP deployment.The baseline DNI value of 1800kWh/m^2/year as revealed in some studies earlier cited (Sharma *et al*., 2015; Mashena and Alkishriwi, 2016) and latitudinal relationships (Ohunakin*et. al*, 2013) are considered better methods of determining suitability of locationsfor CSP application.

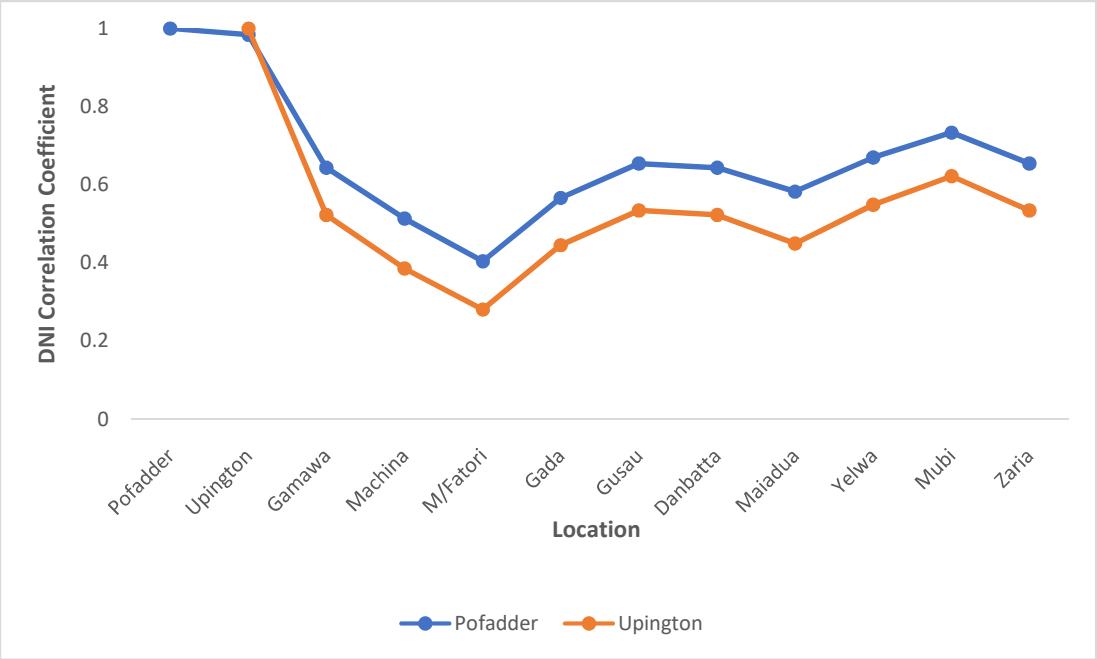

Figure 4.2: Plot of the Correlation Analysis of DNI values for the locations under Review

Table 4.3 presents the descriptive statistics of the hours of sunshine data of the selected locations in South Africa and Nigeria. The statistics reveals that the locations in South Africa have longer sunshine durations compared to all the locations in Nigeria, with Pofadder having the highest value. Meanwhile, Maiadua has the longest mean Sunshine duration in Nigeria, followed by Gada.

Table 4.3: Descriptive Statistics of Average Sunshine Hours of locations under Review

Location	Mean	Median	Range	Average Minimum	Average Maximum	Confidence Level (95.0%)
Pofadder	10.12	10.08	0.68	9.81	10.49	0.15
Upington	10.12	10.13	0.46	9.87	10.33	0.10
Yelwa	7.55	7.33	1.58	6.98	8.56	0.35
Gada	8.11	8.15	1.72	6.99	8.71	0.36
Gusau	7.17	6.82	2.73	6.06	8.79	0.69
Maiadua	8.23	8.25	1.58	7.34	8.92	0.26
Zaria	8.08	8.04	0.99	7.71	8.70	0.22
Danbatta	7.91	7.93	1.18	7.16	8.34	0.23
Gamawa	7.12	7.58	3.20	4.67	7.87	0.73
M/Fatori	8.06	8.04	1.10	7.48	8.58	0.22
Mubi	7.37	7.27	0.88	7.07	7.95	0.20
Machina	8.06	8.04	1.10	7.48	8.58	0.22

Sources: NIMET, 2019; South Africa Weather Services, 2018.

Furthermore,Figure 4.3 is the plot of the maximum, minimum and mean sunshine durations at the locations under Review.

Figure 4.3: Plot of Minimum, Maximum and Average Sunshine Durationsof the Locations under Review

The mean sunshine period for the two locations in South Africa is 10.12 hours while that for the ten selected locations in Nigeria varies from 7.12 hours in Gamawa to 8.23 hours in Maiadua.Maiadua also has the longest maximum sunshine duration (8.92 hours) of all the selected locations in Nigeria, although lower than the maximum 10.49 hours obtained from Pofadder in South Africa.The mean daily sunshine duration in the selected locations in Nigeria, are approximately 80% of the sunshine duration in the two locations in South Africa. The range of sunshine duration (Table 4.3) of the locations in South Africa are also lower relative to the locations under consideration in Nigerian. Amongst the locations indicated in Table 4.3, Upington with 0.46 hours has the lower sunshine duration range between the two locations considered in South Africa while the lowest for locations considered in Nigeria is 0.88 hours in Mubi. The lower sunshine duration range in South Africa suggests a higher level of solar radiation stability relative to Nigeria. Althoughlocations in South Africa have relatively higher levels of stability in terms of solar radiation based on data presented,the variations relative to data obtained for locations in Nigeria are considered not too significant hence the locations in Nigeria could be investigated for CSP deployment.

Table 4.4 presents the descriptive statistics obtained from the average maximum temperature at the locations in South Africa and Nigeria. The statistics reveals that all locations in Nigeria have higher maximum temperature compared to the two locations in South Africa, with Pofadder having the least maximum and mean temperatures. Gada has the highest maximum and mean temperatures of 36.38^{o}C and 35.73^{o}C, respectively while that of Pofadder is 28.17^{o}C and 26.87^{o}C, respectively.However, all the locations have mean temperatures higher than the 25^{o}C used as the ambient temperature in the design of CSP systems (NREL SAM, 2017).

Table 4.4: Descriptive Maximum Temperature

Location	Mean	Median	Average Minimum	Average Maximum	Confidence Level (95.0%)
Pofadder	26.87	26.58	26.03	28.17	0.44
Upington	29.53	29.57	28.95	30.13	0.24
Yelwa	34.65	34.61	34.10	35.50	0.27
Gada	35.73	35.76	35.16	36.38	0.22
Gusau	33.97	33.85	33.29	34.81	0.33
Maiadua	33.90	33.90	33.36	34.41	0.21
Zaria	32.42	31.90	31.63	34.41	0.67
Danbatta	33.35	33.38	32.11	34.19	0.40
Gamawa	33.05	33.08	32.03	34.33	0.39
M/Fatori	35.48	35.53	35.08	35.93	0.19
Mubi	34.98	35.00	34.21	35.73	0.31
Machina	35.48	35.53	35.08	35.93	0.19

Sources: NIMET, 2019; South Africa Weather Services, 2018.

Also, Figure 4.4 presents the maximum, minimum and mean values of the maximum temperature at the selected locations. As shown, the three plots are quite close, and all values meet the design criteria for CSP systems.

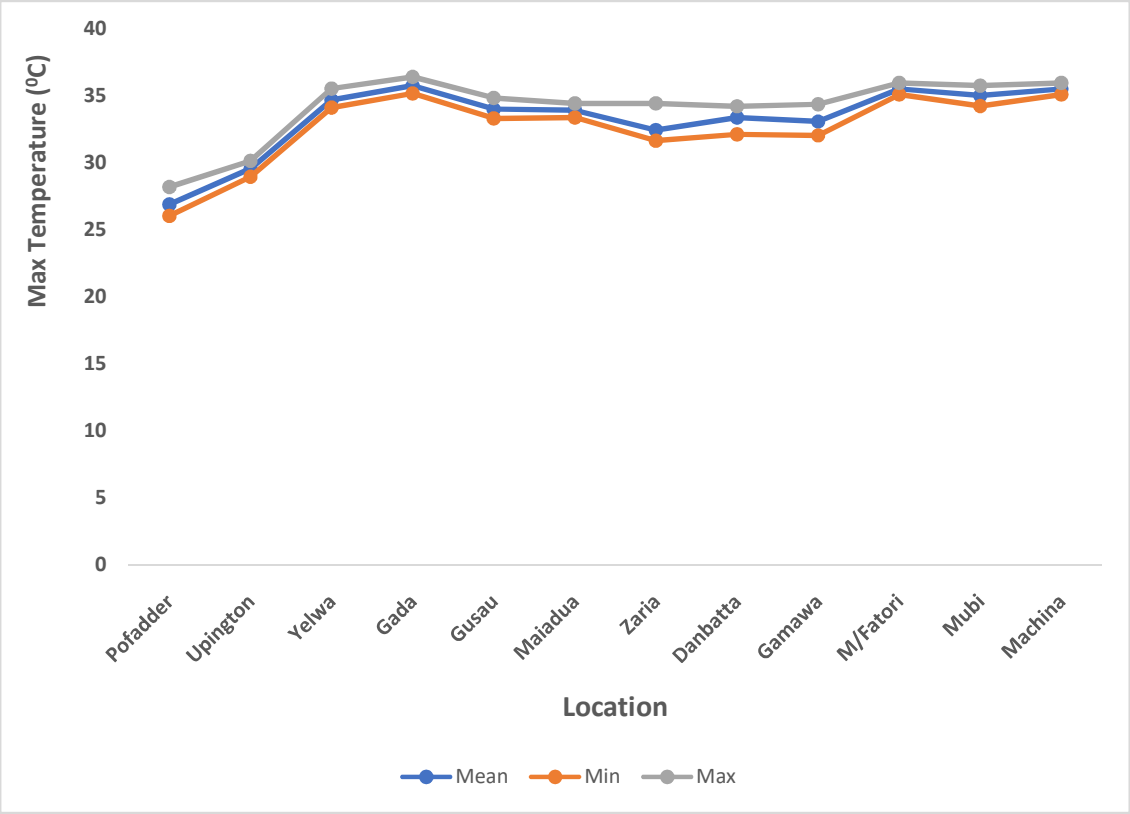

Figure 4.4: Plot of the minimum, maximum and mean values of maximum temperature at the locations under Review

Table 4.5 presents the descriptive statistics obtained from the average minimum temperature of all locations.The statistics reveals that all the locations in Nigeria have higher minimum temperature compared to the two locations in South Africa, with Pofadder having the least minimum temperature of 11.33^{o}C.

Table 4.5: Descriptive Minimum Temperature

	Mean	Median	Average Minimum	Average Maximum	Confidence Level (95.0%)
Pofadder	12.41	12.28	11.33	13.91	0.46
Upington	12.81	12.73	12.03	14.25	0.45
Yelwa	21.76	21.81	20.93	22.32	0.36
Gada	22.70	22.73	22.14	23.28	0.26
Gusau	20.01	20.30	18.43	21.86	0.64
Maiadua	19.59	19.73	18.05	20.62	0.61
Zaria	19.50	19.58	18.38	20.08	0.32
Danbatta	20.33	20.38	19.45	21.30	0.35
Gamawa	19.67	19.53	18.65	20.88	0.48
M/Fatori	20.40	20.43	19.54	21.20	0.34
Mubi	22.84	23.03	22.18	23.44	0.30
Machina	20.40	20.43	19.54	21.20	0.34

Sources: NIMET, 2019; South Africa Weather Services, 2018.

The least minimum temperature of the locations in Nigeria is 18.05^{o}C obtained in Maiadua (Katsina).This least minimum temperature is much higher than the minimum operating temperature of 12^{o}C for Therminol VP-1 HTF (NREL SAM, 2017), which indicates that locations in Nigeria would be more tolerant to different HTF relative to locations in South Africa.Figure 4.5 is the plot of the combination of maximum, minimum and mean values of the minimum temperature at the selected locations. As shown, locations in Nigeria have higher values in comparison to those of South Africa.

Figure 4.5: Plot of the minimum, maximum and mean minimum temperature at the locations under Review

Generally, the two locations in South Africa have higher DNI and sunshine hours relative to the selected locations in Nigeria; the selected locations in Nigeria have relatively higher temperatures in comparison to the locations in South Africa. The differences in all parameters were however considered not too significant, and thus provides one of the bases for investigation. The study then adopted a weighted approach by considering other parameters in addition to the DNI, sunshine duration and temperature. The allocation of weights was guided by the allotted weights in the User's Manual for TMY3 Data Sets (Wilcox and Marion, 2008).

4.3 Determination of Locations' Suitability for CSP Plants

In determining the suitability in order of preference of the locations under review for possible CSP investment, some criteria were selected, and allotted weights using the weighting values employed by the NREL for the development of TMY format data, and deductions from some of the literatures reviewed as a guide. Apart from DNI, ambient temperature, wind velocity and relative humidity identified as factors affecting CSP performance, other criteria considered as important are land availability and slope, sunshine duration and water availability. Habib *et al*., (2012) established sufficient land space for CSP deployment in northern Nigeria with adequate average ground slope of < 3 %, which is an important criterion for CSP deployment. The study examined the land mass in each of the states where locations were considered for CSP deployment taking into consideration, the 5% landmass for each State considered in the work of Habib *et al*., (2012). Furthermore, Eludoyin*et al*., (2014) highlighted that mean values of RH of 10 locations in northern Nigeria in/or adjacent to locations under review ranges from 25.8% to 28.6% and found to be very low compared with the maximum threshold of 80% that will bring about corrosion of metals. Therefore, it can be inferred that the relative humidityof all the selected locations issuitable for conducive for CSP plants.The criteria utilised in selecting proposed locations for CSP plants in Nigeria therefore are: DNI level (50 weighted points), sunshine duration (15 weighted points), ambient temperature (15 weighted points), land availability (10 weighted points), wind velocity (5 weighted points), and availability of water source (5 weighted points). Table 4.6thus highlights the parameters of the locations based on the selected criteria.

Table 4.6: Relevant Parameters of locations under Review based on selected Criteria

Location	Lat (^oN)	Mean DNI ($Wh/m^2/yr$)	Mean Sunshine Duration	Mean Max Temp (^oC)	Mean Temp (^oC)	Wind Speed (m/s)	5% Suitable Landmass of the State (km^2)
Malam-Fatori (Borno)	13.68	2121.26	8.06	35.93	27.74	3.84	3274
Gada (Sokoto)	13.76	2001.57	8.11	36.38	29.26	5.39	562
Yelwa (Kebbi)	10.80	1851.85	7.55	35.50	28.22	2.37	871
Gamawa (Bauchi)	12.13	1989.77	7.12	34.33	26.49	1.87	722
Maiadua (Katsina)	13.13	2012.25	8.23	34.41	26.23	8.38	857
Danbatta (Kano)	12.42	1989.77	7.91	34.19	26.82	5.42	815
Gusau (Zamafara)	12.20	1924.31	7.17	34.81	26.62	4.11	1178
Mubi (Adamawa)	10.26	1933.30	7.37	35.73	28.96	2.00	474
Zaria (Kaduna)	11.18	1924.31	8.08	34.41	26.40	3.91	552
Machina (Yobe)	13.13	2024.33	8.06	36.17	27.31	3.82	1615

Sources: NIMET, 2019; EU PVGIS, 2019; Habib *et al*., 2012.

The weights for the various criteria were allotted as follows:

Direct Normal Irradiance

DNI is the most important criteria needed for the deployment of CSP (World Energy Council, 2016).The annual DNI of each location could be obtained by multiplying the daily DNI by 365.25; the decimal value caters for the leap years in the data employed since a solar year is given as 365.25 days (Brooks, 2012). The yearly DNI for the 10 selected locations are given in Table 4.6. Considering the minimum DNI value of 1800 kWh/m^2/year for CSP deployment (Sharma *et al*., 2015; Mashena and Alkishriwi, 2016), and the maximum DNI of 2600 kWh/m^2/year employed for the projection of LCOE (IEA, 2010), suggested weights for DNI values are given in Table 4.7.

Table 4.7: Allotted Weighted Points for DNI

DNI Range	Allotted Weighted Point
≥ Annual average DNI of 2600 kWh/m^2/ year	50
2500 kWh/m^2/year ≤ DNI ≤ 2599 kWh/m^2/year	45
2400 kWh/m^2/year ≤ DNI ≤ 2499 kWh/m^2/year	40
2300 kWh/m^2/year ≤ DNI ≤ 2399 kWh/m^2/year	35
2200 kWh/m^2/year ≤ DNI ≤ 2299 kWh/m^2/year	30
2100 kWh/m^2/year ≤ DNI ≤ 2199 kWh/m^2/year	25
2000 kWh/m^2/year ≤ DNI ≤ 2099 kWh/m^2/year	20
1900 kWh/m^2/year ≤ DNI ≤ 1999 kWh/m^2/year	15
1800 kWh/m^2/year ≤ DNI ≤ 1899 kWh/m^2/year	10
< 1800 kWh/m^2/year	0

Sunshine Duration

Duration of sunshine determines the period a CSP system can function without TES. Locations having sunshine duration of 10 hours or more, per day such as Upington and Poffader in South Africa, have proven reliable for CSP application. In this regard, suggested weights, based on data from NIMET, are given in Table 4.8.

Table 4.8: Allotted Weighted Points for Sunshine Duration

Sunshine Duration Range	**Allotted Weighted Point**
≥ 10hrs	10
9hrs ≤ Sunshine Period ≤ 9hrs 59 mins	8
8 hrs ≤ Sunshine Period ≤ 8hrs 59 mins	6
7 hrs ≤ Sunshine Period ≤ 7hrs 59 mins	4
6 hrs ≤ Sunshine Period ≤ 6hrs 59 mins	2
< 6 hrs	0

Ambient Temperature

The minimum operating temperature for CSP applications is as 25^{o}C (NREL SAM, 2017). In this regard, suggested weights for mean dry bulb temperature, based on data from NIMET, are given in Table 4.9.

Table 4.9:Allotted Weighted Points for Ambient Temperature

Ambient Temperature Range	**Allotted Weighted Point**
$> 35^{o}C$	10
$30^{o}C <$ temperature $\leq 35^{o}C$	8
$25^{o}C <$ temperature $\leq 30^{o}C$	6
$20^{o}C <$ temperature $\leq 25^{o}C$	4
$15^{o}C <$ temperature $\leq 20^{o}C$	2
$< 15^{o}C$	0

Land Availability

The work of Habib *et al*. (2012) suggested the 5% of total suitable land space. This is also considered for the selected locations.Hence, the suggested weights are given in Table 4.10.

Table 4.10:Allotted Weighted Points for Landmass

Landmass Range	**Allotted Weighted Point**
>2000 km^2 and above	10
1500 $km^2 \leq$ Land size $\leq$ 1999 km^2	8
1000 $km^2 \leq$ Land size $\leq$ 1499 km^2	6
500 $km^2 \leq$ Land size $\leq$ 999 km^2	4
100 $km^2 \leq$ Land size $\leq$ 499 km^2	2
<100 km^2	0

Wind Velocity

Strong wind velocity affects the stability of CSP collectors and its ability to effectively track the Sun. Wind increases the amount of dust deposited on the concentrators, particularly in the desert regions thereby reducing the reflectance of the mirrors (Sansom *et al*., 2014). Furthermore, the cost of CSP system increases with wind speed due to the need for stronger foundation, structures and framework to ensure stability of the system. It has been observed that the operational wind velocity for CSP plants lies between 5 – 8 m/s, while wind velocities above 17.5m/s constitute physical hazard to the mirrors, particularly in locations close to the Sahara Desert (Balza and von Reeken, 2015; Sansom *et al*., 2014).

However, it was also observed that strong winds could improve system efficiency of CSP by convection cooling effect. The force impacting on the collector structure is minimum when the orientation of the collector is parallel to the direction of the wind (Naeeni and Yaghoubi, 2007). It is essential that the proposed CSP plants are properly oriented, to reduce adverse wind effects. Therefore, based on data from NIMET, a lower limit of operational wind velocity of 5m/s and upper limit of 17.5m/s, was used as a benchmark for the allocation of points as indicated in Table 4.11.

Table 4.11:Allotted Weighted Points for Wind Velocity

Wind Velocity Range	Allotted Weighted Point
≤ 5m/s	5
5m/s < wind velocity ≤ 8 m/s	4
8m/s < wind velocity ≤ 11m/s	3
11m/s < wind velocity ≤ 14m/s	2
14m/s < wind velocity ≤ 17.5m/s	1
>17.5m/s	0

Water Sources

The demand for surface water from rivers and lakes in northern Nigeria is very high.In order not to aggravate the living conditions of the populace around the proposed CSP sites, this study shall focus on groundwater as the source of water supply to the proposed CSP plant.The abundance of groundwater in northern Nigeria has been established (JICA and FMWR, 2014). The ratio of groundwater demand to recharge by 2030taking the effect of climate change into consideration in the selected states hosting the locations is highlighted in Table 4.12.

Table 4.12: Ratio of Groundwater Demand to Recharge by 2030 in Selected Parts of Northern Nigeria

State (Location)	Groundwater Demand by 2030 (MCM/year)	Groundwater Recharge (MCM/year)	Ratio of Groundwater Demand to Recharge (%)	Selected Locations for CSP Plant
Borno	278	295	94	Malam-Fatori
Sokoto	207	152	136	Gada
Kebbi	185	965	19	Yelwa
Bauchi	299	2841	11	Gamawa
Katsina	333	405	82	Maiadua
Kano	553	679	81	Danbatta
Zamafara	202	1017	20	Gusau
Adamawa	145	2567	6	Mubi
Kaduna	233	6511	4	Zaria
Yobe	189	265	71	Machina

Source: JICA Project Team/FMWR, 2014

A maximum of five weighted points is allotted based on percentage of groundwater demand to recharge by 2030 because the proposed CSP plant is a dry cooled system. However, it is suggested that the weight of water be increased to 10, while temperature and sunshine durations allotted equal weights of 12.5 for a wet cooled system. In this regard, suggested weights are given in the Table 4.13:

Table 4.13:Allotted Weighted Points for Available Groundwater

% of Groundwater Demand to Recharge	Allotted Weighted Point
0 – 19%	5
20 – 39%	4
40 – 59%	3
60 – 79%	2
80 – 99%	1
≥ 100%	0

The ranking of the selected locations in order of preference for CSP plants is highlighted in Table 4.14.

Table 4.14: Ranking of locations under review for Implementation of CSP Projects

Location	DNI Value (50)	Sunshine Duration (15)	Mean Temperature (15)	Land Availability (10)	Water Availability (5)	Wind Velocity (5)	Total Score (100)	Rank
Malam-Fatori (Borno)	25	9	9	10	1	5	59	1
Machina (Yobe)	20	9	9	8	2	5	53	2
Zaria (Kaduna)	15	9	9	4	5	5	47	3
Maiadua (Katsina)	20	9	9	4	1	3	46	4
Gada (Sokoto)	20	9	9	4	0	4	46	5
Gusau (Zamafara)	15	6	9	6	4	5	45	6
Gamawa (Bauchi)	15	6	9	4	5	5	44	7
Mubi (Adamawa)	15	6	9	2	5	5	42	8
Danbatta (Kano)	15	6	9	4	1	5	40	9
Yelwa (Kebbi)	10	6	9	4	5	5	39	10

An important observation from the study is that the four locations lying between latitudes 13°N and 14°N, which are around the northernmost parts of Nigeria have higher values of DNI compared to the other locations lying within latitudes 10°N – 12°N. These four locations are ranked within the first five positions based on the criteria employed in the study, with Zaria being the only location beneath Latitude 13°N among the top five ranked locations. It can also be observed that the relatively lower groundwater demand to recharge ratio in Kaduna state contributed to the high ranking of Zaria.Although water requirement for the locations in this study was based exclusively on groundwater, availability of surface water could boost the rankings of Maiadua and Gada as well as improve the viability of Malam-Fatori, though it is ranked in the first position. This suggests that prospective CSP plants in Nigeria would likely be more viable if sited within Latitudes 13°N and 14°N and especially in locations with good groundwater reserve.To further determine the suitability of locations in northern Nigeria for CSP application, the study shall investigate the top five ranked locations as highlighted in Table 4.14.

4.4 Determination of Solar Radiation Models

In determining solar radiation models for each of the five locations, the linear, quadratic and cubic variants, based on OLS method of the Angstrom-Page (AP) and Hargreaves-Samani (HS) models were derived for each location using the R Software.

4.4.1 Solar Radiation Model for Malam-Fatori

The Angstrom-Page model based on linear, quadratic and cubic equations are as derived in Equations (4.1), (4.2) and (4.3) respectively:

$$K_T = 0.2075 + 0.3687\frac{n}{N} \quad (4.1)$$

$$K_T = -2.0218 + 6.9102\frac{n}{N} - 4.7325(\frac{n}{N})^2 \quad (4.2)$$

$$K_T = 0.4882 - 4.1882\frac{n}{N} + 11.4746(\frac{n}{N})^2 - 7.8156\ (\frac{n}{N})^3 \quad (4.3)$$

The results of the three regression analyses of the clearness index with the sunshine

duration for Malam-Fatori is in Appendix 2. Summary of the result of the regression analysis from the three equations are highlighted in Table 4.15.

Table 4.15: Regression Statistics of Derived Angstrom-Page Solar Radiation Models forMalam-Fatori

Model	Multiple R	R^2	Adjusted R^2	Standard Error
$K_T = 0.2075 + 0.3687\frac{n}{N}$	0.501868	0.251871	0.249810	0.050558
$K_T = -2.0218 + 6.9102\frac{n}{N} - 4.7325(\frac{n}{N})^2$	0.729993	0.532889	0.530309	0.040005
$K_T = 0.4882 - 4.1882\frac{n}{N} + 11.4746(\frac{n}{N})^2 - 7.8156\ (\frac{n}{N})^3$	0.731866	0.535627	0.531768	0.0399432

Also, the derived monthly mean values of $\frac{n}{N}$ (sunshine fraction), K_T (clearness index), DNI (divided by a factor of 10 for ease of illustration on a plot) and δ are highlighted in Table 4.16.

Table 4.16: Calculated Monthly Mean Values of $\frac{n}{N}$, K_T, DNI and δ

Month	Mean Value of $\frac{n}{N}$	Mean Value of K_T	Mean Value of DNI (kWh/m^2/day)/10	Mean Value of δ
January	0.7035	0.5117	0.646	-20.8471721
February	0.7194	0.5279	0.628	-13.325257
March	0.6651	0.5275	0.619	-2.3891786
April	0.5945	0.4970	0.589	9.49319779
May	0.6801	0.4504	0.573	18.805818
June	0.6399	0.4089	0.488	23.0770588
July	0.5977	0.3689	0.424	21.1014674
August	0.5569	0.3445	0.352	13.2960413
September	0.6011	0.4322	0.477	1.99357263
October	0.7079	0.4739	0.563	-9.8485451
November	0.8008	0.4942	0.645	-19.050509
December	0.7358	0.4426	0.651	-23.095605

Furthermore, the scatter plot of the monthly mean values of $\frac{n}{N}$, K_T and DNI are highlighted in Figure 4.6.

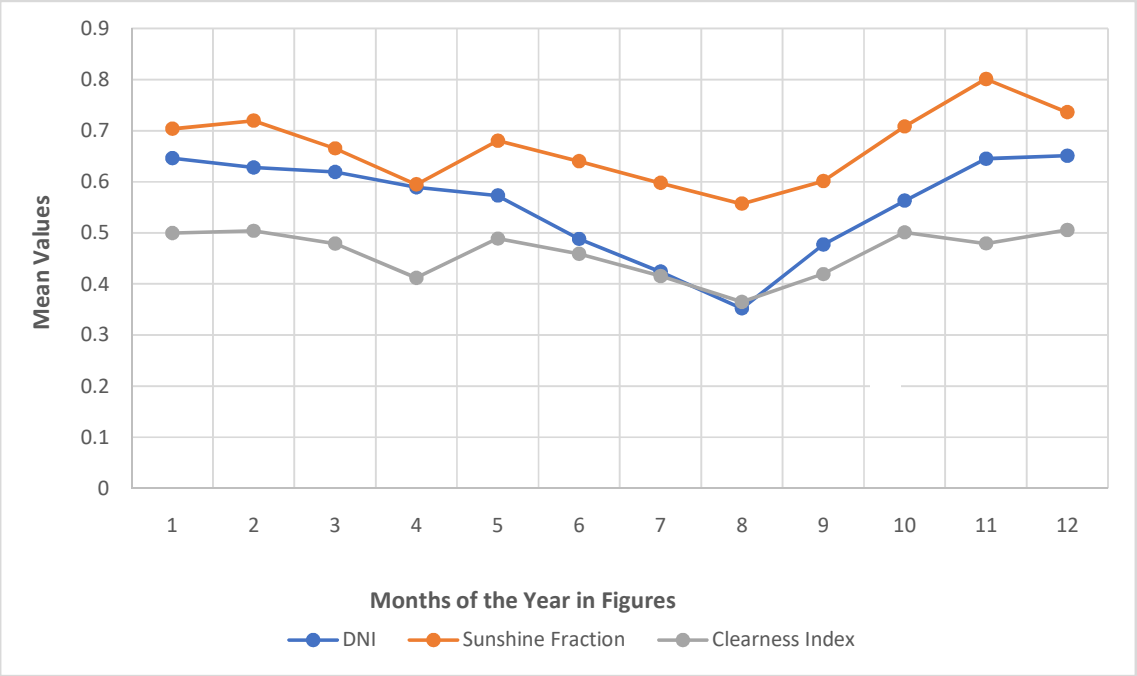

Figure 4.6: Scatter Plot of monthly values of clearness index, sunshine fraction and DNI

Figure 4.6 suggests that there is a direct relationship among the three parameters examined: DNI, clearness index and sunshine fraction. The correlation coefficients of 0.8082, 0.8770 and 0.5945 between $\frac{n}{N}$ and DNI, K_T and DNI, and $\frac{n}{N}$ and K_T respectively, indicated in Table 4.17, confirms the direct (positive) relationship among the three parameters.

Table 4.17: Correlation Coefficients of $\frac{n}{N}$, K_T and DNI

Parameter	$\boldsymbol{\frac{n}{N}}$	$\mathbf{K_T}$	**DNI**
$\boldsymbol{\frac{n}{N}}$	1		
$\mathbf{K_T}$	0.594530791	1	
DNI	0.80822278	0.876959787	1

From the HS model for Malam – Fatori, the linear, quadratic and cubic equations are as derived in Equation (4.4), (4.5) and (4.6) respectively:

$$K_T = 0.0887 + 0.0955\ \Delta T^{0.5} \quad (4.4)$$

$$K_T = -1.0328 + 0.7068\Delta T^{0.5} - 0.0816(\Delta T^{0.5})^2 \quad (4.5)$$

$$K_T = 5.6748 - 4.8476(\Delta T^{0.5}) + 1.4347(\Delta T^{0.5})^2 - 0.1365\ (\Delta T^{0.5})^3 \quad (4.6)$$

The result of the regression analysis from the three HS equations are in Appendix 3. The summary of the result is highlighted in Table 4.18.

Table 4.18: Regression Statistics of Derived HS Solar Radiation Models for Malam-Fatori

Model	Multiple R	R^2	Adjusted R^2	Standard Error
$K_T = 0.0887 + 0.0955\ \Delta T^{0.5}$	0.8582	0.7365	0.7358	0.03
$K_T = -1.0328 + 0.7068\Delta T^{0.5} - 0.0816(\Delta T^{0.5})^2$	0.9039	0.8170	0.8160	0.025
$K_T = 5.6748 - 4.8476(\Delta T^{0.5}) + 1.4347(\Delta T^{0.5})^2 - 0.1365\ (\Delta T^{0.5})^3$	0.9204	0.8472	0.8459	0.0229

Table 4.19 gives the summary of correlation constants, R^2, and adjusted R^2 for the derived AP and HS models.

Table 4.19: Summary of correlation constants, R^2 and Adjusted R^2 for Malam-Fatori.

Model	R^2	Adjusted R^2
$K_T = 0.2075 + 0.3687\frac{n}{N}$	0.2519	0.2498
$K_T = -2.0218 + 6.9102\frac{n}{N} - 4.7325(\frac{n}{N})^2$	0.5329	0.5303
$K_T = 0.4882 - 4.1882\frac{n}{N} + 11.4746(\frac{n}{N})^2 - 7.8156\ (\frac{n}{N})^3$	0.5356	0.5318
$K_T = 0.0887 + 0.0955\ \Delta T^{0.5}$	0.7365	0.7358
$K_T = -1.0328 + 0.7068\Delta T^{0.5} - 0.0816(\Delta T^{0.5})^2$	0.8170	0.8160
$K_T = 5.6748 - 4.8476(\boldsymbol{\Delta T^{0.5}}) + 1.4347(\boldsymbol{\Delta T^{0.5}})^2 - 0.1365\ (\boldsymbol{\Delta T^{0.5}})^3$	0.8472	0.8459

The temperature-based HS model provides better results from the regression analysis relative to the AP model for Malam-Fatori. Furthermore, the cubic equation of the HS model gave the best fit with the data, since it has the highest value of R^2. Equation (4.6) is thus proposed as the solar radiation model for Malam-Fatori.

4.4.2 Solar Radiation Model for Machina

The Angstrom-Page model based on linear, quadratic and cubic equations are as derived in Equations (4.7), (4.8) and (4.9) respectively:

$$K_T = -0.0218 + 0.8393\frac{n}{N} \quad (4.7)$$

$$K_T = -1.7217 + 5.8436\frac{n}{N} - 3.6558(\frac{n}{N})^2 \quad (4.8)$$

$$K_T = -10.3572 + 43.7705\frac{n}{N} - 58.8929(\frac{n}{N})^2 + 26.6815\ (\frac{n}{N})^3 \quad (4.9)$$

The result of the three regression analyses of the clearness index with the sunshine duration for Machina is in Appendix 4.Summary of the result of the regression analysis from the three equations are highlighted in Table 4.20:

Table 4.20: Regression Statistics of Derived Angstrom-Page Solar Radiation Models for Machina

Model	Multiple R	R^2	Adjusted R^2	Standard Error
$K_T = -0.0218 + 0.8393\frac{n}{N}$	0.6944	0.4822	0.4808	0.0514
$K_T = -1.7217 + 5.8436\frac{n}{N} - 3.6558(\frac{n}{N})^2$	0.7177	0.5151	0.5124	0.0498
$K_T = -10.3572+43.7705(\frac{n}{N}) - 58.8929(\frac{n}{N})^2 + 26.6815(\frac{n}{N})^3$	0.7222	0.5215	0.5176	0.0495

From the HS model for Machina, the linear, quadratic and cubic equations are as derived in Equation (4.10), (4.11) and (4.12) respectively:

$$K_T = -0.0445 + 0.1595\ \Delta T^{0.5} \quad (4.10)$$

$$K_T = -1.0273 + 0.6977\Delta T^{0.5} - 0.0727(\Delta T^{0.5})^2 \quad (4.11)$$

$$K_T = 3.3915 - 2.9293(\Delta T^{0.5}) + 0.9129(\Delta T^{0.5})^2 - 0.0887\ (\Delta T^{0.5})^3 \quad (4.12)$$

The result of the regression analysis from the three HS equations for Machina are in Appendix 5;Table 4.21 is the summary of the result.

Table 4.21: Regression Statistics of derived HS Solar Radiation Models for Machina

Model	Multiple R	R^2	Adjusted R^2	Standard Error
$K_T = -0.0445 + 0.1595\ \Delta T^{0.5}$	0.9430	0.8893	0.8890	0.0237
$K_T = -1.0273 + 0.6977\Delta T^{0.5} - 0.0727(\Delta T^{0.5})^2$	0.9516	0.9056	0.9051	0.0220
$K_T = 3.3915 - 2.9293(\Delta T^{0.5}) + 0.9129(\Delta T^{0.5})^2 - 0.0887\ (\Delta T^{0.5})^3$	0.9532	0.9087	0.9079	0.0216

Table 4.22 contains the summary of correlation constants, R^2, and Adjusted R^2 for all derived AP and HS models:

Table 4.22: Summary of correlation coefficient, R^2 and Adjusted R^2 for Machina

Model	R^2	Adjusted R^2
$\mathbf{K_T = -0.0218 + 0.8393\frac{n}{N}}$	0.4822	0.4808
$\mathbf{K_T = -1.7217 + 5.8436\frac{n}{N} - 3.6558(\frac{n}{N})^2}$	0.5151	0.5124
$\mathbf{K_T = -10.3572 + 43.7705\frac{n}{N} - 58.8929(\frac{n}{N})^2 + 26.6815\ (\frac{n}{N})^3}$	0.5215	0.5176
$\mathbf{K_T = -0.0445 + 0.1595\ \Delta T^{0.5}}$	0.8893	0.8890
$\mathbf{K_T = -1.0273 + 0.6977\Delta T^{0.5} - 0.0727(\Delta T^{0.5})^2}$	0.9056	0.9051
$\mathbf{K_T = 3.3915 - 2.9293(\Delta T^{0.5}) + 0.9129(\Delta T^{0.5})^2 - 0.0887(\Delta T^{0.5})^3}$	**0.9087**	**0.9079**

The study also revealed that the temperature-based HS model provides better results from the regression analysis relative to the AP model for Machina. Furthermore, the cubic equation of the HS-based model also gave the best result for the modelled data, since it has the highest value of R^2. Equation (4.12) is proposed as the best model for solar radiation for Machina.

4.4.3 Solar Radiation Model for Zaria

The Angstrom-Page model based on linear, quadratic and cubic equations are as derived in Equations (4.13), (4.14) and (4.15) respectively:

$$K_T = 0.3820 + 0.3264\frac{n}{N} \quad (4.13)$$

$$K_T = -1.1300 + 4.8322\frac{n}{N} - 3.2925(\frac{n}{N})^2 \quad (4.14)$$

$$K_T = -6.7220 + 29.9023\frac{n}{N} - 40.3236(\frac{n}{N})^2 + 18.0255\ (\frac{n}{N})^3 \quad (4.15)$$

The result of the three regression analyses of the clearness index with the sunshine duration for Zaria is in Appendix 6. Summary of the result of the regression analysis from the three equations are highlighted in Table 4.23:

Table 4.23: Regression Statistics of the derived Angstrom-Page Solar Radiation Models forZaria

Model	Multiple R	R^2	Adjusted R^2	Standard Error
$\mathbf{K_T = 0.3820 + 0.3264\frac{n}{N}}$	0.6714	0.4508	0.4493	0.0340
$\mathbf{K_T = -1.1300 + 4.8322\frac{n}{N} - 3.2925(\frac{n}{N})^2}$	0.8794	0.7734	0.7722	0.0219
$\mathbf{K_T = -6.7220 + 29.9023(\frac{n}{N}) - 40.3236(\frac{n}{N})^2 + 18.0255(\frac{n}{N})^3}$	0.9230	0.8520	0.8507	0.0177

From the HS model for Zaria, the linear, quadratic and cubic equations are as derived in Equations (4.16), (4.17) and (4.18) respectively:

$$K_T = 0.2286 + 0.1045\ \Delta T^{0.5} \quad (4.16)$$

$$K_T = -2.1393 + 1.4688\Delta T^{0.5} - 0.1943(\Delta T^{0.5})^2 \quad (4.17)$$

$$K_T = -5.4829 + 4.3570(\Delta T^{0.5}) - 1.0210(\Delta T^{0.5})^2 + 0.0784(\Delta T^{0.5})^3 \quad (4.18)$$

The result of the regression analysis from the three HS equations evaluated for Zaria are in Appendix 7 while Table 4.24 shows the summary of the result.

Table 4.24: Regression Statistics of the derived HS Solar Radiation Models for Zaria

Model	Multiple R	R^2	Adjusted R^2	Standard Error
$K_T = 0.2286 + 0.1045\ \Delta T^{0.5}$	0.8382	0.7026	0.7017	0.0251
$K_T = -2.1393 + 1.4688\Delta T^{0.5} - 0.1943(\Delta T^{0.5})^2$	0.9384	0.8806	0.8800	0.0159
$K_T = -5.4829 + 4.3570(\Delta T^{0.5}) - 1.0210(\Delta T^{0.5})^2 + 0.0784\ (\Delta T^{0.5})^3$	0.9396	0.8829	0.8819	0.0158

Table 4.25 presents summary of the correlation coefficient, R^2 and Adjusted R^2 for all derived AP and HS models.

Table 4.25: Summary of correlation coefficients, R^2 and Adjusted R^2 for Zaria

Model	R^2	Adjusted R^2
$\mathbf{K_T = 0.3820 + 0.3264\frac{n}{N}}$	0.4508	0.4493
$\mathbf{K_T = -1.1300 + 4.8322\frac{n}{N} - 3.2925(\frac{n}{N})^2}$	0.7734	0.7722
$\mathbf{K_T = -6.7220 + 29.9023\frac{n}{N} - 40.3236(\frac{n}{N})^2 + 18.0255(\frac{n}{N})^3}$	0.8520	0.8507
$\mathbf{K_T = 0.2286 + 0.1045\ \Delta T^{0.5}}$	0.7026	0.7017
$\mathbf{K_T = -2.1393 + 1.4688\Delta T^{0.5} - 0.1943(\Delta T^{0.5})^2}$	0.8806	0.8800
$\mathbf{K_T = -5.4829 + 4.3570(\Delta T^{0.5}) - 1.0210(\Delta T^{0.5})^2 + 0.0784(\Delta T^{0.5})^3}$	**0.8829**	**0.8819**

The study also revealed that the temperature-based HS model provides better results from the regression analysis relative to the sunshine-based AP model for Zaria. Furthermore, the cubic equation of the HS-based model also gave the best fit with the data, since it has the highest value of R^2. Equation (4.18) is proposed as the solar radiation model for Zaria.

4.4.4 Solar Radiation Model for Maiadua

The Angstrom-Page model based on linear, quadratic and cubic equations are as derived in Equations (4.19), (4.20) and (4.21) respectively:

$$K_T = -0.0244 + 0.8432\frac{n}{N} \quad (4.19)$$

$$K_T = -1.8013 + 6.0766\frac{n}{N} - 3.8257\left(\frac{n}{N}\right)^2 \quad (4.20)$$

$$K_T = -11.6152 + 49.2025\frac{n}{N} - 66.6787\left(\frac{n}{N}\right)^2 + 30.3861\left(\frac{n}{N}\right)^3 \quad (4.21)$$

The result of the three regression analyses of the clearness index with the sunshine duration for Maiadua is in Appendix 8. Summary of the regression analysis from the three equations are highlighted in Table 4.26:

Table 4.26: Regression Statistics of the derived Angstrom-Page Solar Radiation Models for Maiadua

Model	Multiple R	R^2	Adjusted R^2	Standard Error
$\mathbf{K_T = -0.0244 + 0.8432\frac{n}{N}}$	0.6872	0.4722	0.4707	0.0518
$\mathbf{K_T = -1.8013 + 6.0766\frac{n}{N} - 3.8257(\frac{n}{N})^2}$	0.7113	0.5060	0.5033	0.0502
$\mathbf{K_T = -11.6152 + 49.2025(\frac{n}{N}) - 66.6787(\frac{n}{N})^2 + 30.3861(\frac{n}{N})^3}$	0.7167	0.5136	0.5096	0.0499

From the HS model for Zaria, the linear, quadratic and cubic equations are as derived in Equations (4.22), (4.23) and (4.24) respectively:

$$K_T = -0.0445 + 0.1595\ \Delta T^{0.5} \quad (4.22)$$

$$K_T = -1.0273 + 0.6977\Delta T^{0.5} - 0.0727(\Delta T^{0.5})^2 \quad (4.23)$$

$$K_T = 3.3915 - 2.9293(\Delta T^{0.5}) + 0.9129(\Delta T^{0.5})^2 - 0.0887(\Delta T^{0.5})^3 \quad (4.24)$$

The result of the regression analysis from the three HS equations for Maiadua are in Appendix 9 while the summary of the result is highlighted in Table 4.27.

Table 4.27: Regression Statistics of the derived HS Solar Radiation Models for Maiadua

Model	Multiple R	R^2	Adjusted R^2	Standard Error
$K_T = -0.0445 + 0.1595\ \Delta T^{0.5}$	0.9430	0.8893	0.8890	0.0224
$K_T = -1.0273 + 0.6977\Delta T^{0.5} - 0.0727(\Delta T^{0.5})^2$	0.9516	0.9056	0.9051	0.0220
$K_T = 3.3915-2.9293(\Delta T^{0.5})+0.9129(\Delta T^{0.5})^2-0.0887\ (\Delta T^{0.5})^3$	0.9532	0.9087	0.9079	0.0216

Table 4.28 gives the summary of correlation coefficient, R^2 and Adjusted R^2 for all the derived AP and HS models.

Table 4.28: Summary of correlation coefficient, R^2 and Adjusted R^2 for Maiadua

Model	**R^2**	**Adjusted R^2**
$K_T = -0.0244 + 0.8432\frac{n}{N}$	0.4722	0.4707
$K_T = -1.1803 + 6.0766\frac{n}{N} - 3.8257(\frac{n}{N})^2$	0.5060	0.5033
$K_T = -11.6152 + 49.2025\frac{n}{N} - 66.6787(\frac{n}{N})^2 + 30.3861(\frac{n}{N})^3$	0.5136	0.5096
$K_T = -0.0445 + 0.1595\ \Delta T^{0.5}$	0.8893	0.8890
$K_T = -1.0273 + 0.6977\Delta T^{0.5} - 0.0727(\Delta T^{0.5})^2$	0.9056	0.9051
$K_T = 3.3915 - 2.9293(\boldsymbol{\Delta T^{0.5}}) + 0.9129(\boldsymbol{\Delta T^{0.5}})^2 - 0.0887(\boldsymbol{\Delta T^{0.5}})^3$	0.9087	0.9079

The study also revealed that the temperature-based HS model provides better results from the regression analysis relative to the AP model for Maiadua. Furthermore, the cubic equation of the HS-based model gave the best fit, since it has the highest value of R^2 value. Equation (4.24) is adopted as the solar radiation model for Maiadua.

4.4.5 Solar Radiation Model for Gada

The Angstrom-Page model based on linear, quadratic and cubic equations are as derived in Equations (4.25), (4.26) and (4.27) respectively:

$$K_T = 0.1919 + 0.5201\frac{n}{N} \quad (4.25)$$

$$K_T = 0.5742 - 0.7015\frac{n}{N} + 0.9548(\frac{n}{N})^2 \quad (4.26)$$

$$K_T = 8.3160 - 38.8673\frac{n}{N} + 62.3190(\frac{n}{N})^2 - 32.2793(\frac{n}{N})^3 \quad (4.27)$$

The result of the three regression analyses of the clearness index with the sunshine duration for Gadais in Appendix 10. Summary of the result of the regression analysis from the three equations are highlighted in Table 4.29:

Table 4.29: Regression Statistics of the derived Angstrom-Page Solar Radiation Models for Gada

Model	Multiple R	R^2	Adjusted R^2	Standard Error
$\mathbf{K_T = 0.1919 + 0.5201\frac{n}{N}}$	0.8181	0.6693	0.6684	0.0312
$\mathbf{K_T = 0.5742 - 0.7015\frac{n}{N} + 0.9548(\frac{n}{N})^2}$	0.8364	0.6996	0.6979	0.0298
$\mathbf{K_T = 8.3160 - 38.8673(\frac{n}{N}) + 62.3190(\frac{n}{N})^2 - 32.2793(\frac{n}{N})^3}$	0.9025	0.8146	0.8130	0.0234

From the HS model for Gada, the linear, quadratic and cubic equations are as derived in Equations (4.28), (4.29) and (4.30) respectively:

$$K_T = 0.0835 + 0.1287\ \Delta T^{0.5} \quad (4.28)$$

$$K_T = -0.0562 + 0.2093\Delta T^{0.5} - 0.0115(\Delta T^{0.5})^2 \quad (4.29)$$

$$K_T = -5.8042 + 5.2115(\Delta T^{0.5}) - 1.4536(\Delta T^{0.5})^2 + 0.1377(\Delta T^{0.5})^3 \quad (4.30)$$

The result of the regression analysis from the three HS equations evaluated for Gada are in Appendix 11, while the summary of the result is highlighted in Table 4.30.

Table 4.30: Regression Statistics of the derived HS Solar Radiation Models for Gada

Model	Multiple R	R^2	Adjusted R^2	Standard Error
$\mathbf{K_T = 0.0835 + 0.1287\ \Delta T^{0.5}}$	0.9413	0.8861	0.8858	0.0183
$\mathbf{K_T = -0.0562 + 0.2093\Delta T^{0.5} - 0.0115(\Delta T^{0.5})^2}$	0.9415	0.8865	0.8859	0.0183
$\mathbf{K_T = -5.8042 + 5.2115(\Delta T^{0.5}) - 1.4536(\Delta T^{0.5})^2 + 0.1377(\Delta T^{0.5})^3}$	0.9444	0.8918	0.8909	0.0179

Table 4.31 gives the summary of correlation coefficient, R^2 and Adjusted R^2 values for all the derived AP and HS models.

Table 4.31: Summary of correlation coefficients, R^2 and Adjusted R^2 for Gada

Model	R^2	Adjusted R^2
$\mathbf{K_T = 0.1919 + 0.5201\frac{n}{N}}$	0.6693	0.6684
$\mathbf{K_T = 0.5742 - 0.7015\frac{n}{N} + 0.9548(\frac{n}{N})^2}$	0.6996	0.6979
$\mathbf{K_T = 8.3160 - 38.8673(\frac{n}{N}) + 62.3190(\frac{n}{N})^2 - 32.2793(\frac{n}{N})^3}$	0.8146	0.8130
$\mathbf{K_T = 0.0835 + 0.1287\ \Delta T^{0.5}}$	0.8861	0.8858
$\mathbf{K_T = -0.0562 + 0.2093\Delta T^{0.5} - 0.0115(\Delta T^{0.5})^2}$	0.8865	0.8859
$\mathbf{K_T = -5.8042 + 5.2115(\Delta T^{0.5}) - 1.4536(\Delta T^{0.5})^2 + 0.1377(\Delta T^{0.5})^3}$	**0.8918**	**0.8909**

The study also revealed that the temperature-based HS model provides better results from the regression analysis relative to the AP model for Gada. Furthermore, the cubic equation of the HS-based model gave the best fit with the observed data, since it has the highest value of R^2 values. Equation 4.30 is adopted as the solar radiation model for Gada. Summary of the derived solar radiation models for all the five selected locations are highlighted in Table 4.32.

Table 4.32: Summary of the Derived Solar Radiation Models for the Selected Locations

Location	Derived Solar Radiation Model
Malam-Fatori (Borno)	$K_T = 5.6748 - 4.8476(\Delta T^{0.5}) + 1.4347(\Delta T^{0.5})^2 - 0.1365\ (\Delta T^{0.5})^3$
Machina (Yobe)	$K_T = 3.3915 - 2.9293(\Delta T^{0.5}) + 0.9129(\Delta T^{0.5})^2 - 0.0887\ (\Delta T^{0.5})^3$
Zaria (Kaduna)	$K_T = -5.4829 + 4.3570(\Delta T^{0.5}) - 1.0210(\Delta T^{0.5})^2 + 0.0784(\Delta T^{0.5})^3$
Maiadua (Katsina)	$K_T = 3.3915 - 2.9293(\Delta T^{0.5}) + 0.9129(\Delta T^{0.5})^2 - 0.0887(\Delta T^{0.5})^3$
Gada (Sokoto)	$K_T = -5.8042 + 5.2115(\Delta T^{0.5}) - 1.4536(\Delta T^{0.5})^2 + 0.1377(\Delta T^{0.5})^3$

4.5 Theoretical Determination of Direct Normal Irradiance for the Top Ranked Locations

From Figure 3.1, some of the values obtained as I_{bn} were found to be negative. The negative values were obtained only within the period 6:00p.m to 6:00a.m daily,being periods of low or no solar radiation. The low or no solar radiation within this period is validated byFigure 4.6 where a direct relationship was established among sunshine fraction, clearness index and DNI. Since negative values for the computed DNI were only obtained during periods of low or no solar radiation,the result of the DNIgenerated empirically was therefore validated by the satellite based DNI values. The negative DNI values were discarded in their entirety. The sum of the positive hourly DNI for each day and subsequently for each month and year obtained empirically as well as the satellite-based DNI obtained from EU-PVGIS are indicated in Table 4.33.

Table 4.33: Comparison of Satellite Based and Empirical DNI

Location	**Satellite Based DNI ($kWh/m^2/year$)**	**Theoretical DNI ($kWh/m^2/year$)**
Malam-Fatori	2121.3	2275.7
Machina	2024.3	2347.1
Maiadua	2012.3	2503.3
Gada	2001.6	2385.2
Zaria	1924.3	2407.6

The sum of the positive hourly DNI for each day and subsequently for each month and year obtained empirically as well as the satellite-based DNI obtained from EU-PVGIS both meets the minimum DNI requirement for CSP deployment as indicated in Figure 4.7.

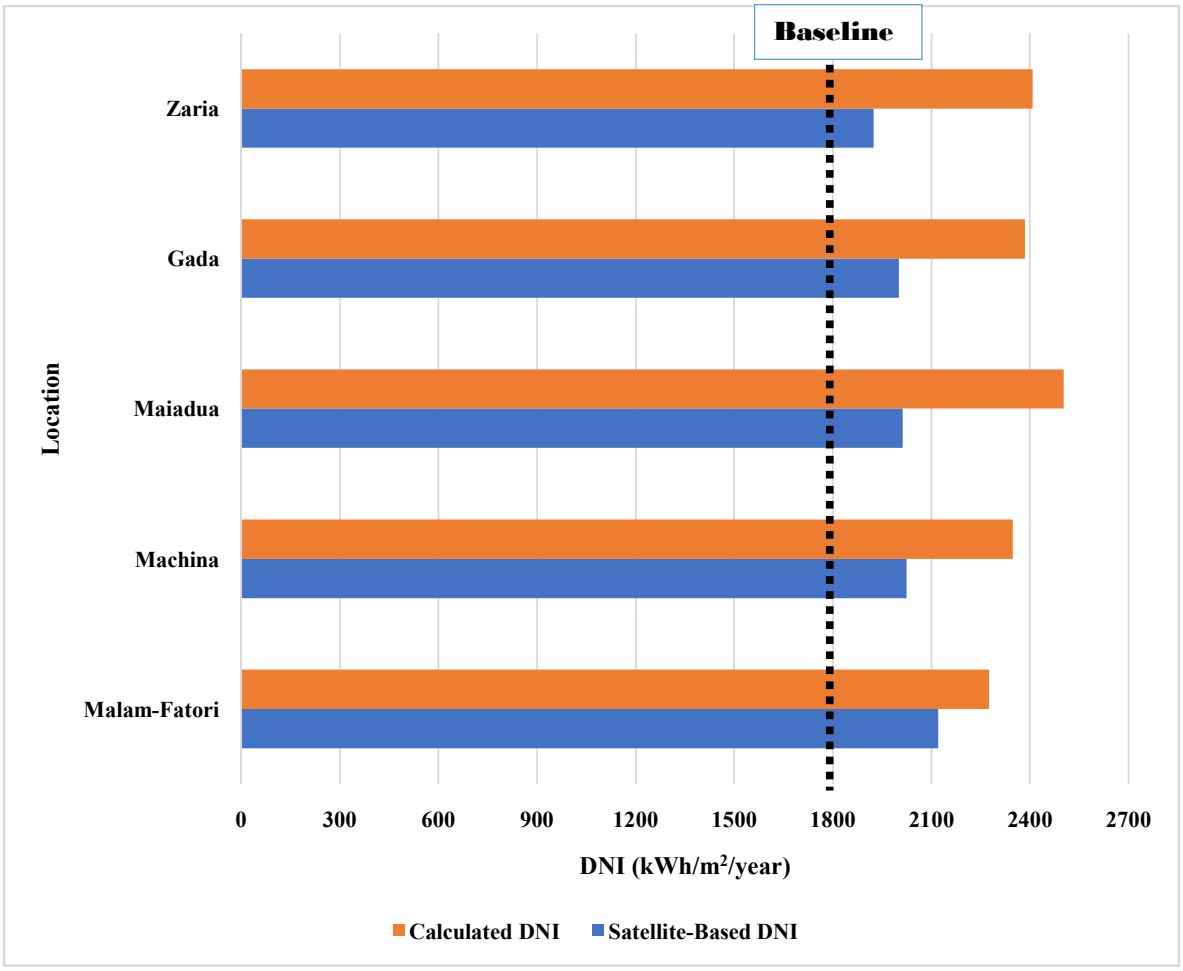

Figure 4.7: Highlight of Calculated vs Satellite-Based DNI

Since the values of the satellite based and empirical DNI of the respective locations meet the minimum requirement for CSP deployment, the locations are considered suitable for the deployment of CSP plants.

4.6 Simulation Results

The results of the simulations of energy outputs and LCOE for each of the top-5 ranked locations under review are discussed subsequently.

4.6.1 Simulation of Relevant Outputs from Malam-Fatori

The simulation of the adopted 100 MW CSP Plant in Malam-Fatori indicated that the plant would run efficiently at the location. The simulation indicated no errors and no warnings as shown in Appendix 12.The results of the simulation for Malam-Fatori indicated annual energy output of 323.48GWh with a capacity factor of 0.37 with LCOE of $0.144/kWh as indicated also in Appendix 12. The simulation also indicated minimum monthly energy output of 25GWh except from June-September as shown also in Appendix 12.

4.6.2 Simulation of Relevant Outputs from Machina

The simulation of the adopted 100MW CSP Plant in Machina indicated six warnings about insufficient temperature to achieve the design boiler pressure input as shown in Appendix 13. Therefore, a 100 MW CSP plant is not recommended for Machina. Rather, a 50MW plant with a boiler operating pressure of 96 Bar; the 100 Barindicated on the NREL SAM, was found unsuitable for the location.The results of the simulation for Machina from a 50MW hypothetical plant indicated annual energy output of 179.17 GWh operating at a capacity factor of 0.41 with LCOE of $0.125/kWh as indicated also in Appendix 13.The simulation also indicated minimum monthly energy output of 13 GWh except for the month of August as highlighted also in Appendix 13.

4.6.3 Simulation of Relevant Outputs fromZaria

The simulation of the adopted 100MW CSP Plant in Zaria indicated four warnings about insufficient temperature to achieve the designed input boiler pressure as shown in Appendix 14.Thus, a 100MW CSP plant is not recommended for Zaria. Rather, a 50MW plant with a boiler operating pressure of 94 bar was found suitable for the location, and not the 100 Bar indicated on the NREL SAM.The results of the simulation for Zaria from a 50MW hypothetical plant indicated annual energy output of 155.71 GWh operating at a capacity factor of 0.36 with LCOE of $0.149/kWh as also indicated in Appendix 14. The simulation also indicated minimum monthly energy output of 13 GWh except for months from May to September as highlighted also in Appendix 14.

4.6.4 Simulation of Relevant Outputs fromMaiadua

The simulation of the adopted 100MW CSP Plant in Maiadua indicated that the plant would run efficiently at that location. The simulation indicated no errors and no warnings as shown in Appendix 15.The results of the simulation for Maiadua indicated annual energy output of 341.70 GWh operating at a capacity factor of 0.39 with LCOE of $0.137/kWh as also indicated in Appendix 15. The simulation also indicated minimum monthly energy output of 25GWh except for the months from June to August (See Appendix 15).

4.6.5 Simulation of Relevant Outputs fromGada

The simulation of the adopted 100MW CSP Plant in Zaria indicated six warnings about insufficient temperature to achieve the design input boiler pressure as shown in Appendix 16. Thus, a 100MW CSP plant is not recommended for Gada. Rather, a 50MW plant with a boiler operating pressure of 95 Bar will be suitable for the location, and not the 100 Bar indicated on the NREL SAM. The results of the simulation for Gada from a 50MW hypothetical plant indicated annual energy output of 170.67 GWh operating at a capacity factor of 0.39 with LCOE of $0.136/kWh as also indicated in Appendix 16. The simulation also indicated minimum monthly energy output of 13GWh except for the months from June to August as highlighted also in Appendix 16.

4.6.6 Summary of Simulation Results

The simulation indicated a solar field of 587 acres (2,376,000m^2) for locations suitable for 100MW plant, while 292 acres (1,182,000m^2) was indicated as the solar field for locations identified as suitable for 50MW. However, the aperture reflective areas for each of the two locations proposed for 100MW plant are 949,888m^2, while those of each location identified for 50MW plants are 472,320m^2,except Machina whose simulated aperture area was 477,568m^2. The two locations identified for the deployment of 100MW CSP plants, Maiadua and Malam-Fatori, could generate a minimum of 25GWh of energy for 9 and 8 months respectively, in a year.Furthermore, the three locations identified for the deployment of 50MW CSP plants including Machina, Gada and Zaria, could generate a minimum of 13 GWh of energy for 11, 9 and 7 months respectively, in a year. Using the annual energy output, LCOE and optimal generation period in a year from simulation, the ranking of the locations suitable for 100 MW CSP plant capacity is highlighted in Table 4.34.

Table 4.34: Ranking of Locations by Simulation of 100MW PTC CSP Plant

Location	Annual Energy Output (GWh)	LCOE ($/kWh)	No of Months with Generation ≥ 25 GWh	Rank
Maiadua	341.70	0.137	9	1
Malam-Fatori	323.48	0.144	8	2

The simulated energy outputs for the proposed 100 MW CSP plants are indicated in Figure 4.8.

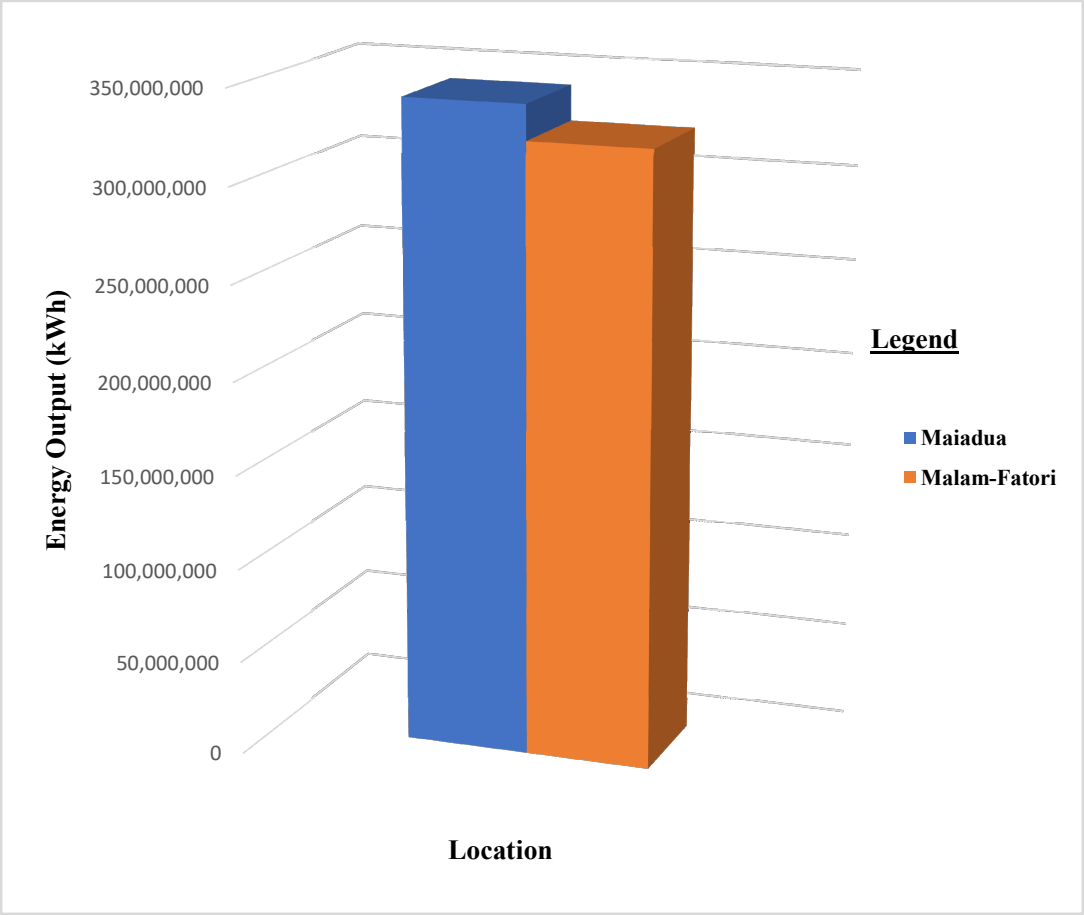

Figure 4.8: Simulated Energy Output from Proposed 100MW CSP Plants at Maiadua and Malam-Fatori.

The ranking of locations suitable for 50 MW CSP plants is indicated at Table 4.35.

Table 4.35: Ranking of Locations by Simulation of 50MW PTC CSP Plant

Location	Annual Energy Output (GWh)	LCOE ($/kWh)	No of Months with Generation ≥ 13 GWh	Rank
Machina	179.18	0.125	11	1
Gada	170.67	0.136	9	2
Zaria	155.71	0.149	7	3

The simulated energy outputs from the proposed 50 MW CSP plants are indicated in figure 4.9.

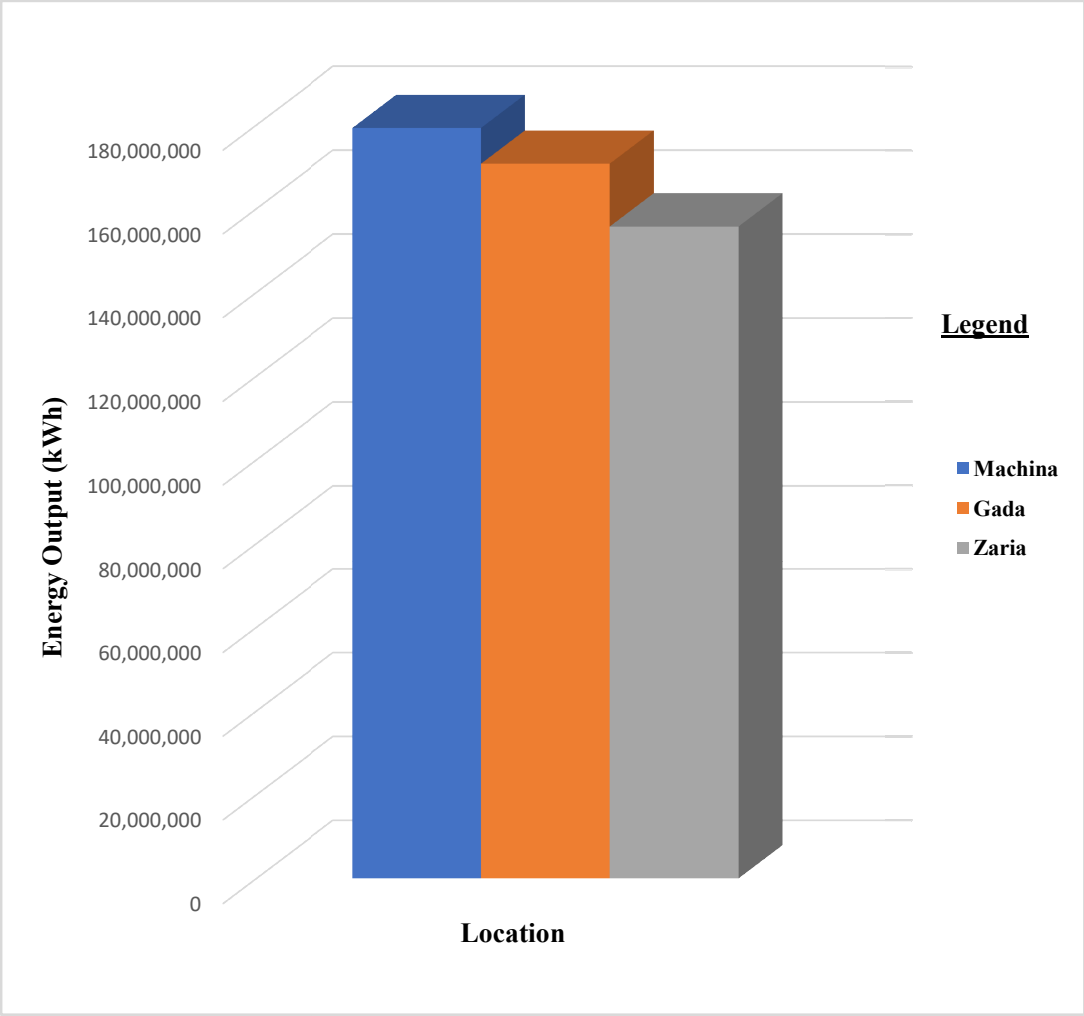

Figure 4.9: Simulated Energy Output from Proposed 50MW CSP Plants at Machina, Gada and Zaria.

4.7 Plant Configuration and Computation of Levelised Cost of Electricity

A dry-cooled CSP is considered more suitable for locations in northern Nigeria because of water limitation as a resource, despite the available groundwater and water bodies like Lake Chad. The design of CSP plant for locations suitable for 100MW CSP plants was based on WorleyParsons' design of a 100MW dry-cooled PTC CSP in Dagget, California, USA, used as a reference plant in NREL SAM (Turchi, 2010).For locations suitable for 50MW CSP plants, the specifications in the NREL SAM were adopted.

The total cost for each plant was categorised into direct, indirect, and operations and maintenance costs. The breakdown of the costs calculated for a 100MW plant in Maiadua and Malam-Fatori are as shown in Appendices 17 and 18 respectively, while the breakdown of costs for a 50MW CSP plant in Machina, Gada and Zaria are in Appendices 19, 20 and 21 respectively. Additionally, the calculated LCOE for Maiadua, Malam-Fatori, Machina, Gada, and Zaria are in Appendices 22-26 respectively. Summary of costs and comparison of calculated, simulated and projected Levelised Cost of Electricity (LCOE) are shown in Table 4.36. Also indicated in Table 4.36 is the derived LCOE, which is the mean of the calculated, simulated and projected LCOE for the respective locations.

Location	Proposed Plant Capacity	Calculated Costs (US$)	Calculated LCOE (US$/kWh)	Simulated LCOE (US$/kWh)	Projected LCOE (US$/kWh)	Derived LCOE (US$/kWh)
Maiadua	100MW	868,743,422.44	0.200	0.137	0.134	0.157
Malam-Fatori	100MW	868,498,428.04	0.212	0.144	0.118	0.158
Machina	50MW	435,328,628.4	0.193	0.125	0.123	0.147
Gada	50MW	432,516,138.49	0.201	0.136	0.126	0.154
Zaria	50MW	432,598,847.54	0.219	0.149	0.127	0.165

Table 4.36: Summary of Calculated Costs and Calculated LCOE

A comparison of the calculated and simulated LCOE for the top-5 rankedlocations (Table 4.36), indicates that the calculated LCOEs for Maiadua, Malam-Fatori, Machina, Gada and Zariaare 31.50%, 32.07%, 35.23%, 32.33% and 31.96% respectively higher than the simulated LCOE of the locations. However, there is smaller disparity between the simulated and projected LCOE of the respective locations.Since the calculated LCOE employed prevailing economic indices in Nigeria, while the projected LCOE gave a global perspective of costs; the average of the three was used as the derived LCOE. The derived LCOE for all the locations was lower than the average LCOE of US $0.184/kWh for solar thermal systems as at 2017 (US DoE, 2017). This indicates that the derived LCOE is viable and could be used for planning purposes in the selected locations. Furthermore, the order of economic viability of the plants based on LCOE are as follows: Machina, Gada, Maiadua, Malam-Fatori, and Zaria.

4.8 Selection of Concentrator, Heat Transfer Fluid and Thermal Energy Storage Medium

The study adopted the Parabolic Trough Concentrator (PTC)technology for the proposed CSP plants owing to the maturity of the technology and its widespread deployment (NREL, 2020). Montes *et al*. (2009) investigated the performance of a 50MW CSP plant by simulating energy outputs at different solar multiples within the range of 1-1.5 and obtained 1.16 as the optimal solar multiple. This study, however, simulated the energy output, levelised cost of electricity (LCOE) and solar field of a 100MW CSP plant,through the SAM,at solar multipleintervals of 0.15 within a range of 1.1-2.0. The study developed typical meteorological year (TMY) data for the locationsinvestigated and adopted the design of the 100MW CSP Reference Plant in California USA,and its 50 MW variant, for the simulations. The simulation results for the selection of solar concentrator and other requirements were based on the derived TMY data of one of the selected locations (Malam-Fatori). The outputs obtained through simulations of the output derivable from three concentrators from different manufacturers (Ogunleye *et. al*, 2020). The concentrators are Sky Fuel Sky Trough 80-mm OD receiver (SF), EuroTrough ET150 (ET)and Siemens SunField 6 (SSF). Relevantcharacteristics of the solar collector assembly (SCA) of the three concentrators whose outputs were simulated are indicated in Table 4.37.

Table 4.37: Characteristics of Selected Parabolic Trough Collectors

PTR Model/Make	SCA Length (m)	SCA Aperture (m)	SCA Aperture Reflective Area (m^2)	Average Focal length (m)	Reflectance	Geometric Accuracy
Sky Fuel Sky Trough	115	6	8	656	0.93	0.952
Siemens SunField 6	95.2	5.776	8	545	0.925	0.968
EuroTrough ET150	150	5.75	12	817.5	0.935	0.98

Source: NREL SAM, 2017

The results of the simulations using the candidate SCAs are shown in Table 4.38.

Table 4.38:Selection Criteria for Solar Concentrator

SM	Energy Output (MWh)			LCOE ($/kWh)			Solar Aperture Area (m^2)		
	SSF	ET	SF	SSF	ET	SF	SSF	ET	SF
1.10	163,267	153,065	168,374	0.2823	0.3008	0.2738	514,480	510,120	524,800
1.25	187,462	177,508	191,926	0.2463	0.2599	0.2407	584,240	582,060	593,024
1.40	211,085	199,288	216,886	0.2192	0.2320	0.2135	654,000	647,460	666,496
1.55	235,735	222,293	241,690	0.1967	0.2084	0.1920	723,760	719,400	734,720
1.70	263,199	246,324	269,524	0.1766	0.1884	0.1726	797,880	791,340	808,192
1.85	289,269	270,185	295,469	0.1610	0.1721	0.1578	867,640	856,740	876,416
2.00	315,360	296,241	323,484	0.1481	0.1574	0.1444	937,400	928,860	949,888

The simulation results (Table 4.38)indicate that the annual energy output obtainable from SF is higher than those of the other three concentrators investigated. Furthermore, the LCOE of SF is lower than those of the other three concentrators for all the solar multiples examined. The simulation results also indicated an inverse relationship between the energy output and LCOE obtained from the various solar concentrators. Although SF had the highest energy output and least LCOE, it however requires about 3% additional land spacecompared to SSF and ET as highlighted in figures 4.10, 4.11 and 4.12, respectively. However, the least LCOEobtainable from SF suggests that the cost of additional land did not diminish the economic viability of SF concentrators.The study therefore proposes the utilisation of SF solar concentrator for potential CSP plants in Malam-Fatori, Borno State Nigeria. The energy output per concentrator at different solar multiples is highlighted at Figure 4.10.

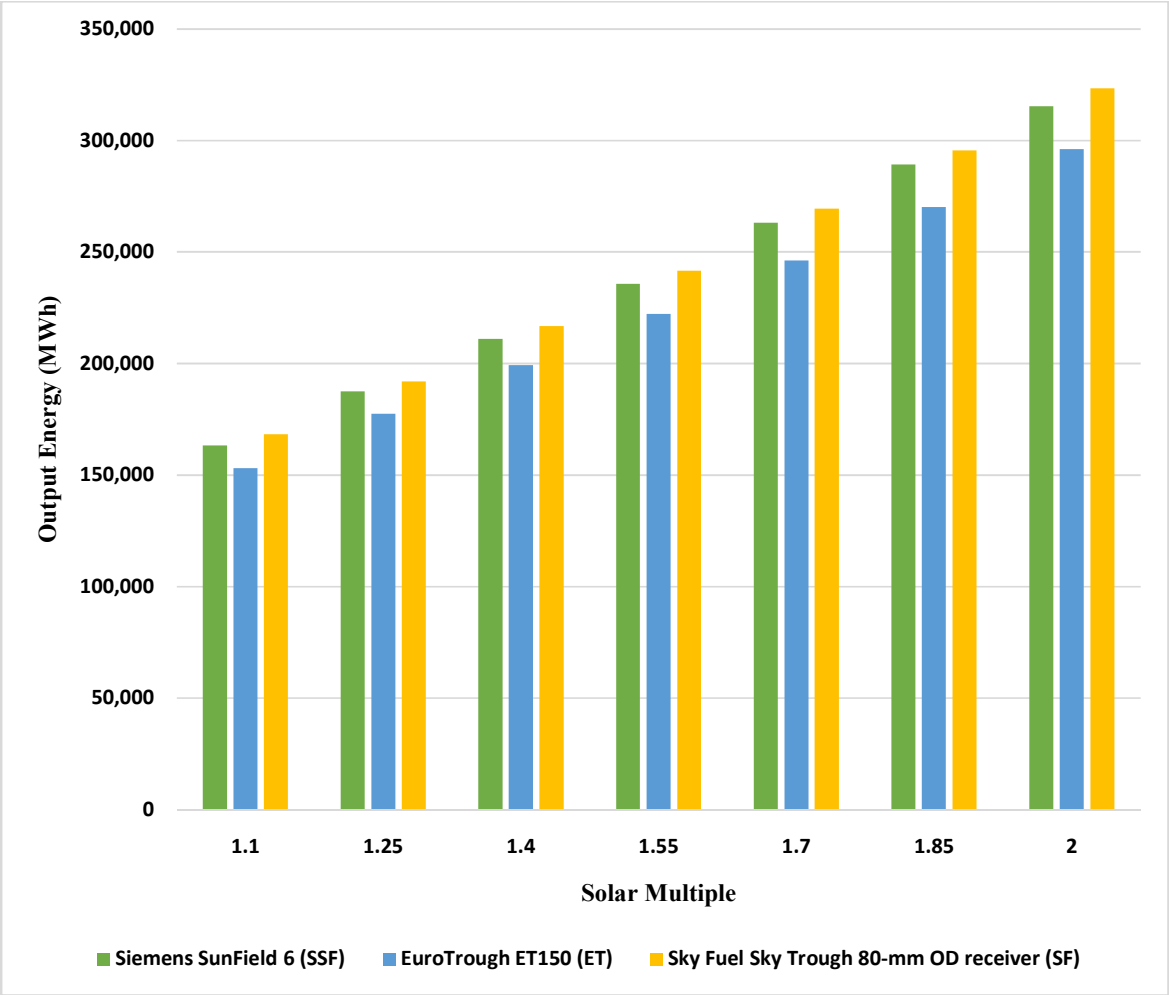

Figure 4.10: Energy output per Concentrator at Different Solar Multiples

The simulated LCOE of concentrators investigated is highlighted at Figure 4.11.

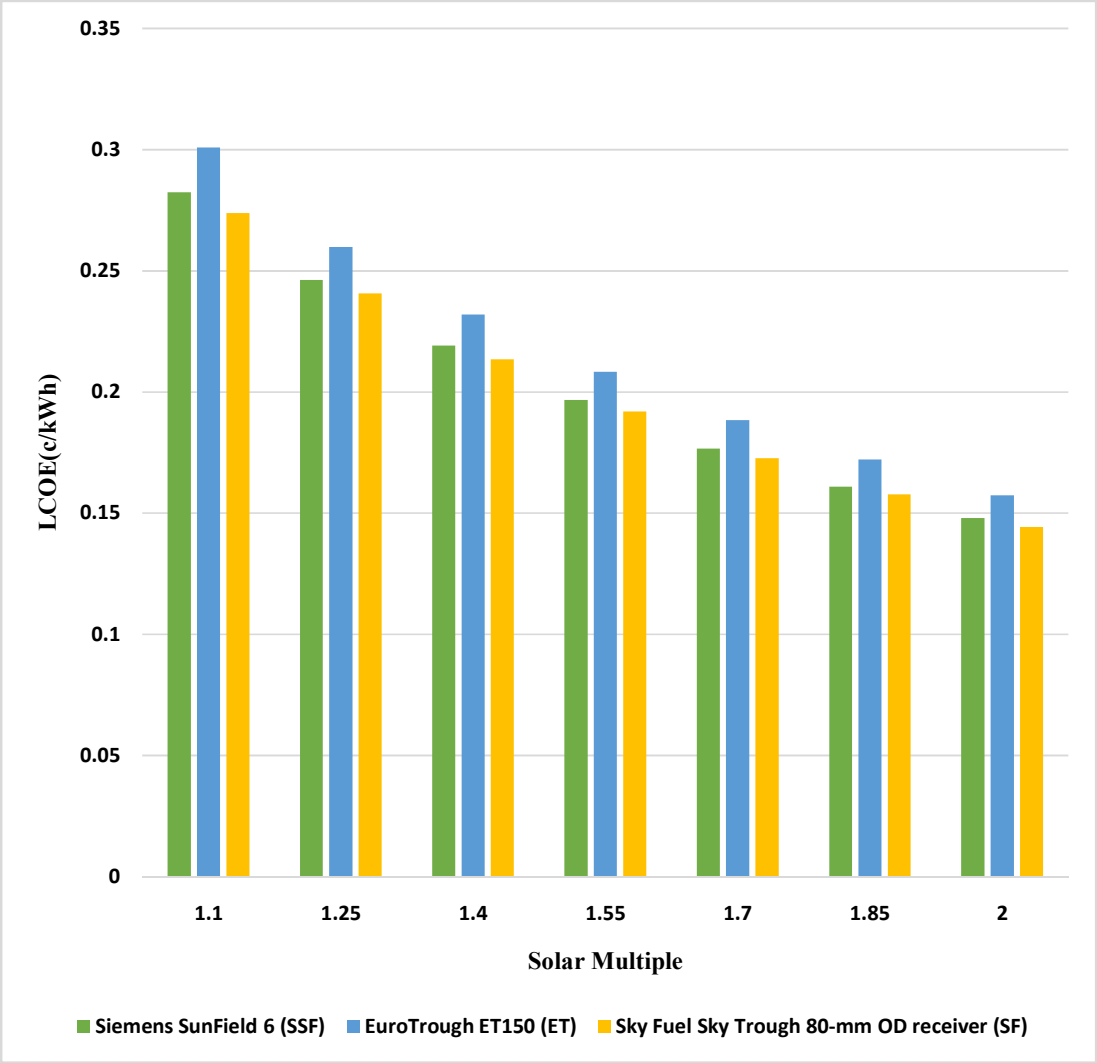

Figure 4.11: Simulated LCOE of Concentrators Investigated.

The simulated solar aperture area for concentrators investigated is indicated at Figure 4.12.

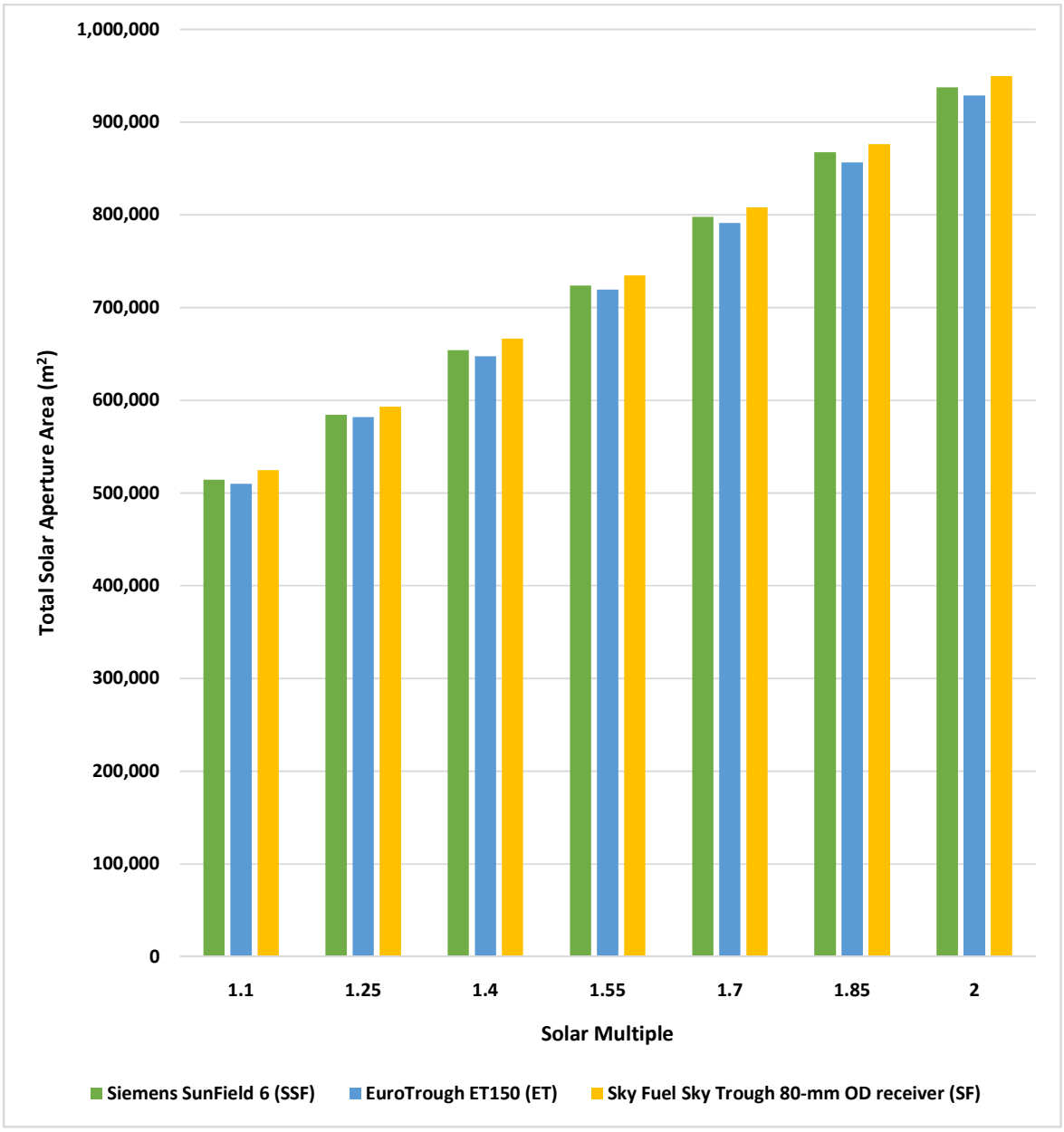

Figure 4.12: Simulated Solar Aperture Area for Concentrators Investigated.

Molten salt and oil were utilised as TES medium and HTF,respectivelyfor the simulation because of their efficient application in PTC CSP technology. Oil has low freezing temperature, below freezing point, while salt remains stable at very high temperatures, above 500^{o}C; these qualities make them suitable as TES medium and HTFrespectively(Kearney *et al*., 2003; Vignaroobane*t al*., 2015). Studies are however investigating the possibility of using molten salt as both TES medium and HTF, particularly in DSGapplications that offers reduced TES cost and enhanced TES performance (Grogan, 2013).

In this regard, the study consideredtwo types of HTF which are Therminol VP-1 and Therminol 59, and four types of TES medium, which are:HITEC Solar Salt, HITEC XL (Eutectic), HITEC XL (low calcium), and HITEC (Ogunleye *et. al*, 2020). Some important characteristics of the two HTF are presented in Table 4.39.

Table 4.39: Comparison of Candidate HTF

	Therminol VP-1	**Therminol 66**
Minimum Operating Temperature	12°C	0°C
Maximum Operating Temperature	400°C	345°C
Solar Field Inlet Temperature	293°C	293°C
Solar Field Outlet Temperature	391°C	391°C
Minimum Field Flow Velocity	0.2686 m/s	0.2703 m/s
Maximum Field Flow Velocity	3.7445 m/s	3.5488 m/s

Source: NREL SAM, 2017.

Some important characteristics of the TES media are presented in Table 4.40.

Table 4.40: Comparison of Candidate TES Medium.

Salt Name	Per Cent Salt Composition				Cover Gas
	$NaNO_3$	KNO_3	$Ca(NO_3)_2$	$NaNO_2$	
HITEC XL (Eutectic)	12	46	42	-	Air (dry, no CO/CO_2)
HITEC XL (Low Calcium)	30	50	20	-	Air (dry, no CO/CO_2)
HITEC (Ordinary)	7	53	-	40	Nitrogen (dry)
Solar Salt (HITEC)	60	40	-	-	Air (dry, no CO/CO_2)

Source: Grogan, 2013.

From Table 4.39, it is evident that the maximum operating temperature and maximum field flow velocity of Therminol VP-1 is higher relative to those of Therminol 66. These upper limits of the parameters are considered more important relative to the lower limits where Therminol 66 has the advantage in view of Nigeria being in a tropical region(Ogunleye *et. al*, 2020). In considering the TES medium, Table 4.40 indicates the presence of corrosive agents that are harmful to the valves, seals and tubes required for CSP system. HITEC XL (Eutectic and low calcium) contain corrosive calcium nitrates [Ca $(NO_3)_2$]andthe bond of their compounds disintegrate significantly at temperatures of about 500^{o}C. The Solar Salt (HITEC) and HITEC (Ordinary) are both suitable for CSP application in Nigeria. The study however adopted Solar Salt (HITEC) due to its higher operating temperature (Grogan, 2013). Therefore, Therminol VP-1 and Solar Salt (HITEC)are adopted as the HTF and TES medium respectively for this study.

4.9 Summary of Discussion

The discussion of results focusses on the meteorological conditions of locations investigated, simulation results and assessed potential of northern Nigeria for deployment of CSP plants.

4.9.1 Meteorological Conditions

The top-5 ranked locations identified for deployment of CSP all satisfy the minimum criteria in terms of DNI value (1800kWh/m^2/year), which is the main criteria for CSP deployment. Other criteria including sunshine duration, ambient temperature and relative humidity were also adequate for CSP deployment. Locations in South Africa have higher levels of DNI relative to locations in Nigeria (maximum of 2924kWh/m^2/year and 2121kWh/m^2/year respectively). They also have relatively higher levels of sunshine duration relative to locations in Nigeria (maximum of 10.49 hours and 8.92 hours respectively). However, correlation analysis of relevant meteorological data of locations investigated in Nigeria with those of locations in South Africa revealed relationship values of about 0.7 for some locations. Moreover, the locations in Nigeria have higher ambient temperatures relative to those in South Africa (Average maximum temperature of about 35^{o}and 30^{o} respectively). These initial findings suggest viability of deploying CSP in parts of northern Nigeria. Consequently, the study proceeded to simulation using the SAM Software.

4.9.2 Simulation Results

The results of simulation using SAM Software indicates that CSP plants would function efficiently in the five selected top-ranked locations in Nigeria. However, only two of the five locations (Malam-Fatori and Machina) were found suitable for the deployment of 100MW CSP plants. The other three locations (Gada, Maiadua and Zaria) could only accommodate 50MW CSP plants based on the meteorological conditions of the locations. The meteorological conditions in the three locations could not generate 100 bar pressure required to activate the 100MW hypothetical plant used for the simulation. This result buttresses the place of DNI as the most important criteria for CSP deployment because Malam-Fatori and Machina higher DNI levels (2121kWh/m^2/year and 2024kWh/m^2/year respectively)relative to those obtainable from Gada, Maiadua and Zaria(2001kWh/m^2/year, 2012kWh/m^2/year and 1924kWh/m^2/year respectively).This suggests that 50MW CSP plants would be more ideal for locations in Nigeria based on prevalent meteorological conditions.

4.9.3 Assessed Potential of Northern Nigeria for Deployment of CSP Plants

The study established the suitability of some locations in northern Nigeria for the deployment of CSP plants. An important observation, however, is that latitudes 13^{o}N and 14^{o}N, which are the northernmost parts of Nigeria are the preferred locations for the deployment of CSP plants in northern Nigeria. This aligns with contemporary practise whereby CSP plants are always located close to desert areas, as obtainable with Xina Solar One CSP Plant in South Africa, located in Pofadder close to the Namib Desert. The Quarzazate Solar Complex in Morocco, comprising the Noor I-IV CSP plants, is also located at the edge of the Sahara Desert (Jezard, 2018). This study thus limits the possible locations for CSP deployment in Nigeria to suitable areas within latitudes 13^{0}N and 14^{0}N for efficient performance of proposed CSP plants in Nigeria.

4.10 Strengths, Weaknesses, Opportunities and Threats(SWOT) Analysis

The simulations and empirical results indicated that some locations in northern Nigeria have good potential for CSP deployment.To further determine the viability of the prospective locations for CSP deployment, it is essential to subject the general area of proposed deployment to analysis using a strategic analytical tool. In this regard, the study employed SWOT analysis to give more insight into the viability of the project in the selected locations. Highlight of the SWOT analysis is given in Table 4.41.

Table 4.41:SWOT Analysis of CSP Deployment inNorthern Nigeria

Strengths	**Weaknesses**
▪ High level of solar resource (DNI) ▪ Long periods of daily sunshine ▪ Availability of large expanse of land ▪ Lower cost of labour relative to other CSP locations (USA, Spain, South Africa). ▪ Lower cost of landlabour relative to other CSP locations (USA, Spain, South Africa). ▪ Relatively competitive for peak load generation ▪ Low operating and maintenance cost relative to non-renewable technologies ▪ Adaptability of system for co-generation with gas ▪ Sustainable means of power generation ▪ Affords higher grid stability relative to Solar PV ▪ Thermal Energy Storage (TES) systems robustly caters for periods of low or no solar radiation	▪ High investment cost ▪ High LCOE ▪ Weak industrial base for the technology ▪ Dusty environment with consequent impact on efficiency of concentrators ▪ Lack of equipment for on-site DNI measurement (Pyrheliometer) ▪ Long distance from seaport to prospective sites ▪ Continuous reduction in cost of solar PV ▪ Non availability of technical and feasibility studies on CSP application in Nigeria ▪ Lack of technical/skilled manpower for CSP deployment in Nigeria
Opportunities	**Threats**
▪ Tran-Sahara gas pipeline as potential for co-generation ▪ Availability of project financing/support options including grant funding, debt financing, equities and guarantees by USAID Power Africa, AfDB, AREF etc. ▪ Global interest/support for renewable energy	▪ Insecurity in Sahel Region and northern Nigeria ▪ Foreign infrastructure and technical support

Deductions from SWOT Analysis

i. The current security situation in northern Nigeria constitutes a huge risk for immediate deployment of CSP in the prospective locations. In this regard, it is essential for the security situation in the region to be relatively stable before the plants are deployed.Moreover, the possibility of deploying the plants close to military locations as much as technically feasible could be considered as a means of enhancing the security of the plants.

ii. The LCOE of the prospective plants is higher than the average cost of electricity in Nigeria based on the current Nigerian Electricity Regulatory Commission (NERC) Multi-Year Tariff Order (MYTO). However, obtained LCOE for the proposed CSP plants relative to the energy charge for the C3 category in the 2021 MYTO of Yola Electricity Distribution Company (YEDC) and Kano Electricity Distribution Company (KEDCO), the electricity distribution companies in the locations of the proposed plants, are quite competitive. The LCOE of 0.137c/kWh obtained for Maiadua for instance, is ₦49.39 at the official exchange rate of ₦360.5 to $1 as at April 2020 (CBN, 2020). The LCOE is thus competitive relative to the ₦56.12/kWh energy charge proposed for the C3 Category of YEDC MYTO for 2021 as highlighted in Appendix27 (NERC, 2020). It is however not competitive relative to the ₦33.66/kWh proposed for same category in KEDCO as highlighted in Appendix28 (NERC, 2020). In this regard, adopting a pricing method based on peak and off-peak periods could enhance the economic viability of the proposed plants since required solar radiation is readily available within the hours of 8a.m to 6p.m, the period for peak load demand. However, government support in the form of power purchase agreement (PPA) and feed-in-tariff (FIT) is essential as a means of encouraging investments in the technology.

iii. Although CSP technology is more expensive relative to other renewable and non-renewable sources, its cost is gradually reducing due to improved technology (Hernandez-Moro and Martínez-Duart, 2012). Additionally, it is essential to further diversify the nation's energy mix as a means of ensuring security of energy supply.

iv. The ability of CSP systems to incorporate TES that robustly caters for periods of low or no solar radiation enhances grid stability. Solar PV technology does not have the capacity to incorporate TES system, hence this is a major strength of CSP technology.

v. Public Private Partnership is proposed as the ownership structure of the prospective CSP plants. This is to ensure efficiency in the running of the plants andmitigate the gap in terms of local technical capacity in infrastructure and skilled manpower. Furthermore, sole private ownership is not advised due to the strategic importance of such plants to the nation.

vi. Local security of the prospective plants could be enhanced if the local populace is part of the ownership of the plants. In this regard, the local population could be encouraged to form a cooperative that would acquire a small percentage, 1 – 2 % of the plant through government instruments like the Bank of Industry. The loan would be repaid from the profit accrued from operating the plant.

4.11 Summary

All the top-5 rankedlocations considered for the deployment of CSP plants in northern Nigeria met the minimum requirement for CSP deployment using available satellite based DNI data and the generated empirical DNI data. These locations were subjected to further analysis where it was established that only two of the locations would be suitable for the deployment of 100MW CSP plants,while the other three locations are suitable for 50MW CSP plants. A SWOT analysis of northern Nigeria for CSP deployment further indicated that the area is viable if the strengths and opportunities are effectively harnessed, while the weaknesses and threats are substantially mitigated.

CHAPTER FIVE
SUMMARY CONCLUSIONAND RECOMMENDATIONS

5.1 Preamble

The study examined selected locations in northern Nigeria to determine their viability for the deployment of PTC CSP plants. The terrain and other meteorological conditions in northern Nigeria, are found to be similar to locations where CSP plants are currently deployed such as that of Northern Cape Province of South Africa. This necessitated the study of potential locations for CSP deployment in Nigeria. Ten locations were selected for assessment; out of these 10 locations, the top five ranked locations were subjected to further analysis to determine their suitability for the establishment of CSP plant. Simulations, empirical derivations, comparative and SWOT analyses were carried out.

5.2 Summary of Findings

The research focussed on investigating the technical and economic viability of CSP in northern Nigeria. This was necessitated by the high level of DNI in northern Nigeria, above baseline of 1800kWh/m^2/year. The DNI obtainable in northern Nigeria was also found to be competitive relative to the DNI of locations where CSP plants are deployed around the world, such as Upington and Pofadder in South Africa. The ability of CSP to provide both grid-tied and distributed power supply that is environmentally friendly and capable of providing power supply for industrial processes brings to fore the need to utilise this technology for power generation. This would be particularly beneficial to the northern parts of Nigeria where poverty levels are relatively higher as the technology would effectively support industrial parks to improve socio-economic activities for improved job creation. It was against this backdrop that the study set out to fulfil the objectives highlighted below to

elucidate the techno-economic potential of northern Nigeria for the deployment of CSP plants. The study addressed four key objectives. Each of the objectives with the respective findings are discussed as follows:

Objective 1: Toconduct a general assessment of potential locations in northern Nigeria to determine suitability for power generation through CSP.
In addressing the objective, the study undertook a general survey of locations in northern Nigeria and selected 10 locations for investigation based on the value of DNI in the respective locations as obtained from the EU-PVGIS Software. Correlation analysis of the DNI values, ambient temperatures and sunshine durations of the selected locations with those of two locations with similar terrain in South Africa, where CSP is currently in operation, was also conducted to assist in determining the suitability of the selected locations. The following were the findings about this objective:

i. All the 10 locations met the minimum criteria of DNI (1800 kWh/m^2/year) for the deployment of CSP plant based using the satellite-based data obtained from EU-PVGIS.

ii. The correlations of these parameters (DNI values, ambient temperatures and sunshine durations) of the selected locations with those of the two locations in South Africa, gave positive values.

iii. The five top-ranked locations all have mean sunshine duration of above 8 hours per day.

iv. Four out of the top five ranked locations, that is, Malam-Fatori, Gada, Maiadua and Machina, are situated withinLatitudes 13°N and 14°N, around the northernmost parts of Nigeria.

v. The locations situated within Latitudes 13°N and 14°N all have higher annual energy output and lower LCOE compared to the location below these latitudes (Zaria) amongst the top five ranked locations.

Objective 2: Establish models for the utilisation of CSP systems in suitable locations in northern Nigeria.

The second objective was addressed by comparing the empirical models obtained through Angstrom-Page and Hargreaves-Samaniexpressions for the top five ranked locations. The model identified as most suitable for each of the locations was determined through the ordinary least square (OLS) method.The models were used to determine the clearness index and empirical derivation of the DNI for each location. The following were the finding about this objective:

i. The cubic model from the Hargreaves-Samani equation was observed to be the most suitable model amongst the three variants of the two models examined for each of the locations.

ii. A direct relationship exists among the DNI, clearness index and the sunshine fraction of the locations investigated.

iii. Among the three variants of concentrators analysed in the study i.e., Sky Fuel Sky Trough 80-mm OD receiver (SF), Siemens SunField 6 (SSF) and EuroTrough ET150 (ET), Sky Fuel Sky Trough 80-mm OD receiver was found to be most suitable concentrator, as it gave the best energy output and the least LCOE.

iv. The preferred HTF was Therminol VP-1 because its higher maximum operating temperature (400^{o}C) and maximum field flow velocity (3.7445 m/s) relative to Therminol 66 (345^{o}C and 3.5488 m/s respectively).

v. Solar Salt (HITEC) was the preferred choice for TES medium among othervarieties of salt examined such as HITEC (Ordinary), HITEC XL (low calcium) and HITEC XL (Eutectic). The decision was based on therelatively higher operating temperature and absence of corrosive calcium nitrates in Solar Salt (HITEC).

Objective 3: Determine the annual electricity outputfrom CSP plants in suitable locations.The following were the findings:

i. Maiadua and Malam-Fatori are suitable for the deployment of 100 MW PTC CSP plant, while Machina, Gada and Zaria are only suitable for the deployment of 50 MW PTC CSP plant.

ii. The estimated annual energy output from the hypothetical CSP plants in Maiadua

and Malam-Fatori are 341.70 GWh and 323.48 GWh, respectively while those of Machina, Gada and Zaria are 179.18GWh, 170.67 GWh and 155.71 GWh, respectively.

Objective 4: Determine the LCOE for CSP plants in suitable locations.The following were the findings:

i. The estimated LCOE of the proposed CSP plants in Maiadua and Malam-Fatori are US$0.157/kWhand US$0.158/kWh,respectively while those of Machina, Gada and Zaria are US$0.147/kWh, US$0.154/kWhand US$0.165/kWh,respectively.

ii. The proposed 50 MW CSP plant in Machina was obtained as the most economically viable CSP plant among the proposed plants for the five locations, based on LCOE.

iii. The order of economic viability of the proposed plants are Machina (50 MW), Gada (50 MW), Maiadua (100 MW), Malam-Fatori (100 MW) and Zaria (50 MW).

5.3 Conclusion

The study undertook a general survey of locations in northern Nigeria with a view to establishing the viability of CSP plants in the region. It was established that PTC CSP plants would function efficiently in five identified locations; two out of these locations were each proposed for the deployment of 100 MW PTC CSP, while the other three locations could each accommodate a 50 MW PTC CSP plant. The security situation in the identified locations is volatile; hence, it may not be feasible to deploy the plants in the short term until when the security situation becomes relatively stable. As a security measure, whenever the plants are to be established, the siting should be as close as possible to military locations. Furthermore, a modality for part ownership by the local communities hosting the plants is essential as a means of enhancing the acceptability of the plants in the proposed locations.

5.4 Recommendations Based on Applications of the Study

The following are recommendations from this study:

i. CSP plants should only be sited within Latitudes 13°N and 14°N in Nigeria.

ii. Prospective CSP plants in northern Nigeria should be sited close to military

locations due to the current state of insecurity in the general area.The deployment of CSP in the proposed locations should only be done when the security situation is relatively stable.

iii. Since the LCOE of the proposed plants is higher than the current electricity cost in Nigeria, the project should be designed to primarily cater for peak load generation using the Pareto Principle as a guide.The model for the proposed project should include the siting of industries and stimulation of SMEs that would mainly be served by the plants. In this regard, the "willing buyer, willing seller" policy of the Federal Government of Nigeria that allows the direct purchase of electricity from generation companies should be implemented for these proposed projects, as a way of stimulating the growth of industries and SMEs in the general area.This would contribute towards addressing insecurity in the northern Nigeria since a nexus has been established between development and security. Furthermore, government support through power purchase agreement (PPA) and feed-in-tariff (FIT) in the short and medium terms is proposed as a means of encouraging investments in CSP and other green energies.

iv. The ownership structure of the proposed CSP plants in northern Nigeria should be a PPP arrangement with the private companies in ownership ofthe majority of the stakes. This proposal is to ensure a more efficient functioning of the plants relative to government ownership structure that has been observed to be usually less efficient in Nigeria. Furthermore, it is also proposed that the local populace (community) hosting the power plant should form part of the ownership, as part of the measures of enhancing security of the plant, through their acceptability of the project.

5.5 Contributions to Knowledge

The following are the contributions to knowledge:

i. **Generation of Empirical Solar Radiation Models for Theoretical Generation of DNI.** The study developed empirical models that could be used to determine parameters such as clearness index, sunshine fraction and subsequently DNI. This could assist in determining the viability of other locations with similar topography and on the same latitude for the deployment of CSP since similar topography and latitudinal relationship are often an indication of strong correlation of solar radiation (Ohunakin, 2013).

ii. **Generation of TMY 3 Data for simulation of potential outputs from CSP plants in northern Nigeria using NREL SAM.** The study has afforded the possibility of simulating energy output and LCOE from potential locations in Nigeria using NREL SAM by evolving a means of generating TMY 3 data.

iii. **Guide for Investment on CSP in Nigeria.** The study identified the general area in northern Nigeria where CSP would be more suitable and viable for exploitation (within latitudes 13°N and 14°N). It also highlighted the potential energy output and LCOE in the potential locations thereby providing focus for further feasibility and technical studies, regarding the deployment of CSP in northern Nigeria.

5.6 Suggestion for Further Work

The impact of hybridizing with co-generation using CSP and gas, leveraging on the proposed Tran Saharan gas pipeline, on the LCOE of proposed CSP plants in northern Nigeria, could be considered for future studies.This suggestion is made because Nigeria has abundant gas reserves, and there is an ongoing gas pipeline project,the Ajaokuta-Kaduna-Kano (AKK) Gas Pipeline. Studies could therefore be undertaken to investigate the viability of CSP-Gas co-generation (hybrid)power plants in northern Nigeria. In this way, the TES medium of the proposed plants could be eliminated while gas could be used to power the thermal plants during periods of low irradiation.This arrangement has great prospects to significantly reduce LCOE of the proposed CSP plants.

REFERENCES

Abdulsalam, D., Mbamali, I., Mamman, M. and Saleh Y.M. 2012. An Assessment of Solar Radiation Patterns for Sustainable Implementation of Solar Home Systems in Nigeria. *American International Journal of Contemporary Research* Vol. 2 No. 6.

Abengoa Solar, 2013. Development of Molten-Salt Heat Transfer Fluid Technology for Parabolic Trough Solar Power Plants. Abengoa Solar Sunshot Conference Project Review: 4-35.

African Development Bank (AfDB). Dec., 2013. Integrated Safeguard Systems: Policy Statement and Operational Safeguards. *Safeguard and Sustainability Series* 1.1: 31-37.

African Development Bank. Dec., 2015. Involuntary Resettlement Policy: Review of Implementation. *Safeguard and Sustainability Series* 1.3: 15 - 26.

Alexopoulos, S. and Hoffschmidt, B. 2017. Advances in solar tower Technology. *WIREs Energy Environ 2016* 6.1: 1-19.

Aliyu, A.S., Dada, J. O. and Adam, I.K. 2015. Current status and future prospects of renewable energy in Nigeria. *Renewable and Sustainable Energy Reviews* 48: 336–346.

Al-Shemmeri, T. 2010. Engineering Thermodynamics. Holland, Tarik Al-Shemmeri&Ventus Publishing, pp. 40-55.

Anon. 2019. Policy research on the imposition of 10% tariff duties on solar components: Making a way for solar in Nigeria. Africa Energy and Utilities Tax Guide. *Renewable Energy Association of Nigeria and RE Stakeholders Publication*.

Retrieved Apr. 10, 2018, fromhttps://ng.boell.org/sites/default/files/uploads/2019/07/final_35_page_-_policy_research_on_the_10_duties_on_solar.pdf.pdf.

Astolfi, M., Alfani, D., Lasala, S. and Macchi, E. 2018. Comparison between ORC and CO_2 Power Systems for the exploitation of Low-Medium Temperature Heat Sources. *Energy* 161:1250-1261.

Balza, M. and von Reeken, F. 2015. Environmental loading conditions for CSP solar fields. *Energy Procedia* 69: 1211 – 1219.

Bishoyi, D. and Sudhakar, K. 2017. Modeling and performance simulation of 100 MW PTC based solar thermal power plant in Udaipur India. *Case Studies in Thermal Engineering*. Volume 10: 216-226. Retrieved Jan. 18, 2018, from http://dx.doi.org/10.1016/j.csite.2017.05.005.

Black & Veatch (B&V) Corporation. 2007. Arizona renewable energy assessment. Final report B&V Project Number 145888: 4-1 – 4-71.Retrieved Nov. 25, 2016, from https://azmemory.azlibrary.gov/digital/collection/statepubs/id/5891/rec/1.

Blanc, P., Espinar, B., Gueder, N., Gueymard, C., Meyer, R., Pitz-Paal, R., Reinhart, B., Renne, D., Sengupta, M., Wald, L. and Wilbert, S. 2014. Direct normal irradiance related definitions and applications: The circumsolar issue. *Solar Energy* 110:561-577. Retrieved Aug. 17, 2019 from https://www.sciencedirect.com/science/article/pii/S0038092X14004824

BP. 2020. Statistical Review of World Energy. Retrieved Aug. 7, 2021 from https://www.bp.com/en/global/corporate/energy-economics/statistical-review-of-world-energy.html

Bravo, J., Casals, X. and Pascua, L. 2007. GIS Approach to the definition of capacity and generation ceilings of renewable energy technologies. *Energy Policy* 35: 4879-4892.

Brooks, D.R. 2012. C Programming: The Essentials for Engineers and Scientists. New York, Springer Science & Business Media, pp. 222.

Breeze. P. 2016, Solar Power Generation. Cambridge, Massachusetts, Academic Press, pp. 25-34.

Carter, R.C., Morgulis, E.D., Dottridge, J. and Agbo, J.U. 1994. Groundwater modelling with limited data: a case study in a semi-arid dune field of North East Nigeria. *Quarterly journal of Engineering Geology* 27: S85-S94.

Cebecauer, T. and Suri, M. 2016. Site-adaptation of Satellite-Based DNI and GHI Time Series: Overview and SolarGIS Approach. *American Institute of Physics Conference Proceedings1734*. Retrieved Aug. 17, 2017, from https://doi.org/10.1063/1.4949234.

Cengel, Y.A. and Boles, M.A. 2005. Thermodynamics: An Engineering Approach, 5th ed, Hightstown, NJ, McGraw-Hill, pp. 752-770.

Chhatbar, K. and Meyer, R. 2011. The Influence of Meteorological Parameters on the Energy Yield of Solar Thermal Power Plants. *SolarPACES 2011 Conference (Concentrating Solar Power and Chemical Energy Systems, 20-23 September 2011 - Granada, Spain*: 1-8. Retrieved May 25, 2016, from https:// http://epic.awi.de/24776/1/Chh2011a.pdf.

Christodoulou, A. and Cullinane, K. 2019. Identifying the Main Opportunities and Challenges from the Implementation of a Port Energy Management System: A SWOT/PESTLE Analysis. *Sustainability* 11, 6046: 1-15.

Chu, Y. 2011. Review and Comparison of Different Solar Energy Technologies. Global Energy Network Institute (GENI). *Heriot-Watt University (Heriot-Watt), ENGINEERIN 6, Mechanical engineering Publication*: 31-52. Retrieved April 19, 2016, from https://www.coursehero.com/file/13369486/Review-and-Comparison-of-Different-Solar-Technologies/.

Corral, N., Anrique, N., Fernandes, D., Parrado, C. and Caceres, G. 2012. Power, placement and LEC evaluation to install CSP plants in northern Chile. *Renewable and Sustainable Energy Review* 16.9: 6678-6685.

Craig, O. 2018. Concentrating Solar Power (CSP) technology adoption in South Africa. PhD. Thesis. Faculty of Engineering. Stellenbosch University, South Africa. iii + 145pp.

Craig, O.O., Brent, A.C. and Dinter, F. 2017. The Current and Future Energy Economics of Concentrating Solar Power (CSP) in South Africa. *South African Journal of Industrial Engineering* 28.3:1-14.

Crowell, B. 2006. *Discover Physics*. Fullerton, California: Light and Matter. Retrieved April 25, 2017, from http://www.lightandmatter.com/dp/dp.pdf.

Dazhia, Y., Jirutitijaroena, P. and Walsh, W.M. 2012. The Estimation of Clear Sky Global Horizontal Irradiance at the Equator. *Energy Procedia* 25: 141 – 148. Retrieved Aug. 25, 2019 from https://www.sciencedirect.com/science/article/pii/S1876610212011812.

Deutsche Gesellschaft für Internationale Zusammenarbeit (GIZ). 2015. The Nigerian

Energy Sector: An Overview with a Special Emphasis on Renewable Energy, Energy Efficiency and Rural Electrification. Retrieved Aug. 7, 2021 fromhttps://s1p.manualzz.com/store/data/008728914.pdf?k=AwAAAXshrsBSAAACWMXSTHQjsbncJT_CIIfcWk1O27U2

DLR Institute of Solar Research. Concentrating solar power (CSP) and parabolic trough technology.Retrieved June 5, 2020, fromhttps://www.dlr.de/sf/en/desktopdefault.aspx/tabid-10436/12676_read-43070/.

Duffie, J.A. and Beckman, W.A. 2013. *Solar Engineering of Thermal Processes*. 4th ed. New Jersey: Wiley.

Eludoyin, O.M., Adelekan, I.O., and Eludoyin, A.O. 2014. Air temperature, relative humidity, climate regionalization and thermal comfort of Nigeria. *International Journal of Climatology*34, 6: 2000-2018.

Environmental Resources Management (ERM). 2017. *Resettlement Action Plan for the Ganjuwa Solar Project, Nigeria. Final Report*. Retrieved Feb. 11, 2019, fromhttps://www3.opic.gov/Environment/EIA/bauchisolar/RAP_June_2017.pdf

Erbs D.G., Klein S.A. and Duffie J.A. 1982. Estimation of the diffuse radiation fraction for hourly, daily and monthly-average global radiation. *Solar Energy* 28.4:293 – 302.

Ernst, M., Thomson, A., Haedrich, I. and Blakers, A. 2016. Comparison of ground-based and satellite-based irradiance data for photovoltaic yield estimation. *Energy Procedia* 92: 546 - 553

European Investment Bank. 2013. *Environmental and Social Handbook*9.0 of 02/12/2013: pp. 52 - 62. Retrieved Jan. 21, 2020, from https://www.academia.edu/21409225/European_Investment_Environmental_and_Social_Handbook

Fadare, D.A. 2010. The Application of Artificial Neural Networks to Mapping of Wind Speed Profile for Energy Application in Nigeria. *Applied Energy* 87: 934–942.

Falobi, E.O. 2019. The Role of Renewables in Nigeria's Energy Policy Mix. *International Association for Energy Economics Energy Forum,*First Quarter 2019.

Federal Ministry of Power (FMP), 2016. National Renewable Energy Action Plans (NREAP) (2015 – 2030).

Fluri, T.P. 2009. The Potential of Concentrating Solar Power in South Africa. *Energy Policy* 37: 5075–5080.

Francis, R.A. 2002. Humidity and Dew Point: Their Effect on Corrosion and Coatings. ACA Annual Conference, Adelaide, Paper 016: 1-10. Retrieved June 20, 2017, from https://www.academia.edu/17021842/Humidity_and_Dew_Point_Their_Effect_on_Corrosion_and_Coatings.

Ganji, D.D., Sedighiamiri, A. andSabzehmeidani, Y. 2018. *Nonlinear Systems in Heat Transfer: Mathematical Modeling and Analytical Methods.* 1st Ed., Amsterdam, Netherlands, Elsevier, pp. 105-151

Gnandesikan, A. and Stouffer, R. J. 2006. Diagnosing atmosphere-ocean general circulation model errors relevant to the terrestrial biosphere using the K¨oppen climate classification, *Geophysical Research Letters*, 33.

Gurel, E. and Tat, M. (2017). SWOT Analysis: A Theoretical Review. *The Journal of International Social Research* 10.51: 994-1006.

Grogan, D. 2013. Public Final Technical Report DE-FC36-08GO18038, Development of Molten Salt HTF for Parabolic CSP Troughs, Abengoa Solar, pp. 4-35. Retrieved June 17, 2019, from https://www.osti.gov/servlets/purl/1090096.

Habib, S.L., Idris, N.A., Ladan, M.J. and Mohammad, A.G. 2012. Unlocking Nigeria's Solar PV and CSP Potentials for Sustainable Electricity Development. *International Journal of Scientific & Engineering Research* 3.5: 1-8.

Hapag-Lloyd AG. Mar., 2016. *Container Specification*: Booklet of Container Specifications: 9-33. Retrieved Oct. 19, 2019, from https://www.hapag-lloyd.com/content/dam/website/downloads/press_and_media/publications/15211_Container_Specification_engl_Gesamt_web.pdf.

Hargreaves, G.H. and Samani, Z.A. 1982. Estimating potential evapotranspiration. *J. Irrig. and Drain Engr*., ASCE, 108(IR3):223-230.

Hayat, M.B, Ali, B., Monyake, K.C., Alagha, L. and Ahmed, N. 2018. Solar energy—A look into power generation, challenges, and a solar-powered future. *International Journal of Energy Research* 2018: 1-9.

Hejase, H.A.N. and Assi, A.H. 2014. Estimation of Global and Diffuse Horizontal Irradiance in Abu Dhabi, United Arab Emirates. *Renewable Energy in the Service of MankindVol II.:Selected Topics from the World Renewable Energy Conference 2014*. A. Sayigh. Ed. Heidelberg: Springer, Cham. 3-14.

Hernandez-Moro, J., and Martínez-Duart, J.M. 2012. CSP electricity cost evolution and grid parities based on the IEA roadmaps. *Energy Policy* 41:184-192.

Ho, J.K.K. 2014. Formulation of a Systemic PEST Analysis for Strategic Analysis. European Academic Research 2.5: 6478-6492.

Hussain, H. A. and Maathe, A.T. 2014. Sustaining thermal power plant production in low water supply regions using cooling towers. *WIT Transactions on Ecology and the Environment* 186:679-690.

Ifediora, C. O., Idoko, O.R. and Nzekwe, J. 2014. Organization's Stability and Productivity: The Role of SWOT Analysis an acronym for Strength, Weakness, Opportunities and Threat. *International Journal of Innovative and Applied Research* 2.9: 23- 32.

Intergovernmental Panel on Climate Change. May 2011. Summary for Policymakers. *IPCC Special Report on Renewable Energy Sources and Climate Change Mitigation*. 5-8 May 2011. Edenhofer, O., Pichs-Madruga, R., Sokona, Y., Seyboth, K., Matschoss, P., Kadner, S., Zwickel, T., Eickemeier, P., Hansen, G., Schlömer, S. and von Stechow, C. Eds. Cambridge University Press, Cambridge, United Kingdom and New York, NY, USA: 60-71.

International Electrotechnical Commission (IEC). 2020. The strategic importance of electrification. Retrieved Aug. 1, 2020, fromhttps://www.iec.ch/smartenergy/importance/.

International Energy Agency (IEA). 2010. *Technology Roadmap: Concentrating Solar Power*. IEA's Renewable Energy Division Publication: 7-38. Retrieved Nov. 7, 2016, from https://www.academia.edu/8150299/Technology_Roadmap_Concentrating_Solar_Power.

International Institute for Environment and Development (IIED). 2012. *Renewable Energy Potential in Nigeria*:Low-carbon approaches to tackling Nigeria's energy poverty. Retrieved Dec. 16, 2019, fromhttps://pubs.iied.org/pdfs/G03512.pdf.

International Renewable Energy Agency (IRENA). 2012. *Renewable Energy Technologies: Cost Analysis Series, Concentrating Solar Power* Vol. 1 Power Sector Issue 2/5: 1-38. Retrieved Apr. 14, 2016, from https://www.irena.org/publications/2013.

International Renewable Energy Agency (IRENA). 2013. *Renewable Power Generation Costs in 2012:* 58-63. Retrieved June 2, 2016, from

https://www.irena.org/publications/2013.

International Renewable Energy Agency (IRENA). 2020. *Renewable Energy Statistics*. Retrieved Dec. 25, 2020, from https://www.irena.org/-/media/Files/IRENA/Agency/Publication/2020/Jul/IRENA_Renewable_Energy_Statistics_2020.pdf

.

Izquierdo, S., Montanes, C., Dopazo, C. and Fueyo, N. 2010. Analysis of CSP plants for the definition of energy policies: The influence on electricity cost of solar multiples, capacity factors and energy storage. *Energy Policy* 38: 6215–6221. Retrieved Sep. 30, 2019 from https://www.sciencedirect.com/science/article/abs/pii/S0301421510004726.

Japan International Cooperation Agency (JICA)/Federal Ministry of Water Resources (FMWR). Jan., 2014. *The Project for Review and Update of Nigeria National Water ResourcesMaster Plan*. Summary Report Vol. 2: 13-25. Retrieved Mar. 15, 2017, from https://openjicareport.jica.go.jp/pdf/12146544.pdf

Jezard, A. 2018. Morocco is building a giant thermosolar farm in the Sahara Desert, World Economic Forum, https://www.weforum.org/agenda/2018/05/morocco-is-building-a-solar-farm-as-big-as-paris-in-the-sahara-desert/

Kalogirou S.A., 2014. *Solar Energy Engineering: Processes and Systems*.2nd ed, Oxford: Academic Press.

Kalvova, J., Halenka, T., Bezpalcova, K., and Nemesova, I. 2003. K¨oppen Climate types in observed and simulated climates, *Science journal on Earth and related environmental sciences*, 47: 185–202.

Kaushik, S.C., Tyagi, S.K., Kumar P. 2017. Finite Time Thermodynamic Analysis of Brayton Cycle. *Finite Time Thermodynamics of Power and Refrigeration Cycles*. Springer, Cham: New Delhi, India. Chapter 3: 37-55.

Kearney, D., Herrmann, U., Nava, P., Kelly, B., Mahoney, R., Pacheco, J. and Price, H. (2003). Assessment of a Molten Salt Heat Transfer Fluid in a Parabolic Trough Solar Field. *Journal of Solar Energy Engineering* 125.2: 170-176.

Khatib, T. and Elmenreich W. 2015. A Model for Hourly Solar Radiation Data Generation from Daily Solar Radiation Data Using a Generalized Regression Artificial Neural Network. *International Journal of Photoenergy* 2015:1-13. Retrieved May 24, 2018, fromhttp://dx.doi.org/10.1155/2015/968024.

Kleidon, A., Fraedrich, K., and Heimann, M. 2000. A green planet versus a desert world: estimating the maximum effect of vegetation on the land surface climate,

Climatic Change 44: 471–493.

Knight, K.M., Klein, S.A. and Duffie J.A. 1991. A methodology for the synthesis of hourly weather data, *Solar Energy* 46: 109-120.

Kottek, M., Grieser, J., Beck, C., Rudolf, B., and Rubel, F. 2006. World Map of the Köppen-Geiger climate classification updated, *MeteorologischeZeitschrift* 15.3: 259-263

Kraemer, S. 2018. Morocco's Noor III Solar Tower CSP to Deliver Power by October, Solar Power and Chemical Energy Systems (SolarPACES).

Lawrence, M.G. 2005. The Relationship between Relative Humidity and the Dewpoint Temperature in Moist Air: A Simple Conversion and Applications. Bulletin of the American Meteorological Society 86, 2: 225-233.

Liu, T., Wang, E., Meng, F., Zhang, F., Zhao, C., Zhang, H. and Zhao, R. 2019. Operation Characteristics and Transient Simulation of an ICE-ORC Combined System. *Applied Sciences* 9, 1639: 1-18.

Liu, B.Y.H. and Jordan, R.C. 1960. The interrelationship and characteristic distribution of direct, diffuse and total solar radiation. *Solar Energy* 4: 1-19

Lloyd, P.J. 2017. The role of energy in development, *Journal of Energy in Southern Africa* 28, 1:54-62.

Lohmann, U., Sausen, R., Bengtsson, L., Cubasch, U., Perlwitz, J., and Roeckner, E. 1993. The K¨oppen climate classification as a diagnostic tool for general circulation models, Clim. Res., 3, 177–193.

Lovegrove, K. and Stein, W. 2012. Introduction to concentrating solar power (CSP) technology. *Concentrating solar power technology: principles, developments and applications*. K. Lovegrove and W. Stein. Eds. Woodhead Publishing Limited: Cambridge, UK. Chapter 1: 3-10.

Lovegrove, K. and Pye, J. 2012 Fundamental principles of concentrating solar power (CSP) systems. *Concentrating solar power technology: principles, developments and applications*. K. Lovegrove and W. Stein. Eds. Woodhead Publishing Limited: Cambridge, UK. Chapter 2: 16-45.

Lubkoll, M. 2011. A Pre-feasibility Study of a Concentrating Solar Power System to Offset Electricity Consumption at the Spier Estate. MSc. Project. Dept. ofMechanical and Mechatronic Engineering. Stellenbosch University. Xiv + 31pp.

Maleki, S.A.M., Hizam H. and Gomes, C. 2017. Estimation of Hourly, Daily and Monthly Global Solar Radiation on Inclined Surfaces: Models Re-Visited. *Energies* 10.134: 1-23.

Mashena, M.E. and Alkishriwi, N.A. 2016. The economics of solar thermal electricity in Libya. *Proceedings of the international Conference on recent advances in Electrical system,Tunisia 2016*. Bouktir, T. and Neji, R. Eds. Retrieved Feb. 22, 2016, from https://journal.esrgroups.org/jes/icraes/CDICRAESFinal/ICRAES16ProcPaper10.pdf. 56-61.

Mason, A. and Reitze, E. 2013. Establishing Bankability for High Performance, Cost Reducing SkyTrough Parabolic Trough Solar Collector. *Energy Procedia* 49: 155-162.

Mastronardo, E. and Coronado, J.M. 2020. High Temperature Chemical Reactions for Thermal Energy Storage.Reference Module in Earth Systems and Environmental Sciences, *Elsevier,*Retrieved Aug. 8, 2021, fromhttps://www.sciencedirect.com/science/article/pii/B9780128197233000020

Merrounia, A.A., Mezrhabb, Ab. and Mezrhaba A. 2013. CSP sites suitability analysis in the Eastern region of Morocco. *Energy Procedia* 49: 2270 – 2279.

Mehta, V.K. and Mehta, R. 2008. Principles of Power Systems. 4th Revised Ed. S. Chand Publications: New Delhi, India. Chapter 1: 1-8.

Meyer, R., Schlecht, M. and Chhatbar, K. 2012. Solar resources for concentrating solar power (CSP) systems. *Concentrating solar power technology: principles, developments and applications*. K. Lovegrove and W. Stein. Eds. Woodhead Publishing Limited: Cambridge, UK. Chapter 3: 68-71.

Mittelman, G. and Epstein, M. 2010. A Novel Power Block for CSP Systems. *Solar Energy* 84: 1761–1771.

Mohammed, Y.S., Mustafa, M.W., Bashir, N. and Ibrahem, I.S.2017. Existing and recommended renewable and sustainable energy development in Nigeria based on autonomous energy and microgrid technologies. *Renewable and Sustainable Energy Reviews*75: 820-838.

Montes, M.J., Abanades, A., Martınez-Val, J.M. and Valdes, M. 2009. Solar multiple optimization for a solar-only thermal power plant, using oil as heat transfer fluid in the parabolic trough collectors. *Solar Energy* 83: 2165–2176.

Moser M., TriebF. and Fichter T., 2013. Potential of Concentrating Solar Power Plants for the Combined Production of Water and Electricity in MENA Countries. *Journal of Sustainable Development of Energy, Water and Environment Systems* 1.2: 122-140.

Naeeni, N. and Yaghoubi, M. 2007. Analysis of wind flow around a parabolic collector (1) fluid flow. *Renewable Energy* 32(11), 1898-1916.

National Bureau of Statistics. 2010. *Annual Abstract of Statistics, 2010*. Retrieved Apr. 30, 2019, from https://nigerianstat.gov.ng/download/71.

National Renewable Energy Laboratory (NREL). 2010. *Parabolic Trough Reference Plant for Cost Modeling with the Solar Advisor Model (SAM)*. Retrieved Mar. 12, 2018, from https://www.nrel.gov/docs/fy10osti/47605.pdf.

National Renewable Energy Laboratory (NREL). 2017. System Advisor Model Version 2017.9.5 r4.

National Renewable Energy Laboratory (NREL). 2018. *Concentrating Solar Power Projects - Ivanpah Solar Electric Generating System.* Retrieved Mar. 10, 2018, from https://solarpaces.nrel.gov/ivanpah-solar-electric-generating-system.

National Renewable Energy Laboratory (NREL). 2020. Concentrating Solar Power Projects. Retrieved June 5, 2020, from https://solarpaces.nrel.gov/

Ngbea, G.T., and Achunike, H.C. 2014. Poverty in Northern Nigeria. *Asian Journal of Humanities and Social Studies* 02.02: 266-272

Nigerian Electricity Regulatory Commission (NERC) Multi-Year Tariff Order (MYTO). 2020. https://nerc.gov.ng/index.php/library/documents/MYTO-2020/.

Nixon, J.D., Dey, P.K. and Davies, P.A. 2010. Which is the best solar thermal collection technology for electricity generation in north-west India? Evaluation of options using the analytical hierarchy process. *Energy* 35.12: 5230-5240. Retrieved June 20, 2018, from https://www.sciencedirect.com/science/article/pii/S0360544210004172.

Nußbaum, S. 2003. Ecological studies on the vegetation of a semi-arid desert following a climatic gradient (Richtersveld, South Africa). PhD. Thesis. Universität zu Köln. 5-28.

Nwokolo, S.C. and Otse, C.Q. 2019. Impact of Sunshine Duration and Clearness Index on Diffuse Solar Radiation Estimation in Mountainous Climate. *Trends in Renewable Energy* 5.3: 307-332.

O'Connel, J.P. and Haile, J.M. 2005. *Thermodynamics: Fundamentals for Application.* 1st ed. Cambridge: Cambridge UP.

Ogunleye, O.A., Diji, C.J. and Abebayo, R.A. 2020. Selection of System Component and Requirements for a Hypothetical Parabolic Trough Concentrated Solar Power Plant in Northern Nigeria. *International Journal of Application or Innovation in Engineering & Management* 9.4: 46-54. Retrieved June 6, 2020, from https://www.ijaiem.org/Volume9Issue4/IJAIEM-2020-04-29-14.pdf.

Ogunmodimu, O. 2012. Potential contribution of solar thermal power to electricity supply in Northern Nigeria. M.Sc. Project. University of Cape Town. xiv + 58pp.

Ogunmodimu, O. and Okoroigwe, E.C. 2018. Concentrating solar power technologies for solar thermal grid electricity in Nigeria: A review. *Renewable and sustainable energy reviews* 90: 104-119.

Ohunakin, O. S., Adaramola, M. S., Oyewola, O. M. and Fagbenle, R. O. 2013. Correlations for Estimating Solar Radiation Using Sunshine Hours and Temperature Measurement in Osogbo, Osun State, Nigeria. *Frontiers in Energy* 7.2: 214-222. Retrieved Apr. 21, 2018, fromhttps://link.springer.com/article/10.1007/s11708-013-0241-2.

Ohunakin, O. S., Adaramola, M. S., Oyewola, O. M., Fagbenle, R. O., Adelekan, D.S., Gill, J. and Abam, F.I. 2018. Photovoltaic performance prediction in Northern Nigeria using generated typical meteorological year dataset. *African Journal of Science, Technology, Innovation and Development* 10.5: 579-591.

Olomiyesan, B.M. and Oyedum, O.D. 2016. Comparative Study of Ground Measured, Satellite-Derived, and Estimated Global Solar Radiation Data in Nigeria. *Journal of Solar Energy* Article ID 8197389: 1-7. Retrieved June 5, 2020, from http://dx.doi.org/10.1155/2016/8197389.

Oyedepo, S.O. 2013. Energy in Perspective of Sustainable Development in Nigeria. *Sustainable Energy* 1. 2: 14-25.

Palenzuela, P., Alarcon-Padilla, D. and Zaragoza G. 2015. *Concentrating Solar Power and Desalination Plants: Engineering and Economics of Coupling Multi-Effect Distillation and Solar Plants*. Switzerland: Spinger. 27-54.

Parrado, C., Marzo, A., Fuentealba, E. and Fernández, A.G. 2016. 2050 LCOE Improvement using New Molten Salts for Thermal Energy Storage in CSP plants. *Renewable and Sustainable Energy Reviews* 57: 505–514.

Patel, V.K., Savsani, V.J., Tawhid, M.A. 2019. Thermal Design and Optimization of Heat Engines and Heat Pumps. In: Thermal System Optimization. Springer, Cham, pp. 99-198, Retrieved Aug. 8, 2021, from https://doi.org/10.1007/978-3-030-10477-1_4

Peatross, J. and Ware, M. 2015. *Physics of Light and Optics*. 5th ed. Utah: Free online textbook. Retrieved Nov. 30, 2019, fromhttps://optics.byu.edu/BYUOpticsBook_2015.pdf

Peel, M. C., Finlayson, B. L., and McMahon, T. A. 2007. Updated world map of the Köppen-Geiger climate classification. *Hydrology and Earth System Sciences* 11.5: 1633-1644. Retrieved Apr. 21, 2016, from https://www.hydrol-earth-syst-sci.net/11/1633/2007/.

Polo, J., Wilbert, S., Ruiz-Arias, J.A., Meyer, R., Gueymard, C., Súri, M., Martín, L., Mieslinger, T., Blanc, P., Grant, I, Boland, J.,Ineichen, P.,Remund, J.,Escobar, R., Troccoli, A.,Sengupta, M.,Nielsen, K.P., Renne, D. and Cebecauer, T. 2016. Preliminary survey on site-adaptation techniques for satellite-derived and reanalysis solar radiation datasets. *Solar Energy*132: 25-37. Retrieved June 5, 2020, from https://www.sciencedirect.com/science/article/abs/pii/S0038092X16001754.

PWC. 2018. *Africa Energy and Utilities Tax Guide 2018*. Retrieved Jan. 15, 2020, fromhttps://www.pwc.com/ng/en/assets/pdf/africa-energy-utilities-tax-guide.pdf.

Razak, A.M.Y. 2007. Industrial Gas Turbines: Performance and Operability. *Thermodynamics of gas turbine cycles.* Woodhead Publishing: Cambridge, UK. Chapter 2: 13-59.

Raziei, T. and Pereira, L.S. 2013. Estimation of ETo with Hargreaves–Samani and FAO-PM temperature methods for a wide range of climates in Iran. *Elsevier: Agricultural Water Management* 121:1-18.

Renewable Energy Policy Network (REN21). 2018. Annual Report 2017. Retrieved Jan. 15, 2020, from https://www.ren21.net/wp-content/uploads/2019/06/REN21_AnnualReport_2017_web.pdf.

Sabri, L. and Benzirar, M. 2015.The Effect of Ambient Conditions on System Efficiency of Concentrated Solar Plants (Parabolic Trough and Central Tower). *International Journal of Application or Innovation in Engineering & Management (IJAIEM)*4.1: 101-105.

Sansom, C., Bhattacharyya, D., Macerol, N. and Comley, P. 2014. A Comparison of Polymer Film and Glass Collectors for Concentrating Solar Power. *Energy Procedia* 49, 209 – 219.

Sawaqed, N.M., Zurigat, Y.H. and Al-Hinai, H. 2005. A step-by-step application of Sandia method in developing typical meteorological years for different locations in Oman. *International Journal of Energy Research* 29:723–737.

Schwerhoff, G. and S. Mouhamadou S. 2017. Financing renewable energy in Africa – Key challenge of the sustainable development goals. *Renewable and Sustainable Energy Reviews* 75: 393–401.

Sengupta, M., Xie Y.,Lopez, A., Habte, A. and Maclaurin,G. 2018. The National Solar Radiation Data Base (NSRDB), *Renewable and Sustainable Energy Reviews*, 51-60. Retrieved June 5, 2020, from https://www.sciencedirect.com/science/article/pii/S136403211830087X.

Sharma, C., Sharma, A.K., Mullick, S.C and Kandpal, T.C. 2015. Assessment of solar thermal power generation potential in India. *Renewable and sustainable Energy Reviews* 42: 902-912.

Sharma, C., Sharma, A.K., Mullick, S.C and Kandpal, T.C. 2016. A Study of the effect of Design Parameters on the Performance of Linear Solar Concentrator-Based Thermal Power Plants in India. *Renewable Energy* 87: 666 – 675.

SIFAX Ports & Cargo (2016). Terminal Tariff as at 20th May 2016. Retrieved July 31, 2019, from http://sifaxgroup.com/wp-content/uploads/2017/06/PCHS-Company-Service-Tariff.pdf.

Smith, J.M., Abbott, M.M.and Van Ness, H.C. 2005. *Introduction to Chemical Engineering Thermodynamics*. 7th ed. New York: McGraw-Hill.

Solargis. 2018. http://solargis.info/doc/_pics/freemaps/1000px/ghi/SolarGIS-Solar-map-Nigeria-en.png

SolarPACES. 2018. CSP Capacity Grew 2% to 5.13 GW in 2017. Retrieved June 5, 2020, from https://www.solarpaces.org/csp-capacity-grew-2-5-13-gw-2017/

Stern, H., de Hoedt, G. and Ernst J. 2000. Objective classification of Australian climates, *Australian Meteorological Magazine* 49: 87-96

Storm, K., 2019. Solar thermal power plant. *Industrial Process Plant Construction Estimating and Man-Hour Analysis*. K. Storm. Ed. Gulf Professional

Publishing: Houston, Texas, USA. Chapter 9: 187-215

Sundaram, S. and Babu, J.S.C. 2014. Theoretical Assessment and Validation of Global Horizontal and Direct Normal Solar Irradiance for a Tropical Climate in India. *Iranica Journal of Energy & Environment* 5.4: 354-368.

Telsnig, T., Eltrop, L., Winkler, H. and Fahl, U. 2013.Efficiency and costs of different concentrated solar power plant configurations for sites in Gauteng and the Northern Cape, South Africa. *Journal of Energy in Southern Africa* 24.1: 77-88.

The Green Optimistic. 2008. Using Solar Power to Change the World. Retrieved June 5, 2020, from https://www.greenoptimistic.com/using-solar-power-to-change-the-world-20080210/.

The Pennsylvania State University. 2018. EME 811 Solar Thermal Energy for Utilities and Industry. Retrieved June 5, 2020, from https://www.e-education.psu.edu/eme811/node/684.

Thomas, D.R. 2006. A General Inductive Approach for Analyzing Qualitative Evaluation Data. *American Journal of Evaluation* 27.2: 237-246.

Thomas, P.F. 2009. The Potential of Concentrating Solar Power in South Africa. *Energy Policy* 37: 5075–5080.

Thompson, J. and Martin, F. 2006. *Strategic Management: Awareness and Change*. 5th ed. London: Cengage Learning.

Transmission Company of Nigeria (TCN). Aug., 2020. Press Release - Power Sector Records New Improved All-Time Peak Of 5,420.30 MW. Retrieved Aug 22, 2020, from https://tcn.org.ng/blog_grid_3.php.

Trieb, F., O'Sullivan, M., Pregger, T., Schillings, C. and Krewitt W. July, 2009. *Characterisation of Solar Electricity Import Corridors from MENA to Europe: Potential, Infrastructure and Cost*. Report of the 7th Framework Programme (FP7) of the European Commission (Theme - Energy-2007-9. 1-01: Knowledge tools for energy-related policy making, Grant agreement no.: 212011). Retrieved March 22, 2019, from https://www.semanticscholar.org/paper/Characterisation-of-Solar-Electricity-Import-from-Trieb-O%E2%80%99Sullivan/004d88650135666ad9e5560ccdba829281dc9b23.

Turchi, C. 2010. Parabolic Trough Reference Plant for Cost Modeling with the Solar Advisor Model (SAM), Technical Report NREL/TP-550-47605 July 2010.

Ubogu, A.E. 2011. The Potentials of Rail-Road Integration for Port-Hinterland Freight Transport in Nigeria. *International Journal for Traffic and Transport Engineering* 1.2: 89 – 107.

United Nations. 2017. The Secretary-General's Advisory Group on Energy and Climate Change (AGECC) Summary Report and Recommendations, 28 April 2010, New York.

United Nations. 2017. Borno State LGAs: Baseline Information for Planners. Retrieved July 17, 2019, from http://earlyrecovery.global/sites/default/files/borno_state_lgaocos.pdf.

United Nations Conference on Trade and Development. 2018. *Review of Maritime Transport*. UNCTAD/RMT/2018: 45-54. Retrieved Aug. 17, 2019, from https://unctad.org/en/PublicationsLibrary/rmt2018_en.pdf.

United Nations Development Program. 2016. Human Development Report 2016, New York.

United Nations Educational, Scientific and Cultural Organization. 2009. Urban Water Security: Managing Risks. B. J. Cisneros, J. B. Rose (eds). Urban Water Series, Vol. 5.

United States Department of Energy. 2017. *Annual Energy Outlook*. Retrieved Oct. 19, 2019, from https://www.eia.gov/outlooks/aeo/pdf/0383(2017).pdf.

United States Department of Energy. 2020. CSP Systems Analysis. Retrieved June 5, 2020, from https://www.energy.gov/eere/solar/csp-systems-analysis

United States Department of Energy Office of Scientific and Technical Information. 2013. *Development of Molten-Salt Heat Transfer Fluid Technology for Parabolic Trough Solar Power Plants*. Public Final Technical Report DE-FC36-08GO18038. Retrieved Sep. 15, 2019, from https://www.osti.gov/biblio/1090096.

Vignarooban, K., Xinhai, X., Arvay, A., Hsu, K. and Kannan, A.M. 2015. Heat transfer fluids for concentrating solar power systems – A review. *Applied Energy* 146: 383–396.

Vignola, F. 2012. GHI Correlations with DHI and DNI and the Effects of Cloudiness on One-Minute Data. *World renewable energy forum*. 621-626.

Wang, M. and Overland, J. E. 2004. Detecting Arctic climate change using K¨oppen climate classification, *Climatic Change*, 67, 43–62.

Weinrebe, G. and Ortmanns, W. 2007. Solar Thermal Power Plants. *Renewable Energy: Technology, Economics and Environment*. M. Kaltschmitt and W. Streicher. Eds. New York: Springer Berlin Heidelberg. Chapter 5: 171-190.

Wilcox, S. and Marion, W. 2008. *Users Manual for TMY3 Data Sets.* National Renewable Energy Laboratory (NREL) Report/Project Number: TP-581-43156. Retrieved June 18, 2016, from https://www.nrel.gov/docs/fy08osti/43156.pdf.

World Bank. 2016. *World's Largest Concentrated Solar Plant Opened in Morocco.* Press release on Feb. 4, 2016.Retrieved Mar. 10, 2018, from https://www.worldbank.org/en/news/press-release/2016/02/04/worlds-largest-concentrated-solar-plant-opened-in-morocco.

World Bank ESMAP. 2011. *Middle East and North Africa Region Assessment of the Local Manufacturing Potential for Concentrated Solar Power (CSP) Projects*. Retrieved Mar. 20, 2020, from http://siteresources.worldbank.org/INTMENA/Resources/CSP-Job-Study-Eng-Sum.pdf.

World Bank Group. 2012. *IFC Performance Standards on Environmental and Social Sustainability*. Performance Standard 5: 31-39.

World Energy Council. 2016. World Energy Resources Solar. Retrieved Sep. 10, 2018, from https://www.worldenergy.org/assets/images/imported/2016/10/World-Energy-Resources-Full-report-2016.10.03.pdf.

World Weather and Climate Information, Retrieved Mar. 9, 2019 from https://weather-and-climate.com/average-monthly-Rainfall-Temperature-Sunshine-in-Nigeria.

WWF-ZA. 2015. *Concentrated solar power: A strategic industrial development opportunity for South Africa*. WWF Technical Report 2015. Retrieved Mar. 18, 2019 from https://dtnac4dfluyw8.cloudfront.net/downloads/concentrated_solar_power_report_final.pdf?14462/Concentrated-Solar-Power---A-strategic-industrial-development-opportunity-for-South-Africa.

Zhang, H.L., Baeyensb, J., Degrevea, J. and Caceresc, G. 2013. Concentrated solar power plants: Review and design methodology. *Renewable and Sustainable Energy Reviews* 22: 466–481.

Zhao, L., Xia, J., Xu, C., Wang, Z., Sobkowiak, L. and Long, C. 2013. Evapotranspiration Estimation Methods in Hydrological Models. *Journal of Geographical Sciences* 23.2: 359-369.

Zhuang, X., Xu, X., Liu, W. and Xu, W. 2019. LCOE Analysis of Tower Concentrating Solar Power Plants Using Different Molten-Salts for Thermal Energy Storage in China, *Energies* 12.1394: 1-17.

APPENDIX 1

PARTIAL SCREENSHOT OF THE GENERATED TMY3 DATA FOR ALL LOCATIONS SHOWING SIMULATION PARAMETERS

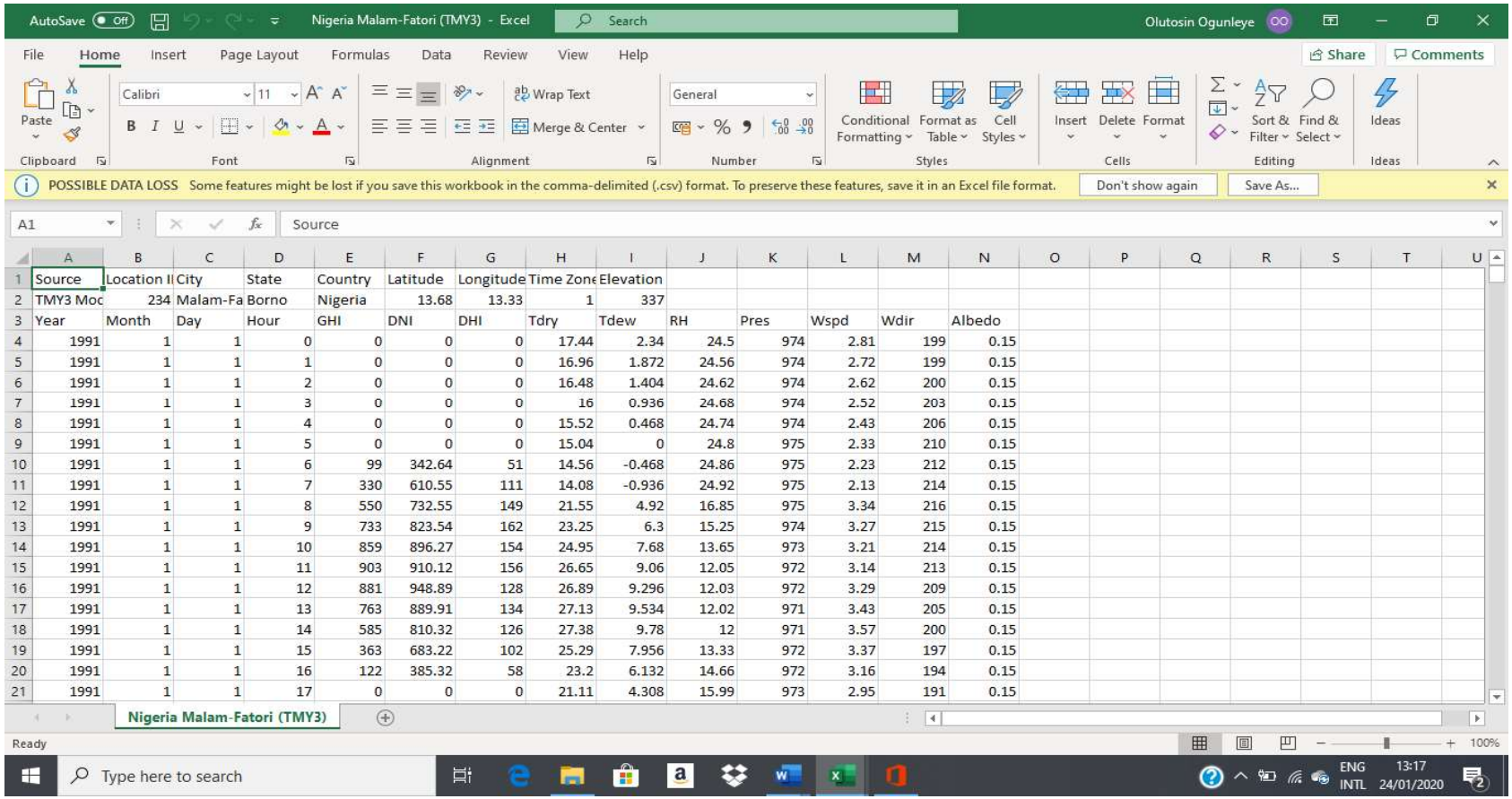

AutoSave Off | Nigeria Malam-Fatori (TMY3) - Excel | Search | Olutosin Ogunleye

File Home Insert Page Layout Formulas Data Review View Help | Share | Comments

Paste | Calibri 11 | Wrap Text | Merge & Center | General | Conditional Formatting | Format as Table | Cell Styles | Insert | Delete | Format | Sort & Filter | Find & Select | Ideas

Clipboard | Font | Alignment | Number | Styles | Cells | Editing | Ideas

POSSIBLE DATA LOSS Some features might be lost if you save this workbook in the comma-delimited (.csv) format. To preserve these features, save it in an Excel file format. Don't show again | Save As...

A1 | Source

	A	B	C	D	E	F	G	H	I	J	K	L	M	N
1	Source	Location II	City	State	Country	Latitude	Longitude	Time Zone	Elevation					
2	TMY3 Moc	234	Malam-Fa	Borno	Nigeria	13.68	13.33	1	337					
3	Year	Month	Day	Hour	GHI	DNI	DHI	Tdry	Tdew	RH	Pres	Wspd	Wdir	Albedo
4	1991	1	1	0	0	0	0	17.44	2.34	24.5	974	2.81	199	0.15
5	1991	1	1	1	0	0	0	16.96	1.872	24.56	974	2.72	199	0.15
6	1991	1	1	2	0	0	0	16.48	1.404	24.62	974	2.62	200	0.15
7	1991	1	1	3	0	0	0	16	0.936	24.68	974	2.52	203	0.15
8	1991	1	1	4	0	0	0	15.52	0.468	24.74	974	2.43	206	0.15
9	1991	1	1	5	0	0	0	15.04	0	24.8	975	2.33	210	0.15
10	1991	1	1	6	99	342.64	51	14.56	-0.468	24.86	975	2.23	212	0.15
11	1991	1	1	7	330	610.55	111	14.08	-0.936	24.92	975	2.13	214	0.15
12	1991	1	1	8	550	732.55	149	21.55	4.92	16.85	975	3.34	216	0.15
13	1991	1	1	9	733	823.54	162	23.25	6.3	15.25	974	3.27	215	0.15
14	1991	1	1	10	859	896.27	154	24.95	7.68	13.65	973	3.21	214	0.15
15	1991	1	1	11	903	910.12	156	26.65	9.06	12.05	972	3.14	213	0.15
16	1991	1	1	12	881	948.89	128	26.89	9.296	12.03	972	3.29	209	0.15
17	1991	1	1	13	763	889.91	134	27.13	9.534	12.02	971	3.43	205	0.15
18	1991	1	1	14	585	810.32	126	27.38	9.78	12	971	3.57	200	0.15
19	1991	1	1	15	363	683.22	102	25.29	7.956	13.33	972	3.37	197	0.15
20	1991	1	1	16	122	385.32	58	23.2	6.132	14.66	972	3.16	194	0.15
21	1991	1	1	17	0	0	0	21.11	4.308	15.99	973	2.95	191	0.15

Nigeria Malam-Fatori (TMY3)

Ready | 100%

Type here to search | ENG INTL 13:17 24/01/2020

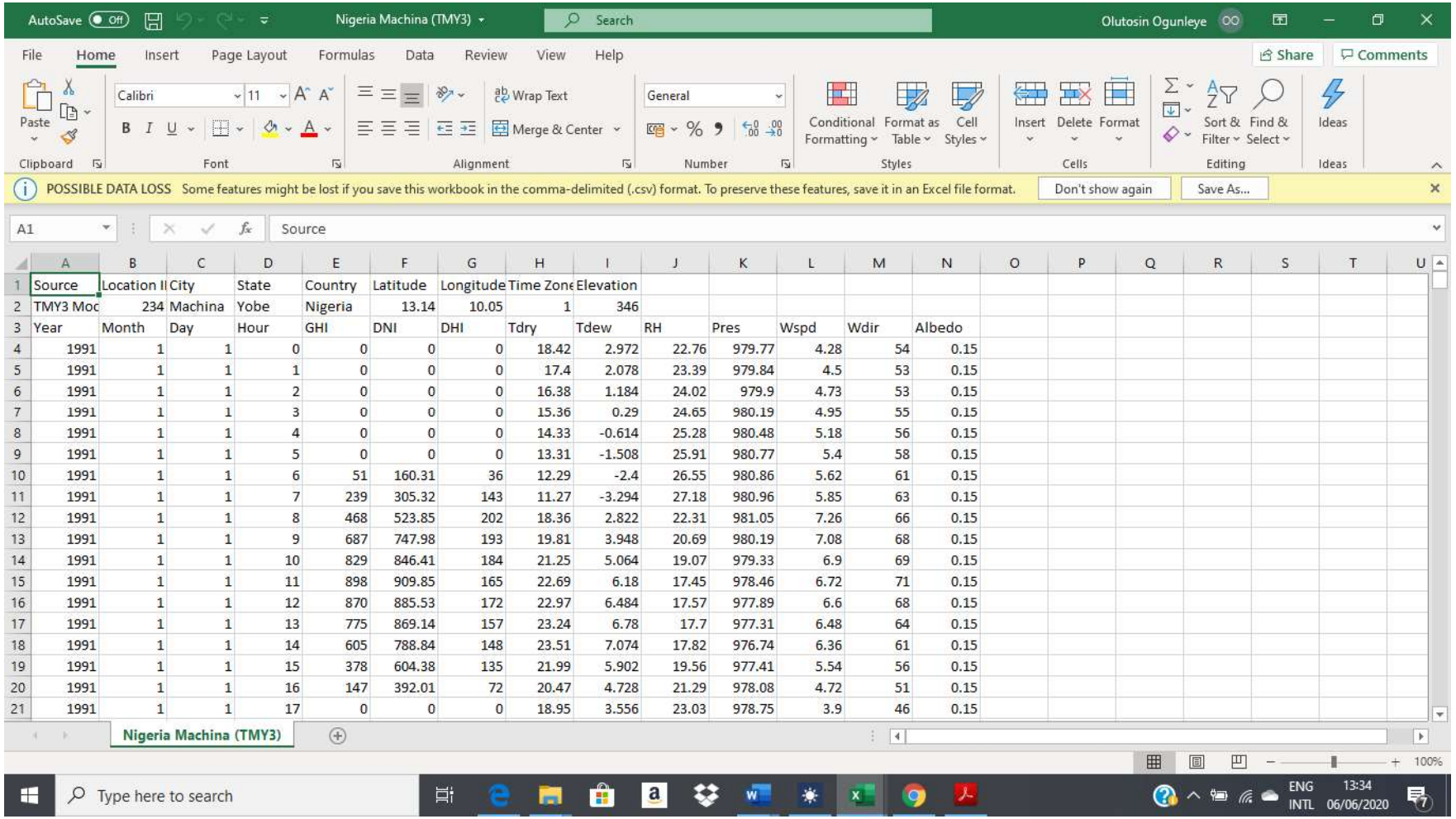

	A	B	C	D	E	F	G	H	I	J	K	L	M	N
1	Source	Location II	City	State	Country	Latitude	Longitude	Time Zone	Elevation					
2	TMY3 Moc	234	Machina	Yobe	Nigeria	13.14	10.05	1	346					
3	Year	Month	Day	Hour	GHI	DNI	DHI	Tdry	Tdew	RH	Pres	Wspd	Wdir	Albedo
4	1991	1	1	0	0	0	0	18.42	2.972	22.76	979.77	4.28	54	0.15
5	1991	1	1	1	0	0	0	17.4	2.078	23.39	979.84	4.5	53	0.15
6	1991	1	1	2	0	0	0	16.38	1.184	24.02	979.9	4.73	53	0.15
7	1991	1	1	3	0	0	0	15.36	0.29	24.65	980.19	4.95	55	0.15
8	1991	1	1	4	0	0	0	14.33	-0.614	25.28	980.48	5.18	56	0.15
9	1991	1	1	5	0	0	0	13.31	-1.508	25.91	980.77	5.4	58	0.15
10	1991	1	1	6	51	160.31	36	12.29	-2.4	26.55	980.86	5.62	61	0.15
11	1991	1	1	7	239	305.32	143	11.27	-3.294	27.18	980.96	5.85	63	0.15
12	1991	1	1	8	468	523.85	202	18.36	2.822	22.31	981.05	7.26	66	0.15
13	1991	1	1	9	687	747.98	193	19.81	3.948	20.69	980.19	7.08	68	0.15
14	1991	1	1	10	829	846.41	184	21.25	5.064	19.07	979.33	6.9	69	0.15
15	1991	1	1	11	898	909.85	165	22.69	6.18	17.45	978.46	6.72	71	0.15
16	1991	1	1	12	870	885.53	172	22.97	6.484	17.57	977.89	6.6	68	0.15
17	1991	1	1	13	775	869.14	157	23.24	6.78	17.7	977.31	6.48	64	0.15
18	1991	1	1	14	605	788.84	148	23.51	7.074	17.82	976.74	6.36	61	0.15
19	1991	1	1	15	378	604.38	135	21.99	5.902	19.56	977.41	5.54	56	0.15
20	1991	1	1	16	147	392.01	72	20.47	4.728	21.29	978.08	4.72	51	0.15
21	1991	1	1	17	0	0	0	18.95	3.556	23.03	978.75	3.9	46	0.15

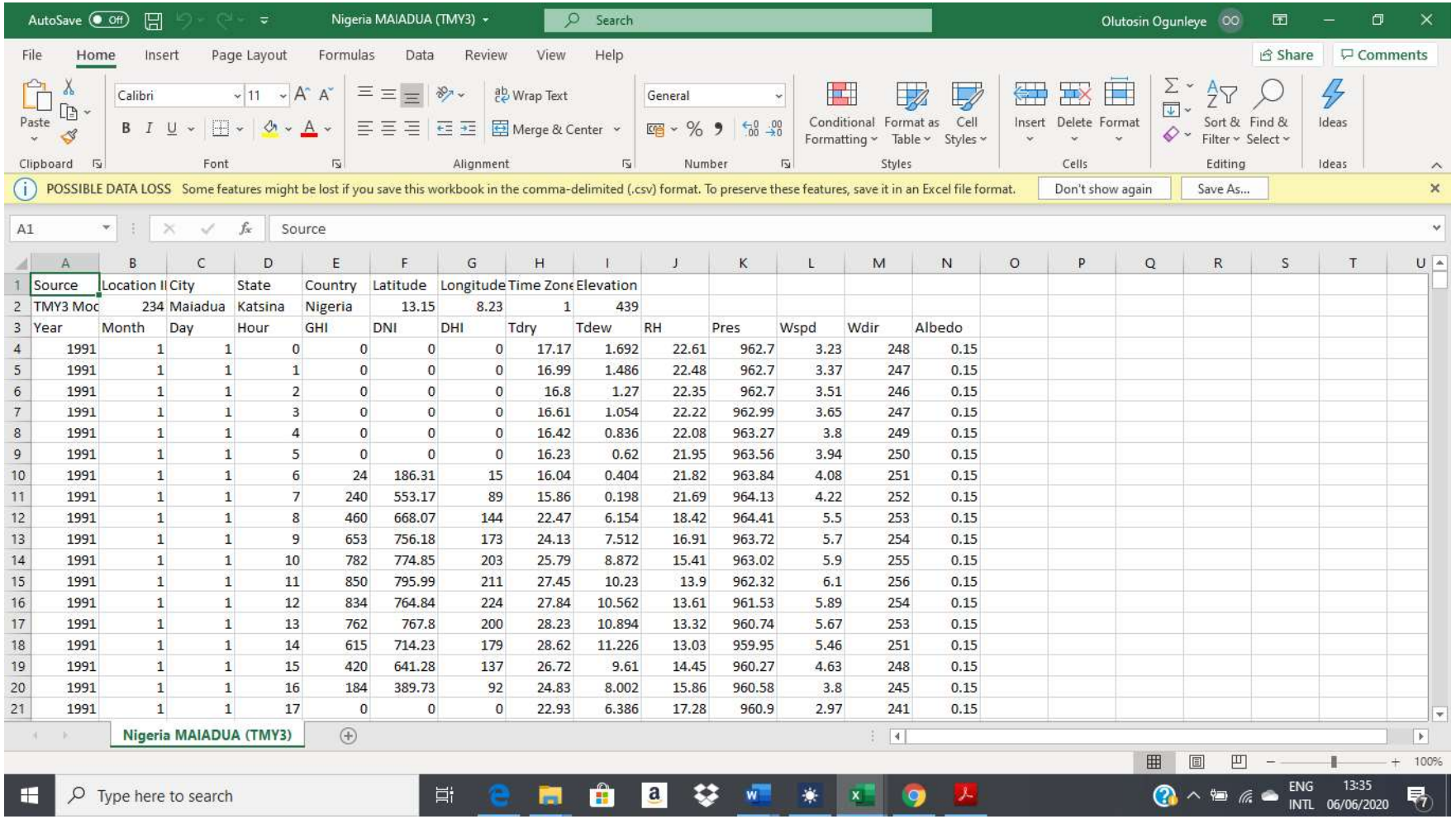

	A	B	C	D	E	F	G	H	I	J	K	L	M	N
1	Source	Location II	City	State	Country	Latitude	Longitude	Time Zone	Elevation					
2	TMY3 Moc	234	Maiadua	Katsina	Nigeria	13.15	8.23	1	439					
3	Year	Month	Day	Hour	GHI	DNI	DHI	Tdry	Tdew	RH	Pres	Wspd	Wdir	Albedo
4	1991	1	1	0	0	0	0	17.17	1.692	22.61	962.7	3.23	248	0.15
5	1991	1	1	1	0	0	0	16.99	1.486	22.48	962.7	3.37	247	0.15
6	1991	1	1	2	0	0	0	16.8	1.27	22.35	962.7	3.51	246	0.15
7	1991	1	1	3	0	0	0	16.61	1.054	22.22	962.99	3.65	247	0.15
8	1991	1	1	4	0	0	0	16.42	0.836	22.08	963.27	3.8	249	0.15
9	1991	1	1	5	0	0	0	16.23	0.62	21.95	963.56	3.94	250	0.15
10	1991	1	1	6	24	186.31	15	16.04	0.404	21.82	963.84	4.08	251	0.15
11	1991	1	1	7	240	553.17	89	15.86	0.198	21.69	964.13	4.22	252	0.15
12	1991	1	1	8	460	668.07	144	22.47	6.154	18.42	964.41	5.5	253	0.15
13	1991	1	1	9	653	756.18	173	24.13	7.512	16.91	963.72	5.7	254	0.15
14	1991	1	1	10	782	774.85	203	25.79	8.872	15.41	963.02	5.9	255	0.15
15	1991	1	1	11	850	795.99	211	27.45	10.23	13.9	962.32	6.1	256	0.15
16	1991	1	1	12	834	764.84	224	27.84	10.562	13.61	961.53	5.89	254	0.15
17	1991	1	1	13	762	767.8	200	28.23	10.894	13.32	960.74	5.67	253	0.15
18	1991	1	1	14	615	714.23	179	28.62	11.226	13.03	959.95	5.46	251	0.15
19	1991	1	1	15	420	641.28	137	26.72	9.61	14.45	960.27	4.63	248	0.15
20	1991	1	1	16	184	389.73	92	24.83	8.002	15.86	960.58	3.8	245	0.15
21	1991	1	1	17	0	0	0	22.93	6.386	17.28	960.9	2.97	241	0.15

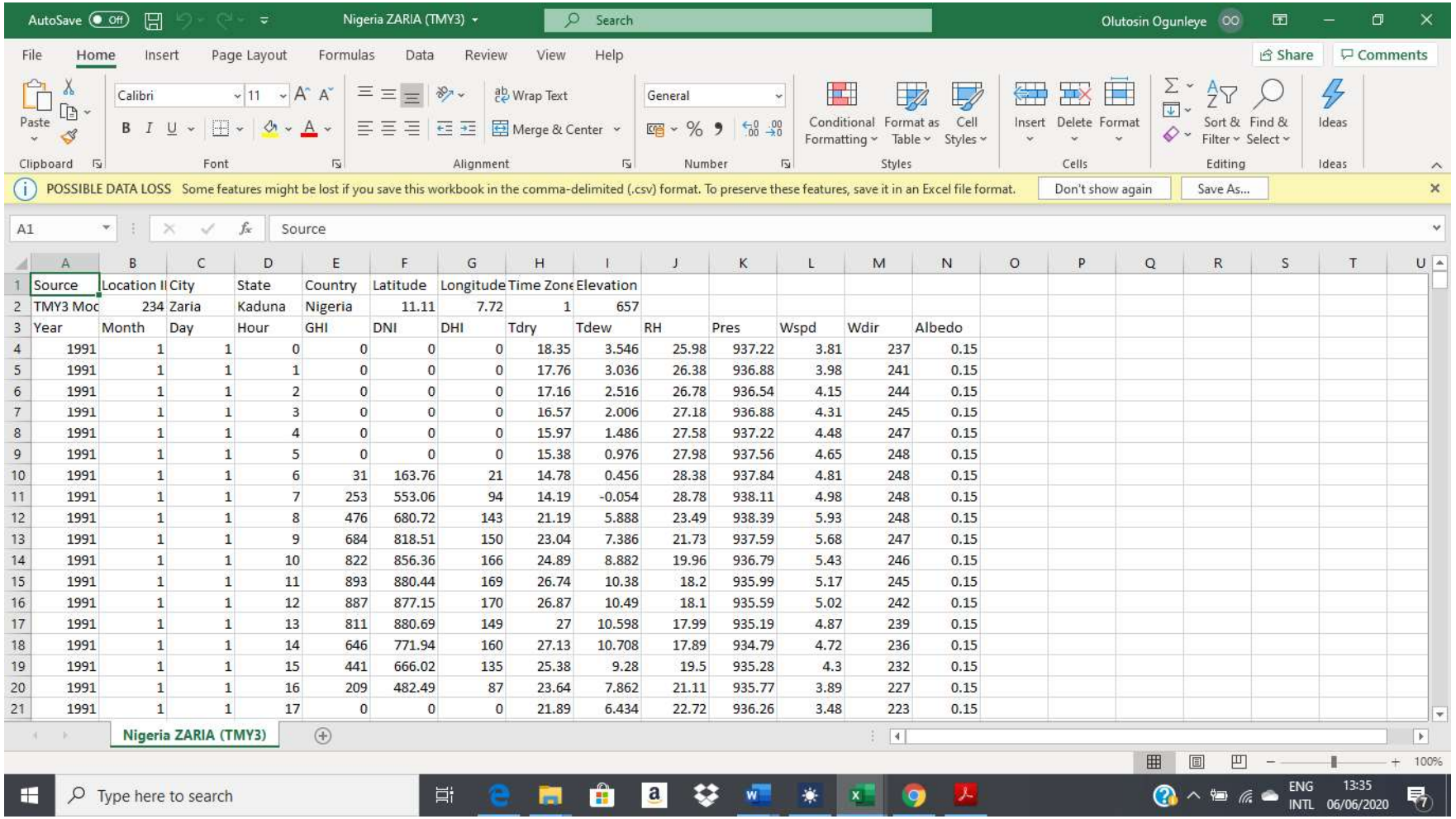

	A	B	C	D	E	F	G	H	I	J	K	L	M	N
1	Source	Location II	City	State	Country	Latitude	Longitude	Time Zone	Elevation					
2	TMY3 Moc	234	Zaria	Kaduna	Nigeria	11.11	7.72	1	657					
3	Year	Month	Day	Hour	GHI	DNI	DHI	Tdry	Tdew	RH	Pres	Wspd	Wdir	Albedo
4	1991	1	1	0	0	0	0	18.35	3.546	25.98	937.22	3.81	237	0.15
5	1991	1	1	1	0	0	0	17.76	3.036	26.38	936.88	3.98	241	0.15
6	1991	1	1	2	0	0	0	17.16	2.516	26.78	936.54	4.15	244	0.15
7	1991	1	1	3	0	0	0	16.57	2.006	27.18	936.88	4.31	245	0.15
8	1991	1	1	4	0	0	0	15.97	1.486	27.58	937.22	4.48	247	0.15
9	1991	1	1	5	0	0	0	15.38	0.976	27.98	937.56	4.65	248	0.15
10	1991	1	1	6	31	163.76	21	14.78	0.456	28.38	937.84	4.81	248	0.15
11	1991	1	1	7	253	553.06	94	14.19	-0.054	28.78	938.11	4.98	248	0.15
12	1991	1	1	8	476	680.72	143	21.19	5.888	23.49	938.39	5.93	248	0.15
13	1991	1	1	9	684	818.51	150	23.04	7.386	21.73	937.59	5.68	247	0.15
14	1991	1	1	10	822	856.36	166	24.89	8.882	19.96	936.79	5.43	246	0.15
15	1991	1	1	11	893	880.44	169	26.74	10.38	18.2	935.99	5.17	245	0.15
16	1991	1	1	12	887	877.15	170	26.87	10.49	18.1	935.59	5.02	242	0.15
17	1991	1	1	13	811	880.69	149	27	10.598	17.99	935.19	4.87	239	0.15
18	1991	1	1	14	646	771.94	160	27.13	10.708	17.89	934.79	4.72	236	0.15
19	1991	1	1	15	441	666.02	135	25.38	9.28	19.5	935.28	4.3	232	0.15
20	1991	1	1	16	209	482.49	87	23.64	7.862	21.11	935.77	3.89	227	0.15
21	1991	1	1	17	0	0	0	21.89	6.434	22.72	936.26	3.48	223	0.15

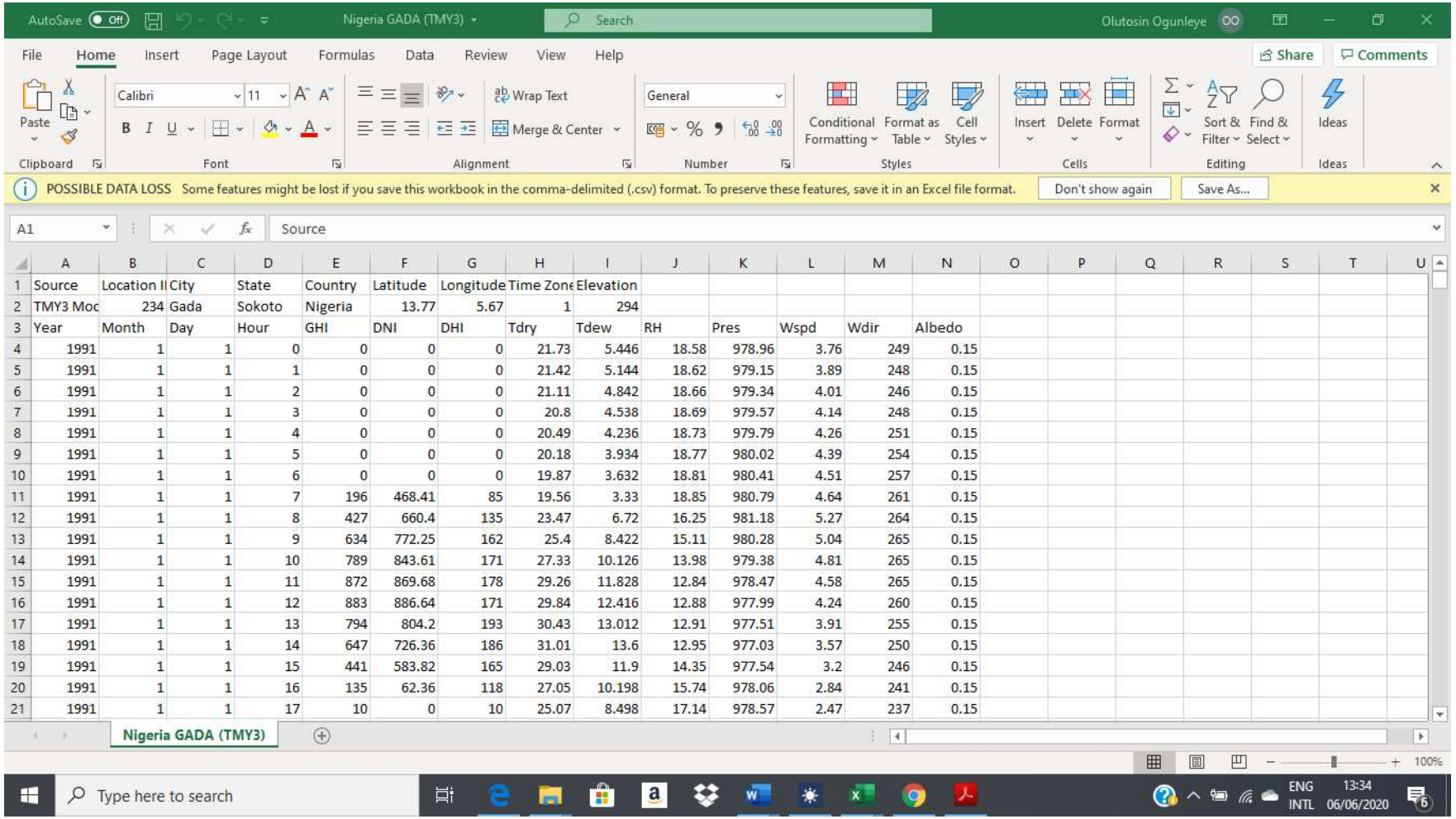

	A	B	C	D	E	F	G	H	I	J	K	L	M	N
1	Source	Location II	City	State	Country	Latitude	Longitude	Time Zone	Elevation					
2	TMY3 Moc	234	Gada	Sokoto	Nigeria	13.77	5.67	1	294					
3	Year	Month	Day	Hour	GHI	DNI	DHI	Tdry	Tdew	RH	Pres	Wspd	Wdir	Albedo
4	1991	1	1	0	0	0	0	21.73	5.446	18.58	978.96	3.76	249	0.15
5	1991	1	1	1	0	0	0	21.42	5.144	18.62	979.15	3.89	248	0.15
6	1991	1	1	2	0	0	0	21.11	4.842	18.66	979.34	4.01	246	0.15
7	1991	1	1	3	0	0	0	20.8	4.538	18.69	979.57	4.14	248	0.15
8	1991	1	1	4	0	0	0	20.49	4.236	18.73	979.79	4.26	251	0.15
9	1991	1	1	5	0	0	0	20.18	3.934	18.77	980.02	4.39	254	0.15
10	1991	1	1	6	0	0	0	19.87	3.632	18.81	980.41	4.51	257	0.15
11	1991	1	1	7	196	468.41	85	19.56	3.33	18.85	980.79	4.64	261	0.15
12	1991	1	1	8	427	660.4	135	23.47	6.72	16.25	981.18	5.27	264	0.15
13	1991	1	1	9	634	772.25	162	25.4	8.422	15.11	980.28	5.04	265	0.15
14	1991	1	1	10	789	843.61	171	27.33	10.126	13.98	979.38	4.81	265	0.15
15	1991	1	1	11	872	869.68	178	29.26	11.828	12.84	978.47	4.58	265	0.15
16	1991	1	1	12	883	886.64	171	29.84	12.416	12.88	977.99	4.24	260	0.15
17	1991	1	1	13	794	804.2	193	30.43	13.012	12.91	977.51	3.91	255	0.15
18	1991	1	1	14	647	726.36	186	31.01	13.6	12.95	977.03	3.57	250	0.15
19	1991	1	1	15	441	583.82	165	29.03	11.9	14.35	977.54	3.2	246	0.15
20	1991	1	1	16	135	62.36	118	27.05	10.198	15.74	978.06	2.84	241	0.15
21	1991	1	1	17	10	0	10	25.07	8.498	17.14	978.57	2.47	237	0.15

APPENDIX 2

REGRESSION ANALYSES OF THE CLEARNESS INDEX FOR MALAM-FATORI USING ANGSTROM-PAGE MODEL

LINEAR MODEL

Regression Statistics	
Multiple R	0.501867645
R Square	0.251871133
Adjusted R Square	0.249810172
Standard Error	0.050558427
Observations	365

ANOVA

	df	*SS*	*MS*	*F*	*Significance F*
Regression	1	0.31238899	0.312389	122.2105	1.10752E-24
Residual	363	0.927884106	0.002556		
Total	364	1.240273097			

	Coefficients	*Standard Error*	*t Stat*	*P-value*	*Lower 95%*	*Upper 95%*	*Lower 95.0%*	*Upper 95.0%*
Intercept	0.207513287	0.02263668	9.167125	3.68E-18	0.162997788	0.252029	0.16299779	0.252028786
x	0.368727909	0.03335429	11.05489	1.11E-24	0.303136008	0.43432	0.30313601	0.43431981

QUADRATIC MODEL

Regression Statistics	
Multiple R	0.729992772
R Square	0.532889448
Adjusted R Square	**0.530308726**
Standard Error	0.040004995
Observations	365

ANOVA

	df	*SS*	*MS*	*F*	*Significance F*
Regression	2	0.660928445	0.330464223	206.4885701	1.462E-60
Residual	362	0.579344651	0.0016004		
Total	364	1.240273097			

	Coefficients	*Standard Error*	*t Stat*	*P-value*	*Lower 95%*	*Upper 95%*	*Lower 95.0%*	*Upper 95.0%*
Intercept	-2.021787663	0.15212078	-13.2906738	4.19651E-33	-2.32093908	-1.722636244	-2.320939081	-1.722636244
X	6.910190663	0.444049662	15.56175187	3.59525E-42	6.03694977	7.783431559	6.036949768	7.783431559
x^2	-4.732491923	0.320684614	-14.7574649	6.42949E-39	-5.36313066	-4.101853184	-5.363130662	-4.101853184

CUBIC MODEL

Regression Statistics	
Multiple R	0.731865517
R Square	0.535627136
Adjusted R Square	**0.531768081**
Standard Error	0.039942797
Observations	365

ANOVA

	Df	*SS*	*MS*	*F*	*Significance F*
Regression	3	0.664323926	0.22144131	138.797513	8.2513E-60
Residual	361	0.57594917	0.00159543		
Total	364	1.240273097			

	Coefficients	*Standard Error*	*t Stat*	*P-value*	*Lower 95%*	*Upper 95%*	*Lower 95.0%*	*Upper 95.0%*
Intercept	0.488169992	1.727189373	0.28263837	0.77761605	-2.908446507	3.884786491	-2.908446507	3.884786491
x	-4.188212482	7.620519956	-0.54959668	0.58293586	-19.1744	10.79797503	-19.1744	10.79797503
x^2	11.4746339	11.1140961	1.03243969	0.30255735	-10.38187053	33.33113832	-10.38187053	33.33113832
x^3	-7.815616317	5.357363033	-1.45885509	0.14547451	-18.35117655	2.719943915	-18.35117655	2.719943915

APPENDIX 3

REGRESSION ANALYSES OF THE CLEARNESS INDEX FOR MALAM-FATORI USING HARGREAVES-SAMANI MODEL

LINEAR MODEL

Regression Statistics	
Multiple R	0.858063139
R Square	0.73627235
Adjusted R Square	0.735545827
Standard Error	0.030017659
Observations	365

ANOVA

	df	*SS*	*MS*	*F*	*Significance F*
Regression	1	0.913152027	0.913152027	1013.419953	4.2413E-107
Residual	363	0.327084724	0.00090106		
Total	364	1.240236751			

	Coefficients	*Standard Error*	*t Stat*	*P-value*	*Lower 95%*	*Upper 95%*	*Lower 95.0%*	*Upper 95.0%*
Intercept	0.088685512	0.011645286	7.615572097	2.29824E-13	0.065784818	0.111586207	0.065784818	0.111586207
ΔT^0.5	0.095519119	0.003000513	31.83425753	4.2413E-107	0.089618548	0.101419691	0.089618548	0.101419691

QUADRATIC MODEL

Regression Statistics	
Multiple R	0.903771769
R Square	0.816803411
Adjusted R Square	0.815791275
Standard Error	0.025052825

Observations	365

ANOVA

	df	*SS*	*MS*	*F*	*Significance F*
Regression	2	1.013029609	0.506514804	807.009664	3.873E-134
Residual	362	0.227207142	0.000627644		
Total	364	1.240236751			

	Coefficients	*Standard Error*	*t Stat*	*P-value*	*Lower 95%*	*Upper 95%*	*Lower 95.0%*	*Upper 95.0%*
Intercept	-1.033145002	0.089459866	-11.54869829	1.76859E-26	-1.209071301	-0.857218703	-1.209071301	-0.857218703
ΔT^0.5	0.706985768	0.048537151	14.56586882	3.77681E-38	0.611535578	0.802435959	0.611535578	0.802435959
(ΔT^0.5)^2	-0.081633039	0.006471257	-12.61471103	1.72218E-30	-0.094359018	-0.068907061	-0.094359018	-0.068907061

CUBIC MODEL

Regression Statistics	
Multiple R	0.92034793
R Square	0.847040313
Adjusted R Square	0.84576918
Standard Error	0.022923831
Observations	365

ANOVA

	df	*SS*	*MS*	*F*	*Significance F*
Regression	3	1.050530525	0.350176842	666.3663224	9.1603E-147
Residual	361	0.189706226	0.000525502		
Total	364	1.240236751			

	Coefficients	*Standard Error*	*t Stat*	*P-value*	*Lower 95%*	*Upper 95%*	*Lower 95.0%*	*Upper 95.0%*
Intercept	5.680661578	0.798962718	7.110045872	6.25619E-12	4.109455783	7.251867373	4.109455783	7.251867373
ΔT^0.5	-4.852543372	0.659615608	-7.35662303	1.28048E-12	-6.149715119	-3.555371624	-6.14971512	-3.555371624
(ΔT^0.5)^2	1.436083552	0.179759842	7.988900833	1.84742E-14	1.082575561	1.789591543	1.082575561	1.789591543
(ΔT^0.5)^3	-0.136633322	0.016174203	-8.44760793	7.37528E-16	-0.168440815	-0.10482583	-0.16844082	-0.10482583

APPENDIX 4

REGRESSION ANALYSES OF THE CLEARNESS INDEX FOR MACHINA USING ANGSTROM-PAGE MODEL

LINEAR MODEL

Regression Statistics	
Multiple R	0.694390269
R Square	0.482177845
Adjusted R Square	0.480751338
Standard Error	0.051352421
Observations	365

ANOVA

	df	*SS*	*MS*	*F*	*Significance F*
Regression	1	0.891363994	0.891363994	338.0128796	7.99097E-54
Residual	363	0.957256807	0.002637071		
Total	364	1.848620801			

	Coefficients	*Standard Error*	*t Stat*	*P-value*	*Lower 95%*	*Upper 95%*	*Lower 95.0%*	*Upper 95.0%*
Intercept	-0.02178056	0.03147181	-0.692065719	0.489338491	-0.083670524	0.040109403	-0.083670524	0.040109403
x	0.839257212	0.045648705	18.38512659	7.99097E-54	0.749488092	0.929026331	0.749488092	0.929026331

QUADRATIC MODEL

Regression Statistics	
Multiple R	0.717692606
R Square	0.515082676
Adjusted R Square	0.512403575
Standard Error	0.049762648
Observations	365

ANOVA

	df	*SS*	*MS*	*F*	*Significance F*
Regression	2	0.952192549	0.476096275	192.2595045	1.27601E-57
Residual	362	0.896428251	0.002476321		
Total	364	1.848620801			

	Coefficients	*Standard Error*	*t Stat*	*P-value*	*Lower 95%*	*Upper 95%*	*Lower 95.0%*	*Upper 95.0%*
Intercept	-1.72168374	0.344337265	-4.999992491	8.95205E-07	-2.398836336	-1.044531143	-2.398836336	-1.044531143
x	5.843619022	1.010682638	5.781853574	1.59719E-08	3.856072388	7.831165657	3.856072388	7.831165657
x^2	-3.655790477	0.737617187	-4.956216503	1.10616E-06	-5.106343305	-2.205237649	-5.106343305	-2.205237649

CUBIC MODEL

Regression Statistics	
Multiple R	0.722173884
R Square	0.521535119
Adjusted R Square	0.517558956
Standard Error	0.049498877
Observations	365

ANOVA

	Df	*SS*	*MS*	*F*	*Significance F*
Regression	3	0.964120669	0.321373556	131.1654455	1.79584E-57
Residual	361	0.884500132	0.002450139		
Total	364	1.848620801			

	Coefficients	*Standard Error*	*t Stat*	*P-value*	*Lower 95%*	*Upper 95%*	*Lower 95.0%*	*Upper 95.0%*
Intercept	-10.35721633	3.928757455	-2.636257507	0.008744452	-18.08334214	-2.631090523	-18.08334214	-2.631090523
x	43.77054498	17.21862656	2.542046244	0.011437825	9.909132918	77.63195705	9.909132918	77.63195705
x^2	-58.89294207	25.04534822	-2.351452316	0.01923719	-108.1460491	-9.63983507	-108.1460491	-9.63983507
x^3	26.68148709	12.0925918	2.20643246	0.027982843	2.900714992	50.46225918	2.900714992	50.46225918

APPENDIX 5

REGRESSION ANALYSES OF THE CLEARNESS INDEX FOR MACHINA USING HARGREAVES-SAMANI MODEL

LINEAR MODEL

Regression Statistics	
Multiple R	0.94302481
R Square	0.889295792
Adjusted R Square	0.888990821
Standard Error	0.023743934
Observations	365

ANOVA

	df	*SS*	*MS*	*F*	*Significance F*
Regression	1	1.643970699	1.6439707	2916.00814	1.4548E-175
Residual	363	0.204650102	0.00056377		
Total	364	1.848620801			

	Coefficients	*Standard Error*	*t Stat*	*P-value*	*Lower 95%*	*Upper 95%*	*Lower 95.0%*	*Upper 95.0%*
Intercept	-0.044493291	0.01116588	-3.98475462	8.1659E-05	-0.066451225	-0.02253536	-0.066451225	-0.022535358
ΔT^0.5	0.159493268	0.002953575	54.0000754	1.455E-175	0.153685002	0.165301534	0.153685002	0.165301534

QUADRATIC MODEL

Regression Statistics	
Multiple R	0.951632121
R Square	0.905603694
Adjusted R Square	0.905082168
Standard Error	0.021955692

Observations	365

ANOVA

	df	*SS*	*MS*	*F*	*Significance F*
Regression	2	1.674117827	0.837058913	1736.447922	2.9299E-186
Residual	362	0.174502974	0.000482052		
Total	364	1.848620801			

	Coefficients	*Standard Error*	*t Stat*	*P-value*	*Lower 95%*	*Upper 95%*	*Lower 95.0%*	*Upper 95.0%*
Intercept	-1.027261076	0.124700686	-8.237814155	3.2416E-15	-1.272489814	-0.782032337	-1.272489814	-0.782032337
ΔT^0.5	0.697685883	0.06811007	10.24350558	8.59446E-22	0.563744787	0.831626979	0.563744787	0.831626979
(ΔT^0.5)^2	-0.072713006	0.009194672	-7.908167174	3.19642E-14	-0.090794687	-0.054631326	-0.090794687	-0.054631326

CUBIC MODEL

Regression Statistics	
Multiple R	0.953246128
R Square	0.90867818
Adjusted R Square	0.907919273
Standard Error	0.021625074
Observations	365

ANOVA

	df	*SS*	*MS*	*F*	*Significance F*
Regression	3	1.679801386	0.5599338	1197.351027	3.5045E-187
Residual	361	0.168819415	0.00046764		
Total	364	1.848620801			

	Coefficients	*Standard Error*	*t Stat*	*P-value*	*Lower 95%*	*Upper 95%*	*Lower 95.0%*	*Upper 95.0%*
Intercept	3.391492046	1.273434589	2.66326365	0.00808529	0.887210232	5.89577386	0.887210232	5.89577386
ΔT^0.5	-2.929262589	1.042532937	-2.8097554	0.005227952	-4.979463124	-0.879062054	-4.979463124	-0.879062054
(ΔT^0.5)^2	0.912913659	0.282867172	3.2273581	0.001363717	0.356639219	1.4691881	0.356639219	1.4691881
(ΔT^0.5)^3	-0.088699287	0.025442954	-3.4862023	0.0005503	-0.138734309	-0.038664264	-0.138734309	-0.038664264

APPENDIX 6

REGRESSION ANALYSES OF THE CLEARNESS INDEX FOR ZARIA USING ANGSTROM-PAGE MODEL

LINEAR MODEL

Regression Statistics	
Multiple R	0.671418582
R Square	0.450802913
Adjusted R Square	0.449289973
Standard Error	0.034041067
Observations	365

ANOVA

	df	*SS*	*MS*	*F*	*Significance F*
Regression	1	0.345280008	0.345280008	297.9649036	3.58038E-49
Residual	363	0.420642301	0.001158794		
Total	364	0.765922309			

	Coefficients	*Standard Error*	*t Stat*	*P-value*	*Lower 95%*	*Upper 95%*	*Lower 95.0%*	*Upper 95.0%*
Intercept	0.381973118	0.012875221	29.66730591	4.6055E-99	0.35665373	0.40729251	0.35665373	0.407292506
X	0.326435067	0.018910989	17.26165993	3.58038E-49	0.289246217	0.36362392	0.289246217	0.363623918

QUADRATIC MODEL

Regression Statistics	
Multiple R	0.879438851
R Square	0.773412693
Adjusted R Square	0.772160829
Standard Error	0.02189555
Observations	365

ANOVA

	df	*SS*	*MS*	*F*	*Significance F*
Regression	2	0.592374035	0.296187018	617.8090867	1.9844E-117
Residual	362	0.173548274	0.000479415		
Total	364	0.765922309			

	Coefficients	*Standard Error*	*t Stat*	*P-value*	*Lower 95%*	*Upper 95%*	*Lower 95.0%*	*Upper 95.0%*
Intercept	-1.130030712	0.067113428	-16.8376247	2.15671E-47	-1.262011873	-0.998049552	-1.262011873	-0.998049552
X	4.832213337	0.19884225	24.30174341	4.68696E-78	4.441182335	5.223244339	4.441182335	5.223244339
x^2	-3.2924503	0.145025365	-22.7025824	1.39254E-71	-3.577648309	-3.007252291	-3.577648309	-3.007252291

CUBIC MODEL

Regression Statistics	
Multiple R	0.923025127
R Square	0.851975385
Adjusted R Square	0.850745264
Standard Error	0.017721714
Observations	365

ANOVA

	df	*SS*	*MS*	*F*	*Significance F*
Regression	3	0.652546954	0.217515651	692.5945261	2.4677E-149
Residual	361	0.113375355	0.000314059		
Total	364	0.765922309			

	Coefficients	*Standard Error*	*t Stat*	*P-value*	*Lower 95%*	*Upper 95%*	*Lower 95.0%*	*Upper 95.0%*
Intercept	-6.722036653	0.407627561	-16.49063335	6.14815E-46	-7.523659521	-5.920413784	-7.523659521	-5.920413784
X	29.90230457	1.818314143	16.44507066	9.45144E-46	26.32648601	33.47812314	26.32648601	33.47812314
x^2	-40.32362643	2.677875075	-15.05806854	4.16117E-40	-45.58982063	-35.05743223	-45.58982063	-35.05743223
x^3	18.02546025	1.302241562	13.84187141	2.99174E-35	15.46452788	20.58639262	15.46452788	20.58639262

APPENDIX 7

REGRESSION ANALYSES OF THE CLEARNESS INDEX FOR ZARIA USING HARGREAVES-SAMANI MODEL

LINEAR MODEL

Regression Statistics	
Multiple R	0.838190071
R Square	0.702562595
Adjusted R Square	0.701743208
Standard Error	0.025051679
Observations	365

ANOVA

	df	*SS*	*MS*	*F*	*Significance F*
Regression	1	0.538108365	0.538108365	857.4248493	1.31565E-97
Residual	363	0.227813944	0.000627587		
Total	364	0.765922309			

	Coefficients	*Standard Error*	*t Stat*	*P-value*	*Lower 95%*	*Upper 95%*	*Lower 95.0%*	*Upper 95.0%*
Intercept	0.228610974	0.012821605	17.83013727	1.59427E-51	0.203397024	0.253824925	0.203397024	0.253824925
ΔT^0.5	0.104513283	0.003569221	29.28181772	1.31565E-97	0.097494336	0.11153223	0.097494336	0.11153223

QUADRATIC MODEL

Regression Statistics	
Multiple R	0.93841696
R Square	0.880626391
Adjusted R Square	0.879966868

Standard Error	0.015892501
Observations	365

ANOVA

	df	*SS*	*MS*	*F*	*Significance F*
Regression	2	0.674491399	0.337245699	1335.248034	8.3254E-168
Residual	362	0.09143091	0.000252572		
Total	364	0.765922309			

	Coefficients	*Standard Error*	*t Stat*	*P-value*	*Lower 95%*	*Upper 95%*	*Lower 95.0%*	*Upper 95.0%*
Intercept	-2.13931689	0.102225601	-20.92740826	2.65075E-64	-2.340347503	-1.938286278	-2.340347503	-1.938286278
ΔT^0.5	1.468770521	0.05875314	24.99901303	7.57878E-81	1.35323019	1.584310852	1.35323019	1.584310852
(ΔT^0.5)^2	-0.19428687	0.008360948	-23.23742157	9.30477E-74	-0.210728993	-0.177844737	-0.210728993	-0.177844737

CUBIC MODEL

Regression Statistics	
Multiple R	0.939638673
R Square	0.882920835
Adjusted R Square	0.881947878
Standard Error	0.015760811
Observations	365

ANOVA

	df	*SS*	*MS*	*F*	*Significance F*
Regression	3	0.676248765	0.225416255	907.4612646	1.0358E-167
Residual	361	0.089673544	0.000248403		
Total	364	0.765922309			

	Coefficients	*Standard Error*	*t Stat*	*P-value*	*Lower 95%*	*Upper 95%*	*Lower 95.0%*	*Upper 95.0%*
Intercept	-5.482899632	1.261151558	-4.34753428	1.79295E-05	-7.963026165	-3.002773099	-7.963026165	-3.002773099
ΔT^0.5	4.357040181	1.087450551	4.006655914	7.48177E-05	2.218506595	6.495573767	2.218506595	6.495573767
(ΔT^0.5)^2	-1.020991473	0.310922622	-3.283747787	0.001124519	-1.632438559	-0.409544387	-1.632438559	-0.409544387
(ΔT^0.5)^3	0.078423483	0.029484489	2.659821682	0.008166741	0.020440552	0.136406413	0.020440552	0.136406413

APPENDIX 8

REGRESSION ANALYSES OF THE CLEARNESS INDEX FOR MAIADUA USING ANGSTROM-PAGE MODEL

LINEAR MODEL

Regression Statistics	
Multiple R	0.687157712
R Square	0.472185721
Adjusted R Square	0.470731687
Standard Error	0.051845367
Observations	365

ANOVA

	df	*SS*	*MS*	*F*	*Significance F*
Regression	1	0.872887456	0.872887456	324.741909	2.59201E-52
Residual	363	0.97572299	0.002687942		
Total	364	1.848610446			

	Coefficients	*Standard Error*	*t Stat*	*P-value*	*Lower 95%*	*Upper 95%*	*Lower 95.0%*	*Upper 95.0%*
Intercept	-0.024378947	0.032249655	-0.755944403	0.450172799	-0.08779856	0.039040667	-0.08779856	0.039040667
x	0.843199198	0.046790859	18.0205968	2.59201E-52	0.751184009	0.935214387	0.751184009	0.935214387

QUADRATIC MODEL

Regression Statistics	
Multiple R	0.711327898
R Square	0.505987379
Adjusted R Square	0.503258028
Standard Error	0.050227023
Observations	365

ANOVA

	df	*SS*	*MS*	*F*	*Significance F*
Regression	2	0.935373554	0.467686777	185.3874005	3.68626E-56
Residual	362	0.913236892	0.002522754		
Total	364	1.848610446			

	Coefficients	*Standard Error*	*t Stat*	*P-value*	*Lower 95%*	*Upper 95%*	*Lower 95.0%*	*Upper 95.0%*
Intercept	-1.801271108	0.358396115	-5.025922531	7.89195E-07	-2.506070978	-1.0964712	-2.50607098	-1.096471238
x	6.076645557	1.052535264	5.773341534	1.67288E-08	4.006794109	8.14649701	4.006794109	8.146497006
x^2	-3.825721711	0.768703943	-4.976846735	1.00136E-06	-5.337407851	-2.3140356	-5.33740785	-2.314035571

CUBIC MODEL

Regression Statistics	
Multiple R	0.716676648
R Square	0.513625417
Adjusted R Square	0.509583523
Standard Error	0.049906204
Observations	365

ANOVA

	df	*SS*	*MS*	*F*	*Significance F*
Regression	3	0.949493312	0.316497771	127.0754286	3.43786E-56
Residual	361	0.899117134	0.002490629		
Total	364	1.848610446			

	Coefficients	*Standard Error*	*t Stat*	*P-value*	*Lower 95%*	*Upper 95%*	*Lower 95.0%*	*Upper 95.0%*
Intercept	-11.61517654	4.137115457	-2.80755436	0.005263032	-19.75105026	-3.479302826	-19.75105026	-3.479302826
x	49.20251956	18.14268521	2.711975598	0.007008333	13.52389342	84.88114571	13.52389342	84.88114571
x^2	-66.67873454	26.40880393	-2.524867643	0.012001898	-118.613155	-14.74431405	-118.613155	-14.74431405

x^3	30.38607172	12.76190406	2.380998288	0.017783785	5.289058863	55.48308457	5.289058863	55.48308457

APPENDIX 9

REGRESSION ANALYSES OF THE CLEARNESS INDEX FOR MAIADUA USING HARGREAVES-SAMANI MODEL

LINEAR MODEL

Regression Statistics	
Multiple R	0.94302481
R Square	0.889295792
Adjusted R Square	0.888990821
Standard Error	0.023743934
Observations	365

ANOVA

	df	*SS*	*MS*	*F*	*Significance F*
Regression	1	1.643970699	1.6439707	2916.00814	1.4548E-175
Residual	363	0.204650102	0.00056377		
Total	364	1.848620801			

	Coefficients	*Standard Error*	*t Stat*	*P-value*	*Lower 95%*	*Upper 95%*	*Lower 95.0%*	*Upper 95.0%*
Intercept	-0.044493291	0.01116588	-3.98475462	8.1659E-05	-0.066451225	-0.02253536	-0.066451225	-0.022535358
ΔT^0.5	0.159493268	0.002953575	54.0000754	1.455E-175	0.153685002	0.165301534	0.153685002	0.165301534

QUADRATIC MODEL

Regression Statistics	
Multiple R	0.951632121
R Square	0.905603694
Adjusted R Square	0.905082168

Standard Error	0.021955692
Observations	365

ANOVA

	df	*SS*	*MS*	*F*	*Significance F*
Regression	2	1.674117827	0.837058913	1736.447922	2.9299E-186
Residual	362	0.174502974	0.000482052		
Total	364	1.848620801			

	Coefficients	*Standard Error*	*t Stat*	*P-value*	*Lower 95%*	*Upper 95%*	*Lower 95.0%*	*Upper 95.0%*
Intercept	-1.027261076	0.124700686	-8.237814155	3.2416E-15	-1.272489814	-0.782032337	-1.272489814	-0.782032337
ΔT^0.5	0.697685883	0.06811007	10.24350558	8.59446E-22	0.563744787	0.831626979	0.563744787	0.831626979
(ΔT^0.5)^2	-0.072713006	0.009194672	-7.908167174	3.19642E-14	-0.090794687	-0.054631326	-0.090794687	-0.054631326

CUBIC MODEL

Regression Statistics	
Multiple R	0.953246128
R Square	0.90867818
Adjusted R Square	0.907919273
Standard Error	0.021625074
Observations	365

ANOVA

	df	*SS*	*MS*	*F*	*Significance F*
Regression	3	1.679801386	0.5599338	1197.351027	3.5045E-187
Residual	361	0.168819415	0.00046764		
Total	364	1.848620801			

	Coefficients	*Standard Error*	*t Stat*	*P-value*	*Lower 95%*	*Upper 95%*	*Lower 95.0%*	*Upper 95.0%*
Intercept	3.391492046	1.273434589	2.66326365	0.00808529	0.887210232	5.89577386	0.887210232	5.89577386
ΔT^0.5	-2.929262589	1.042532937	-2.8097554	0.005227952	-4.979463124	-0.879062054	-4.979463124	-0.879062054
(ΔT^0.5)^2	0.912913659	0.282867172	3.2273581	0.001363717	0.356639219	1.4691881	0.356639219	1.4691881
(ΔT^0.5)^3	-0.088699287	0.025442954	-3.4862023	0.0005503	-0.138734309	-0.038664264	-0.138734309	-0.038664264

APPENDIX 10

REGRESSION ANALYSES OF THE CLEARNESS INDEX FOR GADA USING ANGSTROM-PAGE MODEL

LINEAR MODEL

Regression Statistics	
Multiple R	0.81812205
R Square	0.669323689
Adjusted R Square	0.668412735
Standard Error	0.031229055
Observations	365

ANOVA

	df	*SS*	*MS*	*F*	*Significance F*
Regression	1	0.716568002	0.716568	734.7502418	3.01956E-89
Residual	363	0.354017147	0.00097525		
Total	364	1.070585149			

	Coefficients	*Standard Error*	*t Stat*	*P-value*	*Lower 95%*	*Upper 95%*	*Lower 95.0%*	*Upper 95.0%*
Intercept	0.191908966	0.013117675	14.6298001	1.99735E-38	0.166112787	0.21770514	0.166112787	0.217705145
x	0.520059985	0.019185962	27.1062768	3.01956E-89	0.482330395	0.55778957	0.482330395	0.557789574

QUADRATIC MODEL

Regression Statistics	
Multiple R	0.836423805
R Square	0.699604782
Adjusted R Square	0.69794514
Standard Error	0.02980594
Observations	365

ANOVA

	df	*SS*	*MS*	*F*	*Significance F*
Regression	2	0.74898649	0.374493245	421.539551	2.9003E-95
Residual	362	0.321598659	0.000888394		
Total	364	1.070585149			

	Coefficients	*Standard Error*	*t Stat*	*P-value*	*Lower 95%*	*Upper 95%*	*Lower 95.0%*	*Upper 95.0%*
Intercept	0.574242932	0.064518483	8.900440681	2.7162E-17	0.44736483	0.701121033	0.447364831	0.701121033
x	-0.7015059	0.203047045	-3.454893429	0.00061581	-1.10080579	-0.30220601	-1.100805794	-0.302206006
x^2	0.954848499	0.158066895	6.040787345	3.8085E-09	0.64400381	1.265693183	0.644003815	1.265693183

CUBIC MODEL

Regression Statistics	
Multiple R	0.902537487
R Square	0.814573916
Adjusted R Square	0.813032979
Standard Error	0.023449977
Observations	365

ANOVA

	df	*SS*	*MS*	*F*	*Significance F*
Regression	3	0.872070738	0.290690246	528.6224713	1.102E-131
Residual	361	0.198514411	0.000549901		
Total	364	1.070585149			

	Coefficients	*Standard Error*	*t Stat*	*P-value*	*Lower 95%*	*Upper 95%*	*Lower 95.0%*	*Upper 95.0%*
Intercept	8.315983247	0.519947256	15.99389775	6.61789E-44	7.293477287	9.338489208	7.293477287	9.338489208
x	-38.86733821	2.556028982	-15.2061414	1.05009E-40	-43.89391512	-33.84076131	-43.8939151	-33.84076131
x^2	62.31898423	4.103508439	15.18675669	1.25772E-40	54.24920063	70.38876782	54.24920063	70.38876782
x^3	-32.27926228	2.157569437	-14.9609379	1.02513E-39	-36.52224574	-28.03627881	-36.5222457	-28.03627881

APPENDIX 11

REGRESSION ANALYSES OF THE CLEARNESS INDEX FOR GADA USING HARGREAVES-SAMANI MODEL

LINEAR MODEL

Regression Statistics	
Multiple R	0.941318596
R Square	0.886080699
Adjusted R Square	0.885766872
Standard Error	0.018329725
Observations	365

ANOVA

	df	*SS*	*MS*	*F*	*Significance F*
Regression	1	0.948624837	0.948624837	2823.466178	2.6315E-173
Residual	363	0.121960312	0.000335979		
Total	364	1.070585149			

	Coefficients	*Standard Error*	*t Stat*	*P-value*	*Lower 95%*	*Upper 95%*	*Lower 95.0%*	*Upper 95.0%*
Intercept	0.083493802	0.008732713	9.561038112	1.82376E-19	0.066320742	0.100666863	0.066320742	0.100666863
ΔT^0.5	0.128666811	0.002421449	53.13629812	2.6315E-173	0.123904983	0.13342864	0.123904983	0.13342864

QUADRATIC MODEL

Regression Statistics	
Multiple R	0.941541442
R Square	0.886500288
Adjusted R Square	0.885873218

Standard Error	0.018321191
Observations	365

ANOVA

	df	*SS*	*MS*	*F*	*Significance F*
Regression	2	0.949074043	0.474537021	1413.717701	8.996E-172
Residual	362	0.121511106	0.000335666		
Total	364	1.070585149			

	Coefficients	*Standard Error*	*t Stat*	*P-value*	*Lower 95%*	*Upper 95%*	*Lower 95.0%*	*Upper 95.0%*
Intercept	-0.056225504	0.121092903	-0.464317086	0.642699696	-0.294359399	0.18190839	-0.294359399	0.18190839
ΔT^0.5	0.209282709	0.069729017	3.001371855	0.002874099	0.072157891	0.346407528	0.072157891	0.346407528
(ΔT^0.5)^2	-0.011475667	0.009919939	-1.156828378	0.248105288	-0.030983612	0.008032278	-0.030983612	0.008032278

CUBIC MODEL

Regression Statistics	
Multiple R	0.944366675
R Square	0.891828417
Adjusted R Square	0.890929485
Standard Error	0.017910743
Observations	365

ANOVA

	df	*SS*	*MS*	*F*	*Significance F*
Regression	3	0.954778259	0.31825942	992.0968492	6.5209E-174
Residual	361	0.11580689	0.000320795		
Total	364	1.070585149			

	Coefficients	*Standard Error*	*t Stat*	*P-value*	*Lower 95%*	*Upper 95%*	*Lower 95.0%*	*Upper 95.0%*
Intercept	-5.804191045	1.368237151	-4.242094318	2.8177E-05	-8.494907509	-3.113474581	-8.494907509	-3.113474581
ΔT^0.5	5.211466245	1.188204232	4.386002092	1.51693E-05	2.874794794	7.548137695	2.874794794	7.548137695
(ΔT^0.5)^2	-1.4535583	0.342121441	-4.248661808	2.74019E-05	-2.126359644	-0.780756956	-2.126359644	-0.780756956
(ΔT^0.5)^3	0.137733072	0.032662832	4.216813548	3.13604E-05	0.073499749	0.201966396	0.073499749	0.201966396

APPENDIX 12

SCREENSHOTS OF SIMULATION RESULTS FROM MALAM-FATORI

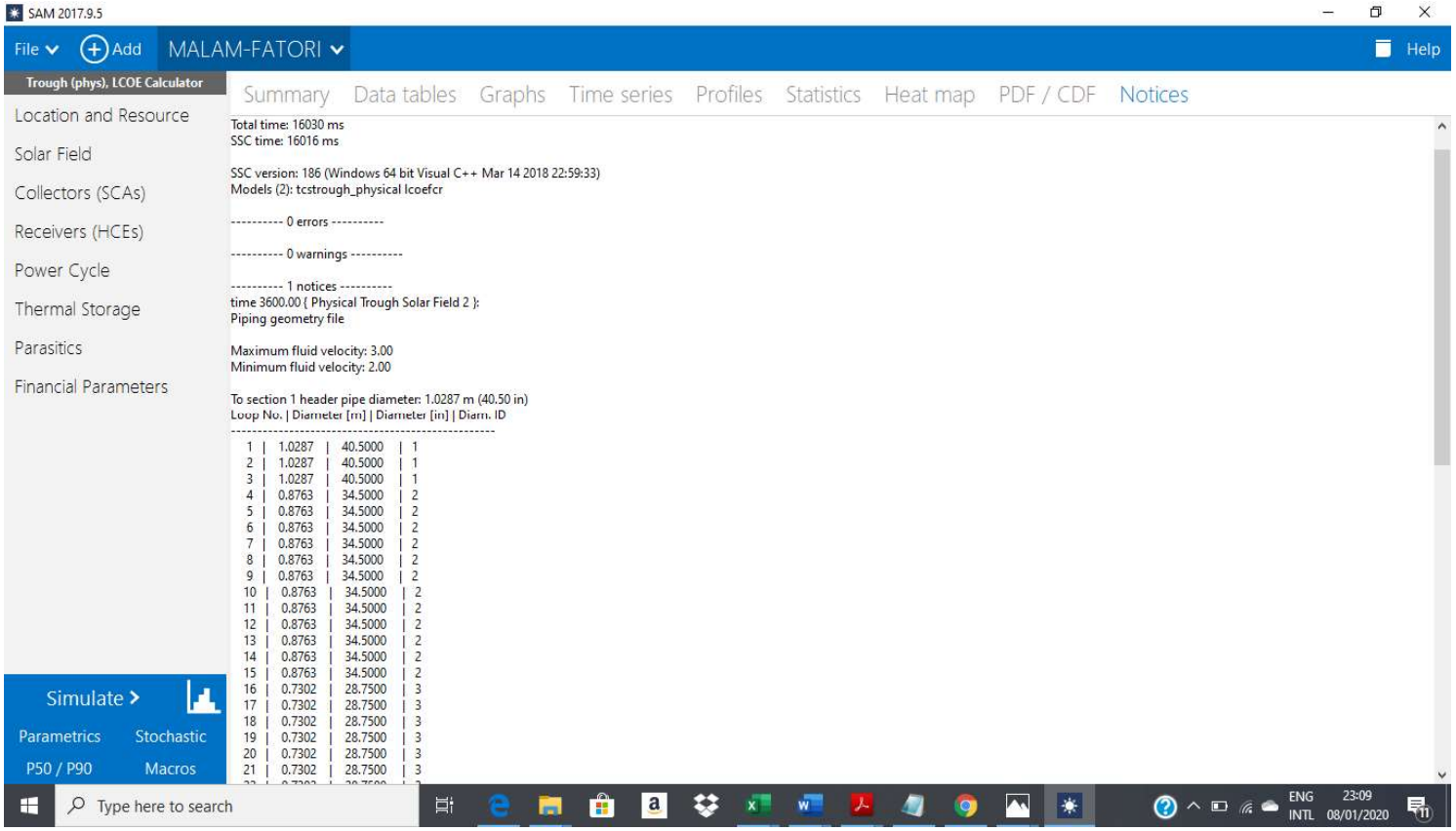

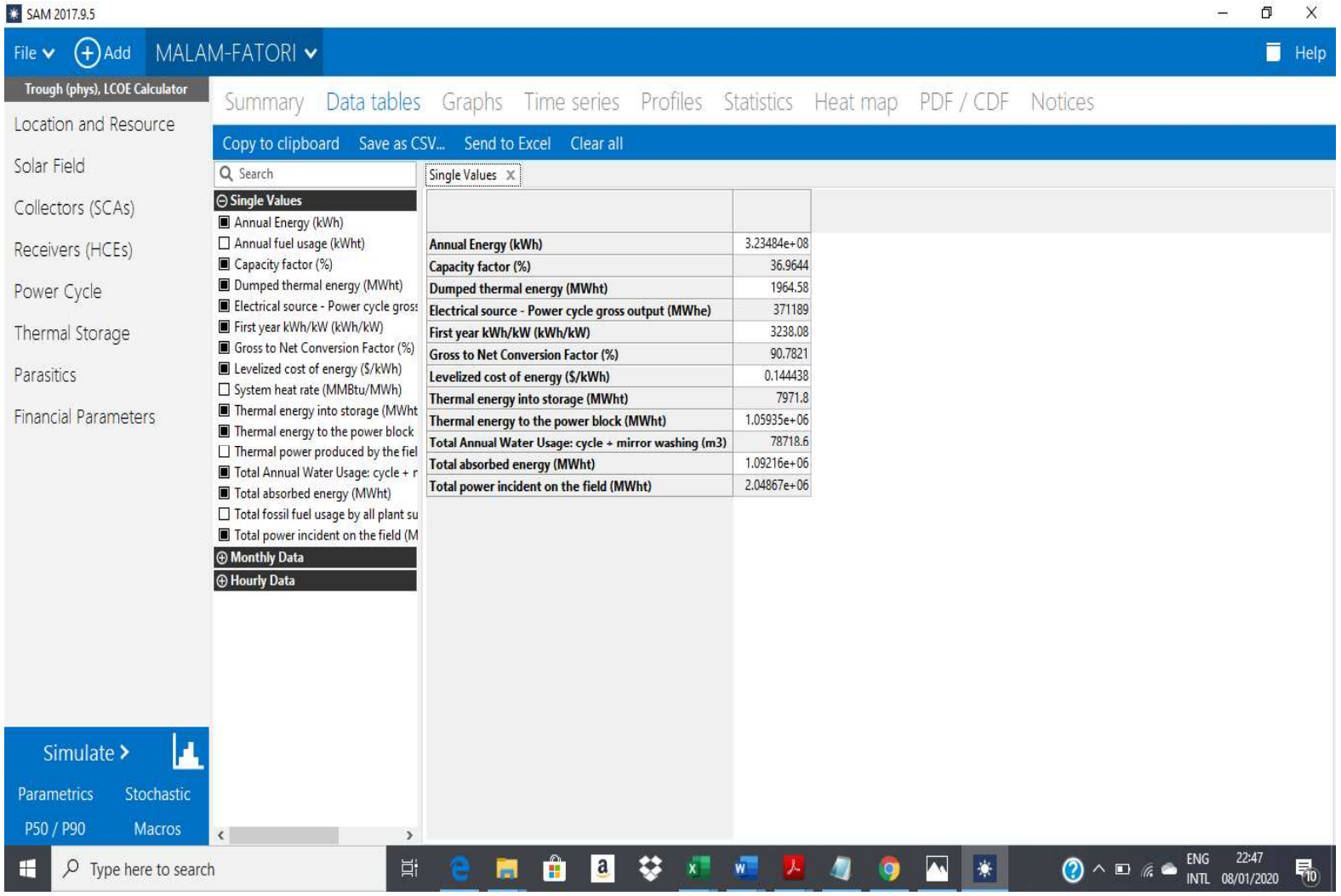
SAM 2017.9.5
File
Add
MALAM-FATORI
Help
Trough (phys), LCOE Calculator
Location and Resource
Solar Field
Collectors (SCAs)
Receivers (HCEs)
Power Cycle
Thermal Storage
Parasitics
Financial Parameters
Simulate
Parametrics
Stochastic
P50 / P90
Macros
Summary
Data tables
Graphs
Time series
Profiles
Statistics
Heat map
PDF / CDF
Notices
Copy to clipboard
Save as CSV...
Send to Excel
Clear all
Search
Single Values
Annual Energy (kWh)
Annual fuel usage (kWht)
Capacity factor (%)
Dumped thermal energy (MWht)
Electrical source - Power cycle gross
First year kWh/kW (kWh/kW)
Gross to Net Conversion Factor (%)
Levelized cost of energy ($/kWh)
System heat rate (MMBtu/MWh)
Thermal energy into storage (MWht
Thermal energy to the power block
Thermal power produced by the fiel
Total Annual Water Usage: cycle + r
Total absorbed energy (MWht)
Total fossil fuel usage by all plant su
Total power incident on the field (M
Monthly Data
Hourly Data
Annual Energy (kWh) 3.23484e+08
Capacity factor (%) 36.9644
Dumped thermal energy (MWht) 1964.58
Electrical source - Power cycle gross output (MWhe) 371189
First year kWh/kW (kWh/kW) 3238.08
Gross to Net Conversion Factor (%) 90.7821
Levelized cost of energy ($/kWh) 0.144438
Thermal energy into storage (MWht) 7971.8
Thermal energy to the power block (MWht) 1.05935e+06
Total Annual Water Usage: cycle + mirror washing (m3) 78718.6
Total absorbed energy (MWht) 1.09216e+06
Total power incident on the field (MWht) 2.04867e+06
Type here to search
ENG
INTL
22:47
08/01/2020

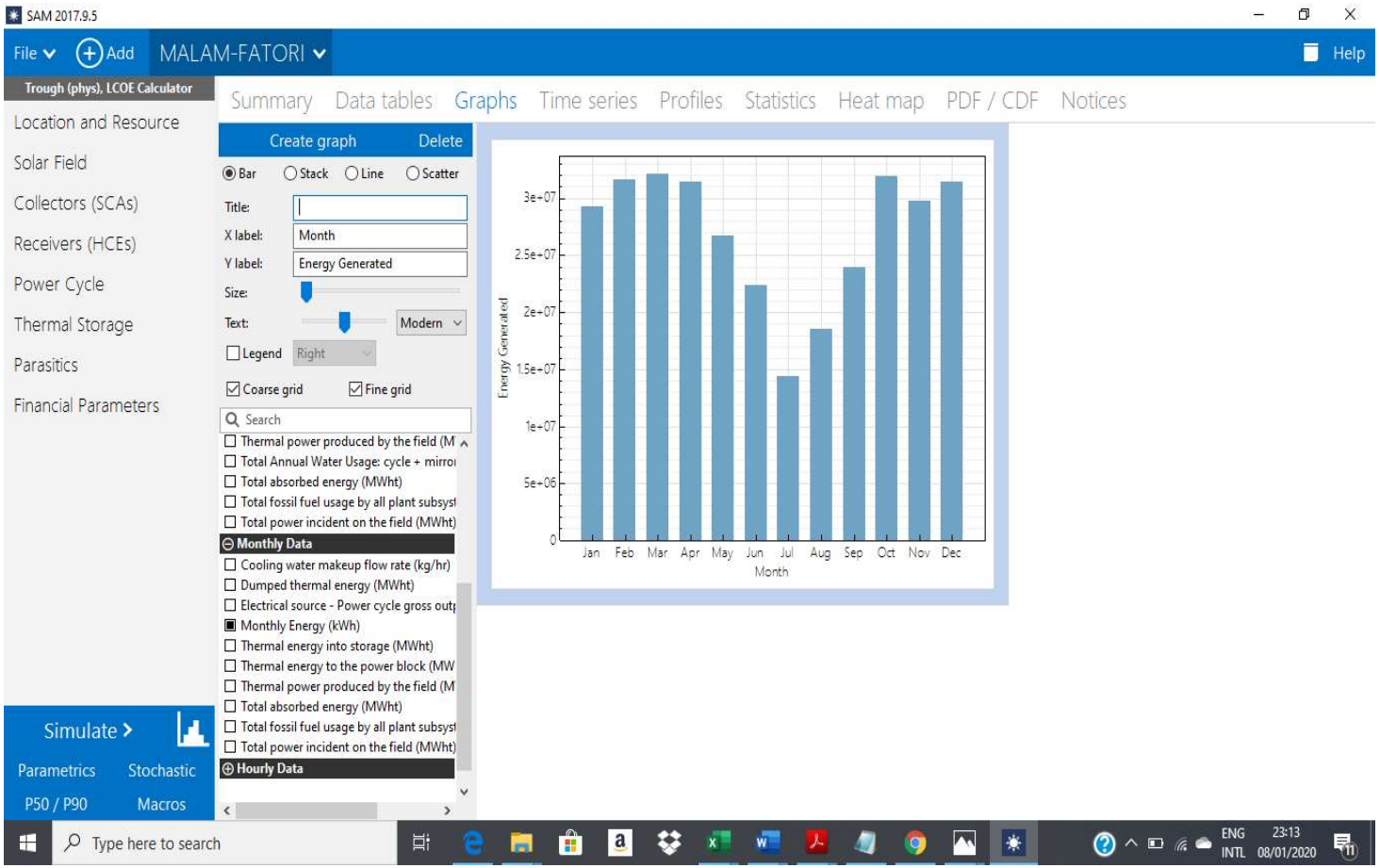
SAM 2017.9.5
File
Add
MALAM-FATORI
Help
Trough (phys), LCOE Calculator
Location and Resource
Solar Field
Collectors (SCAs)
Receivers (HCEs)
Power Cycle
Thermal Storage
Parasitics
Financial Parameters
Summary
Data tables
Graphs
Time series
Profiles
Statistics
Heat map
PDF / CDF
Notices
Create graph
Delete
Bar
Stack
Line
Scatter
Title:
X label:
Month
Y label:
Energy Generated
Size:
Text:
Modern
Legend
Right
Coarse grid
Fine grid
Search
Thermal power produced by the field (M
Total Annual Water Usage: cycle + mirro
Total absorbed energy (MWht)
Total fossil fuel usage by all plant subsyst
Total power incident on the field (MWht)
Monthly Data
Cooling water makeup flow rate (kg/hr)
Dumped thermal energy (MWht)
Electrical source - Power cycle gross outp
Monthly Energy (kWh)
Thermal energy into storage (MWht)
Thermal energy to the power block (MW
Thermal power produced by the field (M
Total absorbed energy (MWht)
Total fossil fuel usage by all plant subsyst
Total power incident on the field (MWht)
Hourly Data
Simulate
Parametrics
Stochastic
P50 / P90
Macros
Energy Generated
3e+07
2.5e+07
2e+07
1.5e+07
1e+07
5e+06
0
Jan
Feb
Mar
Apr
May
Jun
Jul
Aug
Sep
Oct
Nov
Dec
Month
Type here to search
ENG
INTL
23:13
08/01/2020

APPENDIX 13

SCREENSHOTS OF SIMULATION RESULTS FROM MACHINA

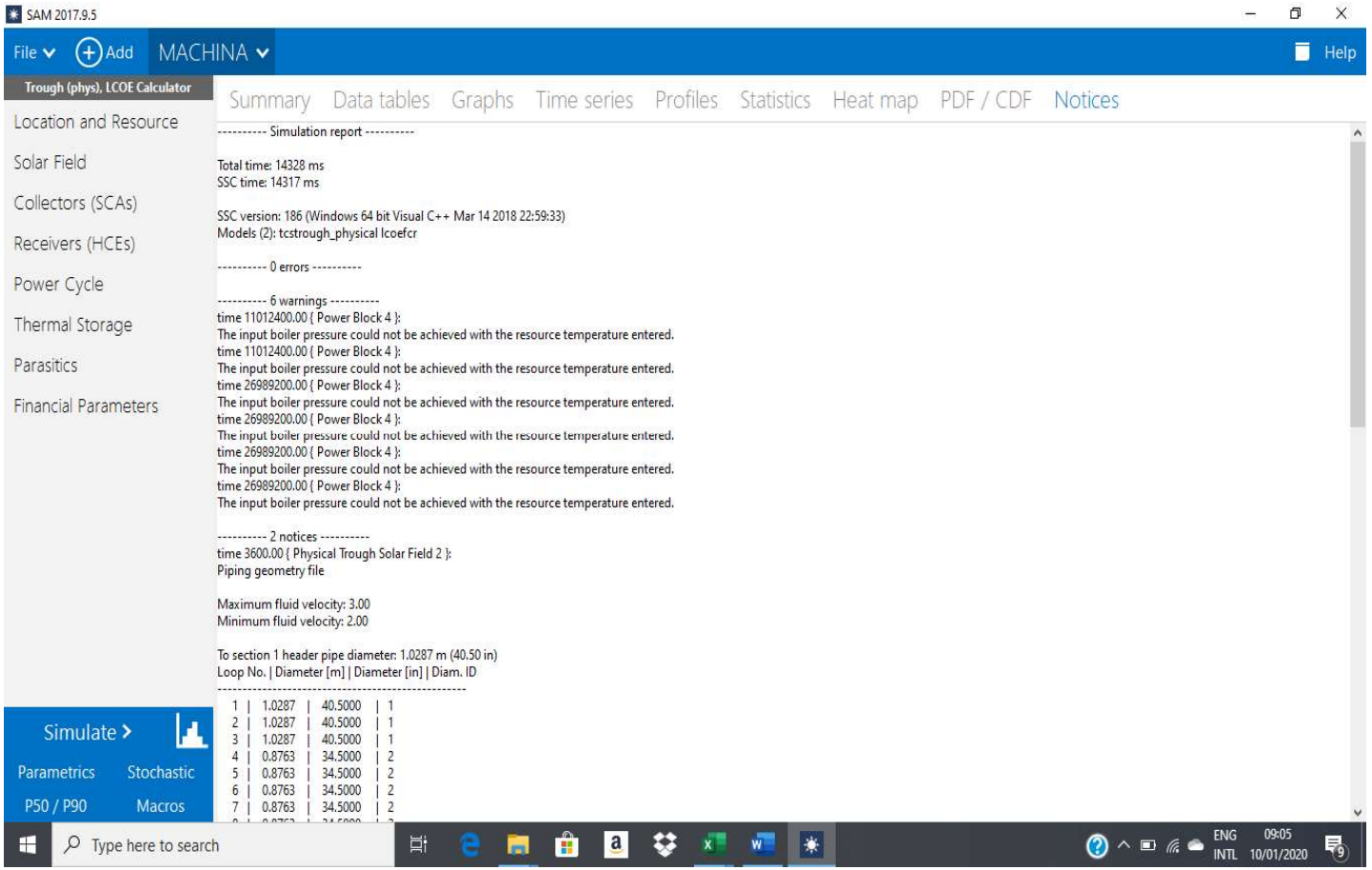

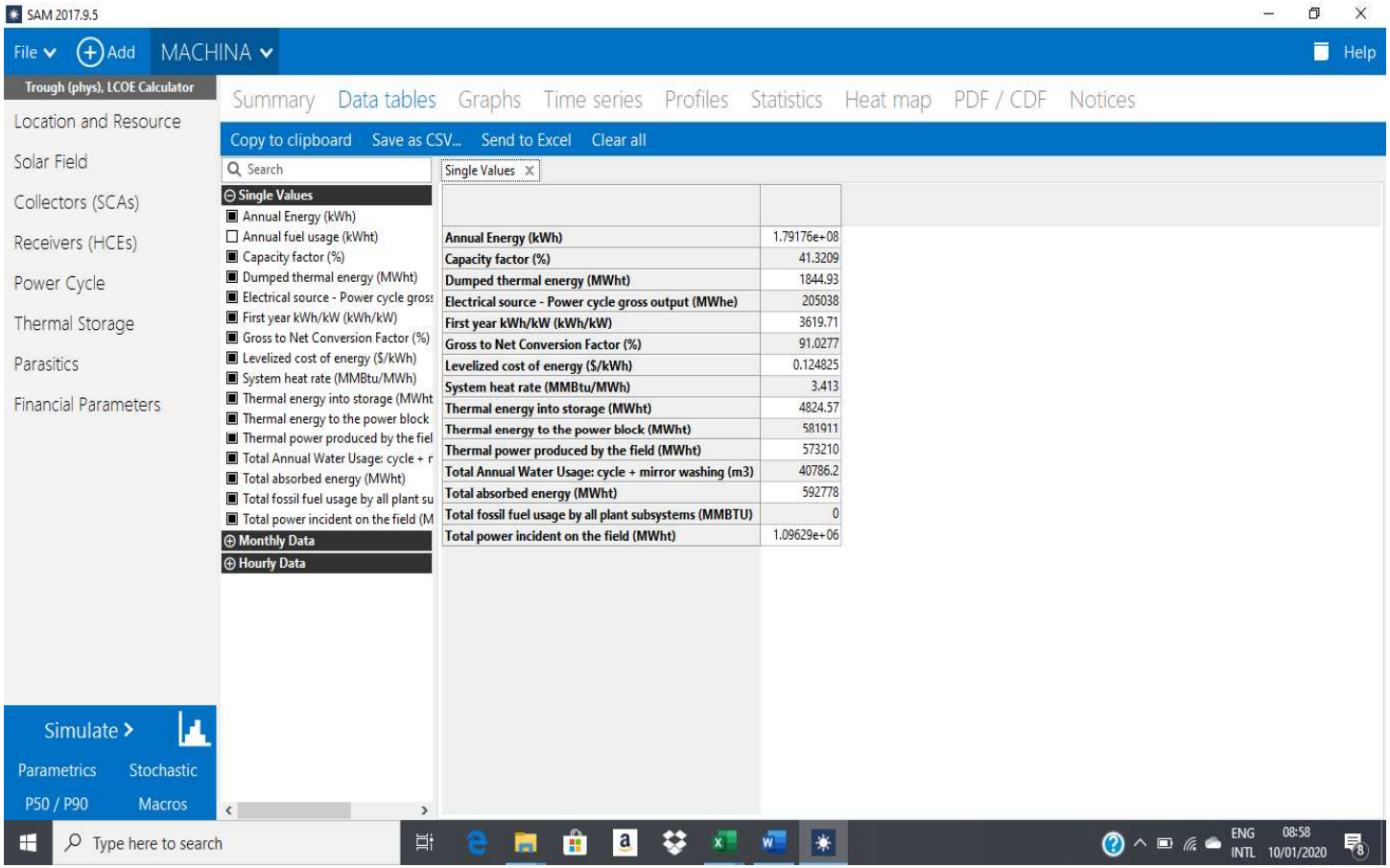
SAM 2017.9.5
File
Add
MACHINA
Help
Trough (phys), LCOE Calculator
Location and Resource
Solar Field
Collectors (SCAs)
Receivers (HCEs)
Power Cycle
Thermal Storage
Parasitics
Financial Parameters
Simulate
Parametrics
Stochastic
P50 / P90
Macros
Summary
Data tables
Graphs
Time series
Profiles
Statistics
Heat map
PDF / CDF
Notices
Copy to clipboard
Save as CSV...
Send to Excel
Clear all
Search
Single Values
Annual Energy (kWh)
Annual fuel usage (kWht)
Capacity factor (%)
Dumped thermal energy (MWht)
Electrical source - Power cycle gross
First year kWh/kW (kWh/kW)
Gross to Net Conversion Factor (%)
Levelized cost of energy ($/kWh)
System heat rate (MMBtu/MWh)
Thermal energy into storage (MWht
Thermal energy to the power block
Thermal power produced by the fiel
Total Annual Water Usage: cycle + r
Total absorbed energy (MWht)
Total fossil fuel usage by all plant su
Total power incident on the field (M
Monthly Data
Hourly Data
Annual Energy (kWh) 1.79176e+08
Capacity factor (%) 41.3209
Dumped thermal energy (MWht) 1844.93
Electrical source - Power cycle gross output (MWhe) 205038
First year kWh/kW (kWh/kW) 3619.71
Gross to Net Conversion Factor (%) 91.0277
Levelized cost of energy ($/kWh) 0.124825
System heat rate (MMBtu/MWh) 3.413
Thermal energy into storage (MWht) 4824.57
Thermal energy to the power block (MWht) 581911
Thermal power produced by the field (MWht) 573210
Total Annual Water Usage: cycle + mirror washing (m3) 40786.2
Total absorbed energy (MWht) 592778
Total fossil fuel usage by all plant subsystems (MMBTU) 0
Total power incident on the field (MWht) 1.09629e+06
Type here to search
ENG
INTL
08:58
10/01/2020

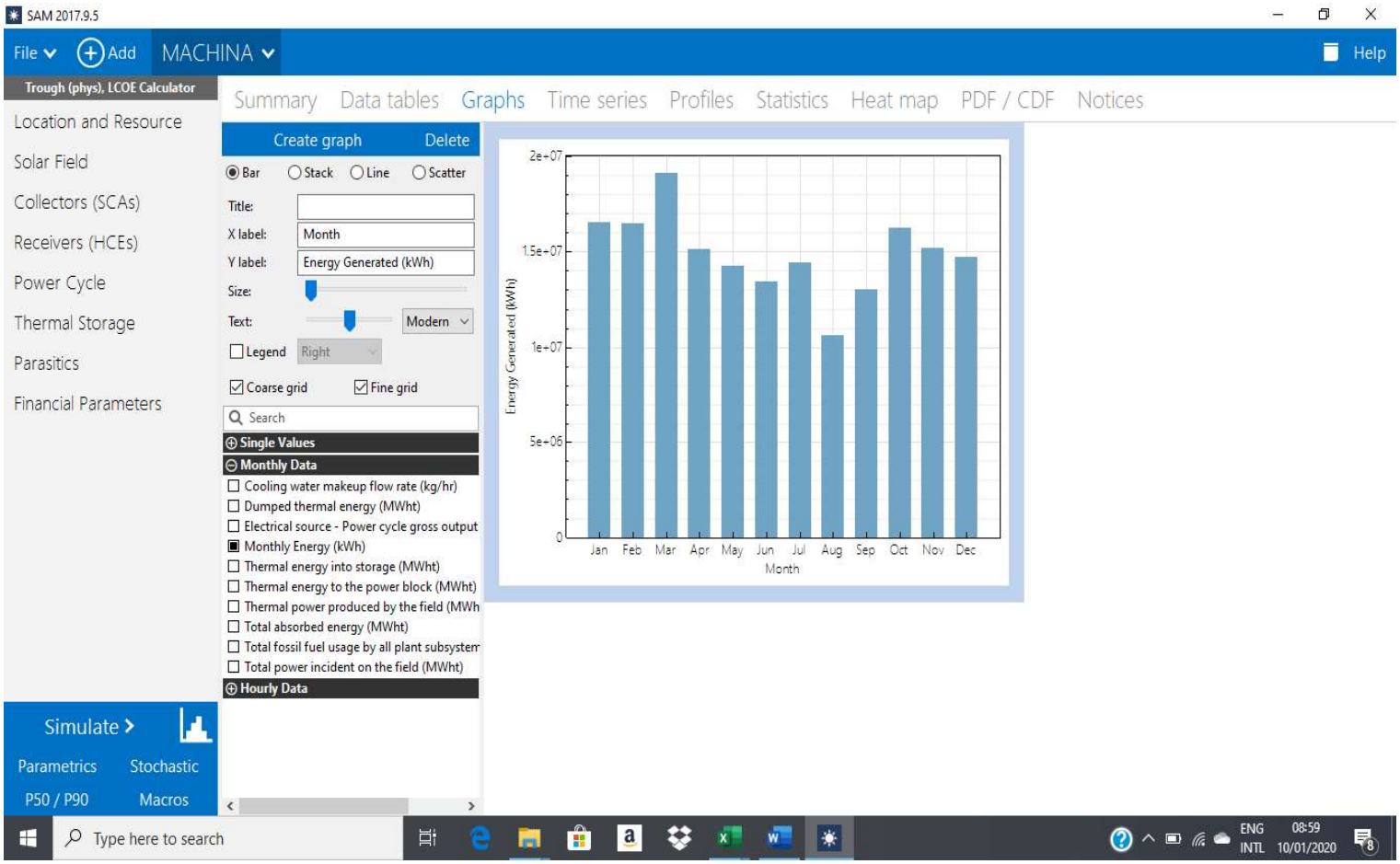
SAM 2017.9.5
File
Add
MACHINA
Help
Trough (phys), LCOE Calculator
Location and Resource
Solar Field
Collectors (SCAs)
Receivers (HCEs)
Power Cycle
Thermal Storage
Parasitics
Financial Parameters
Simulate
Parametrics
Stochastic
P50 / P90
Macros
Summary
Data tables
Graphs
Time series
Profiles
Statistics
Heat map
PDF / CDF
Notices
Create graph
Delete
Bar
Stack
Line
Scatter
Title:
X label:
Month
Y label:
Energy Generated (kWh)
Size:
Text:
Modern
Legend
Right
Coarse grid
Fine grid
Search
Single Values
Monthly Data
Cooling water makeup flow rate (kg/hr)
Dumped thermal energy (MWht)
Electrical source - Power cycle gross output
Monthly Energy (kWh)
Thermal energy into storage (MWht)
Thermal energy to the power block (MWht)
Thermal power produced by the field (MWh
Total absorbed energy (MWht)
Total fossil fuel usage by all plant subsystem
Total power incident on the field (MWht)
Hourly Data
2e+07
1.5e+07
1e+07
5e+06
0
Energy Generated (kWh)
Jan
Feb
Mar
Apr
May
Jun
Jul
Aug
Sep
Oct
Nov
Dec
Month
Type here to search
ENG
INTL
08:59
10/01/2020

APPENDIX 14

SCREENSHOTS OF SIMULATION RESULTS FROM ZARIA

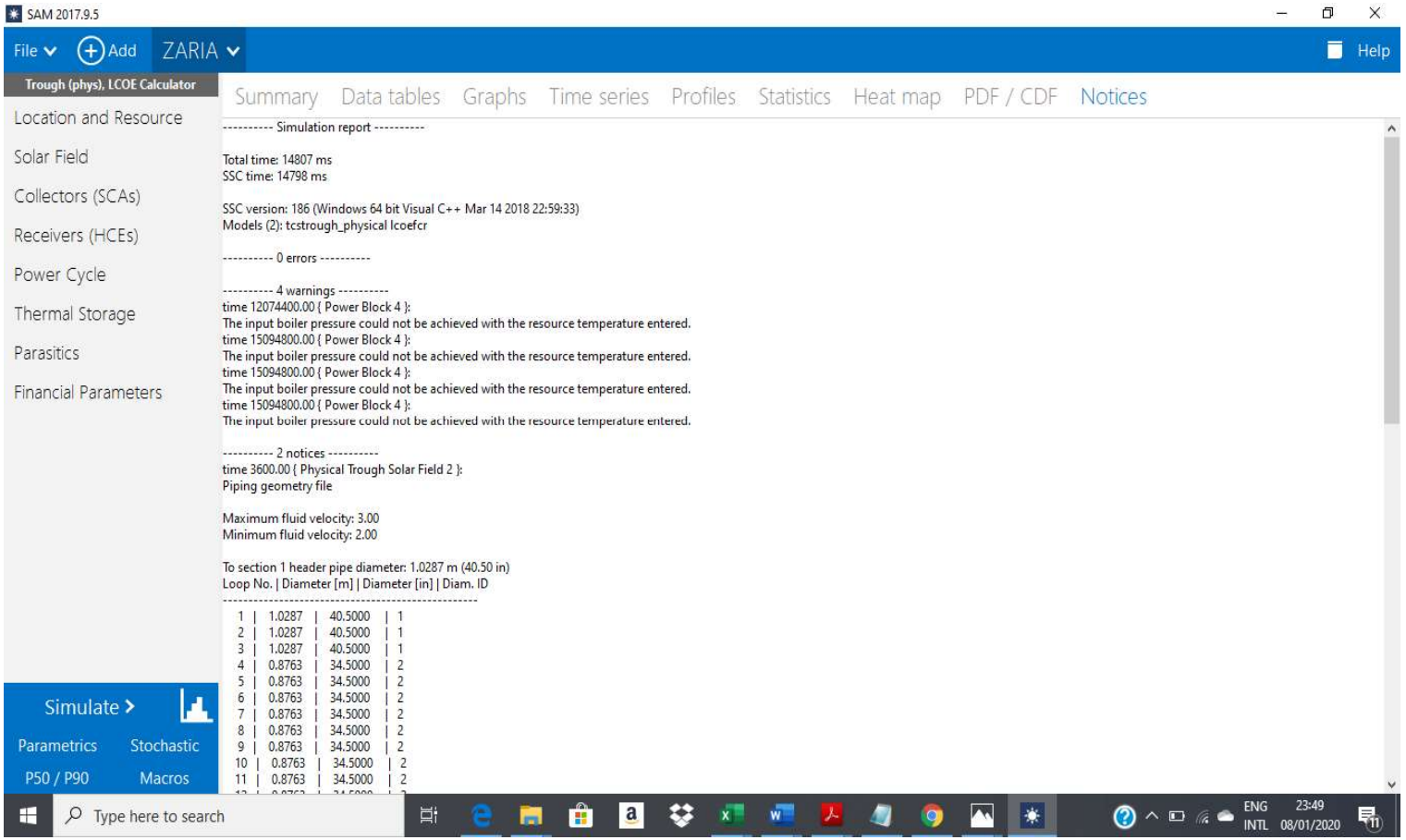

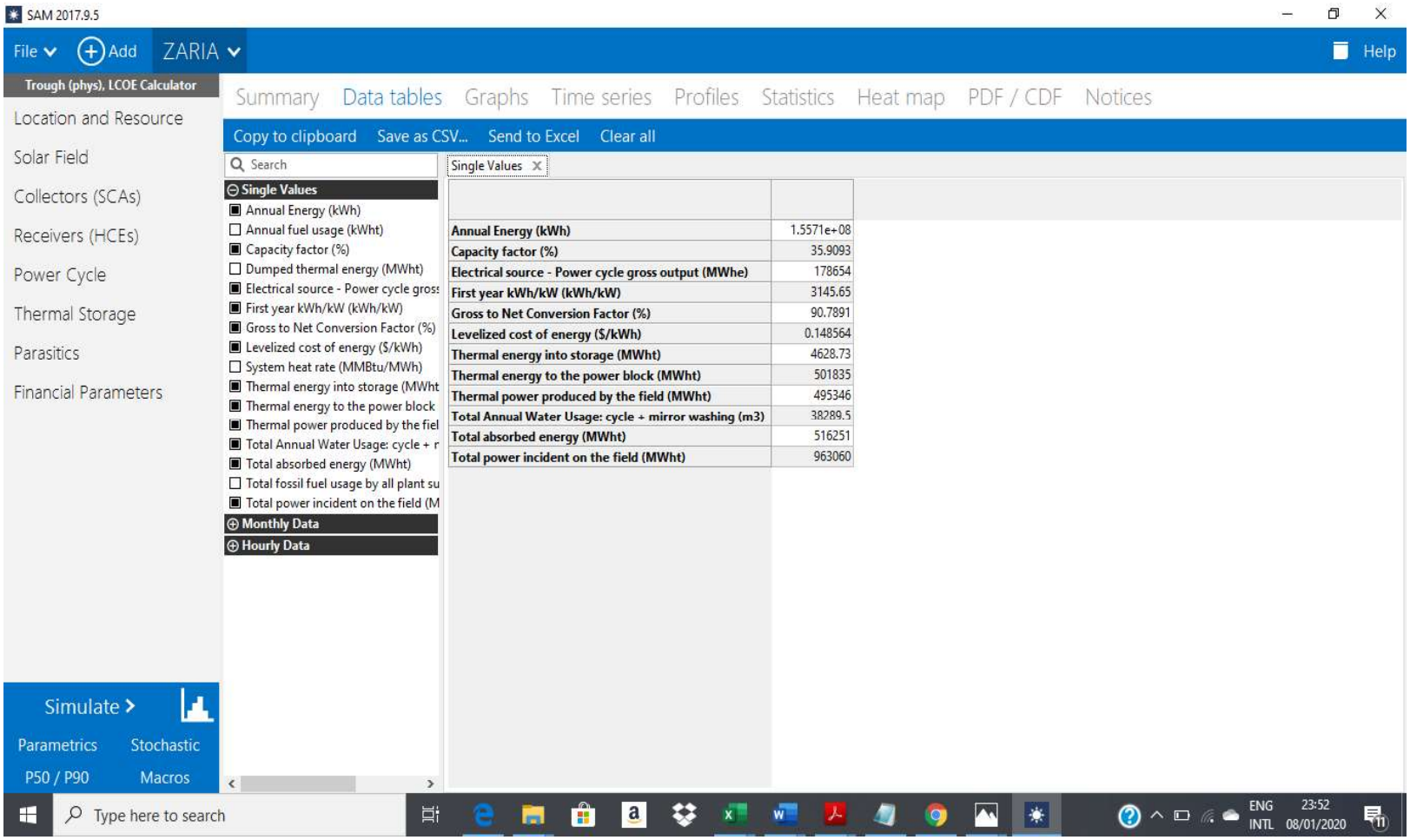
SAM 2017.9.5
File
Add
ZARIA
Help
Trough (phys), LCOE Calculator
Location and Resource
Solar Field
Collectors (SCAs)
Receivers (HCEs)
Power Cycle
Thermal Storage
Parasitics
Financial Parameters
Simulate
Parametrics
Stochastic
P50 / P90
Macros
Summary
Data tables
Graphs
Time series
Profiles
Statistics
Heat map
PDF / CDF
Notices
Copy to clipboard
Save as CSV...
Send to Excel
Clear all
Search
Single Values
Annual Energy (kWh)
Annual fuel usage (kWht)
Capacity factor (%)
Dumped thermal energy (MWht)
Electrical source - Power cycle gross
First year kWh/kW (kWh/kW)
Gross to Net Conversion Factor (%)
Levelized cost of energy ($/kWh)
System heat rate (MMBtu/MWh)
Thermal energy into storage (MWht
Thermal energy to the power block
Thermal power produced by the fiel
Total Annual Water Usage: cycle + r
Total absorbed energy (MWht)
Total fossil fuel usage by all plant su
Total power incident on the field (M
Monthly Data
Hourly Data
Annual Energy (kWh) 1.5571e+08
Capacity factor (%) 35.9093
Electrical source - Power cycle gross output (MWhe) 178654
First year kWh/kW (kWh/kW) 3145.65
Gross to Net Conversion Factor (%) 90.7891
Levelized cost of energy ($/kWh) 0.148564
Thermal energy into storage (MWht) 4628.73
Thermal energy to the power block (MWht) 501835
Thermal power produced by the field (MWht) 495346
Total Annual Water Usage: cycle + mirror washing (m3) 38289.5
Total absorbed energy (MWht) 516251
Total power incident on the field (MWht) 963060
Type here to search
ENG
INTL
23:52
08/01/2020

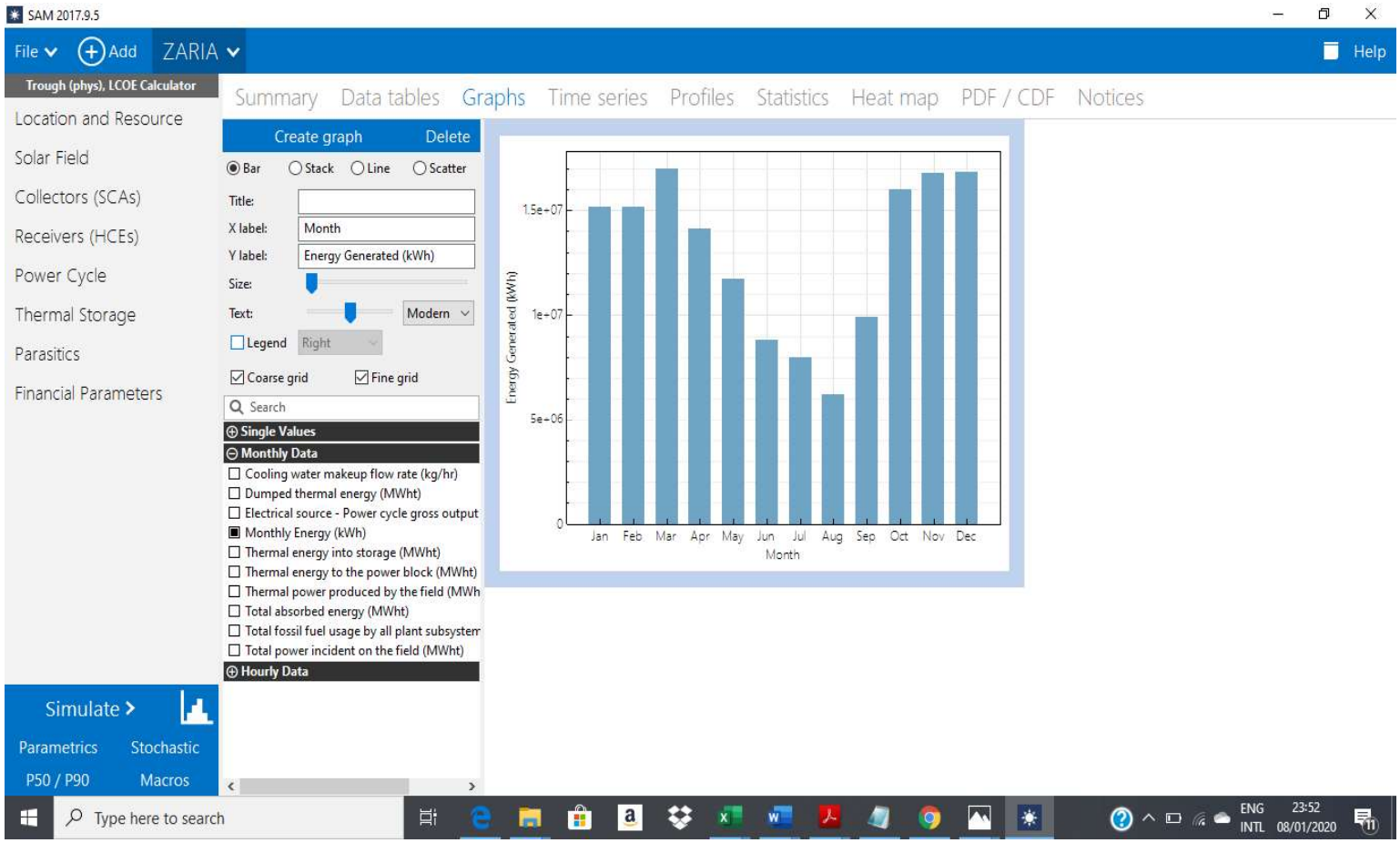
SAM 2017.9.5
File
Add
ZARIA
Help
Trough (phys), LCOE Calculator
Location and Resource
Solar Field
Collectors (SCAs)
Receivers (HCEs)
Power Cycle
Thermal Storage
Parasitics
Financial Parameters
Summary
Data tables
Graphs
Time series
Profiles
Statistics
Heat map
PDF / CDF
Notices
Create graph
Delete
Bar
Stack
Line
Scatter
Title:
X label:
Month
Y label:
Energy Generated (kWh)
Size:
Text:
Modern
Legend
Right
Coarse grid
Fine grid
Search
Single Values
Monthly Data
Cooling water makeup flow rate (kg/hr)
Dumped thermal energy (MWht)
Electrical source - Power cycle gross output
Monthly Energy (kWh)
Thermal energy into storage (MWht)
Thermal energy to the power block (MWht)
Thermal power produced by the field (MWh
Total absorbed energy (MWht)
Total fossil fuel usage by all plant subsystem
Total power incident on the field (MWht)
Hourly Data
Simulate
Parametrics
Stochastic
P50 / P90
Macros
1.5e+07
1e+07
5e+06
0
Energy Generated (kWh)
Jan
Feb
Mar
Apr
May
Jun
Jul
Aug
Sep
Oct
Nov
Dec
Month
Type here to search
ENG
INTL
23:52
08/01/2020

APPENDIX 15

SCREENSHOTS OF SIMULATION RESULTS FROM MAIADUA

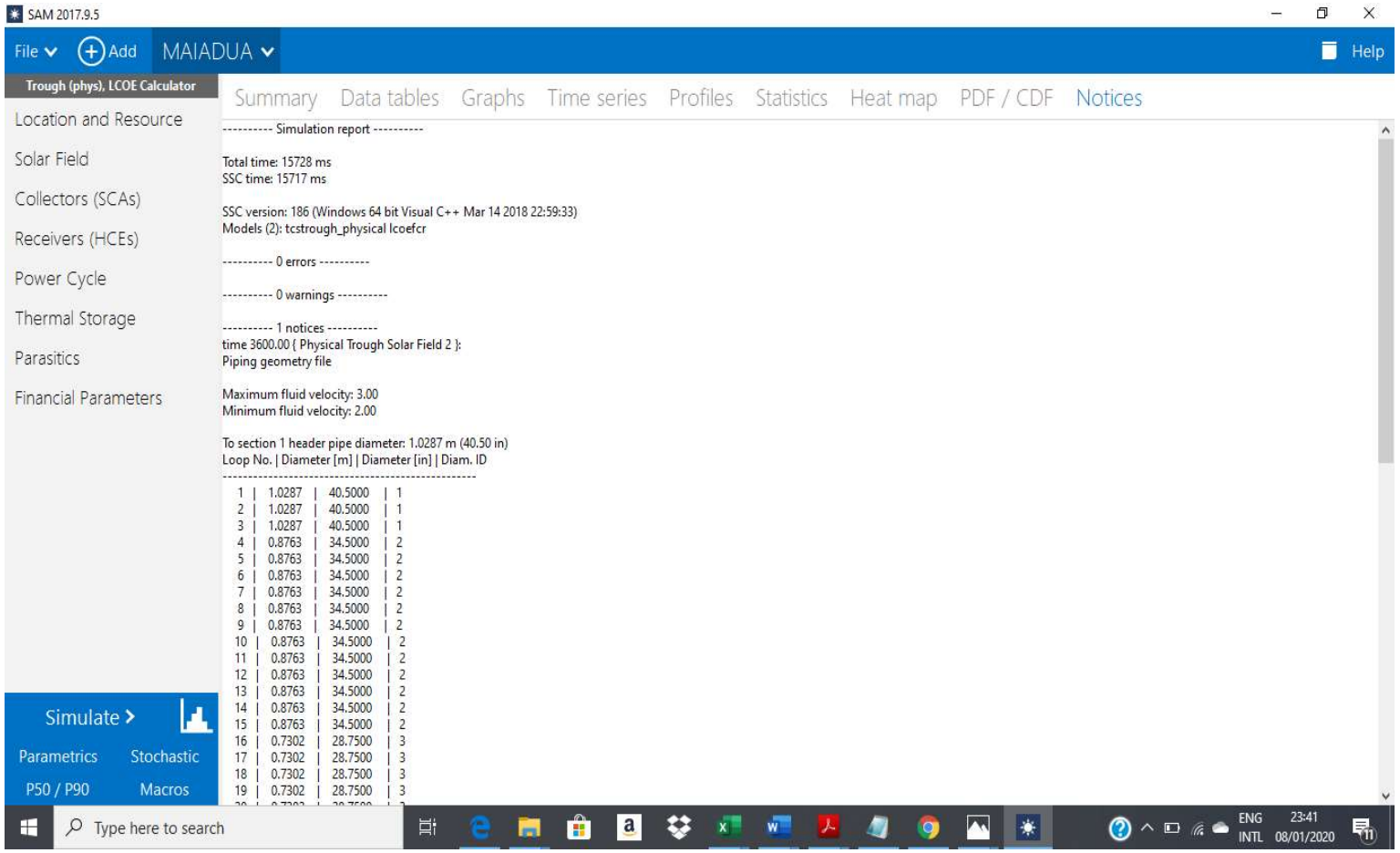

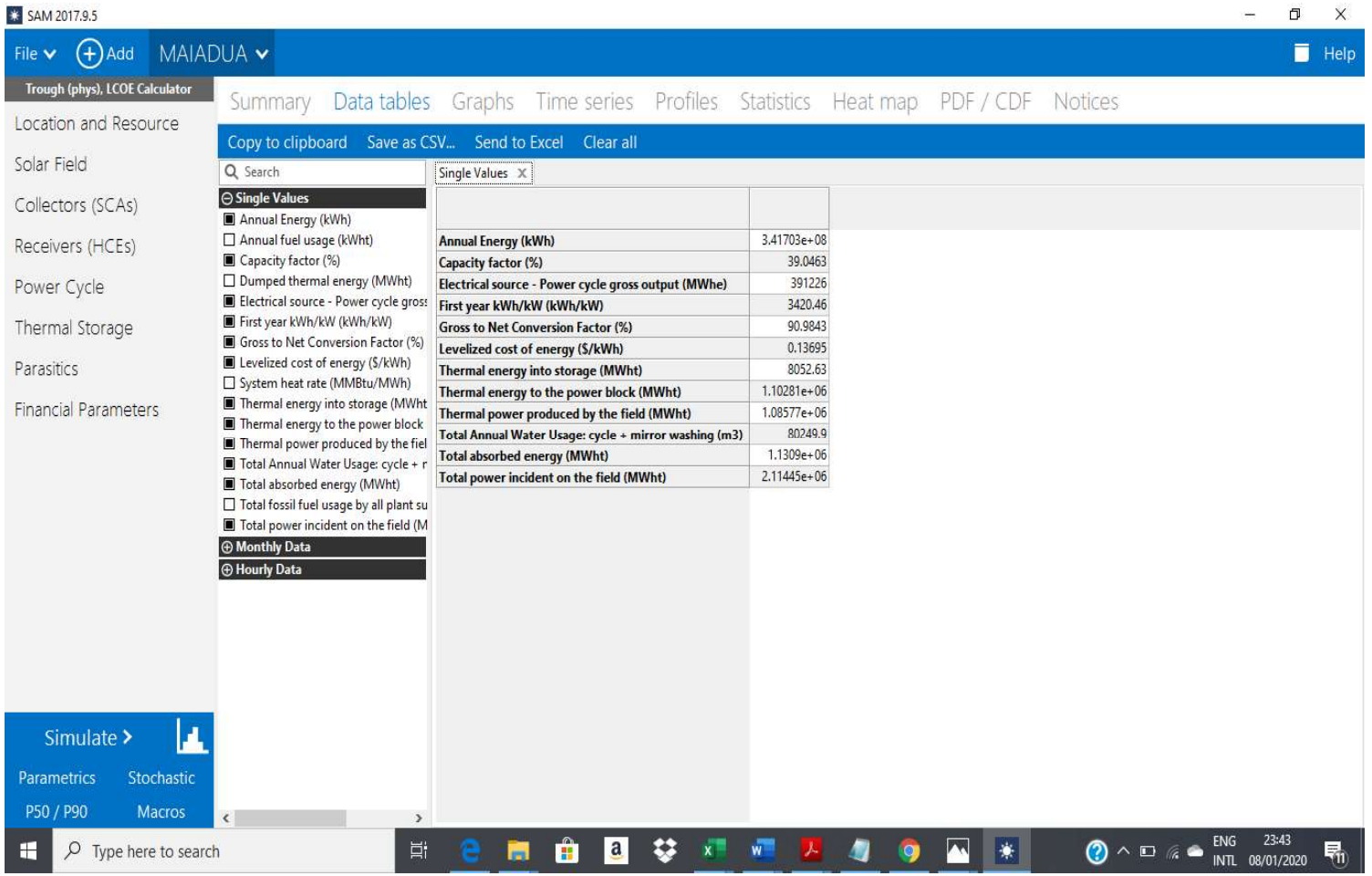
SAM 2017.9.5
File
Add
MAIADUA
Help
Trough (phys), LCOE Calculator
Location and Resource
Solar Field
Collectors (SCAs)
Receivers (HCEs)
Power Cycle
Thermal Storage
Parasitics
Financial Parameters
Simulate
Parametrics
Stochastic
P50 / P90
Macros
Summary
Data tables
Graphs
Time series
Profiles
Statistics
Heat map
PDF / CDF
Notices
Copy to clipboard
Save as CSV...
Send to Excel
Clear all
Search
Single Values
Annual Energy (kWh)
Annual fuel usage (kWht)
Capacity factor (%)
Dumped thermal energy (MWht)
Electrical source - Power cycle gross
First year kWh/kW (kWh/kW)
Gross to Net Conversion Factor (%)
Levelized cost of energy ($/kWh)
System heat rate (MMBtu/MWh)
Thermal energy into storage (MWht
Thermal energy to the power block
Thermal power produced by the fiel
Total Annual Water Usage: cycle + r
Total absorbed energy (MWht)
Total fossil fuel usage by all plant su
Total power incident on the field (M
Monthly Data
Hourly Data
Single Values
Annual Energy (kWh) 3.41703e+08
Capacity factor (%) 39.0463
Electrical source - Power cycle gross output (MWhe) 391226
First year kWh/kW (kWh/kW) 3420.46
Gross to Net Conversion Factor (%) 90.9843
Levelized cost of energy ($/kWh) 0.13695
Thermal energy into storage (MWht) 8052.63
Thermal energy to the power block (MWht) 1.10281e+06
Thermal power produced by the field (MWht) 1.08577e+06
Total Annual Water Usage: cycle + mirror washing (m3) 80249.9
Total absorbed energy (MWht) 1.1309e+06
Total power incident on the field (MWht) 2.11445e+06
Type here to search
ENG
INTL
23:43
08/01/2020

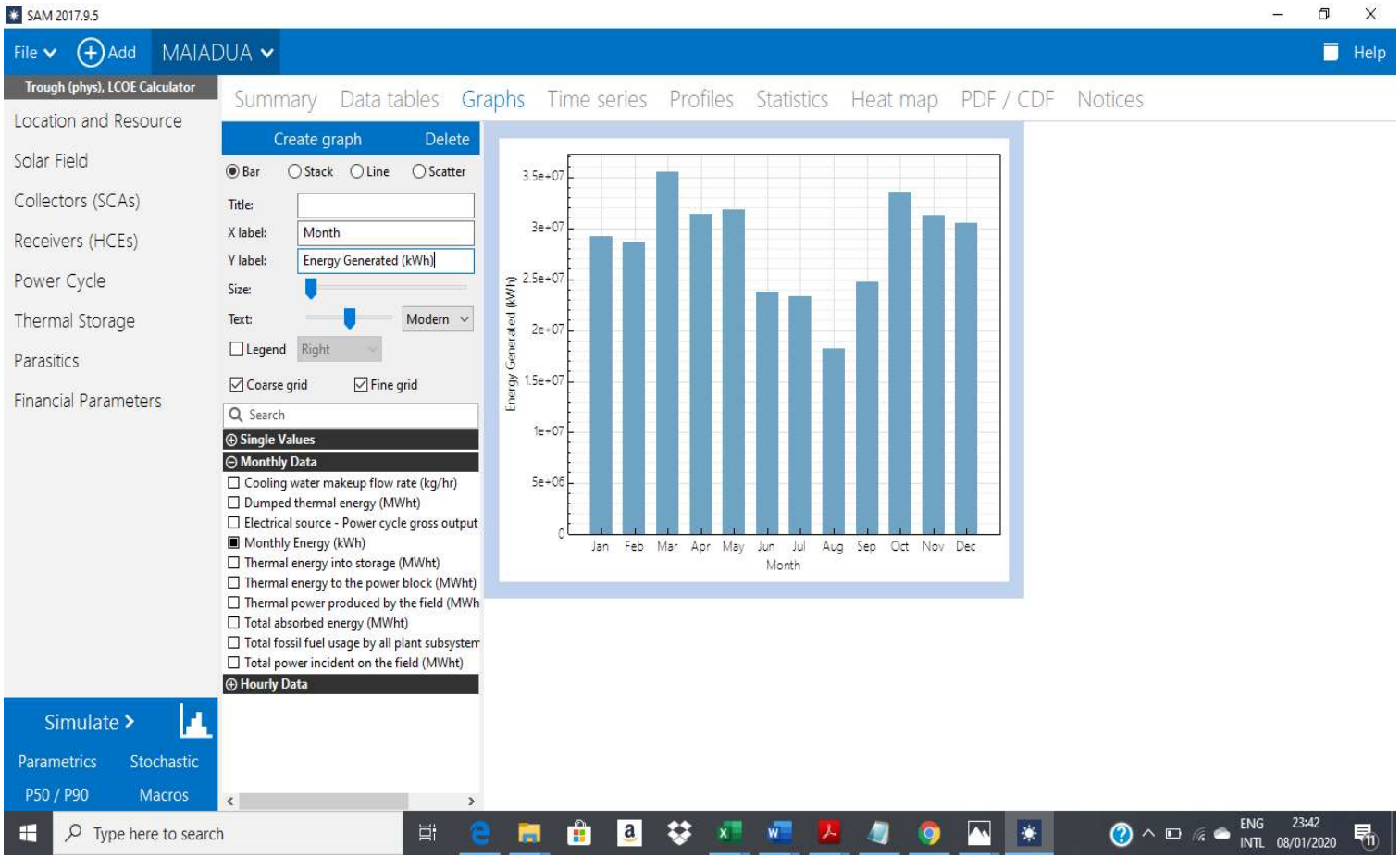
SAM 2017.9.5
File
Add
MAIADUA
Help
Trough (phys), LCOE Calculator
Location and Resource
Solar Field
Collectors (SCAs)
Receivers (HCEs)
Power Cycle
Thermal Storage
Parasitics
Financial Parameters
Summary
Data tables
Graphs
Time series
Profiles
Statistics
Heat map
PDF / CDF
Notices
Create graph
Delete
Bar
Stack
Line
Scatter
Title:
X label:
Month
Y label:
Energy Generated (kWh)
Size:
Text:
Modern
Legend
Right
Coarse grid
Fine grid
Search
Single Values
Monthly Data
Cooling water makeup flow rate (kg/hr)
Dumped thermal energy (MWht)
Electrical source - Power cycle gross output
Monthly Energy (kWh)
Thermal energy into storage (MWht)
Thermal energy to the power block (MWht)
Thermal power produced by the field (MWh
Total absorbed energy (MWht)
Total fossil fuel usage by all plant subsystem
Total power incident on the field (MWht)
Hourly Data
Simulate
Parametrics
Stochastic
P50 / P90
Macros
Energy Generated (kWh)
3.5e+07
3e+07
2.5e+07
2e+07
1.5e+07
1e+07
5e+06
0
Jan
Feb
Mar
Apr
May
Jun
Jul
Aug
Sep
Oct
Nov
Dec
Month
Type here to search
ENG
INTL
23:42
08/01/2020

APPENDIX 16

SCREENSHOTS OF SIMULATION RESULTS FROM GADA

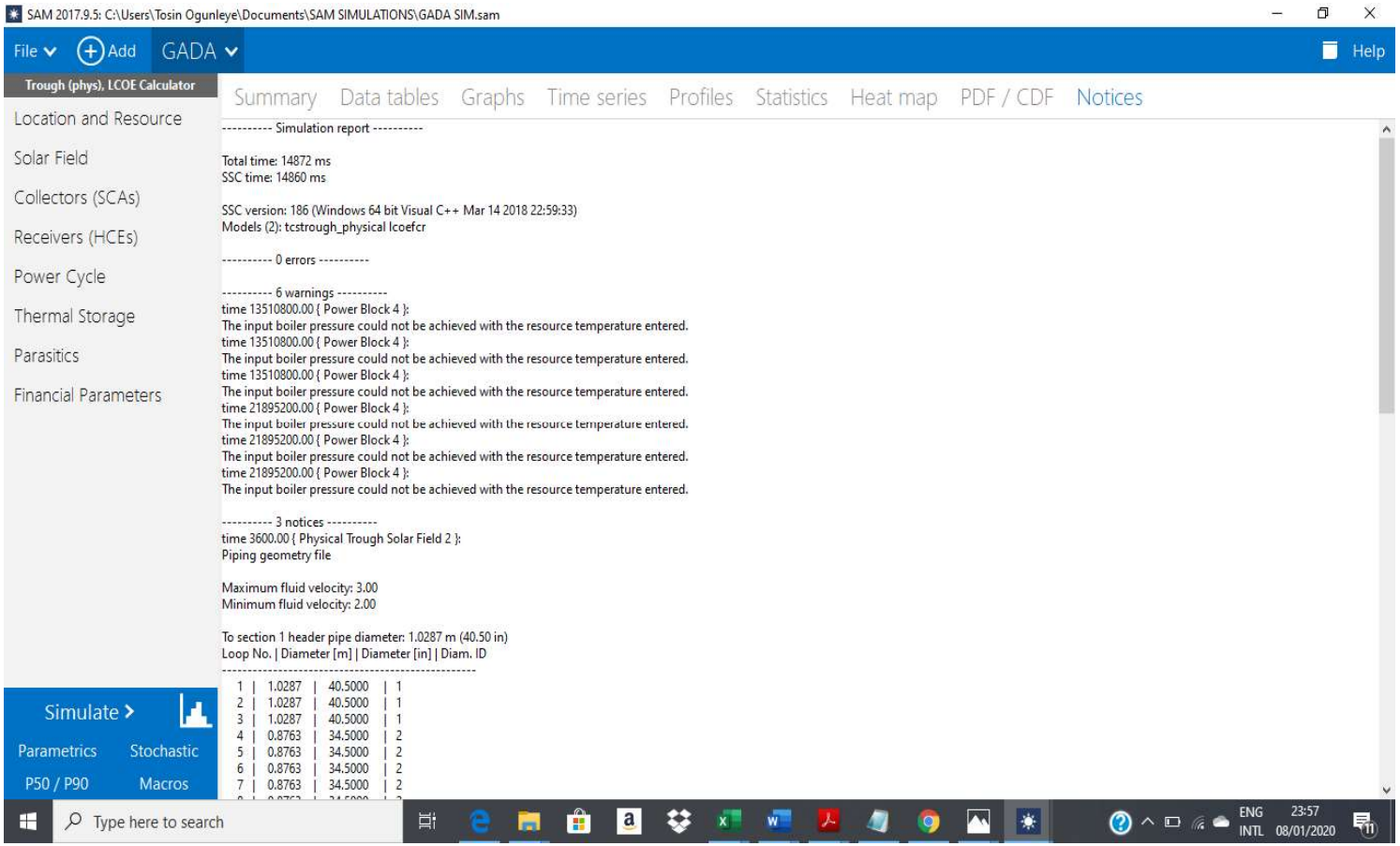

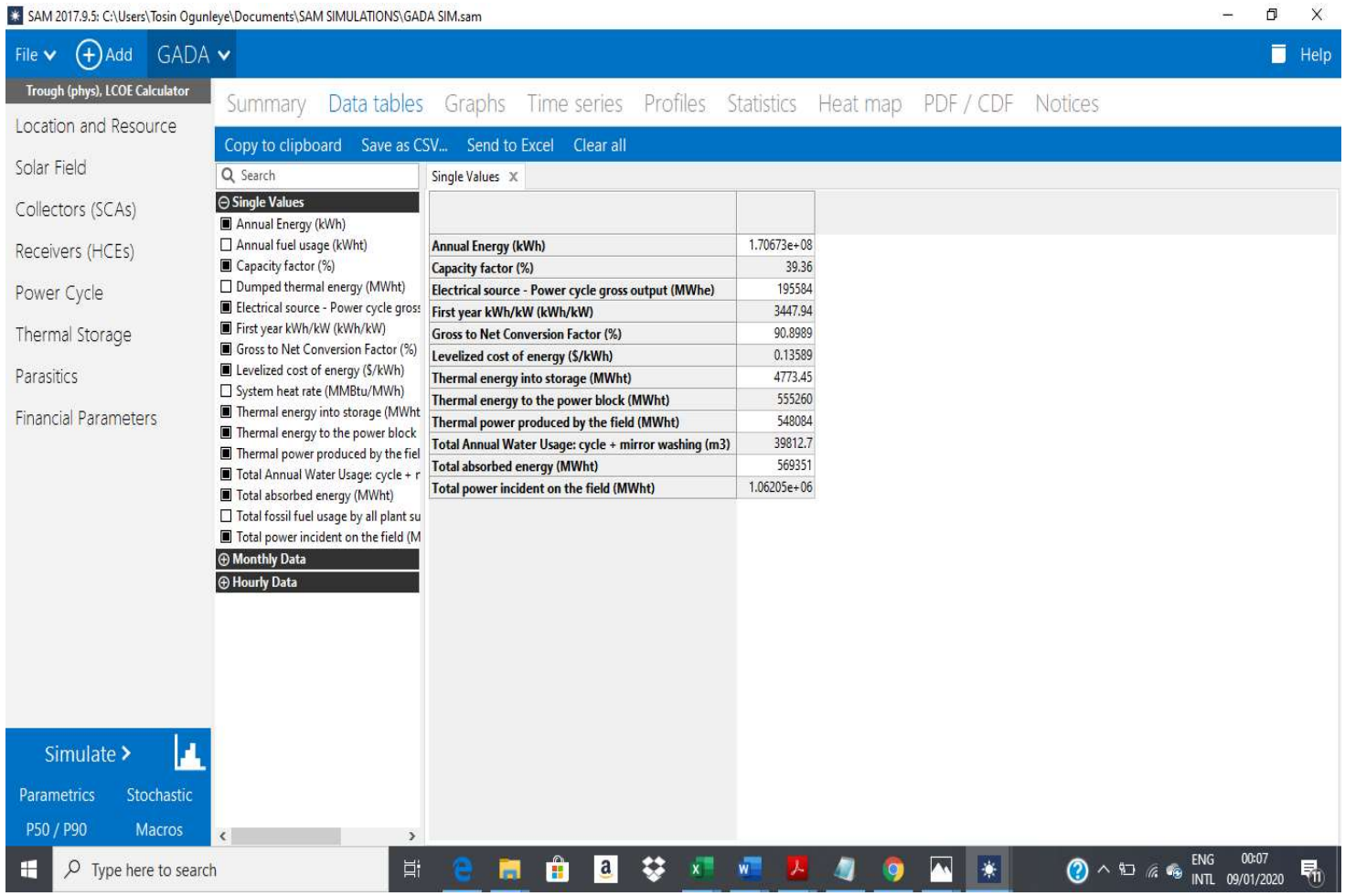
SAM 2017.9.5: C:\Users\Tosin Ogunleye\Documents\SAM SIMULATIONS\GADA SIM.sam
File
Add
GADA
Help
Trough (phys), LCOE Calculator
Location and Resource
Solar Field
Collectors (SCAs)
Receivers (HCEs)
Power Cycle
Thermal Storage
Parasitics
Financial Parameters
Simulate
Parametrics
Stochastic
P50 / P90
Macros
Summary
Data tables
Graphs
Time series
Profiles
Statistics
Heat map
PDF / CDF
Notices
Copy to clipboard
Save as CSV...
Send to Excel
Clear all
Search
Single Values
Annual Energy (kWh)
Annual fuel usage (kWht)
Capacity factor (%)
Dumped thermal energy (MWht)
Electrical source - Power cycle gross
First year kWh/kW (kWh/kW)
Gross to Net Conversion Factor (%)
Levelized cost of energy ($/kWh)
System heat rate (MMBtu/MWh)
Thermal energy into storage (MWht
Thermal energy to the power block
Thermal power produced by the fiel
Total Annual Water Usage: cycle + r
Total absorbed energy (MWht)
Total fossil fuel usage by all plant su
Total power incident on the field (M
Monthly Data
Hourly Data
Single Values
Annual Energy (kWh) 1.70673e+08
Capacity factor (%) 39.36
Electrical source - Power cycle gross output (MWhe) 195584
First year kWh/kW (kWh/kW) 3447.94
Gross to Net Conversion Factor (%) 90.8989
Levelized cost of energy ($/kWh) 0.13589
Thermal energy into storage (MWht) 4773.45
Thermal energy to the power block (MWht) 555260
Thermal power produced by the field (MWht) 548084
Total Annual Water Usage: cycle + mirror washing (m3) 39812.7
Total absorbed energy (MWht) 569351
Total power incident on the field (MWht) 1.06205e+06
Type here to search
ENG
INTL
00:07
09/01/2020

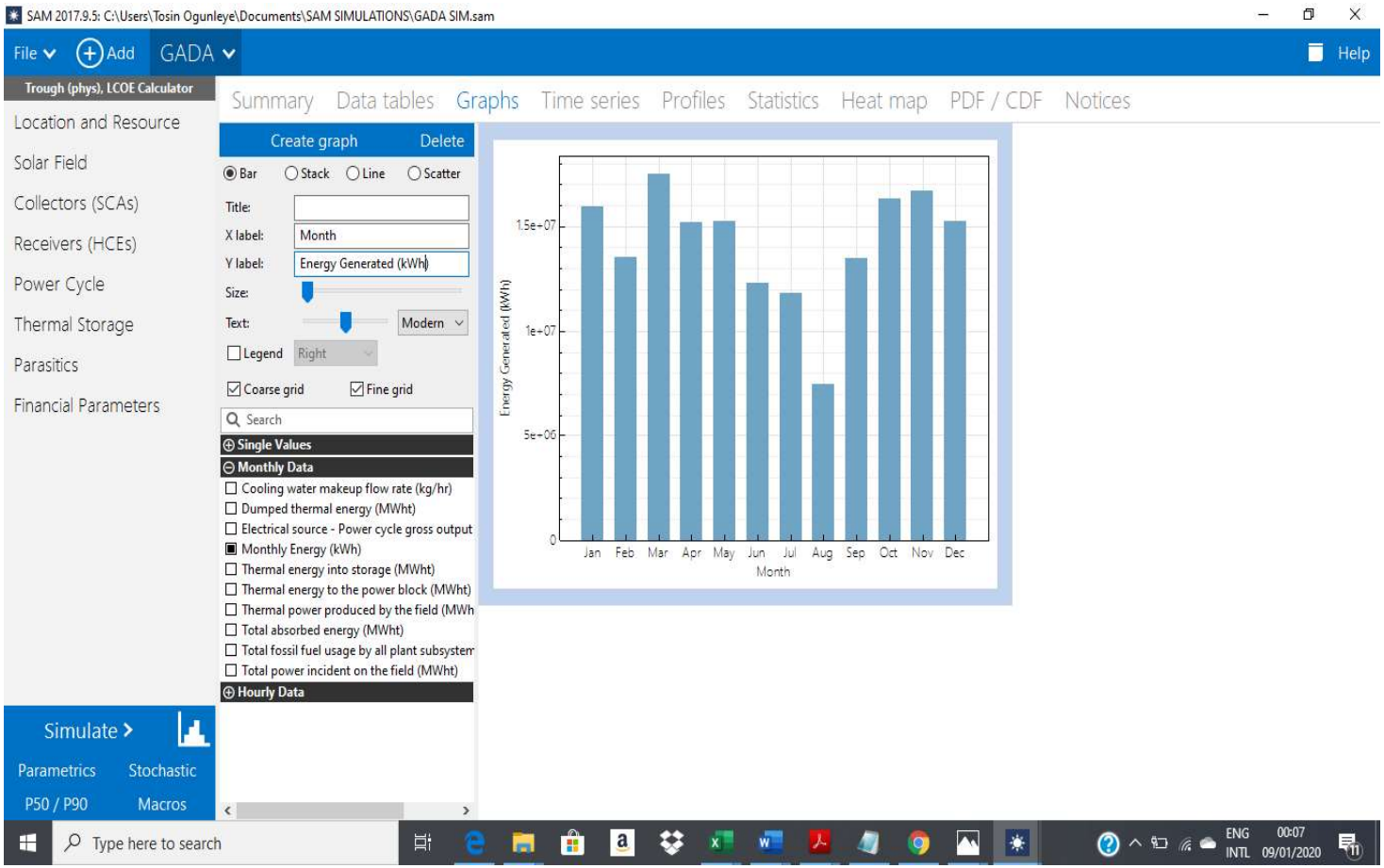
SAM 2017.9.5: C:\Users\Tosin Ogunleye\Documents\SAM SIMULATIONS\GADA SIM.sam
File
Add
GADA
Help
Trough (phys), LCOE Calculator
Location and Resource
Solar Field
Collectors (SCAs)
Receivers (HCEs)
Power Cycle
Thermal Storage
Parasitics
Financial Parameters
Simulate
Parametrics
Stochastic
P50 / P90
Macros
Summary
Data tables
Graphs
Time series
Profiles
Statistics
Heat map
PDF / CDF
Notices
Create graph
Delete
Bar
Stack
Line
Scatter
Title:
X label:
Month
Y label:
Energy Generated (kWh)
Size:
Text:
Modern
Legend
Right
Coarse grid
Fine grid
Search
Single Values
Monthly Data
Cooling water makeup flow rate (kg/hr)
Dumped thermal energy (MWht)
Electrical source - Power cycle gross output
Monthly Energy (kWh)
Thermal energy into storage (MWht)
Thermal energy to the power block (MWht)
Thermal power produced by the field (MWh
Total absorbed energy (MWht)
Total fossil fuel usage by all plant subsystem
Total power incident on the field (MWht)
Hourly Data
1.5e+07
1e+07
5e+06
0
Energy Generated (kWh)
Jan
Feb
Mar
Apr
May
Jun
Jul
Aug
Sep
Oct
Nov
Dec
Month
Type here to search
ENG
INTL
00:07
09/01/2020

APPENDIX 17

BREAKDOWN OF THE CALCULATED COST OF A 100 MW PLANT IN MAIADUA

Direct Cost (DC) Category	Proposed Value	Units	System Value	Cost (US$)	Remarks
(a)	(b)	(c)	(d)	(e)	(f)
Aperture Area	295	$/m^2	949888m^2	280216960	SAM Estimate.
HTF System	90	$/m^2	949888m^2	85489920	SAM Estimate.
Storage	80	$/kWh-t	2144000 kWh-t	171520000	SAM Estimate.
Power Plant (dry-cooled), based on turbine gross	1160	$/kW	100000Kw	116000000	SAM Estimate.
Contingency	10	% of DC		65322688	SAM Estimate.
Estimated DC				**718549568**	
Indirect Cost (IC) category	**Cost in USD (2017 RAP)**	**Proposed/ Applicable Value**	**Units**	**Cost/Cost in USD (2019 Interpolated based on Inflation rate)**	**Remarks**
Land Compensation	815537.11			948,047.51	Average Inflation rate June 2017-September 2019 is 12.8%.
Resettlement of proposed location's inhabitants	242200			281,553.23	Individual household resettlement agreement, livelihood restoration/improvement and resettlement program management.
Preliminary physical design stage	47970			55,764.28	
Detailed physical design stage	46032			53,511.39	
Land preparation	133800			155,540.14	
Site Infrastructure	274000			318,520.17	Roads, drainage, water system.
Housing construction		12500	USD	375000	Quantity 30 portacabins (30-35 feet). Cost of transportation and installation inclusive (REVLYTE Ltd, 2020).
Construction Supervision	96180			111,807.55	
Project Management	127687			148,433.89	Monitoring and evaluation system, public disclosure and incorporation of stakeholder comments.
Engineer, Procure, Construct		5	% of DC	35927478.4	

(a)	(b)	(c)	(d)	(e)	(f)
Shipping Cost		1770	$/Container	88500	Rate as highlighted in UNCTAD (2018). Assume 50 containers from Shanghai-Lagos
Import Duties		5	% of DC	35927478.4	
VAT		7.5	% of DC	53891217.6	
Cargo Handling		1000	$/Container	50000	50 containers and indicated rate assumed. Rate to cover storage/rent charges, equipment hires, transfer charges etc. (Sifax Ports & Cargos, 2016).
Haulage at origin		0.1	/tonne/Km	150,000	Assumptions: $0.1/tonne/Km, distance 1000Km.
Local Haulage		0. 0244	/tonne/Km	37,771.2	30 tonnes for each container assumed. Distance Lagos-Malam Fatori approx. 1032 Km. Rates as indicated in Ubogu A.E. (2011). Average inflation 2011-2019 is 11.59%
Contingency		10	% of IDC	12,855,839.5	
Estimated IDC				**141,414,234.46**	
O&M Cost Category					
Fixed Cost by Capacity		70	$/kW-yr	7,000,000	SAM Estimate. Plant Capacity: 100,000 kW
Variable Cost by Generation		3	$/MWh	1,025,108.7	SAM Estimate. Annual generation: 341702.9 MWh x 25 years
Total Estimated O&M Cost				**8,025,108.7**	
Estimated Total Cost				**868,743,422.44**	

APPENDIX 18

BREAKDOWN OF THE CALCULATED COST OF A 100 MW PLANT IN MALAM-FATORI

Direct Cost (DC) Category	Proposed Value	Units	System Value	Cost (US$)	Remarks
Aperture Area	295	$/m^2	949888m^2	280216960	SAM Estimate.
HTF System	90	$/m^2	949888m^2	85489920	SAM Estimate.
Storage	80	$/kWh-t	2144000 kWh-t	171520000	SAM Estimate.
Power Plant (dry-cooled), based on turbine gross	1160	$/kW	100000kW	116000000	SAM Estimate.
Contingency	10	% of DC		65322688	SAM Estimate.
Estimated DC				**718,549,568**	
Indirect Cost (IC) category	**Cost in USD (2017 RAP)**	**Proposed/ Applicable Value**	**Units**	**Cost in USD (2019 Interpolated based on Inflation rate)**	**Remarks**
Land Compensation	815537.11			948,047.51	Average Inflation rate June 2017-September 2019 is 12.8%.
Resettlement of proposed location's inhabitants	242200			281,553.23	Individual household resettlement agreement, livelihood restoration/improvement and resettlement program management.
Preliminary physical design stage	47970			55,764.28	
Detailed physical design stage	46032			53,511.39	
Land preparation	133800			155,540.14	
Site Infrastructure	274000			318,520.17	Roads, drainage, water system.
Housing construction		12500	USD	375000	Quantity 30 portacabins (30-35 feet). Cost of transportation and installation inclusive (REVLYTE Ltd, 2020).
Construction Supervision	96180			111,807.55	
Project Management	127687			148,433.89	Monitoring and evaluation system, public disclosure and incorporation of stakeholder comments.
Engineer, Procure, Construct		5	% of DC	35,927,478.4	
(a)	**(b)**	**(c)**	**(d)**	**(e)**	**(f)**

(a)	(b)	(c)	(d)	(e)	(f)
Shipping Cost		1770	$/Container	88500	Rate as highlighted in UNCTAD (2018). Assume 50 containers from Shanghai-Lagos
Import Duties		5	% of DC	35927478.4	
VAT		7.5	% of DC	53891217.6	
Cargo Handling	1000		$/Container	50000	50 containers and indicated rate assumed. Rate to cover storage/rent charges, equipment hires, transfer charges etc. (Sifax Ports & Cargos, 2016).
Haulage at origin	0.1		/tonne/Km	150,000	Assumptions: $0.1/tonne/Km, distance 1000Km.
Local Haulage	0. 0244		/tonne/Km	49,483.2	30 tonnes for each container assumed. Distance Lagos-Malam Fatori approx. 1352 Km. Rates as indicated in Ubogu A.E. (2011). Average inflation 2011-2019 is 11.59%
Contingency		10	% of IDC	12853233.58	
Estimated IDC				**141,385,569.34**	
O&M Cost Category					
Fixed Cost by Capacity		70	$/kW-yr	7,000,000	SAM Estimate. Plant Capacity: 100,000 kW
Variable Cost by Generation		3	$/MWh	970,452.6	SAM Estimate. Annual generation: 323484.2 MWh x 25 years
Total Estimated O&M Cost				**7,970,452.7**	
Estimated Total Cost				**868,498,428.04**	

APPENDIX 19

BREAKDOWN OF THE CALCULATED COST OF A 50 MW PLANT IN MACHINA

Direct Cost (DC) Category	Proposed Value	Units	System Value	Cost (US$)	Remarks
Aperture Area	295	$/m^2	477568m^2	140882560	SAM Estimate.
HTF System	90	$/m^2	477568m^2	42981120	SAM Estimate.
Storage	80	$/kWh-t	1072000 kWh-t	85760000	SAM Estimate.
Power Plant (dry-cooled), based on turbine gross	1160	$/kW	50000kW	58000000	SAM Estimate.
Contingency	10	% of DC		32762368	SAM Estimate.
Estimated DC				**360,386,048**	
Indirect Cost (IC) category	**Cost in USD (2017 RAP)**	**Proposed/ Applicable Value**	**Units**	**Cost in USD (2019 Interpolated based on Inflation rate)**	**Remarks**
Land Compensation	407768.56			474,023.76	Average Inflation rate June 2017-September 2019 is 12.8%.
Resettlement of proposed location's inhabitants	121100			140,776.62	Individual household resettlement agreement, livelihood restoration/improvement and resettlement program management.
Preliminary physical design stage	23985			27882.14	
Detailed physical design stage	23016			26755.70	
Land preparation	66900			77770.07	
Site Infrastructure	137000			159260.09	Roads, drainage, water system.
Housing construction		12500	USD	187500	Quantity 15 portacabins (30-35 feet). Cost of transportation and installation inclusive (REVLYTE Ltd, 2020).
Construction Supervision	48090			55903.78	
Project Management	63843.5			74216.95	Monitoring and evaluation system, public disclosure and incorporation of stakeholder comments.
Engineer, Procure, Construct		5	% of DC	18019302.4	

(a)	(b)	(c)	(d)	(e)	(f)
Shipping Cost		1770	$/Container	44250	Rate as highlighted in UNCTAD (2018). Assume 25 containers from Shanghai-Lagos
Import Duties		5	% of DC	18019302.4	
VAT		7.5	% of DC	27028953.6	
Cargo Handling	1000		$/Container	25000	25 containers and indicated rate assumed. Rate to cover storage/rent charges, equipment hires, transfer charges etc. (Sifax Ports & Cargos, 2016).
Haulage at origin	0.1		/tonne/Km	75,000	Assumptions: $0.1/tonne/Km, distance 1000Km.
Local Haulage	0. 0244		/tonne/Km	23241	30 tonnes for each container assumed. Distance Lagos-Malam Fatori approx. 1270 Km. Rates as indicated in Ubogu A.E. (2011). Average inflation 2011-2019 is 11.59%
Contingency		10	% of IDC	6445913.77	
Estimated IDC				**70,905,051.5**	
O&M Cost Category					
Fixed Cost by Capacity		70	$/kW-yr	3,500,000	SAM Estimate. Plant Capacity: 50,000 kW
Variable Cost by Generation		3	$/MWh	537528.9	SAM Estimate. Annual generation: 179,176.3MWh x 25 years
Total Estimated O&M Cost				**4,037,528.9**	
Estimated Total Cost				**435,328,628.4**	

APPENDIX 20

BREAKDOWN OF THE CALCULATED COST OF A 50 MW PLANT IN GADA

Direct Cost (DC) Category	**Proposed Value**	**Units**	**System Value**	**Cost (US$)**	**Remarks**
Aperture Area	295	$\$/m^2$	$472320m^2$	139334400	SAM Estimate.
HTF System	90	$\$/m^2$	$472320m^2$	42508800	SAM Estimate.
Storage	80	$/kWh-t	1072000 kWh-t	85760000	SAM Estimate.
Power Plant (dry-cooled), based on turbine gross	1160	$/kW	50000kW	58000000	SAM Estimate.
Contingency	10	% of DC		32560320	SAM Estimate.
Estimated DC				**358,163,520**	
Indirect Cost (IC) category	**Cost in USD (2017 RAP)**	**Proposed/ Applicable Value**	**Units**	**Cost in USD (2019 Interpolated based on Inflation rate)**	**Remarks**
Land Compensation	407768.56			474,023.76	Average Inflation rate June 2017-September 2019 is 12.8%.
Resettlement of proposed location's inhabitants	121100			140,776.62	Individual household resettlement agreement, livelihood restoration/improvement and resettlement program management.
Preliminary physical design stage	23985			27882.14	
Detailed physical design stage	23016			26755.70	
Land preparation	66900			77770.07	
Site Infrastructure	137000			159260.09	Roads, drainage, water system.
Housing construction		12500	USD	187500	Quantity 15 portacabins (30-35 feet). Cost of transportation and installation inclusive (REVLYTE Ltd, 2020).
Construction Supervision	48090			55903.78	
Project Management	63843.5			74216.95	Monitoring and evaluation system, public disclosure and incorporation of stakeholder comments.
Engineer, Procure, Construct		5	% of DC	17908176	

(a)	(b)	(c)	(d)	(e)	(f)
Shipping Cost		1770	$/Container	44250	Rate as highlighted in UNCTAD (2018). Assume 25 containers from Shanghai-Lagos
Import Duties		5	% of DC	17908176	
VAT		7.5	% of DC	26862264	
Cargo Handling	1000		$/Container	25000	25 containers and indicated rate assumed. Rate to cover storage/rent charges, equipment hires, transfer charges etc. (Sifax Ports & Cargos, 2016).
Haulage at origin	0.1		/tonne/Km	75,000	Assumptions: $0.1/tonne/Km, distance 1000Km.
Local Haulage	0. 0244		/tonne/Km	19910.4	30 tonnes for each container assumed. Distance Lagos-Malam Fatori approx. 1088 Km. Rates as indicated in Ubogu A.E. (2011). Average inflation 2011-2019 is 11.59%
Contingency		10	% of IDC	6394599.93	
Estimated IDC				**70,340,599.22**	
O&M Cost Category					
Fixed Cost by Capacity		70	$/kW-yr	3,500,000	SAM Estimate. Plant Capacity: 50,000 kW
Variable Cost by Generation		3	$/MWh	512019.27	SAM Estimate. Annual generation: 170,673.09MWh x 25 years
Total Estimated O&M Cost				**4,012,019.27**	
Estimated Total Cost				**432,516,138.49**	

APPENDIX 21

BREAKDOWN OF THE CALCULATED COST OF A 50 MW PLANT IN ZARIA

Direct Cost (DC) Category	Proposed Value	Units	System Value	Cost (US$)	Remarks
Aperture Area	295	$/m^2	472320m^2	139334400	SAM Estimate.
HTF System	90	$/m^2	472320m^2	42508800	SAM Estimate.
Storage	80	$/kWh-t	1072000 kWh-t	85760000	SAM Estimate.
Power Plant (dry-cooled), based on turbine gross	1160	$/kW	50000kW	58000000	SAM Estimate.
Contingency	10	% of DC		32560320	SAM Estimate.
Estimated DC				**358,163,520**	
Indirect Cost (IC) category	**Cost in USD (2017 RAP)**	**Proposed/ Applicable Value**	**Units**	**Cost in USD (2019 Interpolated based on Inflation rate)**	**Remarks**
Land Compensation	407768.56			474,023.76	Average Inflation rate June 2017-September 2019 is 12.8%.
Resettlement of proposed location's inhabitants	121100			140,776.62	Individual household resettlement agreement, livelihood restoration/improvement and resettlement program management.
Preliminary physical design stage	23985			27882.14	
Detailed physical design stage	23016			26755.70	
Land preparation	66900			77770.07	
Site Infrastructure	137000			159260.09	Roads, drainage, water system.
Housing construction		12500	USD	187500	Quantity 15 portacabins (30-35 feet). Cost of transportation and installation inclusive (REVLYTE Ltd, 2020).
Construction Supervision	48090			55903.78	
Project Management	63843.5			74216.95	Monitoring and evaluation system, public disclosure and incorporation of stakeholder comments.
Engineer, Procure, Construct		5	% of DC	17908176	

(a)	(b)	(c)	(d)	(e)	(f)
Shipping Cost		1770	$/Container	44250	Rate as highlighted in UNCTAD (2018). Assume 25 containers from Shanghai-Lagos
Import Duties		5	% of DC	17908176	
VAT		7.5	% of DC	26862264	
Cargo Handling	1000		$/Container	25000	25 containers and indicated rate assumed. Rate to cover storage/rent charges, equipment hires, transfer charges etc. (Sifax Ports & Cargos, 2016).
Haulage at origin	0.1		/tonne/Km	75,000	Assumptions: $0.1/tonne/Km, distance 1000Km.
Local Haulage	0. 0244		/tonne/Km	15042.6	30 tonnes for each container assumed. Distance Lagos-Malam Fatori approx. 822 Km. Rates as indicated in Ubogu A.E. (2011). Average inflation 2011-2019 is 11.59%
Contingency		10	% of IDC	6406199.77	
Estimated IDC				**70,468,197.48**	
O&M Cost Category					
Fixed Cost by Capacity		70	$/kW-yr	3,500,000	SAM Estimate. Plant Capacity: 50,000 kW
Variable Cost by Generation		3	$/MWh	467130.06	SAM Estimate. Annual generation: 155,710.02MWh x 25 years
Total Estimated O&M Cost				**3,967,130.06**	
Estimated Total Cost				**432,598,847.54**	

APPENDIX 22

CALCULATED LCOE FOR A 100 MW PLANT IN MAIADUA

INPUT

Simulated Energy Output (kWh)	**341,702,879.00**
Calculated Capital Investment (USD)	**859963802.5**
Projected Annual Inflation Rate (%)	**7.5**
System Annual Degradation (%)	**2**

O&M (USD)			
Year	**O&M**		**Total for Year**
(a)	**(b)**	**(c)**	**(d)**
Year 1	-		
Year 2	8025108.7		8025108.7
Year 3	8626991.853		8626991.853
Year 4	9274016.241		9274016.241
Year 5	9969567.46		9969567.46
Year 6	10717285.02		10717285.02
Year 7	11521081.4		11521081.4
Year 8	12385162.5		12385162.5
Year 9	13314049.69		13314049.69
Year 10	14312603.41		14312603.41
Year 11	15386048.67		15386048.67

Energy Production			
Year	**Energy Code**	**System Degradation**	**Energy Output (kWh)**
(a)	**(b)**	**(c)**	**(d)**
Year 1	P_{Y1}	100.00	341,702,879
Year 2	P_{Y2}	98.00	334,868,821
Year 3	P_{Y3}	96.04	328,171,445
Year 4	P_{Y4}	94.12	321,608,016
Year 5	P_{Y5}	92.24	315,175,856
Year 6	P_{Y6}	90.39	308,872,339
Year 7	P_{Y7}	88.58	302,694,892
Year 8	P_{Y8}	86.81	296,640,994
Year 9	P_{Y9}	85.08	290,708,174
Year 10	P_{Y10}	83.37	284,894,011
Year 11	P_{Y11}	81.71	279,196,130

(a)	(b)	(c)	(d)
Year 12	16540002.32		16540002.32
Year 13	17780502.49		17780502.49
Year 14	19114040.18		19114040.18
Year 15	20547593.2		20547593.2
Year 16	22088662.68		22088662.68
Year 17	23745312.39		23745312.39
Year 18	25526210.82		25526210.82
Year 19	27440676.63		27440676.63
Year 20	29498727.37		29498727.37
Year 21	31711131.93		31711131.93
Year 22	34089466.82		34089466.82
Year 23	36646176.83		36646176.83
Year 24	39394640.09		39394640.09
Year 25	42349238.1		42349238.1
Total	500004296.8		**500004296.8**

(a)	(b)	(c)	(d)
Year 12	P_{Y12}	80.07	273,612,208
Year 13	P_{Y13}	78.47	268,139,964
Year 14	P_{Y14}	76.90	262,777,164
Year 15	P_{Y15}	75.36	257,521,621
Year 16	P_{Y16}	73.86	252,371,189
Year 17	P_{Y17}	72.38	247,323,765
Year 18	P_{Y18}	70.93	242,377,290
Year 19	P_{Y19}	69.51	237,529,744
Year 20	P_{Y20}	68.12	232,779,149
Year 21	P_{Y21}	66.76	228,123,566
Year 22	P_{Y22}	65.43	223,561,095
Year 23	P_{Y23}	64.12	219,089,873
Year 24	P_{Y24}	62.83	214,708,075
Year 25	P_{Y25}	61.58	210,413,914
Total			**6,774,862,173**

OUTPUT

Total O&M Life Cycle cost (USD)	**500004296.8**
Life Cycle cost of System (USD)	**1359968099**
Lifetime Energy Production (kWh)	**6774862173**
LCOE (USD/kWh)	**0.200737382**

APPENDIX 23

CALCULATED LCOE FOR A 100 MW PLANT IN MALAM-FATORI

INPUT

Simulated Energy Output (kWh)	**323484204**
Calculated Capital Investment (USD)	**859935137.3**
Projected Annual Inflation Rate (%)	**7.5**
System Annual Degradation (%)	**2**

O&M (USD)			
Year	**O&M**		**Total for Year**
(a)	**(b)**	**(c)**	**(d)**
Year 1	-		
Year 2	7970452.7		7970452.7
Year 3	8568236.653		8568236.653
Year 4	9210854.401		9210854.401
Year 5	9901668.482		9901668.482
Year 6	10644293.62		10644293.62
Year 7	11442615.64		11442615.64
Year 8	12300811.81		12300811.81
Year 9	13223372.7		13223372.7
Year 10	14215125.65		14215125.65
Year 11	15281260.07		15281260.07
Year 12	16427354.58		16427354.58

Energy Production			
Year	**Energy Code**	**System Degradation**	**Energy Output (kWh)**
(a)	**(b)**	**(c)**	**(d)**
Year 1	P_{Y1}	100.00	323484204
Year 2	P_{Y2}	98.00	317014519.9
Year 3	P_{Y3}	96.04	310674229.5
Year 4	P_{Y4}	94.12	304460744.9
Year 5	P_{Y5}	92.24	298371530
Year 6	P_{Y6}	90.39	292404099.4
Year 7	P_{Y7}	88.58	286556017.4
Year 8	P_{Y8}	86.81	280824897.1
Year 9	P_{Y9}	85.08	275208399.2
Year 10	P_{Y10}	83.37	269704231.2
Year 11	P_{Y11}	81.71	264310146.5
Year 12	P_{Y12}	80.07	259023943.6

(a)	(b)	(c)	(d)
Year 13	17659406.17		17659406.17
Year 14	18983861.64		18983861.64
Year 15	20407651.26		20407651.26
Year 16	21938225.1		21938225.1
Year 17	23583591.99		23583591.99
Year 18	25352361.38		25352361.38
Year 19	27253788.49		27253788.49
Year 20	29297822.63		29297822.63
Year 21	31495159.32		31495159.32
Year 22	33857296.27		33857296.27
Year 23	36396593.49		36396593.49
Year 24	39126338		39126338
Year 25	42060813.35		42060813.35
Total	**496598955.4**		**496598955.4**

(a)	(b)	(c)	(d)
Year 13	P_{Y13}	78.47	253843464.7
Year 14	P_{Y14}	76.90	248766595.4
Year 15	P_{Y15}	75.36	243791263.5
Year 16	P_{Y16}	73.86	238915438.3
Year 17	P_{Y17}	72.38	234137129.5
Year 18	P_{Y18}	70.93	229454386.9
Year 19	P_{Y19}	69.51	224865299.2
Year 20	P_{Y20}	68.12	220367993.2
Year 21	P_{Y21}	66.76	215960633.3
Year 22	P_{Y22}	65.43	211641420.7
Year 23	P_{Y23}	64.12	207408592.2
Year 24	P_{Y24}	62.83	203260420.4
Year 25	P_{Y25}	61.58	199195212
Total			**6413644812**

OUTPUT

Total O&M Life Cycle cost (USD)	**496598955.4**
Life Cycle cost of System (USD)	**1356534093**
Lifetime Energy Production (kWh)	**6413644812**
LCOE (USD/kWh)	**0.211507518**

APPENDIX 24

CALCULATED LCOE FOR A 50 MW PLANT IN MACHINA

INPUT

Simulated Energy Output (kWh)	**179176312**
Calculated Capital Investment (USD)	**435328628.4**
Projected Annual Inflation Rate (%)	**7.5**
System Annual Degradation (%)	**2**

O&M (USD)			
Year	**O&M**		**Total for Year**
(a)	**(b)**	**(c)**	**(d)**
Year 1	-		
Year 2	4037528.9		4037528.9
Year 3	4340343.568		4340343.568
Year 4	4665869.335		4665869.335
Year 5	5015809.535		5015809.535
Year 6	5391995.25		5391995.25
Year 7	5796394.894		5796394.894
Year 8	6231124.511		6231124.511
Year 9	6698458.85		6698458.85
Year 10	7200843.263		7200843.263
Year 11	7740906.508		7740906.508
Year 12	8321474.496		8321474.496

Energy Production			
Year	**Energy Code**	**System Degradation**	**Energy Output (kWh)**
(a)	**(b)**	**(c)**	**(d)**
Year 1	P_{Y1}	100.00	179,176,312
Year 2	P_{Y2}	98.00	175,592,786
Year 3	P_{Y3}	96.04	172,080,930
Year 4	P_{Y4}	94.12	168,639,311
Year 5	P_{Y5}	92.24	165,266,525
Year 6	P_{Y6}	90.39	161,961,195
Year 7	P_{Y7}	88.58	158,721,971
Year 8	P_{Y8}	86.81	155,547,531
Year 9	P_{Y9}	85.08	152,436,581
Year 10	P_{Y10}	83.37	149,387,849
Year 11	P_{Y11}	81.71	146,400,092
Year 12	P_{Y12}	80.07	143,472,090

(a)	(b)	(c)	(d)
Year 13	8945585.083		8945585.083
Year 14	9616503.965		9616503.965
Year 15	10337741.76		10337741.76
Year 16	11113072.39		11113072.39
Year 17	11946552.82		11946552.82
Year 18	12842544.29		12842544.29
Year 19	13805735.11		13805735.11
Year 20	14841165.24		14841165.24
Year 21	15954252.63		15954252.63
Year 22	17150821.58		17150821.58
Year 23	18437133.2		18437133.2
Year 24	19819918.19		19819918.19
Year 25	21306412.05		21306412.05
Total	**251558187.4**		**251558187.4**

(a)	(b)	(c)	(d)
Year 13	P_{Y13}	78.47	140,602,649
Year 14	P_{Y14}	76.90	137,790,596
Year 15	P_{Y15}	75.36	135,034,784
Year 16	P_{Y16}	73.86	132,334,088
Year 17	P_{Y17}	72.38	129,687,406
Year 18	P_{Y18}	70.93	127,093,658
Year 19	P_{Y19}	69.51	124,551,785
Year 20	P_{Y20}	68.12	122,060,749
Year 21	P_{Y21}	66.76	119,619,534
Year 22	P_{Y22}	65.43	117,227,144
Year 23	P_{Y23}	64.12	114,882,601
Year 24	P_{Y24}	62.83	112,584,949
Year 25	P_{Y25}	61.58	110,333,250
Total			**3,552,486,365**

OUTPUT

Total O&M Life Cycle cost (USD)	**251558187.4**
Life Cycle cost of System (USD)	**686886815.8**
Lifetime Energy Production (kWh)	**3552486365**
LCOE (USD/kWh)	**0.193353822**

APPENDIX 25

CALCULATED LCOE FOR A 50 MW PLANT IN GADA

INPUT

Simulated Energy Output (kWh)	**170673093**
Calculated Capital Investment (USD)	**428504119.2**
Projected Annual Inflation Rate (%)	**7.5**
System Annual Degradation (%)	**2**

O&M (USD)			
Year	**O&M**		**Total for Year**
(a)	**(b)**	**(c)**	**(d)**
Year 1	-		
Year 2	4012019.27		4012019.27
Year 3	4312920.715		4312920.715
Year 4	4636389.769		4636389.769
Year 5	4984119.002		4984119.002
Year 6	5357927.927		5357927.927
Year 7	5759772.521		5759772.521
Year 8	6191755.46		6191755.46
Year 9	6656137.12		6656137.12
Year 10	7155347.404		7155347.404
Year 11	7691998.459		7691998.459
Year 12	8268898.343		8268898.343

Energy Production			
Year	**Energy Code**	**System Degradation**	**Energy Output (kWh)**
(a)	**(b)**	**(c)**	**(d)**
Year 1	P_{Y1}	100.00	170,673,093
Year 2	P_{Y2}	98.00	167,259,631
Year 3	P_{Y3}	96.04	163,914,439
Year 4	P_{Y4}	94.12	160,636,150
Year 5	P_{Y5}	92.24	157,423,427
Year 6	P_{Y6}	90.39	154,274,958
Year 7	P_{Y7}	88.58	151,189,459
Year 8	P_{Y8}	86.81	148,165,670
Year 9	P_{Y9}	85.08	145,202,356
Year 10	P_{Y10}	83.37	142,298,309
Year 11	P_{Y11}	81.71	139,452,343
Year 12	P_{Y12}	80.07	136,663,296

(a)	(b)	(c)	(d)
Year 13	8889065.719		8889065.719
Year 14	9555745.648		9555745.648
Year 15	10272426.57		10272426.57
Year 16	11042858.56		11042858.56
Year 17	11871072.96		11871072.96
Year 18	12761403.43		12761403.43
Year 19	13718508.69		13718508.69
Year 20	14747396.84		14747396.84
Year 21	15853451.6		15853451.6
Year 22	17042460.47		17042460.47
Year 23	18320645.01		18320645.01
Year 24	19694693.38		19694693.38
Year 25	21171795.38		21171795.38
Total	**249968810.2**		**249968810.2**

(a)	(b)	(c)	(d)
Year 13	P_{Y13}	78.47	133,930,030
Year 14	P_{Y14}	76.90	131,251,430
Year 15	P_{Y15}	75.36	128,626,401
Year 16	P_{Y16}	73.86	126,053,873
Year 17	P_{Y17}	72.38	123,532,796
Year 18	P_{Y18}	70.93	121,062,140
Year 19	P_{Y19}	69.51	118,640,897
Year 20	P_{Y20}	68.12	116,268,079
Year 21	P_{Y21}	66.76	113,942,717
Year 22	P_{Y22}	65.43	111,663,863
Year 23	P_{Y23}	64.12	109,430,586
Year 24	P_{Y24}	62.83	107,241,974
Year 25	P_{Y25}	61.58	105,097,135
Total			**3,383,895,053**

OUTPUT

Total O&M Life Cycle cost (USD)	**249968810.2**
Life Cycle cost of System (USD)	**678472929.5**
Lifetime Energy Production (kWh)	**3383895053**
LCOE (USD/kWh)	**0.200500583**

APPENDIX 26

CALCULATED LCOE FOR A 50 MW PLANT IN ZARIA

INPUT

Simulated Energy Output (kWh)	**155710024**
Calculated Capital Investment (USD)	**428631717.5**
Projected Annual Inflation Rate (%)	**7.5**
System Annual Degradation (%)	**2**

O&M (USD)			
Year	**O&M**		**Total for Year**
(a)	**(b)**	**(c)**	**(d)**
Year 1	-		
Year 2	3967130.06		3967130.06
Year 3	4264664.815		4264664.815
Year 4	4584514.676		4584514.676
Year 5	4928353.276		4928353.276
Year 6	5297979.772		5297979.772
Year 7	5695328.255		5695328.255
Year 8	6122477.874		6122477.874
Year 9	6581663.715		6581663.715
Year 10	7075288.493		7075288.493
Year 11	7605935.13		7605935.13
Year 12	8176380.265		8176380.265

Energy Production			
Year	**Energy Code**	**System Degradation**	**Energy Output (kWh)**
(a)	**(b)**	**(c)**	**(d)**
Year 1	P_{Y1}	100.00	155,710,024
Year 2	P_{Y2}	98.00	152,595,824
Year 3	P_{Y3}	96.04	149,543,907
Year 4	P_{Y4}	94.12	146,553,029
Year 5	P_{Y5}	92.24	143,621,968
Year 6	P_{Y6}	90.39	140,749,529
Year 7	P_{Y7}	88.58	137,934,538
Year 8	P_{Y8}	86.81	135,175,848
Year 9	P_{Y9}	85.08	132,472,331
Year 10	P_{Y10}	83.37	129,822,884
Year 11	P_{Y11}	81.71	127,226,426
Year 12	P_{Y12}	80.07	124,681,898

(a)	(b)	(c)	(d)
Year 13	8789608.785		8789608.785
Year 14	9448829.444		9448829.444
Year 15	10157491.65		10157491.65
Year 16	10919303.53		10919303.53
Year 17	11738251.29		11738251.29
Year 18	12618620.14		12618620.14
Year 19	13565016.65		13565016.65
Year 20	14582392.9		14582392.9
Year 21	15676072.36		15676072.36
Year 22	16851777.79		16851777.79
Year 23	18115661.12		18115661.12
Year 24	19474335.71		19474335.71
Year 25	20934910.89		20934910.89
Total	**247171988.6**		**247171988.6**

(a)	(b)	(c)	(d)
Year 13	P_{Y13}	78.47	122,188,260
Year 14	P_{Y14}	76.90	119,744,495
Year 15	P_{Y15}	75.36	117,349,605
Year 16	P_{Y16}	73.86	115,002,613
Year 17	P_{Y17}	72.38	112,702,560
Year 18	P_{Y18}	70.93	110,448,509
Year 19	P_{Y19}	69.51	108,239,539
Year 20	P_{Y20}	68.12	106,074,748
Year 21	P_{Y21}	66.76	103,953,253
Year 22	P_{Y22}	65.43	101,874,188
Year 23	P_{Y23}	64.12	99,836,704
Year 24	P_{Y24}	62.83	97,839,970
Year 25	P_{Y25}	61.58	95,883,171
Total			**3,087,225,822**

OUTPUT

Total O&M Life Cycle cost (USD)	**247171988.6**
Life Cycle cost of System (USD)	**675803706.1**
Lifetime Energy Production (kWh)	**3087225822**
LCOE (USD/kWh)	**0.218903231**

APPENDIX 27

EXTRACT OF MULTI-YEAR TARIFF ORDER FOR YOLA ELECTRICITY DISTRIBUTION COMPANY:2020-2022

Serial	Customer Classification	Description	MYTO Energy Charge (₦/kWh)		
			2020	2021	2022
1.	R1	Life - Line (50kWh)	4.00	4.00	4.00
2.	R2S	Single Phase	27.74	24.05	22.25
3.	R2T	Three Phase	30.37	26.43	24.36
4.	R3	Low Voltage Maximum Demand	55.47	48.10	44.50
5.	C1S	Single Phase	43.81	37.99	35.14
6.	C1T	Three Phase	50.41	43.72	40.44
7.	C2	Low Voltage Maximum Demand	54.15	46.96	43.44
8.	C3	High Voltage Maximum Demand (11/33KV)	64.72	56.12	51.91
9.	D1S	Single Phase	43.81	37.99	35.14
10.	D1T	Three Phase	50.41	43.72	40.44
11.	D2	Low Voltage Maximum Demand	59.43	51.54	47.68
12.	D3	High Voltage Maximum Demand (11/33KV)	66.04	57.26	52.97

APPENDIX 28

EXTRACT OF MULTI-YEAR TARIFF ORDER FOR KANO ELECTRICITY DISTRIBUTION COMPANY:2020-2022

Serial	Customer Classification	Description	MYTO Energy Charge (₦/kWh)		
			2020	2021	2022
1.	R1	Life - Line (50 kWh)	4.00	4.00	4.00
2.	R2S	Single Phase	18.75	18.81	18.60
3.	R2T	Three Phase	24.67	24.75	24.47
4.	R3	Low Voltage Maximum Demand	35.53	35.64	35.24
5.	C1S	Single Phase	35.53	35.64	35.24
6.	C1T	Three Phase	19.74	19.81	19.58
7.	C2	Low Voltage Maximum Demand	24.68	24.76	24.48
8.	C3	High Voltage Maximum Demand (11/33KV)	33.55	33.66	33.28
9.	D1S	Single Phase	33.55	33.66	33.28
10.	D1T	Three Phase	26.65	26.73	26.43
11.	D2	Low Voltage Maximum Demand	34.54	34.65	34.26
12.	D3	High Voltage Maximum Demand (11/33KV)	34.54	34.65	34.26